

Medical /
Mary

(THRY)

front

(NASA CR OR TMX OR AD NUMBER)

FACILITY FORM 602



ENGINE RESTART AND THERMODYNAMIC
ANALYSIS OF APOLLO SPACECRAFT
ENGINE TESTS (VOLUME I)

THE *BOEING* COMPANY · AEROSPACE GROUP
SOUTHEAST DIVISION

NASA → MSC

DOCUMENT NO. D2-118246-1

TITLE ENGINE RESTART AND THERMODYNAMIC ANALYSIS OF APOLLO
SPACECRAFT ENGINE TESTS (VOLUME I)

MODEL NO. APOLLO-TIE CONTRACT NO. NASw-1650

Prepared by:
PROPULSION AND POWER
5-2940

Prepared for:
NATIONAL AERONAUTICS AND SPACE ADMINISTRATION
MANNED SPACECRAFT CENTER
HOUSTON, TEXAS

Prepared by: B. F. Kerkam
A. A. Wood
M. G. Foley
D. W. Smith

Approved by: *A. M. Momen* 8/25/69
A. M. Momen
Propulsion Performance

Approved by: *J. M. Carter*
J. M. Carter (5-2940)
Propulsion and Power Systems

D2-118246-1

REVISIONS

REV. SYM	DESCRIPTION	DATE	APPROVED

ABSTRACT

This report presents analyses of results obtained from cold flow and hot firing tests conducted on the LM Ascent, LM Descent, and Service Propulsion System engines. The purposes of these analyses were to provide a basis for defining the thermodynamic processes and hardware variables that lead to a hypergol engine hard restart after a short duration firing, and to determine if cold flow tests can be formulated to provide data that will allow a reduction in the requirements for costly hypergol engine hot firing restart performance tests. Engine restart characteristics were related to the results from thermodynamic analyses of propellant behavior during the coast phase of cold flow and hot firing tests. Hard restarts were related to the accumulation of frozen propellants in the injector assemblies and the accumulation of nitrates in the thrust chambers. Recommendations were made concerning the conduct of future cold flow test programs and for further experimental and analytical investigations.

KEY WORDS

Aerojet
Aerozine-50
Arnold Engineering Development Center
Atlantic Research Corporation
Boeing Tulalip Test Site
Chamber Pressure Overshoot
Hydrazine
Injector
Injector Freezing
LM Ascent Engine
LM Descent Engine
Mixed Hydrazines
Nitrogen Tetroxide
Propellant Temperature
Propellant Thermodynamics
Restart
Rocket Engine Restart
Rocketdyne
Service Propulsion System Engine
TRW
UDMH

CONTENTS

Paragraph		Page
	Revisions	ii
	Abstract and Key Words	iii
	Contents	iv
	Illustrations	vii
	Tables	xii
	Definitions	xiv
	Nomenclature	xv
	Acknowledgements	xvi
	References	xvii

VOLUME I

SECTION 1 - INTRODUCTION

1.0	Purpose	1-1
1.1	Scope	1-1
1.2	Background	1-2

SECTION 2 - SUMMARY

2.0	Summary	2-1
-----	---------	-----

SECTION 3 - INJECTOR COLD FLOW TESTS AT ARC

3.0	General	3-1
3.1	Test Results	3-3

SECTION 4 - ROCKETDYNE ASCENT ENGINE TESTS AT SEATTLE

4.0	General	4-1
4.1	Test Objectives and Requirements	4-3
4.2	Test Results	4-7

SECTION 5 - TRW DESCENT ENGINE TESTS AT SEATTLE

5.0	General	5-1
5.1	Test Objectives and Requirements	5-3
5.2	Test Results	5-5

SECTION 6 - SPS ENGINE AND INJECTOR TESTS AT AEDC

6.0	General	6-1
6.1	Test Objectives and Requirements (Engine Restart)	6-2
6.2	Test Results (Engine Restart)	6-5
6.3	Test Objectives and Requirements (Injector Cold Flow)	6-12
6.4	Test Results (Injector Cold Flow)	6-14

CONTENTS (CONTINUED)

Paragraph		Page
SECTION 7 - ANALYSIS OF TEST DATA		
7.0	General	7-1
7.1	Thermodynamics and Flow	7-2
7.2	ARC Cold Flow Test Analysis	7-20
7.3	Ascent Engine Test Analysis	7-45
7.4	Descent Engine Test Analysis	7-71
7.5	SPS Cold Flow Test Analysis	7-88
7.6	SPS Engine Test Analysis	7-96
SECTION 8 - CORRELATION OF TEST RESULTS AND APPLICATION TO FLIGHT		
8.0	General	8-1
8.1	Correlation of APS, DPS, and SPS Restarts	8-2
8.2	Correlation of Cold Flow and Hot Firing Tests	8-6
8.3	Application to Flight	8-10
SECTION 9 - CONCLUSIONS AND RECOMMENDATIONS		
9.1	Conclusions	9-1
9.2	Recommendations	9-2
VOLUME II - APPENDICES		
APPENDIX A - INJECTOR COLD FLOW TESTING AT ARC		
A.0	General	A-1
A.1	Test Facility and Test Apparatus	A-2
A.2	Bell Ascent Engine Injector Tests, Phase I	A-9
A.3	Bell Ascent Engine Injector Tests, Phase II	A-16
A.4	TRW Descent Engine Injector Tests	A-22
A.5	Rocketdyne Ascent Engine Injector Tests	A-28
A.6	Evaluation of Injector Cold Flow Testing	A-34
APPENDIX B - ASCENT ENGINE TESTING AT SEATTLE		
B.0	General	B-1
B.1	Test Facility and Test Apparatus	B-2
B.2	Test Series Description	B-12
B.3	Test Results	B-16

CONTENTS (CONTINUED)

Paragraph		Page
APPENDIX C - DESCENT ENGINE TESTING AT SEATTLE		
C.0	General	C-1
C.1	Test Facility and Test Apparatus	C-2
C.2	Test Series Description	C-8
C.3	Test Results	C-8
APPENDIX D - SPS ENGINE TESTING AT AEDC		
D.0	General	D-1
D.1	Test Facility and Test Apparatus (Engine Restart)	D-2
D.2	Test Series Description (Engine Restart)	D-15
D.3	Test Results (Engine Restart)	D-18
D.4	Test Facility and Test Apparatus (Cold Flow)	D-19
D.5	Test Series Description (Cold Flow)	D-23
D.6	Test Results (Cold Flow)	D-24
APPENDIX E - RESTART COLD FLOW RECOMMENDATIONS		
E.0	General	E-1
E.1	Required Cold Flow Test Results	E-2
E.2	Evaluation of APS, DPS, and SPS Cold Flow Test Programs	E-3
E.3	Recommended Test Program	E-4

ILLUSTRATIONS

FIGURE		PAGE
3-1	Measured Fuel Residual Volumes, Bell Injector	3-4
3-2	Measured Fuel Residual Volumes, TRW Injector	3-6
3-3	Measured Fuel Residual Volumes, Rocketdyne Injector	3-7
4-1	Seattle APS Camera Views	4-10
4-2	LM Ascent Engine Chamber Windows and Cameras	4-11
5-1	Seattle DPS Camera Views	5-8
5-2	LM Descent Engine Thrust Chamber Windows and Cameras	5-9
7-1	Nitrogen Tetroxide Phase Diagram	7-4
7-2	Phase Diagram for 50% UDMH + 50% Hydrazine	7-6
7-3	Solubility of Helium in 50-50 and N_2O_4	7-10
7-4	Mass Residual Ascent Engine Fuel Side	7-14
7-5	Mass Residual Ascent Engine Oxidizer Side	7-15
7-6	Mass Residual for Descent Engine Fuel Side	7-16
7-7	Mass Residual for Descent Engine Oxidizer Side	7-17
7-8	Temperature History for Bell Injector, Repeated Pulses	7-21
7-9	Temperature History for Bell Injector	7-23
7-10	Temperature History for Bell Injector	7-24
7-11	Temperature History for Bell Injector	7-25
7-12	Temperature History for Bell Injector	7-26
7-13	Fuel Phase History, First Pulse, Bell Injector	7-27
7-14	Fuel Phase History, Second Pulse, Bell Injector	7-28
7-15	Temperature History for Descent Injector	7-31
7-16	Fuel Phase History for Descent Injector	7-32

ILLUSTRATIONS (CONTINUED)

FIGURE		PAGE
7-17	Fuel Phase History for Descent Injector	7-33
7-18	Oxidizer Phase History for Descent Injector	7-34
7-19	Temperature History for Descent Injector	7-35
7-20	Temperature History for Descent Injector Oxidizer Duct	7-35
7-21	Temperature History for Rocketdyne Injector	7-39
7-22	Temperature History for Rocketdyne Injector	7-40
7-23	Temperature History for Rocketdyne Injector	7-41
7-24	Temperature History for Rocketdyne Injector	7-42
7-25	Maximum Accelerometer Reading at Ignition vs. Ascent Engine Coast Period	7-46
7-26	Fuel Phase History for Ascent Engine	7-48
7-27	Fuel Phase History for Ascent Engine	7-49
7-28	Oxidizer Phase History for Ascent Engine	7-50
7-29	Fuel Phase History for Ascent Engine	7-51
7-30	Fuel Phase History for Ascent Engine	7-52
7-31	Fuel Phase History for Ascent Engine	7-53
7-32	Oxidizer Phase History for Ascent Engine	7-55
7-33	Oxidizer Phase History for Ascent Engine	7-56
7-34	Oxidizer Phase History for Ascent Engine	7-57
7-35	Time to Ignition vs. Ascent Engine Coast Period	7-61
7-36	Fuel and Oxidizer Injector Priming Times vs. Ascent Engine Coast Period	7-62
7-37	Maximum Oxidizer Interface Pressure vs. Ascent Engine Coast Period	7-63

ILLUSTRATIONS (CONTINUED)

FIGURE		PAGE
7-38	Maximum Fuel Interface Pressure vs. Ascent Engine Coast Period	7-65
7-39	Interface Pressure Records for Ascent Engine Firings A-7a and A-7b	7-67
7-40	Chamber Pressure and Manifold Pressure Records for Ascent Engine Firings A-7a and A-7b	7-68
7-41	Fuel Phase History for Descent Engine	7-72
7-42	Oxidizer Phase History for Descent Engine	7-74
7-43	Fuel Phase History for Descent Engine	7-75
7-44	Fuel Phase History for Descent Engine	7-76
7-45	Oxidizer Phase History for Descent Engine	7-77
7-46	Oxidizer Phase History for Descent Engine	7-78
7-47	Peak Chamber Pressure vs. Descent Engine Oxidizer Gas Content	7-84
7-48	Peak Chamber Pressure vs. Descent Engine Propellant Temperature	7-84
7-49	Peak Chamber Pressure vs. Descent Engine Coast Period	7-86
7-50	Time to Ignition vs. Descent Engine Coast Period	7-87
7-51	Oxidizer Phase Histories SPS Injector Inlet Duct	7-89
7-52	Temperature Histories SPS Injector Manifold and Inlet Duct	7-90
7-53	Fuel Phase Histories SPS Injector Inlet Duct	7-92
7-54	Temperature Histories SPS Injector Manifold and Inlet Duct	7-93
7-55	Temperature Histories SPS Injector Inlet Duct - Comparison Fuel Only and Fuel Plus Simulated Oxidizer	7-95
7-56	Histories SPS Injector and Combustion Chamber Pressure	7-97

ILLUSTRATIONS (CONTINUED)

FIGURE		PAGE
7-57	Temperature Histories SPS Injector and Inlet Duct	7-98
7-58	Temperature Histories SPS Injector and Manifold	7-100
7-59	Phase Histories SPS Injector	7-102
7-60	Phase Histories SPS Injector	7-103
7-61	Maximum Acceleration vs. Coast Time for SPS Engine	7-105
7-62	Maximum Chamber Pressure Spike vs. Coast Time for SPS Engine	7-106
7-63	Maximum Acceleration vs. Coast Time for SPS Engine	7-107
7-64	Fuel Manifold Priming Time vs. Coast Duration for SPS Engine	7-108
8-1	Correlation of Hot Firing Coast Phase Results (35°F)	8-8
8-2	Correlation of Hot Firing Coast Phase Results (65°F)	8-8
A-1	Propellant Supply System, Bell Injector Phase I Tests	A-3
A-2	Modified Propellant Supply System	A-4
A-3	Fuel Residual Distillation Apparatus	A-6
A-4	Test Orientation for Bell Injector	A-10
A-5	Instrumentation Locations on Bell Injector	A-11
A-6	Instrumentation Locations on TRW Injector	A-24
A-7	Instrumentation Locations on Rocketdyne Injector	A-29
A-8	Beaker Configuration and Instrumentation	A-31
A-9	Temperature Histories for Bell Injector Oxidizer Manifold	A-37
A-10	Temperature History of Bell Injector Fuel Manifold	A-39
A-11	Temperature History of TRW Injector Oxidizer Duct	A-40
A-12	Temperature History of TRW Injector Fuel Manifold	A-41

ILLUSTRATIONS (CONTINUED)

FIGURE		PAGE
A-13	Pressure History for TRW Injector and ARC Test Facility	A-45
B-1	Seattle Test Facility	B-3
B-2	Seattle APS Engine Pressure Measurements	B-6
B-3	Seattle APS Engine Temperature Measurements	B-7
C-1	Seattle DPS Instrumentation Locations	C-3
D-1	Propellant System Schematic and Instrumentation Locations	D-4
D-2	Cross Section SPS Engine Injector	D-7
D-3	Engine Instrumentation Locations	D-10
D-4	Apollo SPS Injector Cold Flow Test System Schematic	D-20

TABLES

TABLE

3-1	Summary of Cold Flow Testing at Atlantic Research Corporation	3-2
4-1	Ascent Engine Test Conditions	4-2
4-2	Planned Test Matrix for Seattle LMAE Tests	4-5
4-3	Ascent Engine Test Results Summary	4-8
5-1	Descent Engine Test Conditions	5-2
5-2	Planned Test Matrix For Seattle LMDE Tests	5-4
5-3	Descent Engine Test Results Summary	5-6
6-1	SPS Engine Test Conditions	6-6
6-2	SPS Engine Test Results Summary	6-9
6-3	SPS Injector Cold Flow Test Conditions	6-15
7-1	Physical Properties of the 50/50 Fuel Blend and N ₂ O ₄	7-3
8-1	Comparison of APS, DPS, SPS Engine Configurations	8-3
8-2	Coast Phase Test Results Summary	8-7
A-1	Distillation Apparatus Calibration Data	A-7
A-2	Bell Injector Phase I Test Summary	A-12
A-3	Bell Injector Phase II Test Summary	A-18
A-4	TRW Injector Test Summary	A-25
A-5	Rocketdyne Injector Test Summary	A-32
A-6	Rocketdyne Injector, Beaker Simulation Test Summary	A-33
B-1	LMAE Phase I Instrumentation	B-8
B-2	LMAE Phase II Instrumentation	B-10
B-3	Ascent Engine Nozzle Choking Summary	B-18

TABLES (CONTINUED)

TABLE		PAGE
C-1	LMDE Phase I Instrumentation	C-4
C-2	LMDE Phase II Instrumentation	C-7
C-3	Descent Engine Nozzle Choking Summary	C-14
D-1	Test Article Components	D-6
D-2	Instrumentation List	D-13
D-3	AEDC Test Summary SPS Restart	D-17
D-4	Apollo SPS Injector Cold Flow Instrumentation Summary	D-22
E-1	Required Cold Flow Test Results	E-3
E-2	Cold Flow Test Evaluation	E-5

DEFINITIONS

AEDC	Arnold Engineering Development Center
ARC	Atlantic Research Corporation
Bell	Bell Aerospace Corporation
TRW	TRW Systems Group
SPS	Service Propulsion System
APS	Ascent Propulsion System
DPS	Descent Propulsion System
LMAE	Lunar Module Ascent Engine
LMDE	Lunar Module Descent Engine
GAEC	Grumman Aircraft Engineering Corporation
GAC	Grumman Aerospace Corporation
Dry Start	An engine start mode with no fuel or oxidizer between the engine ball valves, and (APS and DPS only) no fuel in the valve actuator lines.
Wet Start	An engine start mode with propellants between the engine ball valves and (APS and DPS) fuel in the valve actuator lines.
Initial Start	The first start of a test series.
Hard Start	An engine firing which produced higher chamber pressure and accelerometer readings at ignition than initial starts made at the same test conditions.

D2-118246-1

NOMENCLATURE

m	mass
C_p	specific heat capacity
T	temperature (absolute)
τ	time
h_{lv}	enthalpy of vaporization
e	base of natural logarithms
S	solubility
p	pressure
scc	standard cubic centimeters
C_D	discharge coefficient
A	area
γ	ratio of specific heats, C_p/C_v
n	molecular weight
R_0	gas constant (universal)

D2-118246-1

ACKNOWLEDGEMENTS

The Apollo spacecraft engine restart analysis presented in this report is, in part, the result of a compilation and study of data and test reports made available by personnel of the Primary Propulsion Branch, Propulsion and Power Division of the Manned Spacecraft Center. Assistance provided by M. Lausten, R. Kahl, and R. Polifka in discussions and data was particularly valuable. Further information was obtained first-hand from personnel of the Boeing Tulalip Test Facility, the Atlantic Research Corporation, and the Grumman Aerospace Corporation who had directly participated in these test programs. These people have significantly contributed to the results in this report and their willing cooperation and assistance are recognized and appreciated.

REFERENCES

1. Atlantic Research Corporation Status Reports to Grumman Aerospace Corporation for Contract P.O. 4-61666-C.
2. Venting of Propellants From The Manifolds of The LM Engines After Shutdown, Final Report, Atlantic Research Corporation, (June 1969).
3. Hot Fire Testing of the LM Ascent and Descent Engine Restart Capabilities Phase I Test Report, Vol. I and II. The Boeing Company - Space Division; D2-114434-1 (December 1968).
4. Hot Fire Testing of the LM Ascent and Descent Engine Restart Capabilities Test Phase II Test Reports, The Boeing Company - Space Division; D2-114434-2, D2-114434-5.
5. Hot Fire Testing of the LM Ascent and Descent Engine Restart Capabilities Test Program Final Report, The Boeing Company - Space Division; D2-114434-3 (May 1969).
6. Investigation of the Apollo SPS Engine (AJ10-137) Reignition Characteristics at Pressure Altitudes Above 200,000 Feet, ARO, Inc.; AEDC-TR-69-13 (March 1969).
7. Apollo Service Propulsion System Injector Cold Flow Test, ARO, Inc.; AEDC-TR-68-132 (July 1968).
8. The Reignition Characteristics of the Apollo Service Propulsion System Engine at Pressure Altitudes Above 200,000 Feet, R. Kahl and R. Smith, Proceedings of 11th Liquid Propulsion Meeting (to be published).
9. Nitrogen Tetroxide, Product Bulletin Allied Chemical - Nitrogen Division.
10. Determination of Thermodynamic Properties of Aerozine-50, Atlantic Research Corporation, J. P. Copeland, J. A. Simmons, (May 1968).
11. Study of Pressurant Gas Solubility in Nitrogen Tetroxide and Aerozine-50, Chemistry Support to the LMDE 500 Hz Program Final Report, TRW Report 01827-6205-R0-00 (December 1968)
12. CSM/LM Spacecraft Operational Data Book, Volume II LM Data Book, National Aeronautics and Space Administration, Manned Spacecraft Center, SNA-8-D-027 (II) Rev. 1 (March 1969).
13. Handling and Checkout Instructions for LMDE Engine SK-403936-1 for Engine Restart Verification Program at the Boeing Tulalip Test Site, TRW Report 01827-6187-T000.

D2-118246-1

REFERENCES (CONTINUED)

14. Handling and Usage Procedures for Modified Injector Assembly (SK-402632-1) for Atlantic Research Corporation, TRW Report 01827-6161-T000, C. M. James, April 30, 1968.

SECTION 1 - INTRODUCTION

1.0 PURPOSE

This report presents analyses of results obtained from cold flow and hot firing tests conducted using Apollo spacecraft primary propulsion system engines. The purposes of these analyses were to:

1. Provide a basis for defining the thermodynamic processes and hardware variables that lead to a hypergol engine hard restart after a short duration firing.
2. Determine if cold flow tests can be formulated to provide data that would allow a reduction in the requirements for costly hypergol engine hot firing restart performance tests.

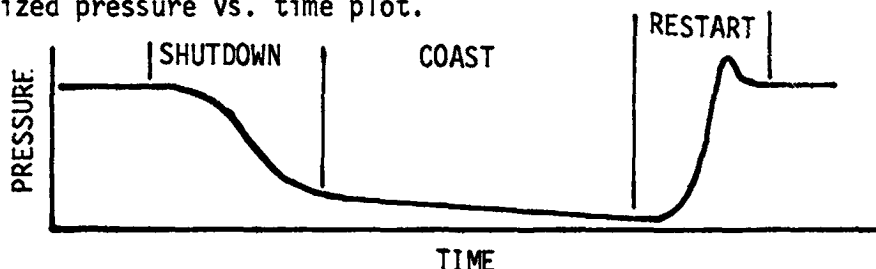
1.1 SCOPE

Results obtained from cold flow and hot firing spacecraft engine tests are analyzed to determine the significant parameters and phenomena affecting engine restarts. Comparisons between cold flow and hot firing tests are used to determine the feasibility of developing a hot firing/cold flow test correlation. The Apollo spacecraft primary propulsion system engine restart tests, supplying data for the analyses, are summarized and evaluated. This summary and evaluation covers test hardware, test conditions, and data validity.

1.2 BACKGROUND

Early in the Apollo program, it was realized that residual propellants could freeze in spacecraft engine injectors and/or propellant manifolds after the engines were shut down. This freezing can occur because the propellants in the injector and manifolds are exposed to space vacuum conditions which results in propellant cooling by evaporation. Heat transferred from the thrust chamber and injector will vaporize part of the residual propellants, but short duration firings (on the order of 1 second) do not transfer enough heat to prevent propellant freezing.

Engine restart characteristics are affected by the engine and propellant behavior during the preceding shutdown and coast periods. The three time periods of interest are shown schematically on the following generalized pressure vs. time plot.



1.2 BACKGROUND (Continued)

During the shutdown period, the thrust chamber, fuel manifold, and oxidizer manifold pressures rapidly decrease below steady state operating levels. Combustion continues, at a low level, for several seconds after the engine valves close as some of the residual propellants are ejected into the thrust chamber. During the coast phase, the fuel and oxidizer manifold pressures decay below the fuel and oxidizer vapor pressures. The fuel and oxidizer residuals are then cooled by boiling and evaporation and can be frozen if the propellant temperatures decrease to the fuel and oxidizer freezing points. Upon engine restart, the injector fuel and oxidizer manifolds are refilled with propellants, and engine ignition follows. The engine restart characteristics will be influenced by the volume and thermodynamic state (solid or liquid) of the residual propellants present at restart.

As a result of concern over the effect that frozen propellants could have on engine restarts, a comprehensive test program to investigate restart phenomena was initiated by the Propulsion and Power Division of the Manned Spacecraft Center, Houston, Texas. This program included a series of injector cold flow tests at the Atlantic Research Corporation (ARC) and Arnold Engineering Development Center (AEDC) followed by a series of engine hot firings at AEDC and Boeing test facilities. These tests emphasized short duration firings which minimize the heat input from combustion and maximizes the possibility of propellant freezing. This report provides a comprehensive summation, comparison, and analyses of the results obtained from these cold flow and hot firing tests covering all three of the Apollo spacecraft primary propulsion system engines.

SECTION 2 - SUMMARY

2.0 SUMMARY

Analyses were conducted to define hypergol engine restart limits using data from tests on Apollo spacecraft Ascent, Descent, and Service Propulsion System (SPS) primary engines. These analyses included data from: Ascent and Descent engine cold flow tests conducted at the Atlantic Research Corporation (ARC); Ascent and Descent engine hot firings conducted at the Boeing (Seattle) Tulalip Test Facility; Service Propulsion System engine cold flow and hot firing tests conducted at the Arnold Engineering Development Center (AEDC). The LM Ascent and Descent engine tests were directed by the Grumman Aerospace Corporation; the SPS tests were directed by NASA/MSFC.

Bell and Rocketdyne Ascent engine injectors and a TRW Descent engine injector were cold flow tested at ARC using oxidizer or fuel plus an oxidizer simulant. These tests were conducted to emphasize the coast phase and observation of propellant behavior after termination of propellant flow. Propellant freezing in injector manifolds and passages was experienced. Techniques were developed during these tests for the measurement of propellant residual volumes in the injectors.

The Ascent (APS) engine was tested at Seattle using short duration (0.5 second) firings, coast periods from 1 to 1500 seconds, propellant temperatures from 40 to 65°F, and propellant helium saturation levels from 33 to 100%. The tests were conducted at altitudes generally above 200,000 feet. During these hot firing tests, hard restarts were experienced at coast times of 15 to 90 seconds. Analyses of the test data, coupled with an evaluation of motion pictures covering the injector flow, showed that all but two hard restarts were caused by frozen oxidizer plugging the engine injector filters sufficiently to reduce the normal oxidizer lead. The two restarts that gave no evidence of oxidizer plugging occurred after coast periods of 30 and 90 seconds. Their cause was not determined. On another test, the engine did not restart during the second restart attempt after a 60 second coast.

The Descent (DPS) engine was tested at Seattle using short duration (2 to 3.5 seconds) firings, coast periods from 2 to 1819 seconds, propellant temperatures from 40 to 65°F, and propellant helium saturation levels from 9 to 100%. All tests were conducted at a 10% thrust setting on this throttleable engine and the test altitudes were generally above 200,000 feet. During these hot firing tests, one hard restart was noted. There were several tests in which restarts showed a transient chamber pressure well above the steady state pressure, however, these could not be classified as hard starts because the transient pressures were within the range of pressures observed during initial starts. Analyses of the test data, coupled with an evaluation

2.0 SUMMARY (Continued)

of motion pictures covering the injector flow, gave evidence that propellants froze in the engine ducts and manifolds. This freezing had little effect on the restart characteristics and it is believed that this is due to the normally slow start transient on this engine.

An SPS (Block I) injector was cold flow tested at AEDC using fuel, fuel plus an oxidizer simulant, and oxidizer. These tests were conducted to emphasize the coast phase and observation of propellant behavior after the injector was exposed to a low pressure environment. Propellant freezing in the injector manifold and passages was experienced.

The SPS engine, using a Block I injector, was tested at AEDC using short duration (0.37 and 0.50 second) firings, coast periods from 7 to 1800 seconds, propellant temperatures of 35 and 65°F. The tests were conducted at altitudes generally above 245,000 feet. During these hot firing tests, random hard restarts were experienced after 0.37 second firings. Analyses of the data from multiple 0.37 second duration restart tests indicated that detonable compounds collected in the combustion chamber causing increasingly hard restarts. No evidence was found that these detonable compounds were formed following 0.5 second firings.

Analyses of the cold flow and hot firing restart test data were performed using phase diagrams to determine the thermodynamic state of the propellants. Selected APS, DPS, and SPS cold flow and hot firing test results were compared. Propellant mass residuals were calculated for the APS and DPS hot firings and the results compared with cold flow residual measurements from ARC tests. The effect of engine injector and manifold volumes, thermodynamic state of propellant residuals, gas saturation, propellant temperature, and gravity on restart characteristics were evaluated. Results from these analyses provide an understanding of the transient thermodynamic processes involved in hypergol engine restarts and the background for developing a technical basis for establishing engine restart limits and mission constraints. In addition, the analyses show that adequately conducted cold flow tests can be useful in reducing the scope of a hot firing test program.

SECTION 3 - INJECTOR COLD FLOW TESTS AT ARC

3.0 GENERAL

This section summarizes the cold flow test program conducted at the Atlantic Research Corporation (ARC) High Altitude Test Facility between September 18, 1967 and March 8, 1969. The test conditions for each test series are summarized, and significant test results are presented. The information and data presented in this section were obtained from the ARC weekly status reports (Reference 1) and the ARC final report (Reference 2). Descriptions of the test facility, instrumentation, and test article configuration are provided in Appendix A.

The objective of the ARC test program was to determine the extent of injector cooling and accumulation of frozen propellants during venting, freezing, and sublimation processes. To meet these objectives, sufficient injector tests were conducted to determine the degree of flow obstruction, and the pressure, temperature, and mass residual histories as a function of time after propellant valve closure. Additional beaker tests were conducted to obtain photographic records of the phenomena occurring after propellants were suddenly exposed to a vacuum environment and to investigate the effects of beaker orientation on the propellant expulsion process.

Four series of cold flow tests were conducted using a Bell ascent injector (Phases I and II), a Rocketdyne ascent injector and a TRW descent injector. The test series were conducted in accordance with the requirements of Grumman Aerospace Corporation contract P.O. 4-61666-C with the Atlantic Research Corporation (ARC). The scope of the test series is indicated in Table 3-1. Fuel tests and oxidizer tests were conducted separately to prevent combustion. During most fuel tests, the oxidizer cooling effects were simulated by flowing Freon MF or TF through the oxidizer side of the test injector. No simulation of fuel cooling effects was attempted during any of the nitrogen tetroxide tests. Test article temperatures, pressures, and propellant mass residuals were recorded as a function of time. Photographic coverage of the injector external flow characteristics was obtained.

In addition to the injector tests, a series of transparent beaker tests was conducted. The beaker approximated the fuel side volume and orifice area of the Bell ascent injector. For each test, the beaker was filled with Aerozine-50 or nitrogen tetroxide, and then exposed to the low pressure environment of the ARC High Altitude Test Facility. Photographic coverage of these tests was obtained, and limited temperature histories were taken. The beakers had no provisions for pressure instrumentation.

TABLE 3-1
SUMMARY OF COLD FLOW TESTING AT ATLANTIC RESEARCH CORPORATION

BELL INJECTOR	BELL INJECTOR	TRW INJECTOR	ROCKETDYNE INJECTOR
PHASE I	PHASE II		
OBJECTIVES 1. DETERMINE EXTENT OF OBSTRUCTION 2. DETERMINE QUANTITY OF TRAPPED PROPELLANT 3. OBTAIN DATA ON BOILING RATES	OBJECTIVES 1. VERIFY DISTILLATION PROCEDURE 2. DETERMINE RESIDUAL FOR SINGLE & DUAL-PULSE TEST 3. DETERMINE PRESSURE AND TEMPERATURE HISTORIES	OBJECTIVES 1. VERIFY DISTILLATION PROCEDURE 2. DETERMINE RESIDUAL FOR SINGLE & DUAL-PULSE TESTS 3. DETERMINE PRESSURE AND TEMPERATURE HISTORIES	OBJECTIVES 1. EVALUATE EFFECT OF FILTERS 2. DETERMINE RESIDUAL FOR SINGLE-PULSE 3. DETERMINE PRESSURE AND TEMPERATURE HISTORIES
TESTS 6 LM-1 MDC FUEL 1 5-PULSE FUEL 2 LM-1 MDC OXID. 3 BEAKER TESTS, FUEL 4 5-PULSE OXID. 1 BEAKER TEST, OXID. 4 1-PULSE FUEL DISTILLATION	TESTS 1 SINGLE-PULSE 40°F FUEL DISTILLATION 8 SINGLE-PULSE 70°F FUEL DISTILLATION 9 DUAL-PULSE 40°F FUEL DISTILLATION 8 DUAL-PULSE 70°F FUEL DISTILLATION	TESTS 9 SINGLE-PULSE 40°F FUEL 8 SINGLE-PULSE 70°F FUEL 3 DUAL-PULSE 70°F FUEL 2 SINGLE-PULSE 40°F OXID. 2 SINGLE-PULSE 40°F OXID. SIMULANT (FREON TF)	TESTS 9 SINGLE-PULSE 40°F FUEL 5 SINGLE-PULSE 70°F FUEL 16 BEAKER, FUEL 3 BEAKER, OXID.
INJECTOR ORIENTATION INJECTOR FACE 30° ABOVE HORIZONTAL	INJECTOR ORIENTATION INJECTOR FACE 30° ABOVE HORIZONTAL	INJECTOR ORIENTATION INJECTOR FACE 8° FORWARD FROM VERTICAL	INJECTOR ORIENTATION INJECTOR FACE 8° FORWARD FROM VERTICAL

3.1 TEST RESULTS

A detailed review of the data from cold flow tests is presented in Section 7.3 of this report. The significant test results for each of the four injector test series are summarized below.

3.1.1 Bell Injector Phase I Test Results Summary

1. Propellant residuals in the injector and ducts boil violently following termination of propellant flow. This causes significant amounts of liquid to be expelled through the injector orifices.
2. The Bell injector was cooled below the freezing temperature of A-50 and N_2O_4 by the evaporation of fuel and oxidizer, or oxidizer simulant, residuals.
3. The oxidizer injector orifices were not plugged by frozen oxidizer residuals during any of the oxidizer tests.
4. The fuel injector orifices were not plugged by frozen fuel residuals when no oxidizer simulant (Freon MF) was used.
5. The fuel injector orifices were partially plugged by frozen fuel residuals when 535-1070 ml of oxidizer simulant (Freon MF) was used at initial fuel temperatures of 62°F or less, and after three or more pulses.

3.1.2 Bell Injector Phase II Test Results Summary

1. The residual fuel started to boil approximately 3 seconds after the start of the fuel flow pulse. This time is independent of initial fuel and injector temperatures over the temperature range of 40 to 70°F, and is the same for first coast periods and second coast periods.
2. The temperature of the residual fuel decreased to the freezing level in 15-20 seconds after the start of the fuel flow pulse. This time is independent of initial fuel and injector temperatures over the temperature range of 40 to 70°F, and is the same for first coast periods and second coast periods.
3. Small amounts (up to 3 in³) of frozen fuel residuals were present in the injector ducts one-half hour after the second fuel pulse. Additional fuel residual data are presented in Figure 3-1.

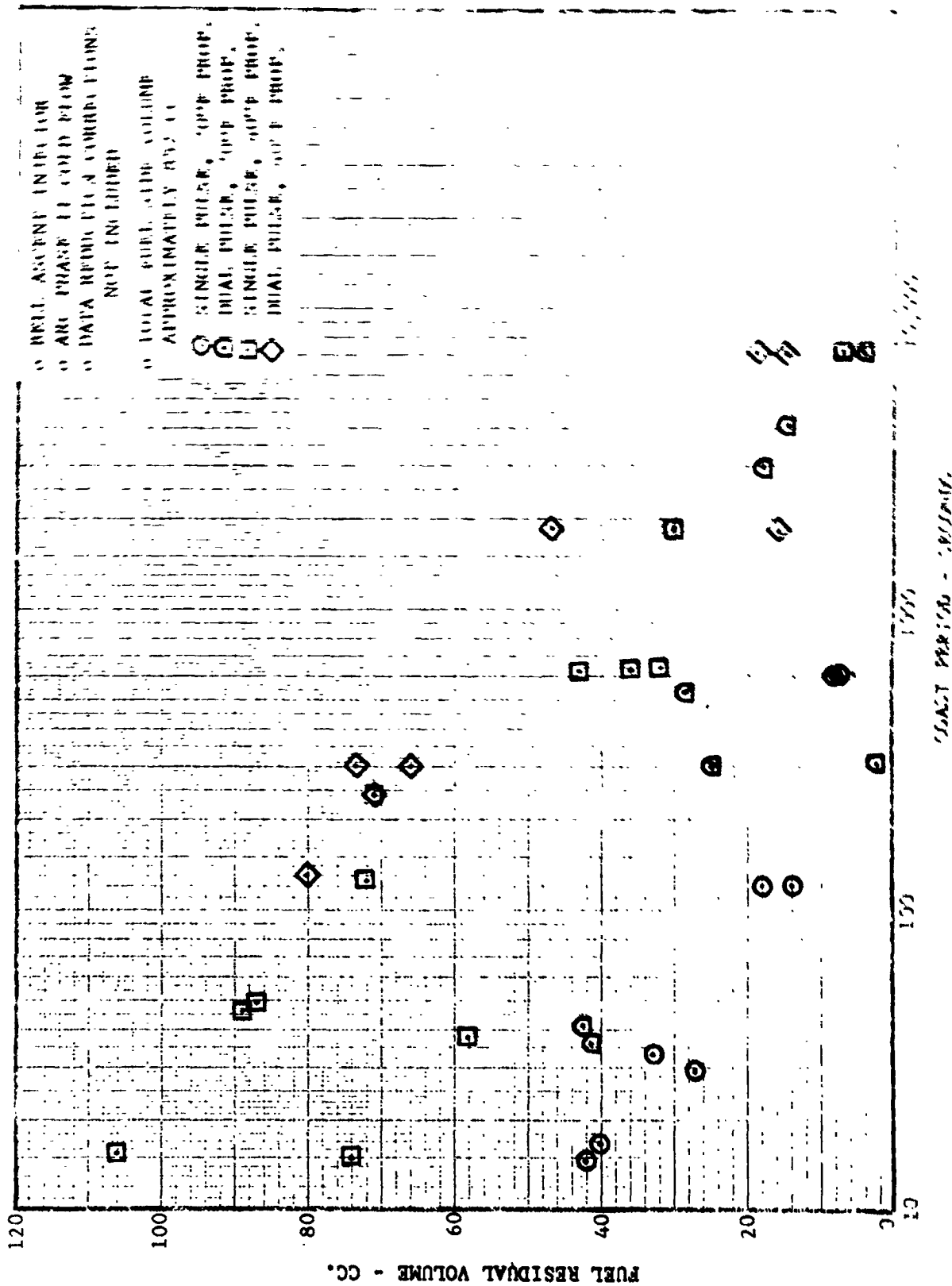


FIGURE 3-1 MEASURED FUEL RESIDUAL VOLUMES, BELL INJECTOR

3.1.2 Bell Injector Phase II Test Results Summary (Continued)

4. The volume of fuel residuals is decreased by an increase in initial fuel and injector assembly temperatures.

3.1.3 TRW Injector Test Results Summary

1. The residual fuel started to boil approximately 5 to 25 seconds after the start of the fuel flow pulse. The time to the start of boiling was decreased by an increase in initial fuel and injector assembly temperatures.
2. The fuel temperature decreased to the freezing level in 90 to 100 seconds following the start of the first fuel flow pulse. The time was independent of the initial fuel temperature.
3. The fuel temperature decreased to the freezing level in 45 to 60 seconds following the start of the second fuel flow pulse (40°F fuel).
4. Small amounts (0-4 in³) of frozen fuel residuals were present in the injector assembly one hour after the fuel flow pulse. Additional fuel residual data are presented in Figure 3-2.
5. The volume of fuel residuals was decreased by an increase in the initial fuel and injector assembly temperature.
6. A nitrogen tetroxide flow pulse cooled the injector fuel manifold approximately 8°F from an initial temperature of 40°F.

3.1.4 Rocketdyne Injector Test Results Summary

1. The injector and propellant ducts were cooled below the freezing point of Aerozine-50.
2. The propellant ducts reached much lower temperatures than the injector, indicating that the propellant residuals were located in the propellant ducts.
3. Measurable amounts (up to 0.8 in³) of frozen fuel residuals were present for as long as 1 hour after the propellant flow pulse. Additional fuel residual data are presented in Figure 3-3.
4. The volume of fuel residuals was increased by a decrease in the initial propellant and injector assembly temperatures.

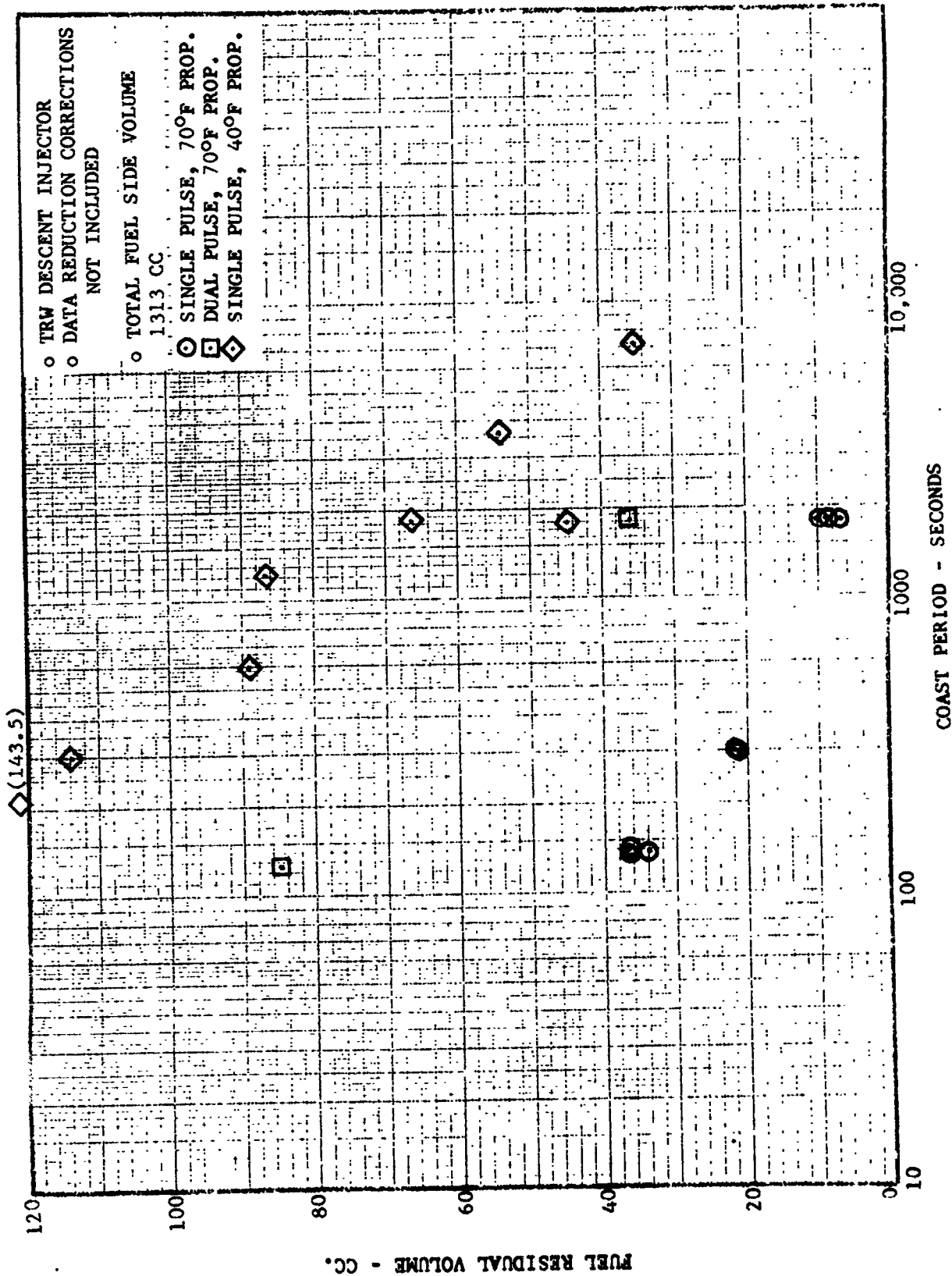


FIGURE 3-2 MEASURED FUEL RESIDUAL VOLUMES, TRW INJECTOR

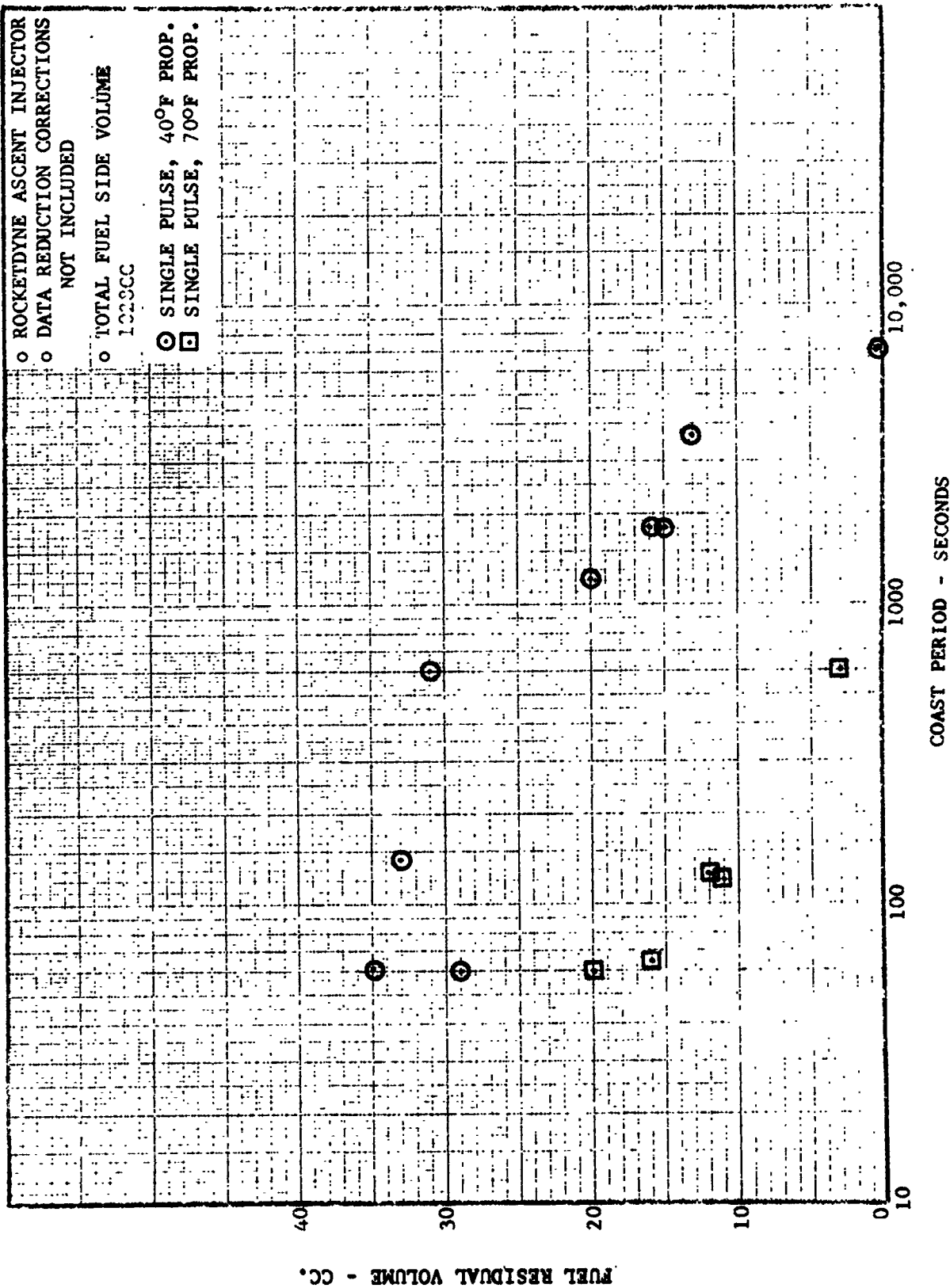


FIGURE 3-3 MEASURED FUEL RESIDUAL VOLUMES, ROCKETDYNE INJECTOR

SECTION 4 - ROCKETDYNE ASCENT ENGINE TESTS AT SEATTLE





4.0 GENERAL


The LM ascent engine hot-firing restart test program was conducted at the Boeing Tulalip Test Facility near Seattle, Washington during the period from October, 1968 to February, 1969. The tests were planned and supervised by GAC, in accordance with GAC Contract Number NAS9-1100. Contract Item CCA 1041 titled, "Test Requirements for LM Ascent and Descent Engine Restart Capabilities Test Program".


The test program was divided into Phase I and Phase II. Phase I tests were run with nominal initial propellant and hardware temperatures of 65°F, with an uncontrolled propellant helium saturation level and no photographic coverage of injector phenomena during coast or firing periods. Phase II tests were run with nominal initial propellant and hardware temperatures of 50°F, with helium saturated propellants and photographic coverage of the interior of the engine thrust chamber during firing and coast periods. Propellant samples were obtained prior to all Phase I and Phase II tests to determine the dissolved gas content (He, N₂, etc.) of the propellants.


A summary of the ascent engine test conditions and the as-run test matrix are in Table 4-1.

Detailed information on the Seattle APS test facility, engine configuration, instrumentation, and test series conduct is presented in Appendix B.

TEST NO.	FIRE TIME SEC.	NO. OF STARTS	COAST PER. SEC.	START ALTITUDE INITIAL 10 ³ FT.	RESTART 10 ³ FT.	INITIAL TEMP. PROP. °F	INITIAL TEMP. HDW. °F	PROP. FUEL %	HELIUM SAT. OXID. %	REMARKS
PHASE I  										
Ac/o	.72	1		210	-	64	65	NA	NA	Dry start
A1	.52	2	1500	212	225	62	65	70	NA	Dry start
A2	.52	2	300	218	218	63	65	58	33	Dry start
A3	.52	2	90	215	218	62	65	51	60	Dry start
A4	.52	2	30	200	200	61	65	45	69	Dry start
PHASE II 										
A01	.5	1	-	225	-	36	40	92	86	Wet start
A02	.5	1	-	221	-	44	45	97	55	Dry start
A5	.5	3	200	212	210	48	50	96	100	Dry start
A6	.5	3	90	228	216	48	48	100	92	Dry start
A7	.5	3	60	232	205	49	48	90	100	Dry start
A8	.5	2	30	244	208	50	51	100	100	Wet start
A9	.5	2	15	212	206	45	44	100	100	Wet start
A10	.5	2	10	222	187	44	45	100	100	Wet start
A11	.5	2	2.5	224	191	47	47	97	100	Wet start
A12	.5	2	1.0	214	186	46	46	90	100	Wet start

 No attempt was made to saturate the propellants with helium during Phase I tests.

 No cryopanelts were used during Phase I tests.

 Propellant helium saturation procedure was performed prior to each test.


 Altitude loss after engine shutdown invalidates coast period data.

TABLE 4-1
ASCENT ENGINE TEST CONDITIONS

4.1 TEST OBJECTIVES AND REQUIREMENTS

4.1.1 Test Objectives

The objective of the LM Ascent Engine Restart Capabilities Test Program was to determine the constraints for ascent engine restarts which may follow short duration (0.5 second) firings. The hazards associated with this type of operation result primarily from the evaporative freezing of the propellants in the injector and ducts following shutdown, and the effect of the frozen propellants on a subsequent restart attempt.

An additional area to be investigated was the deposition of detonable compounds on the cold injector face or combustion chamber walls. These compounds are formed by incomplete combustion of the propellants and may be deposited on the combustion chamber surfaces. It is probable that combustion chamber overpressures would result if sufficient amounts of these compounds were present and were ignited during an engine restart.

4.1.2 Test Requirements

In order to investigate these potential problem areas, the following requirements were established by Grumman Aircraft Engineering Corporation for the Restart Capabilities Testing:

1. The Ascent and Descent Engines to be mounted with the thrust axis (+X) 8° above the horizontal and with the valve packages located at the bottoms of the engines.
2. The engine mount fixture spring rate design target to be 60×10^4 lb per inch.
3. The engine and propellant to be thermally conditioned at $65 \pm 5^\circ\text{F}$ for a minimum of 30 minutes prior to the first firing for Phase I and 40° to 50°F for Phase II.
4. Low speed (24 frames per second) motion pictures to be taken of the engine shutoff valve actuator vent line exits for observation of the formation of frozen propellant during the shutdown sequence in Phase I. In Phase II, additional cameras, a low-speed and a high speed, to be trained on the injector through windows in the engine thrust chamber.
5. The test cell altitude to be in excess of 200,000 ft. prior to the first start of each Phase I test series, and in excess of 250,000 ft. prior to the first start for each Phase II test series. Recovery back to 200,000 ft. after first firing shutdown to be at the maximum facility rate and remain at 200,000 ft. for the remainder of the "coast" time and for restarts.

4.1.2 Test Requirements (Continued)

6. Propellant residue on the injector or combustion chamber walls to be sampled at the end of the run and held for analysis.

4.1.3 Test Planning

The test plans for the LM primary engines called for two phases of testing. The Phase I tests were to investigate single-restart phenomena at propellant and hardware temperatures of 65°F. The Phase II tests were to investigate multiple restart phenomena at colder (50°F) temperatures. High temperatures were not considered to present as severe a problem as low temperatures, and were not tested. Tests were run at a minimum engine firing time of 0.5 seconds, which increased the probability of injector freezing and was at the same time a best condition for the altitude facility, which had a limited mass removal capability.

The primary variable in the test program was the "coast" time between an engine shutdown and the subsequent restart. In this way, a constraint on coast time for minimum impulse multiple restarts could be established. The planned test conditions and sequences are shown in Table 4-2. The coast times for the LMAE were to be determined by thermodynamic considerations before the tests began.

The Phase I and Phase II test programs differed significantly from the planned test matrix, especially in the number of tests actually performed. Greater difficulties than imagined were met in setting up the engines and in meeting cleanliness requirements. As a consequence, the number of Phase I tests was reduced to meet the October 31, 1968 deadline for Phase I test completion. The initial Phase II test matrix was significantly modified by NASA and Grumman. The "as-run" test matrix is shown in Table 4-1.

The following Grumman requirements were incorporated in the detailed test plans, facility buildup, and procedures:

1. The propellants to be nitrogen tetroxide (N_2O_4) oxidizer per MSC Specification MSC PPD-2 Rev. A and mixed hydrazines (50% hydrazine and 50% UDMH) fuel per Specification MIL-P-27402.
2. The pressurizing gas for the propellants to be helium per specification MIL-P-27407 or Bureau of Mines, Grade A.
3. The purging gas to be nitrogen per Specification MIL-P-27401B.

D2-118246-1

TABLE 4-2
PLANNED TEST MATRIX FOR SEATTLE LMAE TESTS

PHASE I

TEST SERIES	ENGINE	NO. OF STARTS	ENGINE FIRING TIME-SEC.	INITIAL PROPELL. & HARDWARE TEMP. °F	PROPELLANT SATURATION LEVEL - %	COAST TIME - SEC.
A-1	Ascent	2	0.5	65	0	TBD
A-2	↓	↓	↓	↓	↓	↓
A-3	↓	↓	↓	↓	↓	↓
A-4	↓	↓	↓	↓	↓	↓
A-5	↓	↓	↓	40	↓	↓
A-6	↓	↓	↓	↓	↓	↓
A-7	↓	↓	↓	↓	↓	↓
A-8	↓	↓	↓	↓	↓	↓
A-9	↓	↓	↓	↓	↓	↓

PHASE II

A-10	Ascent	5	2	65	100	TBD
A-11	↓	↓	↓	↓	↓	↓
A-12	↓	↓	↓	↓	↓	↓
A-13	↓	↓	↓	↓	↓	↓
A-14	↓	↓	↓	↓	↓	↓
A-15	↓	↓	0.5	↓	↓	↓
A-16	↓	↓	↓	↓	↓	↓
A-17	↓	↓	↓	↓	↓	↓
A-18	↓	↓	↓	↓	↓	↓
A-19	↓	↓	2	40	↓	↓
A-20	↓	↓	↓	↓	↓	↓
A-21	↓	↓	↓	↓	↓	↓
A-22	↓	↓	↓	↓	↓	↓
A-23	↓	↓	↓	↓	↓	↓
A-24	↓	↓	↓	↓	↓	↓
A-25	↓	↓	0.5	↓	↓	↓
A-26	↓	↓	↓	↓	↓	↓
A-27	↓	↓	↓	↓	↓	↓

4.1.3 Test Planning (Continued)

4. The fluid and hardware cleanliness levels shall be as specified in the applicable GAEC, TRW, and Rocketdyne documents.
5. Ascent engine propellant feed line length and diameter to be consistent with the LM vehicle drawings. The length, diameter, wall thickness, and material of the engine shutoff valve actuator vent lines to be consistent with vehicle drawings. Reasonable approximations of line configurations are acceptable.
6. Descent engine propellant feed line diameter shall be 2 0 inches. Reasonable approximations of line length and configuration are acceptable. The length, diameter, wall thickness, and material of the engine shutoff valve actuator vent lines to be consistent with LM vehicle drawings, however, reasonable approximations of vent line configurations will be acceptable for the line segments downstream of the flexible hose sections.
7. The engine prevalues and/or shutoff valve actuator pilot valves to be supplied with the required electrical voltage and amperage.
8. Sufficient instrumentation to be available to record the desired pressure, temperature, acceleration, and other parameters necessary to evaluate engine and facility performance.
9. Engine and test facility hardware to be examined after each test series and photographs taken of any damage noted.
10. A facility and engine checkout firing to be conducted for each engine prior to each phase of testing.

4.2 TEST RESULTS

4.2.1 Significant Results

The Seattle Phase I and Phase II tests produced one failure to restart and several restarts which had significantly higher peak chamber pressures and accelerometer readings than the initial starts. Low temperatures, significantly below the fuel and oxidizer freezing temperatures, were observed in the fuel and oxidizer ducts between the engine valves and the injector. The presence of frozen oxidizer residuals was found to result in partial plugging of the oxidizer side, causing hard restarts. A summary of the Seattle test results is presented in Table 4-3. A detailed analysis of the test data is in Section 7.3.

4.2.2 Photographic Results

Three cameras were used for observation of the Ascent engine during Phase II tests. A 1000 frames-per-second Photosonic camera and a 24 frames-per-second Milliken camera (Milliken I) photographed the injector through quartz glass windows in the combustion chamber wall. An additional 24 frames-per-second Milliken camera (Milliken II) was directed at the shut-off valve vent line exits. Figure 4-1 shows sketches of the projected images from the cameras, and Figure 4-2 shows the location of the combustion chamber ports, cameras, and light source. This configuration was maintained constant until the last Ascent Engine test (A-12), when the Photosonics camera was removed and replaced by the Milliken II camera. This camera was pointed towards the thrust chamber throat to determine if fuel puddles were formed after the firing. Despite a successful checkout, the camera did not function properly during the test, and did not produce usable photographs. Color film was used in the Milliken cameras, and black and white film was used in the Photosonics camera. A "fire switch" event light and a 1000 Hertz timing light were used in the Photosonics camera. There were no marker lights used in the Milliken cameras.

Film coverage was obtained from the Photosonics camera for all tests except A-0II-1, A-0II-2, A-5 and A-12 and from the Milliken I camera for all tests except A-5. The Milliken II camera produced no usable films except for test A-11.

Films from the Photosonics camera showed the injection of propellants until the injector was obscured by propellant spray. The floodlight was also obscured, causing the film to darken for a few frames. Ignition was indicated by a sudden increase in light intensity, caused by the incandescence of the burning propellants.

Following engine shutdown, the chamber clears rapidly. The decay of the combustion process is accompanied by combustion oscillations which are detected by the chamber pressure and fuel and oxidizer manifold pressure transducers. When the injector face and baffle became visible,

PHASE I

TEST NO.	DATE	COAST PER. SEC.	CHAMBER PRESS.		FUEL		MANIFOLD PRESSURE		MAX. ACC.		REMARKS
			PEAK PSIA	STEADY STATE PSIA	PEAK PSIA	STEADY STATE PSIA	PEAK PSIA	STEADY STATE PSIA	FLY. GND. GPP	READING	
Ac/o	10/28/68	-	175	127	NA	220	NA	165	Sat.	532	Flight accelerometers saturated
A1	10/29/68	1500	170	130	189	163	287	166	Sat.	129	Smooth restart
A2	10/30/68	300	165	136	230	197	880	186	17	36	
			150	130	110	181	505	170	21	62	
A3	10/30/68	90	146	129	150	161	850	160	31	10	Smooth restart
			156	129	NA	145	NA	140	20	0	Smooth restart
A4	10/31/68	30	174	118	NA	167	NA	140	Sat.	126	
			180	107	NA	174	NA	166	Sat.	161	Roughest ascent
			268	123	NA	159	NA	151	Sat.	>1000	restart on Phase I

PHASE II

A01	1/15/69	-	131.3	126.46	239	154	235	150	41.8	309	Test not acceptable
A02	1/20/69	-	153.9	125	280	175	252	171	29.4	17.5	Checkout acceptable
A5	1/24/69	200	170	124.7	240	189	253	177	44	54	On 3rd firing FM tape recorder failed, data required were lost
			165	122	230	189	232	172	38.5	54	
			NA	123	NA	NA	NA	NA	NA	NA	Rough restarts
A6	1/28/69	90	179	124.7	318	172	275	170	37.2	40.8	
			429.6	126	279	172	250	171	Sat.	Sat.	
A7	1/30/69	60	838	130	NA	160	NA	168	Sat.	Sat.	Engine failed to fire
			172	127.9	290.8	160	260	165	31.5	70.7	3rd start, oxidizer apparently frozen
			473	122	383	160	240	175	Sat.	Sat.	
			0	0	346	153	0	0	37.1	0	
A8	2/3/69	30	182	126	331	174	272	162	37.1	0	
			1090	108	390	174	435	161	Sat.	2558	Rough restart
A9	2/6/69	15	178.9	100	316	186.5	324	182.7	34	20.8	
			243	94.7	1138	191	284	187.8	Sat.	700	Rough restart

TABLE 4-3
ASCENT ENGINE TEST RESULTS SUMMARY

PHASE II (CONTINUED)

TEST NO.	DATE	COAST PER. SEC.	CHAMBER PRESS.			FUEL			MANIFOLD PRESSURE			OXIDIZER			MAX. ACC.			REMARKS
			PEAK PSIA	STEADY STATE PSIA	STEADY STATE PSIA	PEAK PSIA	STEADY STATE PSIA	STEADY STATE PSIA	PEAK PSIA	STEADY STATE PSIA	PEAK PSIA	STEADY STATE PSIA	PEAK PSIA	STEADY STATE PSIA	MAX. ACC. READING FLT. GPP	ACC. READING GND. GPP	ACC. READING GPP	
A10	2/6/69	10	173.5	122.4	122.4	316	188	188	282	188	282	188	188	188	28	90	90	Reasonably smooth restart
A11	2/7/69	2.5	173.5	117.3	117.3	425	193	193	288	188	288	188	188	188	75	50	50	Smooth restart
A12	2/8/69	1.0	170	123.1	123.1	318	187	187	270	187	270	187	187	187	20	62	62	Smooth restart
			225	112.8	112.8	433	199	199	350	187	350	187	187	187	23	0	0	Smooth restart
			179	134.3	134.3	336	211	211	283	191	283	191	191	191	38.5	0	0	Smooth restart
			174	124.4	124.4	442	201	201	462	170	462	170	170	170	86	82	82	

TABLE 4-3
ASCENT ENGINE TEST RESULTS SUMMARY (CONTINUED)

D2-118246-1

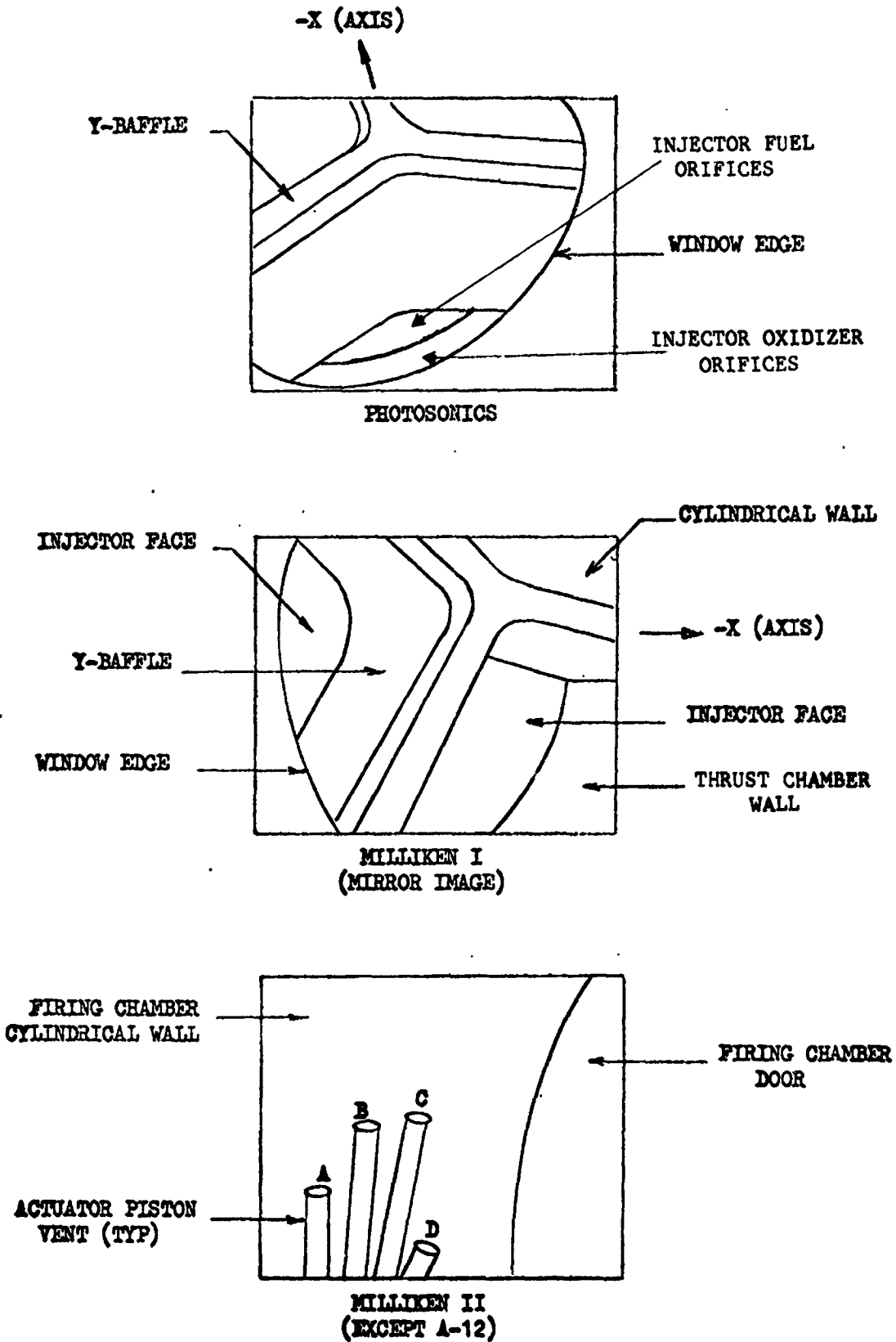


FIGURE 4-1 SEATTLE APS CAMERA VIEWS

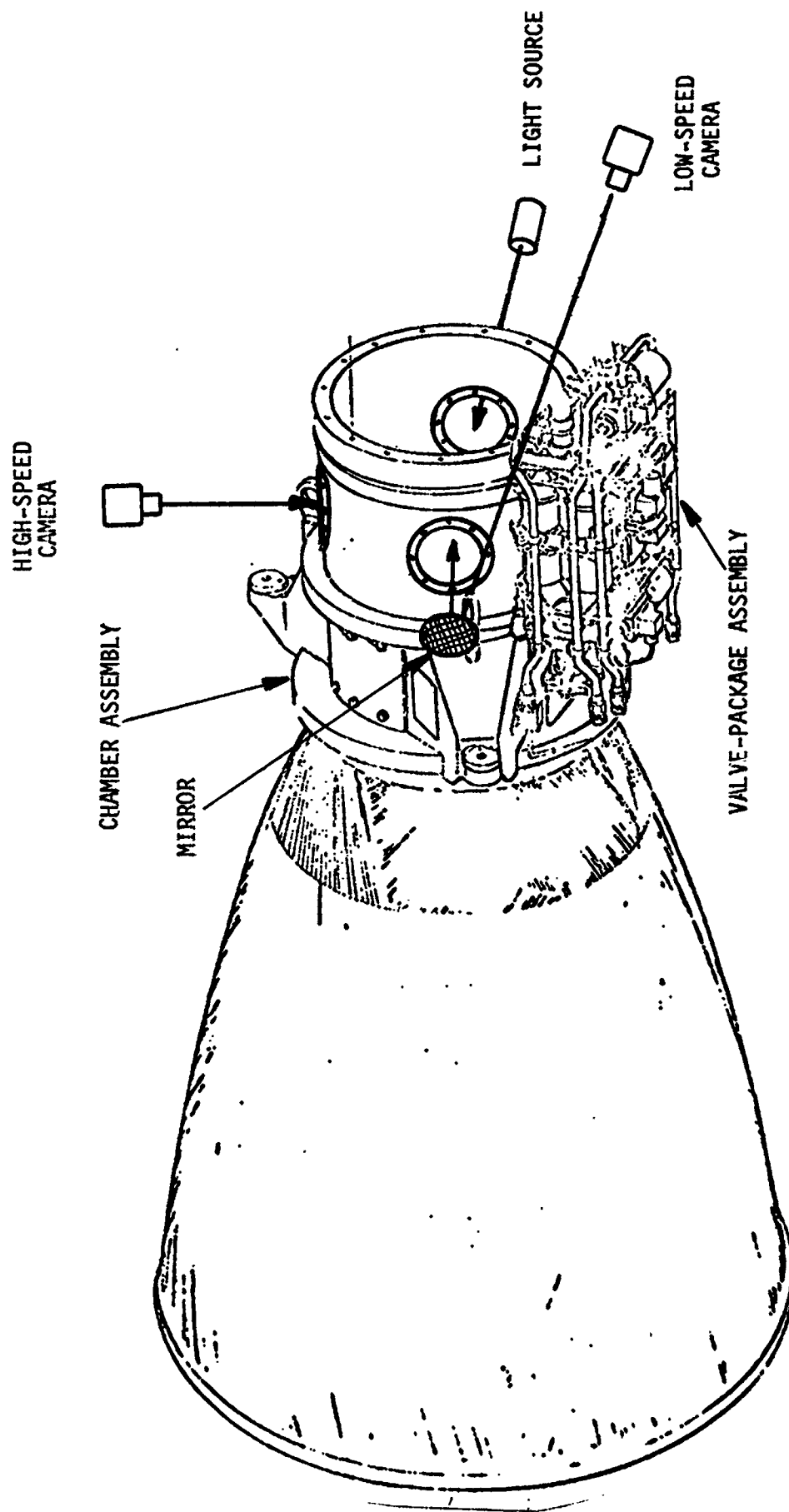


FIGURE 4-2 LM ASCENT ENGINE CHAMBER WINDOWS AND CAMERAS

4.2.2 Photographic Results (Continued)

approximately 0.3 seconds after shutdown, large amounts of foam were observed on the injector face and baffle. The foam appeared to have a consistency which was slightly less viscous than shaving foam. This liquid was undoubtedly oxidizer, because at the existing chamber pressure (10-15psia), fuel would not have been boiling. Boiling and violent agitation of the foam continued for about 2 to 3 seconds after shutdown. At this time, the injector face was essentially clear of all foam. Small amounts of boiling liquid appeared about 8 seconds after shutdown, and persisted for approximately 1 second. During this time period, fuel duct pressure and temperature data indicated that the fuel was beginning to boil.

The Milliken I camera showed that frozen white deposits were formed on the side thrust chamber window about 3.5 seconds after shutdown. These deposits sublimed rapidly. About 8 seconds after shutdown, partly frozen liquid was deposited on the side window, completely obscuring the view of the injector. The liquid froze rapidly and then melted or sublimed. The frozen material had essentially disappeared within 15 seconds after shutdown, although a few small frozen particles remained on the window for up to 50 seconds after shutdown. Frozen fuel and oxidizer were occasionally extruded from the injector orifices for up to 50 seconds after shutdown. However, there was no evidence of the large frozen propellant deposits that were observed during cold-flow testing at ARC.

The second restart of test A-7 did not burn normally. The Photosonic camera showed fuel issuing from the fuel ports in the injector following the opening of the valves, but oxidizer did not appear. After a few frames, the injector was obscured by floodlight reflection from the fuel droplets. Exhaust gas temperatures following the third firing rose to 540°F compared with 1270°F and 1000°F for the first and second firings, indicating that partial combustion occurred. Film from the Milliken I camera showed a reddish gas in the combustion chamber following shutdown of the third firing. This gas, apparently nitrogen tetroxide, was not visible on the black and white film from the Photosonic camera. The appearance of the gas on the color film of the Milliken I camera was evidence of partial oxidizer flow during this firing. Additional data, presented in Section 7.3, confirm that significant oxidizer side blockage occurred during the second restart. The blockage is believed to occur in the injector inlet filter.

The film from the Milliken I camera on test A-8 showed an unusual accumulation of solid material in the combustion chamber following the test. This material apparently was cooling water from the Photocon transducer which ruptured during the A-8 test.

The Milliken I camera for test A-7 (also test A-6) was focused on the window surface instead of the injector head of the ascent engine. This focusing was done deliberately, at GAC's request, to obtain a

4.2.2 Photographic Results (Continued)

better view of deposits which were observed on the windows after engine shutdown.

The film from the Milliken II camera, used to observe the propellant valve actuator vent line exits, showed that the vent lines were capped with frozen fuel at the beginning of the test. These plugs were blown clear when the valves were vented. Thereafter, the plugs reformed. Venting of the valve actuators for shutdown of the second pulse produced a snowflake like deposit on the test chamber wall. During test A-12, the Milliken II camera was used to observe the throat area of the ascent engine. The objective was to obtain photographs of a propellant puddle, if one formed, in the combustion chamber. With the engine orientation used in the tests, the low point of the combustion chamber was just forward of the throat. Film from the Milliken II camera showed the throat plainly while the camera was being checked prior to test. During test A-12, the film showed only an overexposure. It was verified that the camera was not moved following checkout, but no reason for the overexposure could be established.

4.2.3 Detonable Compound Residuals

No significant amount of residue was found in the ascent engine after any of the test firings. As a result, no samples were taken for analysis. The absence of nitrated residues is confirmed by the movie coverage of the thrust chamber interior. These movies show that the viscous brown deposits observed after LMDE firings were not present after ascent engine firings.

SECTION 5 - TRW DESCENT ENGINE TESTS AT SEATTLE




5.0 GENERAL


The LM descent engine hot-firing restart test program was conducted at the Boeing Tulalip Test Facility near Seattle, Washington during the period from October, 1968 to February, 1969. The tests were planned and supervised by GAC, in accordance with GAC Contract Number NAS9-1100, Contract Item CCA 1041 titled, "Test Requirements for LM Ascent and Descent Engine Restart Capabilities Test Program".


The test program was divided into Phase I and Phase II. Phase I tests were run with nominal initial propellant and hardware temperatures of 65°F, with an uncontrolled propellant helium saturation level and no photographic coverage of injector phenomena during coast or firing periods. Phase II tests were run with nominal initial propellant and hardware temperatures of 50°F, with helium saturated propellants and photographic coverage of the interior of the engine thrust chamber during firing and coast periods. Propellant samples were obtained prior to all Phase I and Phase II tests to determine the dissolved gas content (He, N₂, etc.) of the propellants.


A summary of the descent engine test conditions and the as-run test matrix are shown in Table 5-1.

Detailed information on the Seattle DPS test facility, engine configuration, instrumentation, and test series conduct is presented in Appendix C.

TEST NO.	FIRE TIME SEC.	NO. OF STARTS	COAST PER. SEC.	START ALTITUDE INITIAL 10 ³ FT.	RESTART 10 ³ FT.	INITIAL TEMP. PROP. °F	INITIAL TEMP. HDW. °F	PROP. FUEL %	HELIUM SAT. OXID. %	REMARKS
PHASE I  										
Dc/o	3	1	-	205	-	61	65	48	46	Dry Start
D1	3.5	2	1819	197	197	62	65	43	9	Dry Start
D2	3	2	316	220	220	65	65	64	42	Dry Start
D3	3	2	120	210	212	62	65	33	17	Dry Start
D4	3	2	43.5	220	225	66	65	22	42	Dry Start
PHASE II 										
D011	3.5	1	-	213	-	37	41	78	84	Dry Start
D5	3.5	3	120	265	240	41	44	90	91	Dry Start
D6	3.5	3	90	220	233	48	48	100	94	Dry Start
D7	3.5	3	50	214	238	46	51	100	98	Wet Start
D8	3	3	15	250	227	50	54	92	100	Wet Start
D9	3	3	5	224	195	41	44	92	81	Wet Start
D10	3	3	2	249	132	44	48	85	90	Wet Start
D11	3,2,2	3	375	227	116	46	48	87	95	Wet Start
D12	3,2,2	3	170	222	232	49	48	83	92	Wet Start
				230	239					
				232						

 No attempt was made to saturate the propellants with helium during Phase I tests.

 No cryopanelts were used during Phase I tests.

 Propellant helium saturation procedure was performed prior to each test.

 Helium saturation questionable - fuel tank depressurized to 10 psig for 1 minute.

TABLE 5-1

DESCENT ENGINE TEST CONDITIONS

5.1 TEST OBJECTIVES AND REQUIREMENTS

5.1.1 Test Objectives

The objective of the LM Descent Engine Restart Capabilities Test Program was to determine the constraints for descent engine restarts which may follow short duration (3.5 second) firings. The hazards associated with this type of operation result primarily from the evaporative freezing of the propellants in the injector and ducts following shutdown, and the effect of the frozen propellants on a subsequent restart attempt.

An additional area to be investigated was the deposition of detonable compounds on the cold injector face or combustion chamber walls. These compounds are formed by incomplete combustion of the propellants and may be deposited on the combustion chamber surfaces. It is probable that combustion chamber overpressures will result if sufficient amounts of these compounds were present and were ignited during an engine restart.

5.1.2 Test Requirements

The test requirements for both the LMAE and the LMDE Restart Capabilities Test Programs are listed in Section 4.1.2.

5.1.3 Test Planning

The test planning for both the Ascent and Descent test programs was a single effort. Thus, Section 4.1.3 also describes the test planning for the LMDE tests. Table 5-2 is the planned test matrix for the LMDE tests. Table 5-1 is the as-run test matrix, which evolved from the one planned due to the circumstances enumerated in Section 4.1.3.

D2-118246-1

TABLE 5-2
PLANNED TEST MATRIX FOR SEATTLE LMDE TESTS

PHASE I

TEST SERIES	ENGINE	NO. OF STARTS	ENGINE FIRING TIME-SEC.	INITIAL PROPELL. & HARDWARE TEMP. °F	PROPELLANT SATURATION LEVEL - %	COAST TIME - SEC.
D-1	Descent	2	2	65	0	120
D-2	↓	↓	↓	↓	↓	60
D-3	↓	↓	↓	↓	↓	30
D-4	↓	↓	↓	↓	↓	10
D-5	↓	↓	↓	40	↓	300
D-6	↓	↓	↓	↓	↓	120
D-7	↓	↓	↓	↓	↓	60
D-8	↓	↓	↓	↓	↓	30
D-9	↓	↓	↓	↓	↓	10

PHASE II

D-10	Descent	5	5	65	100	120
D-11	↓	↓	↓	↓	↓	60
D-12	↓	↓	↓	↓	↓	30
D-13	↓	↓	↓	↓	↓	TBD
D-14	↓	↓	2	↓	↓	120
D-15	↓	↓	↓	↓	↓	60
D-16	↓	↓	↓	↓	↓	30
D-17	↓	↓	↓	↓	↓	TBD
D-18	↓	↓	↓	↓	↓	300
D-19	↓	↓	5	40	↓	120
D-20	↓	↓	↓	↓	↓	60
D-21	↓	↓	↓	↓	↓	30
D-22	↓	↓	↓	↓	↓	TBD
D-23	↓	↓	↓	↓	↓	300
D-24	↓	↓	2	↓	↓	120
D-25	↓	↓	↓	↓	↓	60
D-26	↓	↓	↓	↓	↓	30
D-27	↓	↓	↓	↓	↓	TBD

5.2 TEST RESULTS

5.2.1 Significant Results

The Seattle Phase I and Phase II tests resulted in one restart which had a peak chamber pressure higher than the range of initial starts. Temperatures significantly below the fuel and oxidizer freezing temperatures were observed on the propellant ducts between the engine valves and the injector. Frozen propellant residuals did not appear to affect restart characteristics. The test results are summarized in Table 5-3, and a detailed analysis of the test data is in Section 7.4.

5.2.2 Photographic Results

Three cameras were used for observation of the Descent engine during Phase II tests. A 1000 frames per second Photosonic camera and a 24 frames per second Milliken camera photographed the injector through quartz glass windows in the combustion chamber wall. An additional Milliken camera (24 frames per second) was directed at the shut-off valve vent line exits. Figure 5-1 shows sketches of the projected images from the cameras, and Figure 5-2 shows the location of the combustion chamber ports, cameras, and light source. This configuration was maintained constant throughout the Descent Engine test series. Color film was used to photograph the injector, and black and white film was used to photograph the vent line exits. A "fire switch" event light and an IRIG "B" timing light were used in the Photosonics camera. There were no marker lights used in the Milliken cameras. All motion pictures were successfully obtained on the Descent Engine test series, with the exception that the Milliken II camera film was broken on the checkout test D-0-1, and the engine floodlight fuse was blown on test D-10.

Engine restarts at coast times of 15 to 375 seconds appear to be very similar to initial starts. At shorter coast times, up to 15 seconds, the restarts are obscured by the shutdown transient from the preceding start. The films from the Photosonic camera showed that the initial starts and observable restarts had oxidizer leads. Following development of the oxidizer spray, a dull red color was observed in the chamber. This could have been caused by low level combustion with fuel vapor, or could have been caused by red-colored N_2O_4 vapor. The films then darkened as the density of the propellant spray increased and obscured the light source. Ignition was indicated by a bright red flash of light in the chamber. The red flame gradually turned white and increased in brilliance as steady state conditions were reached.

Following shutdown, the Photosonic films showed a gradual decrease in the brilliance of the combustion, accompanied by the flow of large droplets of oxidizer toward the chamber window. The chamber cleared briefly, showing that the pintle end was covered with oxidizer foam. The injector pintle was then obscured by further combustion. This

PHASE I

TEST NO.	DATE	COAST PER. SEC.	CHAMBER PRESS.				FUEL		OXIDIZER		MAX. ACC. READING		REMARKS
			PEAK PSIA	STEADY STATE PSIA	PEAK PSIA	STEADY STATE PSIA	PEAK PSIA	STEADY STATE PSIA	FLT. GPP	GND. GPP			
Dc/o D1	10/19/68	-	25	10	10	78.5	78.5	37	140	Checkout satisfactory Reasonably smooth restart Roughest restart of any descent firing (Phase I and Phase II) Reasonably smooth restart Smooth restart			
	10/21/68	1819	12.5	14	21	89	89	7	52				
D2	10/22/68	316	38.5	14	27	90	90	70	400				
			20	12.4	20	73	73	49	292				
			75	13	21	85	85	140	640				
D3	10/23/68	120	6	13	20	81	81	7	69				
D4	10/24/68	43.5	31	13.2	19	86	86	130	262				
			17	13.2	21	88	88	0	23				
			0	13	20	90	90	0	0				

5-6

PHASE II

D011	2/12/69	120	33.1	14.5	19.2	19.2	81.6	81.6	70	386	Checkout satisfactory Smooth restarts		
D5	2/13/69		30	12.3	19.1	19.1	83.1	83.1	29	175			
D6	2/15/69	90	13.1	14.4	21.2	21.2	87.1	87.1	23.8	107			
			8.2	13.4	21.2	21.2	88.1	88.1	9.8	37.4			
D7	2/17/69	50	16	11.7	18.7	18.7	84.3	84.3	20.6	100.5	Smooth restarts		
			20.8	11.7	18.7	18.7	82.2	82.2	54.9	174.6			
D8	2/18/69	15	18.2	11.7	17.7	17.7	84.3	84.3	44.5	100.5	Smooth restarts		
			8.5	10.7	17.3	17.3	82.9	82.9	11.2	40.4			
D9	2/19/69	5	18.1	13.8	18.4	18.4	81.7	81.7	80	212			
			7.5	10.7	17.3	17.3	83.8	83.8	15	50.5			
			8.6	11.3	17.2	17.2	83.8	83.8	11.2	50.8	Reasonably smooth restarts		
			5.7	11.3	17.2	17.2	78.6	78.6	8.2	15.2			
			26.9	11.3	19.2	19.2	78.6	78.6	207	630			
			55	12	20.1	20.1	79.9	79.9	256	592			
			0	12	18.0	18.0	74.7	74.7	0	0	No readable pressure overshoot or accelerometer readings for last two firings		
			0	12.3	19.1	19.1	72	72	0	0			

TABLE 5-3
DESCENT ENGINE TEST RESULTS SUMMARY

PHASE II (CONTINUED)

TEST NO.	DATE	COAST PER. SEC.	CHAMBER PRESS.						MANIFOLD PRESSURE						REMARKS		
			PEAK PSIA			STEADY STATE PSIA			FUEL			OXIDIZER				MAX. ACC. READING	
			PEAK PSIA	STEADY STATE PSIA	STEADY STATE PSIA	PEAK PSIA	STEADY STATE PSIA	STEADY STATE PSIA	FLT. GPP	GND. GPP							
D10	2/19/69	2	24.9 0 0	11.3 11.6 12	20.5 16.4 17.4	85 73.3 74.4	85 73.3 74.4	20.5 16.4 17.4	85 73.3 74.4	154 0 0	283 0 0	Very smooth restarts Voltage drop on 2nd restart makes data questionable Smooth restarts					
D11	2/20/69	375	52 8.7 38.5	15.5 8.45 7.4	18.6 14 8.4	84.5 68.6 119.3	84.5 68.6 119.3	18.6 14 8.4	84.5 68.6 119.3	NA 28 NA	532 68.6 568						
D12	2/21/69	170	24 12.4 14.6	11.5 10.5 9.6	19.5 15.4 18.5	81.3 70.7 79.2	81.3 70.7 79.2	19.5 15.4 18.5	81.3 70.7 79.2	137 37 42	321 75 100						

TABLE 5-3
DESCENT ENGINE TEST RESULTS SUMMARY (CONTINUED)

D2-178246-1

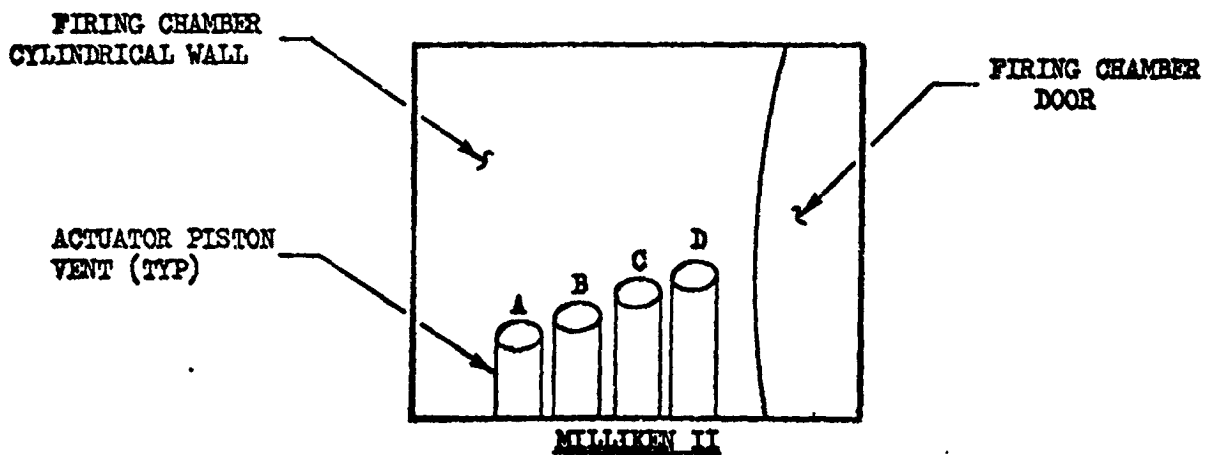
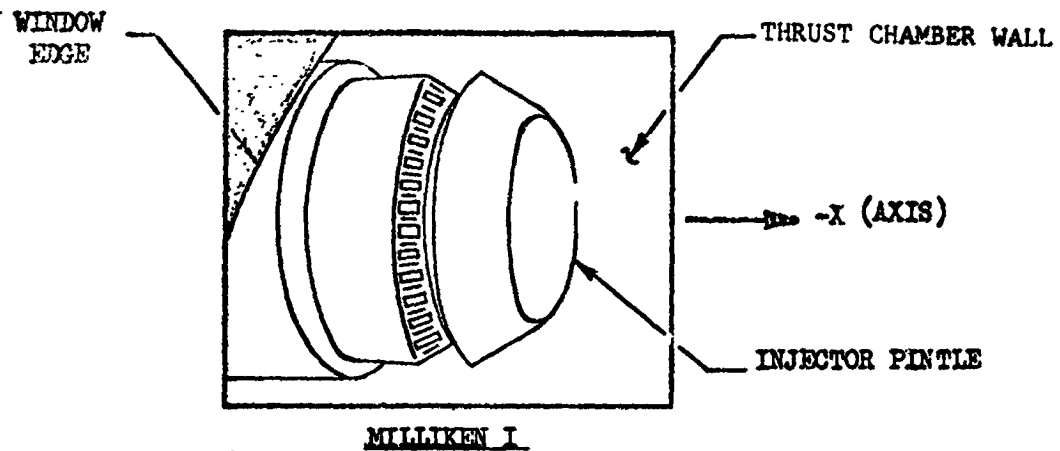
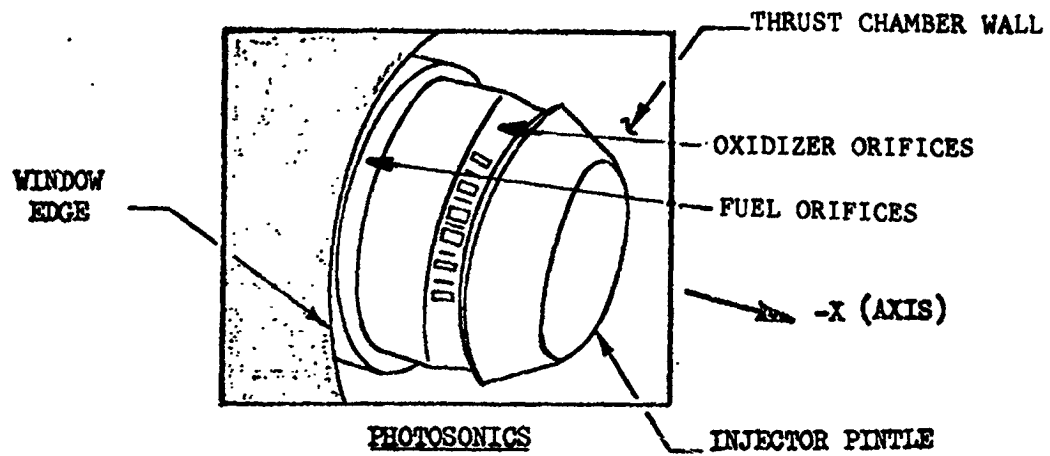


FIGURE 5-1 SEATTLE DPS CAMERA VIEWS

D2-118246-1

TOP VIEW OF DESCENT ENGINE INSTALLATION FOR SEATTLE TESTS

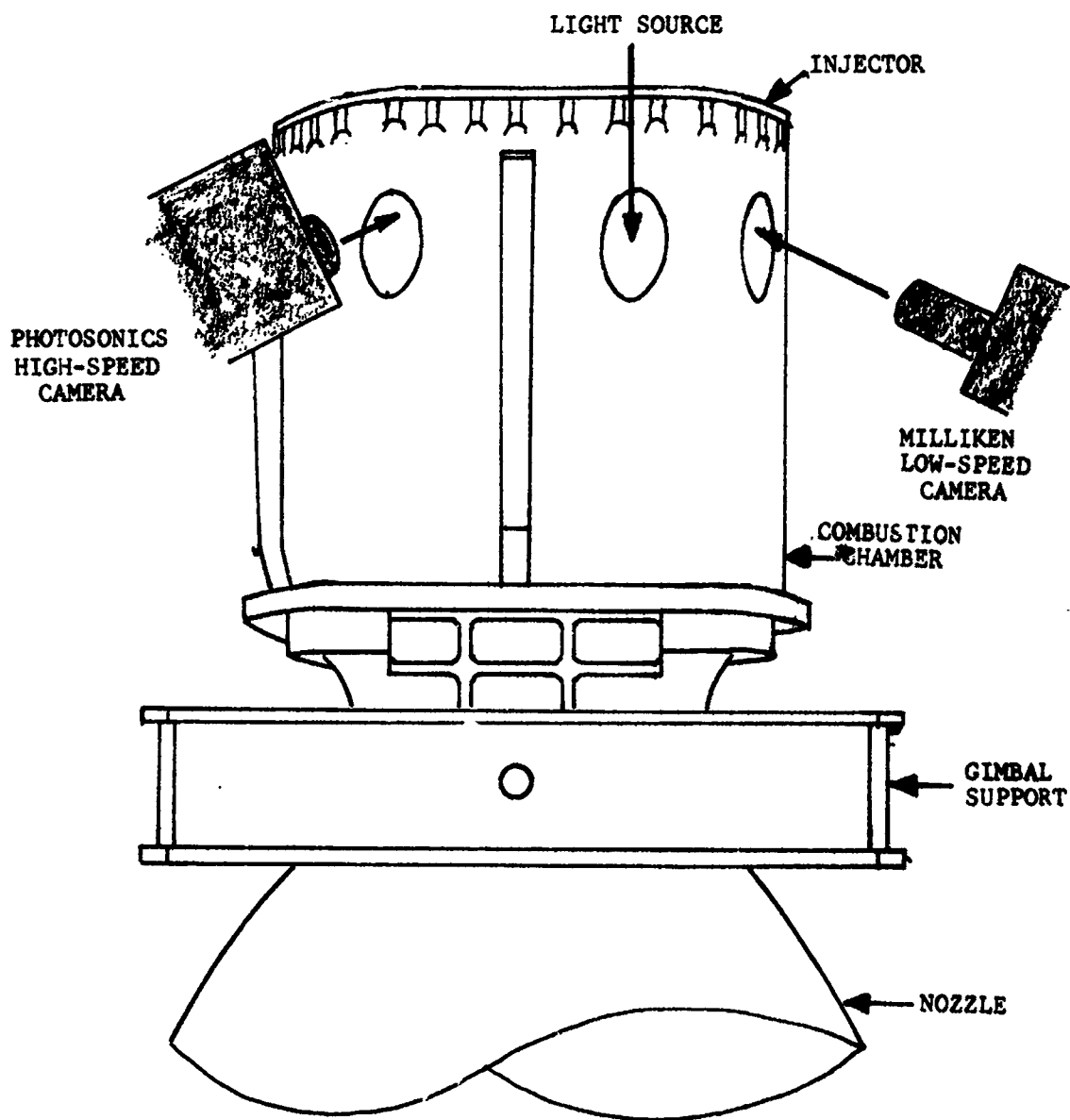


FIGURE 5-2 LM DESCENT ENGINE THRUST CHAMBER WINDOWS AND CAMERAS

5.2.2 Photographic Results. (Continued)

combustion process had a red color, oscillated at a frequency of approximately 50 Hz, and persisted for approximately 1 second of real time.

The pulsations in light intensity were accompanied by pressure pulsations. The presence of pressure pulsations was confirmed by pulsations in the size of foam-like propellant globules that could be seen clinging to the injector. Proof that the light pulsations originate from incandescent processes in the combustion chamber and not from the floodlight was obtained from films of test D-10. The fuse on the engine floodlight was blown on test D-10, with the result that combustion provided the only observable light source for the films. When the engine ignited, incandescence from the combustion process was visible. After shutdown, the light pulsations were visible, proving that the light pulsations were not caused by the floodlight.

The chamber window for the Milliken I camera was partially obscured by brown-colored liquid deposits which were formed during the shutdown phase. It is believed that these deposits were nitrate compounds, formed by incomplete reaction between the fuel and oxidizer. The brown liquid was viscous, and was observed to boil slowly at a time when fuel and oxidizer were observed to freeze on the injector pintle and on the combustion chamber walls. The brown deposits were present for more than 3 minutes after shutdown, and were observed to slowly boil away without freezing. There was no observable increase in the amount of deposits following successive firings.

Frozen fuel and oxidizer deposits were formed at the fuel and oxidizer orifices within five seconds after shutdown. The frozen deposits were formed over the lower third of the injector, and appeared to have low mechanical strength. The deposits reached a maximum length of approximately 1/2 to 1 inch before being ejected from the injector orifices. The oxidizer orifices appeared to be clear at approximately 15 seconds after shutdown, and the fuel orifices appeared to be clear at approximately 1 minute after shutdown.

5.2.3 Detonable Compound Deposits

Samples of the brown-colored deposits observed on movie films were obtained after several runs. Sample analyses were obtained for runs D-1, D-2, D-3, D-4, D-5, D-7, D-8 (two locations), and D-10. All samples contained nitrated fuel and absorbed water. The nitrate concentration ranged from 20% to 67%. The remaining content varied somewhat between samples, but included hydrated nitrates, hydrocarbons, ammonium nitrate, and minor amounts of metal nitrates.

The presence of nitrated fuel in these samples was significant. Nitrated fuel (such as $N_2H_5NO_3$) and ammonium nitrate are expected products from

D2-118246-1

5.2.3 Detonable Compound Deposits (Continued)

non-hypergolic reaction of the propellants. The nitrated fuel in crystalline form as found on the pintle tip, post run D-8, was a unique observation. Heretofore, it had been produced during engine testing only in liquidous residues.

SECTION 6 - SPS ENGINE AND INJECTOR TESTS AT AEDC

6.0 GENERAL

The engine restart tests at Arnold Engineering Development Center (AEDC) were conducted to investigate the restart performance of the SPS engine and establish flight restart constraints. Tests were conducted in the J-2A horizontal test cell under simulated space conditions. Testing was begun in May, 1968 and completed in September, 1968.

The AEDC "A" test series was divided into seven "air periods" - AA through AG. In the course of these tests, there were 68 engine starts made, for a total burn time of 25.2 seconds. Tests were conducted under nominal conditions, except for propellant and hardware temperatures, which were varied from 35 ± 5 to $65 \pm 5^\circ\text{F}$.

The SPS injector cold flow tests at AEDC were conducted to investigate propellant venting characteristics, evaporative freezing effects, and the sublimation rate of frozen propellant remaining in the injector manifold, when exposed to vacuum.

The cold flow testing consisted of three phases: phase I - oxidizer, phase II - fuel, and phase III - fuel and simulated oxidizer. Propellant temperatures were conditioned between 20°F to 80°F prior to the start of a test.

Detailed information covering the AEDC test facility, engine configuration, instrumentation, and test series conduct is presented in Appendix D for both the restart and cold flow test series.

6.1 TEST OBJECTIVES AND REQUIREMENTS (ENGINE RESTART)

6.1.1 Test Objectives

The AEDC SPS engine restart tests were conducted to verify the SPS restart capability at simulated space conditions and nominal and cold (35°F) system and propellant temperatures. In addition, the tests were to: establish any flight constraints required to avoid undesirable or detrimental restart conditions; establish flight instrumentation which would verify that a safe condition exists for engine restarts; identify modifications which would provide for unlimited restart capability; obtain adequate data to define any potential problem such that the results and conclusions can be applied to both the LMAE and LMDE restart capabilities.

6.1.2 Test Requirements

This test plan included the following test requirements:

1. The simulated altitude pressure must be equal to or greater than 180,000 feet.
2. The engine hardware and propellants to be conditioned at $35 \pm 5^\circ\text{F}$.
3. Engine propellant inlet pressure shall be set for a nominal mixture ratio (O/F) of 2.00.
4. The propellants used shall meet the following specifications:

Fuel	MIL-P-27402
Oxidizer	MSC-PPD-2A
5. After each test period, provided test chamber conditions permit, the test hardware shall be inspected through the view ports for any residues, salts, or other foreign or unknown deposits. Samples shall be taken of deposits and chemically analyzed.
6. During the checkout firings, the propellant feed system dynamics shall be evaluated to determine if modifications are necessary to more closely represent flight conditions.
7. All firings will be conducted with the bipropellant valve in the "dual-bore" (AB) mode.

6.1.3 Test Planning

The test plan for the SPS engine restart investigation called for engine restarts at simulated space conditions to establish any flight constraints required to avoid undesirable or detrimental restart conditions. A full-scale, flight-type injector-chamber (area ratio 6:1)-propellant valve was to be tested at simulated altitude conditions to determine the restart characteristics. The hardware and propellants were to be conditioned to the temperatures estimated for the lunar voyage (40-60°F). The firing durations were to be such as to produce the most adverse condition (propellant freezing) for restarts. The coast periods (time between restart and initial firing) was to be reduced in time until an adverse condition is achieved or the test cell capabilities are exceeded. A second restart was to be conducted at each condition with a firing time of sufficient duration to assure that the engine is operating properly as indicated by chamber pressure. Since the test condition achieved during the restart investigation may not be as severe as those experienced in space, tests were also planned to be conducted with propellants which were artificially inbled into the injector prior to ignition. The propellant inbleed rate was to be sufficient to induce propellant freezing.

The SPS engine restart test plan included two phases: phase I - checkout phase and phase II - restart investigation. The primary objective of the checkout phase was to:

1. Determine test cell capability
2. Verify instrumentation and data systems
3. Verify inlet propellant pressure and losses due to line lengths
4. Determine the minimum firing duration required to fill the injector cavities with propellant without inducing a temperature rise in the injector face or ablative chamber walls. This will be called T_1 . (The initial firing will not be used for timing because the volume between the series redundant balls of the propellant valve are not filled with propellant.)
5. Determine the minimum firing duration to obtain the nominal engine rated thrust level (based on chamber pressure) for 0.05 to 0.1 second duration. This will be defined as T_2 .
6. The time between firings will not be critical. Initial data review will be from control room parameters.

6.1.3 Test Planning (Continued)

The test cell, hardware, and propellants were to be at ambient (70°F) temperature conditions. Five to ten firings were to be conducted to determine T_1 and T_2 .

The planned SPS engine restart investigation tests are as follows:

<u>TEST SERIES</u>	<u>NO. OF STARTS</u>	<u>ENGINE * FIRING TIME-SEC.</u>	<u>INITIAL PROP. & HDWR. TEMP.</u>	<u>COAST TIME SEC.</u>
I	3	0.37	35 \pm 5°F	1800
II	3	0.37	35 \pm 5°F	600
III	3	0.37	35 \pm 5°F	180
IV	3	0.37	35 \pm 5°F	60
V	3	0.37	35 \pm 5°F	20
VI	3	0.37	35 \pm 5°F	8
VII	3	0.37	35 \pm 5°F	FACILITY MINIMUM

*The last firing in each series will be of a duration to obtain the nominal engine rated thrust level (based on chamber pressure).

6.2 TEST RESULTS (ENGINE RESTART)

6.2.1 Significant Results

Significant results of the AEDC SPS engine testing include meeting test objectives in Section 6.1, the occurrence of freezing temperatures in the injector manifolds, and the occurrences of hard starts. The results of the SPS engine tests are summarized in Tables 6-1 and 6-2. Test series AA and AB are not included in the summary because they were facility checkout firings and data were not evaluated. A more detailed treatment of the AEDC test results is presented in Section 7.7.

6.2.2 Photographic Results

The photographic coverage of the SPS restart tests was limited because of the technique used, i.e., fiber optics. The photography did show frozen propellant on the injector face, hub, and baffles immediately after every shutdown, and prior to ignition for the propellant inbleed tests. It was not possible to determine any correlation between frozen propellant as photographed and the characteristics of a restart. Photographic coverage was discontinued after the quartz window was found damaged during the AE test series.

TEST NO.	DATE	FIRE TIME SEC.	COAST PER. MIN.**	ALT. (X1000) FT.		INITIAL TEMP.		REMARKS
				INITIAL	RESTART	PROP. °F	HDW. °F	
AC-01	6/24/68	0.37	22	295	251	55	35	Problems with propellant temperature conditioning
AC-02A			22	297	230			
AC-02B			26	297	223			
AC-02C			646	299	257			
AC-03	6/25/68		-	295	80	44		Canister door malfunctioned
AD-01	7/10/68		158	80	238	35		
AD-02			1242	298	80	36		Canister door malfunctioned
AD-03	7/11/68		167	307	80	38		Oxidizer inbleed test
AD-04			175	266	80	41		
AD-05			-	288	80	42		Oxidizer inbleed test
AE-01	8/14/68		236	80	240	35+5	35+5	
AE-02A			15	295	226			
AE-02B			15	295	216			
AE-02C			42	258	214			
AE-03			462	295	80			
AE-04A	8/15/68		10	295	222			
AE-04B			10	286	217			
AE-04C			200	286	217			
AE-05A			3	295	221			
AE-05B			3	250	218			
AE-05C			95	245	195			
AE-06A			1	295	201			
AE-06B			1	218	189			
AE-06C			49	207	175			
AE-07A			20 sec.	295	193			
AE-07B			20 sec.	209	170			
AE-07C			-	191	152			Terminated photographic coverage
AG-01	9/24/68	0.47	70	30	80			Added low response Pc gage (Taber)
AG-02A		0.37	3	295	242			

** Coast period occurred prior to the next listed engine firing

TABLE 6-1
SPS ENGINE TEST CONDITIONS

TEST NO.	DATE	FIRE TIME SEC.	COAST PER. MIN.**	ALT. (X1000) FT.		INITIAL TEMP.		REMARKS
				INITIAL	RESTART	PROP. °F	HDW. °F	
AG-02B	9/24/68	0.37	3	252	220	35+5	35+5	
AG-02C		0.46	301	252	216			
AG-03A	9/25/68	0.37	1	293	247			
AG-03B		0.38	1	255	226			
AG-03C		0.47	221	238	217			
AG-04A		0.37	7 sec.	278	243			
AG-04B		0.37	156	258	212			
AG-05		0.50	417	80	230			
AG-06A		0.38	7 sec.	320	261			
AG-06B		0.38	7 sec.	265	255			
AG-06C		0.50	175	235	230			
AG-07A		0.37	10	290	250			
AG-07B			60	260	248			
AG-08A	9/25/68		3	300	258			
AG-08B			3	270	238			
AG-08C	9/26/68	0.50	242	250	224			
AG-09A		0.50	1	326	248			
AG-09B		0.50	253	257	226	65+5	40+5	
AG-10A		0.37	1	310	246			
AG-10B		0.37	1	257	232			
AG-10C		0.50	141	245	222			
AG-11A		0.37	7 sec.	309	244			
AG-11B		0.50	120	250	228			
AG-12A		0.50	1	307	246			
AG-12B		0.50	226	255	226			
AG-13		0.52	340	310	246			Warm propellant temperature

** Coast period occurred prior to the next listed engine firing

TABLE 6-1
SPS ENGINE TEST CONDITIONS (CONTINUED)

TEST NO.	DATE	FIRE TIME SEC.	COAST PER. MIN. **	ALT. (X1000) FT.		INITIAL TEMP.		REMARKS
				INITIAL	RESTART	PROP. °F	HDM. °F	
AG-14A	9/26/68	0.37	30	296	255	35+5	35+5	Fuel inbleed test ↓
AG-14B		0.37	30	285	261	↓	↓	
AG-14C		0.50	191	264	250	↓	↓	
AG-15A		0.37	20 sec.	293	261	↓	↓	
AG-15B	9/27/68	0.50	177	268	238	↓	↓	
AG-16		0.50	121	312	175	↓	↓	
AG-17		0.50	81	310	199	↓	↓	
AG-18		0.50	-	336	246	↓	↓	

**Coast period occurred prior to the next listed engine firing

TABLE 6-1
SPS ENGINE TEST CONDITIONS (CONTINUED)

TEST NO.	DATE	COAST PER. MIN.**	CHAMBER PRESS.		MANIFOLD PRESSURE			MAX. ACC. READING	REMARKS
			PEAK PSIA	STEADY STATE PSIA	PEAK PSIA	STEADY STATE PSIA	OXIDIZER PEAK PSIA		
AC-01	6/24/68	22	420	NA	28*	NA	No data	2660	Initial start of "air period"
AC-02A		22	315		14*			1235	
AC-02B		26	420		14*			1030	
AC-02C		546	262		0*			1155	
AC-03	6/25/68	-	210		0*			1235	Canister door mal-functioned - "air period" terminated
AD-01	7/10/68	158	710		67*		59	3260	Initial start of "air period"
AD-02	7/10/68	1242	830		27*		Not oper.	1520	
AD-03	7/11/68	167	735		54*			2310	Oxidizer inbleed tests - rough starts
AD-04	7/11/68	175	1220		41*			2480	
AD-05		-	1330		54*			2000	
AE-01	8/14/68	236	1273		Not oper.		40	3460	Initial start of "air period"
AE-02A	8/14/68	15	342				No data	769	
AE-02B		15	390					2690	
AE-02C		42	995					3460	
AE-03		462	1424				141	6920	Hard start
AE-04A	8/15/68	10	1369				No data	5920	Hard start
AE-04B		10	1369				20	4620	Hard start

* Data Questionable

** Coast period occurred prior to the next listed engine firing

TABLE 6-2
SPS ENGINE TEST RESULTS SUMMARY

TEST NO.	DATE	COAST PER. MIN. **	CHAMBER PRESS.		FUEL		MANIFOLD PRESSURE		MAX. ACC. READING	REMARKS
			PEAK PSIA	STEADY STATE PSIA	PEAK PSIA	STEADY STATE PSIA	PEAK PSIA	STEADY STATE PSIA		
AE-04C	8/15/68	200	1360	NA	Not oper.	NA	14	NA	6160	Hard start
AE-05A	9/24/68	3	1424	85	164	NA	28	130	4230	Hard start
AE-05B		3	1275				28		4390	Hard start
AE-05C		95	1360				57		1620	Hard start
AE-06A		1	340				28		785	
AE-06B		1	1424				31		1745	
AE-06C		49	1310				28		1620	
AE-07A		20 sec.	383				No data		-	
AE-07B	9/24/68	20 sec.	1390	85	164	NA	28	130	1890	Initial start of "air period"
AE-07C		-	1860				37		1215	
AG-01		70	178				Not oper.		2590	
AG-02A	9/25/68	3	366	NA	117	NA	1740	NA	1740	Smooth start
AG-02B		3	158	NA	107				3380	
AG-02C		301	293	82	160				2900	
AG-03A		1	158	NA	117				1970	
AG-03B		1	146	NA	85				2820	
AG-03C		221	268	82	150				3150	
AG-04A		7 sec.	36	NA	96				1125	
AG-04B	9/25/68	156	80	NA	107	NA	No data	NA	1125	Smooth start
AG-05		417	158	82	No data				2900	
AG-06A		7 sec.	260	NA	154				3430	

** Coast period occurred prior to the next listed engine firing

TABLE 6-2
SPS ENGINE TEST RESULTS SUMMARY (CONTINUED)

TEST NO.	DATE	COAST PER. MIN. **	CHAMBER PRESS.		MANIFOLD PRESSURE				MAX. ACC. READING	REMARKS
			PEAK PSIA	STEADY STATE PSIA	PEAK PSIA	FUEL	STEADY STATE PSIA	OXIDIZER		
AG-06B	9/25/68	7 sec.	22	NA	99	NA	NA	Not oper.	0	Smooth start
AG-06C		175	0	84	148	126	NA		0	Smooth start
AG-07A		10	0	NA	139	NA			1320	
AG-07B		60	0	NA	95				1715	
AG-08A		3	61	NA	66				1143	
AG-08B		3	219	NA	78				3780	
AG-08C		242	1770	81	132	126			3430	Hard start
AG-09A	9/26/68	1	No data	83	159				0	No deflections from high response data
AG-09B		253	158	86	236	214			4000	
AG-10A		1	0	NA	97	NA			915	
AG-10B		1	22	NA	94				1143	Smooth start
AG-10C		141	122	80	160				4570	
AG-11A		7 sec.	35	NA	102				1370	
AG-11B		128	0	NA	154				0	Smooth start
AG-12A		1	122	83	168	100			1765	Smooth start
AG-12B		226	85	82	134	NA			0	
AG-13		340	85	83	168	NA			1765	Very low Pc
AG-14A		30		NA	89	0			1715	Very low Pc
AG-14B		30		NA	61	0			2940	
AG-14C		191	264	80	179	NA			1410	Very low Pc
AG-15A		20 sec.		NA	74	0			4570	
AG-15B		177	122	80	72	No data				
AG-16	9/27/68	121	329	69	186	137			3430	Fuel inbleed - hard start
AG-17		81	378	69	O.R.	99			8000	
AG-18		-	158	78	O.R.	184			4570	

** Coast period occurred prior to the next listed engine firing

TABLE 6-2
SPS ENGINE TEST RESULTS SUMMARY (CONTINUED)

6.3 TEST OBJECTIVES AND REQUIREMENTS (INJECTOR COLD FLOW)

6.3.1 Test Objectives

The SPS injector cold flow tests were conducted to establish baseline data for an engine restart. The basic test objectives of the injector cold flow tests were to:

1. Determine propellant venting characteristics under vacuum conditions.
2. Determine the relationship of venting characteristics and initial propellant and hardware temperatures.
3. Determine if propellant freezing occurs in the injector manifolding, and the mass of frozen propellant remaining.
4. Determine the sublimation rate of frozen propellant and time for all propellant to vent from the injector manifolding.
5. Determine if frozen residuals tend to obstruct propellant flow passages and orifices.

6.3.2 Test Requirements

The test plan included the following requirements:

1. The injector will be initially filled with the test fluid and be confined in the test chamber at the vapor pressure of the fluid concerned.
2. Tests will be conducted using N_2O_4 , Aerozine-50, and Freon MF.

6.3.3 Test Planning

The test plan for the SPS injector cold flow testing called for simulating the effects of engine short firings and shutdown in a vacuum. The short burn adds very little heat to the system and residual propellants remain in the injector manifolds after shutdown. These propellants can evaporatively freeze and remain in the injector manifold for long periods after shutdown. The cold flow tests will be conducted to define the magnitude of these effects and indicate any additional testing that would be required.

The SPS injector cold flow planned tests are as follows:

D2-118246-1

6.3.3 Test Planning (Continued)

TEST NO.	INITIAL TEMPERATURE (PROPELLANT & INJECTOR)	FUEL SIDE	OX SIDE
1	60°F	A-50	
2	60°F	A-50	
3	80°F	A-50	
4	80°F	A-50	
5	40°F	A-50	
6	40°F	A-50	
7	60°F		N ₂ O ₄
8	60°F		N ₂ O ₄
9	80°F		N ₂ O ₄
10	80°F		N ₂ O ₄
11	40°F		N ₂ O ₄
12	40°F		N ₂ O ₄
13	60°F	A-50	Simulated Oxid.
14	60°F	A-50	Simulated Oxid.
15	80°F	A-50	Simulated Oxid.
16	80°F	A-50	Simulated Oxid.
17	40°F	A-50	Simulated Oxid.
18	40°F	A-50	Simulated Oxid.

6.4 TEST RESULTS (INJECTOR COLD FLOW)

6.4.1 Significant Results

Significant results of the AEDC SPS injector cold flow tests include meeting test objectives in Section 6.3.1 (except determination of mass residuals), the occurrence of freezing temperatures in the injector manifolds and inlet ducts for all three test phases, and the accumulation of frozen propellants in the injector and inlet duct during the tests with cold (30°F) propellants. Test conditions are summarized in Table 6-3.

6.4.2 Visual and Photographic Results







Visual and photographic coverage indicated several modes of venting. Immediately after the 10 inch valve was opened, initial boiling forced a large percentage of the propellant through the orifices in liquid form. At warm temperatures (55 to 80°F) it is estimated that a majority of the initial propellant fill vented in this manner. This venting mode lasted less than 5 seconds and was characterized by a shower of porous ice crystals as evaporative freezing took place outside the injector. Most of this ice was blown clear of the injector face as it formed. In Phase II and Phase III runs, some of the liquid remained on the injector face and formed a dense ice sheet similar in appearance to water frozen at atmospheric conditions. After forming, the ice crystals, or sheets, remained up to several hours.

The venting process was observed internally through glass view ports located in the manifold and duct areas. As the antechamber was opened to vacuum conditions, violent boiling could be seen in both the manifold and the duct. The manifold view ports quickly cleared in the 65 to 80°F initial temperature runs. Various sizes of flakes formed at 55°F, and complete visual blockage of the port occurred with propellants around 30°F. Similar action could be seen in more detail in the duct view port.

As soon as the boiling had subsided enough for observation of the duct interior, the liquid level was near or below the bottom of the view port. The boiling continued, splashing liquid on the view port. In general, as the internal pressure in the injector dropped, this liquid would start abruptly to freeze on the window and later to sublime. This action was most apparent in the tests made with initial propellant temperatures below 55°F and occurred from 3 to 5 seconds into the oxidizer runs and from 30 to 50 seconds into the fuel and combined fuel and simulated oxidizer runs. Ice activity usually decreased shortly after this occurred.

D2-118246-1

TABLE 6-3
SPS INJECTOR COLD FLOW TEST CONDITIONS

PUN NO.	DATE	TEST FLUID	FLUID TEMPERATURE*
<u>OXIDIZER</u>			
I-2	12-15-67	N_2O_4  	75°F
I-3	12-20-67		75°F
I-4	12-20-67		80°F
I-5	12-20-67		55°F
I-6	12-20-67		45°F
I-7	12-20-67		40°F
I-8	12-20-67		25°F
I-9	12-20-67		20°F
I-10	12-21-67		70°F
I-11	12-21-67	N_2O_4	20°F
<u>FUEL</u>			
II-1	1-23-68	A-50	80°F
II-2**	-	-	-
II-3**	-	-	-
II-4**	-	-	-
II-5	1-26-68	A-50  	30°F
II-6	1-29-68		80°F
II-7	1-29-68		55°F
II-8	1-29-68		30°F
II-9	1-30-68		55°F
II-10	1-30-68	A-50	80°F
<u>FUEL & SIMU- LATED OXID.</u>			
III-1	1-31-68	A-50 & Freon MF  	80°F
III-2	1-31-68		55°F
III-3	2-1-68		80°F
III-4	2-1-68		55°F
III-5	2-1-68		30°F
III-6	2-1-68		30°F

* Value reflects desired results of pre-test temperature conditioning. Actual propellant temperature at start of test varied slightly.

** Data improperly recorded and could not be evaluated.

6.4.2 Visual and Photographic Results (Continued)

At temperatures near 30°F and colder, the boiling started and an ice slush began to form within a few seconds. The duct view port quickly became covered from the slush forming in place and also from large pieces falling from the duct above the port. The manifold view port also became obscured, indicating that the slush formed on surfaces throughout the injector.

SECTION 7 - ANALYSIS OF TEST DATA

7.0 GENERAL

Residual propellants remain in the Apollo spacecraft primary propulsion system engine injectors and ducts after shutdown. These residuals often lead to abnormal engine restarts because the normal oxidizer lead time is reduced and/or the residuals freeze and obstruct injector orifices or filters.

Experimental data were obtained on the volume of fuel residuals and on the temperatures of the fuel, oxidizer, and injector assemblies during cold flow testing. These data were used to select coast periods and initial temperatures which were expected to produce hard restarts during engine test firings.

The technical approach for the analysis of restart testing and cold flow testing consisted of four basic steps:

1. Determination of fluid properties which affect the propellant expulsion phenomena.
2. Analysis of cold flow and hot firing test data to determine the volume and thermodynamic state of the residual propellants present at engine restart.
3. Analysis of hot firing tests to determine the effect of residual propellants on engine restart characteristics.
4. Correlation of test results between engines and between cold flow and hot firing tests.

This section presents an analysis of data from ARC and AEDC cold flow tests, Boeing/Seattle hot firing tests and AEDC hot firing tests. The correlation of test results between the three engines and between cold flow and hot firing tests is presented in Section 8.

7.1 THERMODYNAMICS AND FLOW

This section provides the technical basis for the analysis of propellant behavior following engine shutdown in a vacuum environment. The quantity and thermodynamic state (solid, liquid, vapor) of the propellants which are present in an engine can have a significant effect on the engine restart characteristics. The following paragraphs present the propellant property data used to evaluate the thermodynamic state of the propellants, and describe the boiling, sublimation and gas solubility phenomena which affect the amount and state of the residual propellants.

7.1.1 Propellant Properties and Phase Diagrams

A summary of fuel (50% hydrazine + 50% unsymmetrical dimethyl hydrazine) and oxidizer (nitrogen tetroxide) properties is presented in Table 7-1. This table provides the basic characteristics of the propellants at specified values of temperature and/or pressure. However, the effect of temperature and/or pressure variations on the properties cannot be conveniently presented in brief tables. It is more convenient, when analyzing thermodynamic processes, to employ phase diagrams plotted as a function of pressure and temperature. This form of the phase diagram allows the thermodynamic state of the propellants to be determined from experimental measurements of pressure and temperature.

7.1.1.1 Oxidizer Phase Diagram

Figure 7-1 shows the N_2O_4 phase diagram with the phase regions identified. These data were obtained from Reference 9. The phase boundary lines separate the pressure and temperature regions in which the oxidizer can exist in equilibria as a single gas, liquid or solid phase. The boundary lines define pressure and temperature conditions at which phase changes occur. When the fluid exists at pressure and temperature values which permit a phase change (i.e. on a phase boundary), the fluid can exist as a single phase (gas, liquid or solid) or as a mixture of two phases. At the triple point, where all three phase boundaries meet, the oxidizer can exist as a mixture of solid, liquid and vapor. The proportion of each phase present at triple point, or along a phase boundary, depends on the energy content of the fluid. The amounts of energy required to produce phase changes are called the heat of vaporization, heat of fusion and heat of sublimation for the liquid-gas, liquid-solid and solid-gas transitions respectively.

7.1.1.2 Fuel Phase Diagrams

The fuel used in the APS, DPS and SPS engines is Aerozine-50. The allowable composition limits for Aerozine-50, per Mil Spec Mil P27402A, are as follows:

D2-118246-1

TABLE 7-1
PHYSICAL PROPERTIES OF THE 50/50 FUEL BLEND AND N_2O_4

PROPERTY	50/50	N_2O_4
Molecular Weight (avg)	45.0	92.016
Melting Point	18.8°F	11.84
Boiling Point UDMH at 14.7 psia	146°F	
Boiling Point N_2H_4 at 14.7 psia	235°F	
Boiling Point N_2O_4 at 14.7 psia		70.07°F
Physical State	Colorless Liquid	Red Brown Liquid
Density of Liquid at 77°F and 14.7 psia	56.1 lb/ft ³	89.34 lb/ft ³
Viscosity of Liquid at 77°F	54.9 × 10 ⁻⁵ lb/ft-sec	.0002796 lb/ft-sec
Vapor Pressure at 77°F	2.75 psia	17.7 psia
Critical Temperature	634°F	316.8°F
Critical Pressure	1696 psia	1469 psia
Heat of Vaporization	425.8 BTU/lb ◁1	178 BTU/lb
Heat of Formation at 77°F	527.6 BTU/lb	-87.62 BTU/lb
Specific Heat at 77°F	0.694 BTU/lb-°F	.374 BTU/lb-°F
Thermal Conductivity at 77°F	0.151 BTU/ft-hr-°F	.0755 BTU/ft-hr-°F
Heat of Fusion	N.A.	68.5 BTU/lb

◁1 Enthalpy charge required to change liquid 50-50 to vapor 50-50 at 75°F.

D2-118246-1

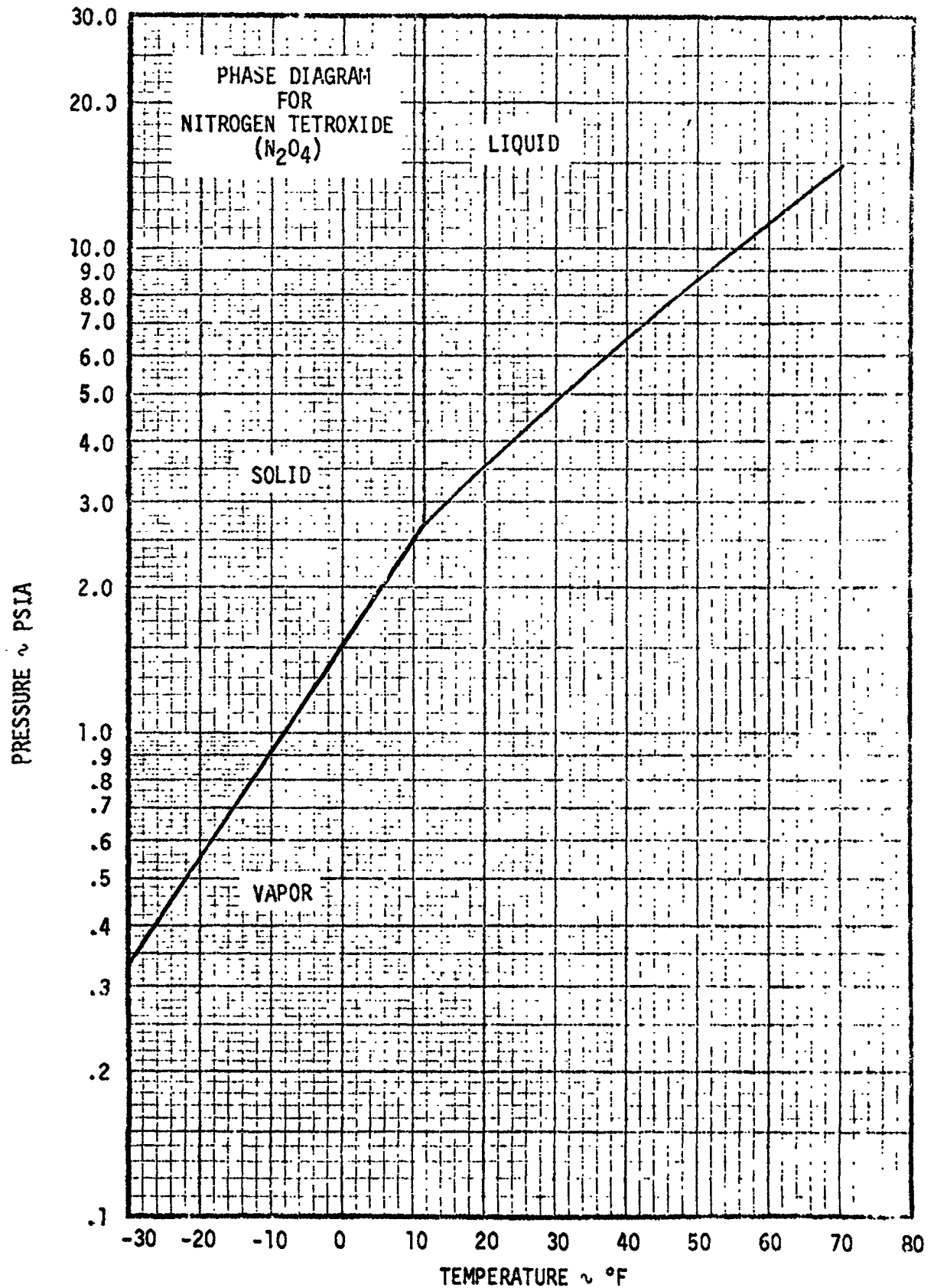


FIGURE 7-1 NITROGEN TETROXIDE PHASE DIAGRAM

7.1.1.2 Fuel Phase Diagrams (Continued)

Physical and Chemical Properties

<u>Properties</u>	<u>Limits</u>
N_2H_4 , percent by weight	51 max
UDMH plus amines, percent by weight	47 min
Water	1.8 max
Total hydrazine - uns-dimethyl-hydrazine and amines, percent by weight	98.2 min

As a result of the allowable concentration variations for Aerozine-50, no single thermodynamically consistent set of property data exist for Aerozine-50. The 50-50 (50% by weight of UDMH and 50% by weight of hydrazine) phase diagram is a good approximation to the known properties of typical Aerozine-50 mixtures and will be used in this report. The data used in the preparation of the 50-50 phase diagrams were obtained from Reference 10.

Since 50-50 is a mixture of hydrazine and UDMH, the phase diagram shown in Figure 7-2 is more complex than that of a pure substance. In Figure 7-2, a liquid + vapor region divides the liquid region and the vapor region. This region is a line on a pure substance phase diagram. For 50-50, it is a region because the composition of both the liquid and the vapor continually changes from point to point in this region. In the upper part of this region, the liquid phase has more than 50% hydrazine. In the lower regions, the liquid is practically all hydrazine while the vapor has less than 50% hydrazine. Along the lower line, the liquid has all been converted to vapor so that the vapor composition is 50% hydrazine and 50% UDMH.

The liquid + vapor region is separated from the solid hydrazine + vapor region by an almost vertical line. As this line is approached from the liquid + vapor side, the pressure and temperature are sufficient to define the composition of each phase. When the line is reached and the pressure and temperature are held constant, all of the UDMH will vaporize and all of the hydrazine in the liquid will solidify. If the pressure and temperature are now adjusted to move to the solid hydrazine + vapor region, the solid hydrazine will exist in equilibrium with the vapor phase, with the composition of the vapor phase continually changing by gaining or losing hydrazine to the solid. As the lower line in this region is reached, the solidified hydrazine is completely sublimed and only 50-50 vapor is present.

In the solid hydrazine + liquid region shown in the upper left of the figure, hydrazine is simply solidifying out of the solution as temperature is decreased making the remaining liquid rich in UDMH. At any particular position in this region, the composition of the liquid and the percent hydrazine solidified is completely defined by the pressure and temperature. There are additional phase regions at temperatures lower than shown on Figure 7-2, but these will not be discussed since they are of no interest to this study.

D2-118246-1

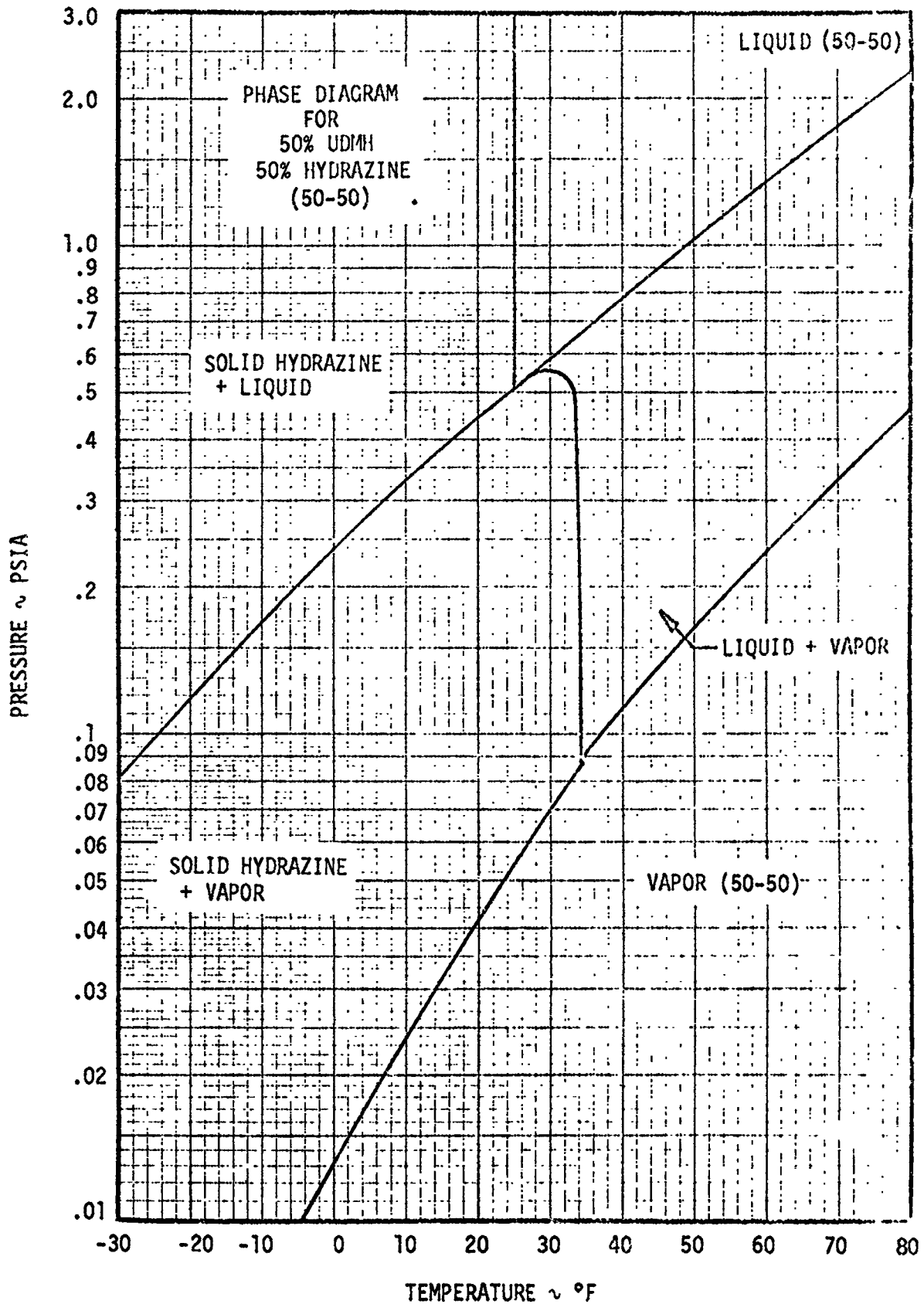


FIGURE 7-2 PHASE DIAGRAM FOR 50% UDMH + 50% HYDRAZINE

7.1.1.2 Fuel Phase Diagrams (Continued)

The 50-50 phase diagram applies to a closed system which always has a total composition of 50% UDMH and 50% hydrazine. In an injector, the vapor pressure is vented to the vacuum chamber or space. In the solid hydrazine-vapor region, the vapor in the venting case will be pure hydrazine so that the 50-50 diagram is not applicable and the sublimation curve for pure hydrazine should be used. However, the phase diagram for hydrazine has a sublimation line which is very close to the dividing line between the solid + vapor and 50-50 vapor phases and a boiling line very close to the lower 50-50 liquid-vapor line. The freezing line is an extension of the line dividing the solid hydrazine vapor-liquid vapor regions. The triple point temperature of hydrazine is 34°F and the pressure is .058 psia. Therefore, a separate diagram is not needed since the lower part of the 50-50 phase diagram is adequate.

7.1.2 Boiling and Sublimation

Boiling can occur when the injector manifold pressure drops below the vapor pressure of the propellant. The type or character of the boiling is governed by the degree to which the liquid is superheated, the characteristics of the surfaces in contact with the liquid, and the presence of nucleation sites within the liquid. When the pressure and temperature data from the tests are plotted so that they can be compared to the propellant phase data, it is obvious that the liquid is sufficiently superheated to cause very violent boiling. Specifically, the vapor pressure of the liquid is significantly higher than the ambient pressure to which the propellant is exposed. The important point is that the rate of boiling is controlled by the difference between the injector manifold pressure and propellant vapor pressure and not by the rate of heat addition to the liquid.

The total amount of propellant boiled off prior to reaching the freezing point is, however, determined by the heat input to the liquid. Thus, there is an upper and lower limit on the amount of propellant that can be converted to vapor by the boiling process. The upper limit is attained when the heat added is equal to the heat of vaporization of all of the liquid. The lower limit occurs when no heat is added to the liquid and the heat of vaporization is supplied by the heat capacity of the liquid. The heat balance for this case is

$$mC_p \frac{dT}{d\tau} = - h_{1v} \frac{dm}{d\tau}, \text{ or, } \frac{m_f}{m_i} = e^{-\left(\frac{\Delta T C_p}{h_{1v}}\right)}$$

after integrating and solving for the ratio of final mass (m_f) to the initial mass (m_i). The heat balance uses the propellant mass (m), the constant pressure specific heat (C_p), temperature (T), time (τ), and the enthalpy of vaporization (h_{1v}). The mass of propellant which must be vaporized to produce a temperature change of ΔT degrees is ($m_i - m_f$), or, the fraction vaporized is $(1 - m_f/m_i)$.

7.1.2 Boiling and Sublimation (Continued)

The table below shows values for the mass ratio (m_f/m_i) required to produce a range of temperature changes for N_2O_4 , UDMH, and hydrazine. Since the initial boiling of Aerozine-50 is primarily the vaporization of UDMH, the data given for UDMH is representative of A-50 boiling.

FINAL MASS/INITIAL MASS

ΔT °F	<u>UDMH</u>	<u>HYDRAZINE</u>	<u>N₂O₄</u>
10	.9728	.9873	.9793
20	.9462	.9748	.9592
30	.921	.9705	.9395
40	.896	.950	.920
50	.871	.938	.901

For the N_2O_4 , an evaporation of only 10% of the liquid will cause a 50°F temperature drop in the remaining liquid. For the Aerozine-50, about 13% evaporation is required to drop the temperature 50°F.

The amount of oxidizer which must be evaporated to solidify the remaining oxidizer can be determined from an energy balance. Equating the energy released during solidification to the energy required for vaporization gives the relation

$$(1-x)h_f = xh_{1v} \text{ or } x = 1/(1 + h_{1v}/h_f)$$

where x is the fraction of fluid evaporated, h_f is the enthalpy of fusion and h_{1v} is the enthalpy of vaporization. For N_2O_4 , the ratio (h_{1v}/h_f) is 2.60. Therefore, evaporation of 27.8% of the N_2O_4 at the freezing temperature would freeze the remaining 72.2% of the N_2O_4 . To drop the N_2O_4 temperature 50°F and then freeze the remainder would require the evaporation of 35% of the N_2O_4 , leaving the remaining 65% to be removed by sublimation.

A similar analysis for the 50-50 fuel is more complicated because the fuel is a mixture which has several phase boundaries (see Figure 7-2). The boiling and freezing processes are actually fractional distillations because the composition of the vapor, liquid and solid phases is, in general, a function of temperature and pressure. Since the UDMH vapor pressure is significantly higher than the hydrazine vapor pressure, the main boiloff product is UDMH. An approximate analysis can be made by assuming that all of the cooling and freezing processes are caused by the evaporation of UDMH, and that the amount of hydrazine remains constant. Evaporative cooling of the 50-50 fuel mixture will require evaporation of approximately twice as much UDMH as would cooling of the UDMH component alone. Thus, cooling the 50-50 mixture by 40°F will require evaporation or boiloff of 20.8% of the UDMH. The amount of UDMH boiloff required

7.1.2 Boiling and Sublimation (Continued)

to freeze hydrazine can be determined from the ratio of the hydrazine heat of fusion to the UDMH heat of vaporization. This ratio is .678, which means that .678 lbs. of UDMH must be evaporated to freeze 1 lb. of hydrazine. Therefore, 88.6% of the UDMH must be evaporated to cool the mixture 40°F and to freeze all of the hydrazine.

When all of the liquid has boiled off or solidified, the remaining solid must be removed by sublimation. The rate at which sublimation can occur for a given solid is proportional to the area available for sublimation and to the difference between the pressure of the vapor in contact with the solid and the vapor pressure of the solid. Thus, the rate of sublimation is zero when the solid is in equilibrium with its vapor. Test results indicate that the sublimation process is far out of equilibrium because the measured manifold pressures are much lower than the vapor pressures of the solidified propellants.

7.1.3 Gas Solubility

Helium and nitrogen are dissolved in the propellants during the propellant storage and propulsion system pressurization periods. When the pressure on the propellants is reduced, these gases come out of solution, or, effervesce. Following engine shutdown, the propellant manifold pressures fall rapidly, allowing dissolved gases to come out of solution. As the gas bubbles form, propellants are displaced and are forced out through the injector orifices. This section describes the relationship between the amount of dissolved helium and the volume of fuel and oxidizer which can be displaced as the gas comes out of solution after engine shutdown.

Figure 7-3 shows the solubility of helium in N_2O_4 and Aerozine 50. These data were taken from Reference 12. The difference in the solubility at two different pressures is

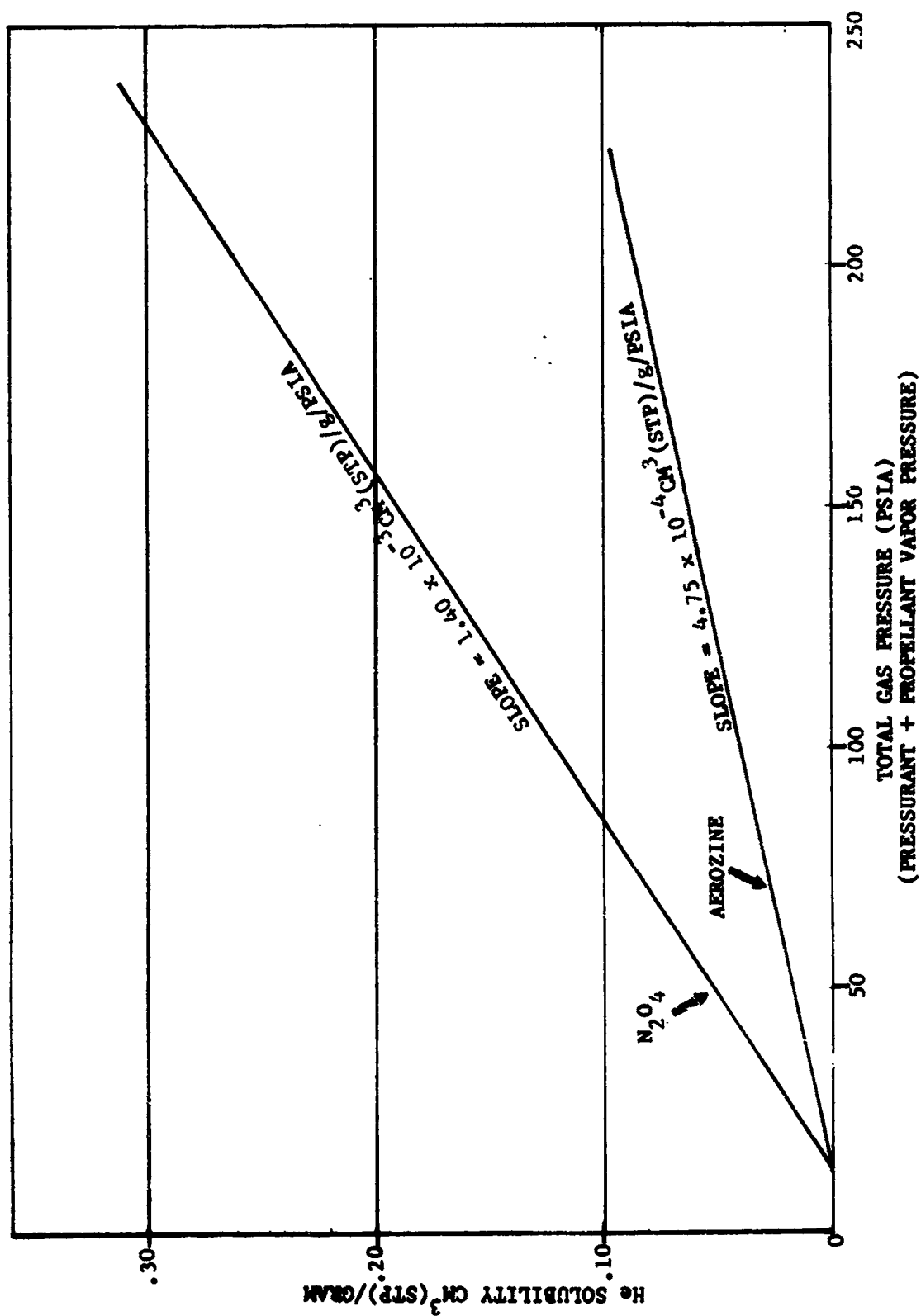
$$\Delta S = k \Delta P$$

where k is the slope of the curves shown in Figure 7-3. Note that the solubility is zero when the total pressure equals the vapor pressure of the propellant. The volume of helium liberated per gram of propellant in going from a saturated pressure, P_s , to some lower pressure, P , is given by

$$\begin{aligned} S_{cc} &= 1.4 (10)^{-3} (P_s - P) & N_2O_4 \\ S_{cc} &= 4.75 (10)^{-4} (P_s - P) & A-50 \end{aligned}$$

The volume (V) occupied by 1 standard cubic centimeter of helium at any pressure, P , and a temperature of 75°F is

$$V(cc) = \frac{17.1}{P} (scc)$$

FIGURE 7-3 SOLUBILITY OF HELIUM IN 50-50 and N₂O₄

7.1.3 Gas Solubility (Continued)

Thus, the volume of helium that can be liberated when the pressure drops from the saturated pressure to some lower pressure, P , is given by

$$V(\text{cc}) = 17.1 (1.4) (10)^{-3} \frac{(P_s - P)}{P} \text{ per gram of } \text{N}_2\text{O}_4$$

$$V(\text{cc}) = 17.1 (4.75) (10)^{-4} \frac{(P_s - P)}{P} \text{ per gram of A-50}$$

Using a vapor pressure of 17 psia for N_2O_4 and 2 psia for A-50, and a saturation pressure P_s of 190 psia (Seattle saturation pressure for the ascent engine) the following liberated volumes are obtained:

N_2O_4	.243 cc per gram
A-50	.765 cc per gram

For the descent engine the saturation pressure was 240 psia and the volumes liberated using the vapor pressures previously stated are:

N_2O_4	.313 cc per gram
A-50	.97 cc per gram

Note that in each case that the volume liberated from the A-50 is considerably greater than for the oxidizer. This occurs because the vapor pressure of the A-50 is so much lower than the N_2O_4 . On the basis of standard cubic centimeters, the following values are obtained:

	<u>Ascent</u>	<u>Descent</u>
A-50	.098 scc	.102 scc
N_2O_4	.225 scc	.31 scc

Thus, by the time the manifold pressure reaches standard pressure (14.7 psia) approximately one tenth of the volume of the A-50 could be displaced by helium and by the time the boiling point of A-50 is reached around 80% of the volume of A-50 could be displaced. With the N_2O_4 , about 45% can be displaced at the standard pressure condition, which is close to the boiling point of N_2O_4 .

The preceding calculations show that the effervescence of dissolved gases can displace significant amounts of fuel and oxidizer from the injector and ducts. This can occur during the shutdown phase, before boiling commences.

7.1.4 Determination of Mass Residuals

The volume of propellant residuals will affect the manifold priming times during engine restarts. Significant differences between fuel and oxidizer residual volumes will affect the normal propellant lead/lag relationship, and may cause hard restarts. Fuel residual volumes were measured during the ARC cold flow tests, but no residual measurements were made during the Seattle hot-firing tests. The fuel and oxidizer residual masses for the Seattle tests were estimated by calculating gas flow rates through the injector orifices. Calculations began at the start of boiling. The mass flow rate equation for isentropic choked flow of a perfect gas is:

$$\frac{dm}{d\tau} = \frac{C_D P A}{\sqrt{T}} \sqrt{\frac{\gamma n}{R_0} \left(\frac{2}{\gamma+1} \right)^{\frac{\gamma+1}{\gamma-1}}}$$

where A is the orifice area, T is the gas temperature, n is the gas molecular weight, P is pressure, R₀ is the universal gas constant, m is mass, τ is time, C_D is the orifice discharge coefficient and γ is the specific heat ratio. The total mass removed in a given time period is obtained by integrating the mass flow rate equation:

$$\Delta m = \frac{C_D A}{\sqrt{T}} \sqrt{\frac{\gamma n}{R_0} \left(\frac{2}{\gamma+1} \right)^{\frac{\gamma+1}{\gamma-1}}} \int P d\tau$$

This equation assumes that the gas properties, orifice area, discharge coefficient, and average temperature are constant over the time interval. When this method is used, there are several sources for error. First, the orifice area and the discharge coefficient may be changed by frozen deposits in the injector holes. For this analysis, the discharge coefficient was estimated to be 0.8 for a square edge orifice discharge into a vacuum, and the injector orifices were assumed to be clear of frozen deposits. During the first few seconds of boiling, some of the holes may be flowing liquid or two phase fluid which would increase the actual mass flow rate. In addition, the molecular weight of the gas products is not constant. For the fuel side, the predominant species during the early stages of the coast period is UDMH and during the final stages it is hydrazine. For the same pressure and temperature conditions, the flow of UDMH is about 37% greater than the flow of hydrazine. The temperature of the vapor is not necessarily the same as the temperature of the liquid by the time the vapor reaches the injector holes. However, since the flow rate is inversely proportional to the square root of the absolute temperature, a 10° to 20° error in temperature could cause only a 1% error in flow rate.

Calculation of the Rocketdyne injector fuel residuals was based on an injector orifice area of .20 in², molecular weight of 60.08, specific heat ratio of 1.125 and discharge coefficient of 0.8. Using these values and an average temperature of 470°R, the mass flow rate equation becomes:

7.1.4 Determination of Mass Residuals (Continued)

$$\Delta m = .00516 \int p d\tau$$

Assuming that all of the UDMH is gone at 100 seconds, the integral $p d\tau = 36.2$ and the mass of UDMH expelled is .187 pounds. Since the original mixture had even weights of UDMH and hydrazine, the total initial mass is calculated to be .374 pounds. The integral from 100 to 800 seconds gives a mass of .2 pounds when based on hydrazine flow during this period. This is good agreement with the UDMH flow calculation since the initial composition was approximately 50% hydrazine and 50% UDMH.

Using the value of .374 pounds for the residual fuel at the start of boiling, and assuming that the flow is entirely UDMH for the first 100 seconds and entirely hydrazine during the remainder of the time gives a mass residual curve as shown in Figure 7-4 for the ascent fuel side. Also shown are the mass residuals data obtained from the ARC distillation tests. The experimental data are significantly lower than the calculated values for coast times of less than 300 seconds. The experimental data are believed to be in error because approximately 300 cc of fuel (.6 lbs) cannot drain from the fuel duct, and should be present when boiling starts. The calculated value of .374 lbs is reasonably close to the amount of trapped fuel, but the experimental data are significantly lower.

Figure 7.6 shows the mass residual curve obtained for the fuel side of the descent injector. This curve was generated in the same way as discussed for the ascent engine. The injector orifice area used in the calculation was .084 in². Also shown are data from the descent injector distillation tests performed at ARC. The calculated residuals show excellent agreement with the measured residuals.

Figures 7.5 and 7.7 show the mass residual curves for the ascent and descent engine oxidizer sides. No distillation test for the oxidizer was conducted at ARC.

The table below shows the total injector and duct volume for each of the engines and the volume of mass residual calculated for a 10 second coast period.

	Total Volume	Residual Volume	<u>Empty Volume</u> <u>Total Volume</u>	% Change in Priming Time
Ascent				
Fuel	62.7 in ³	11.05 in ³	.825	-17.5
Oxidizer	20.1	4.4	.782	-21.8
Descent				
Fuel	80.1	17.35	.783	-21.7
Oxidizer	56.6	11.25	.801	-19.9

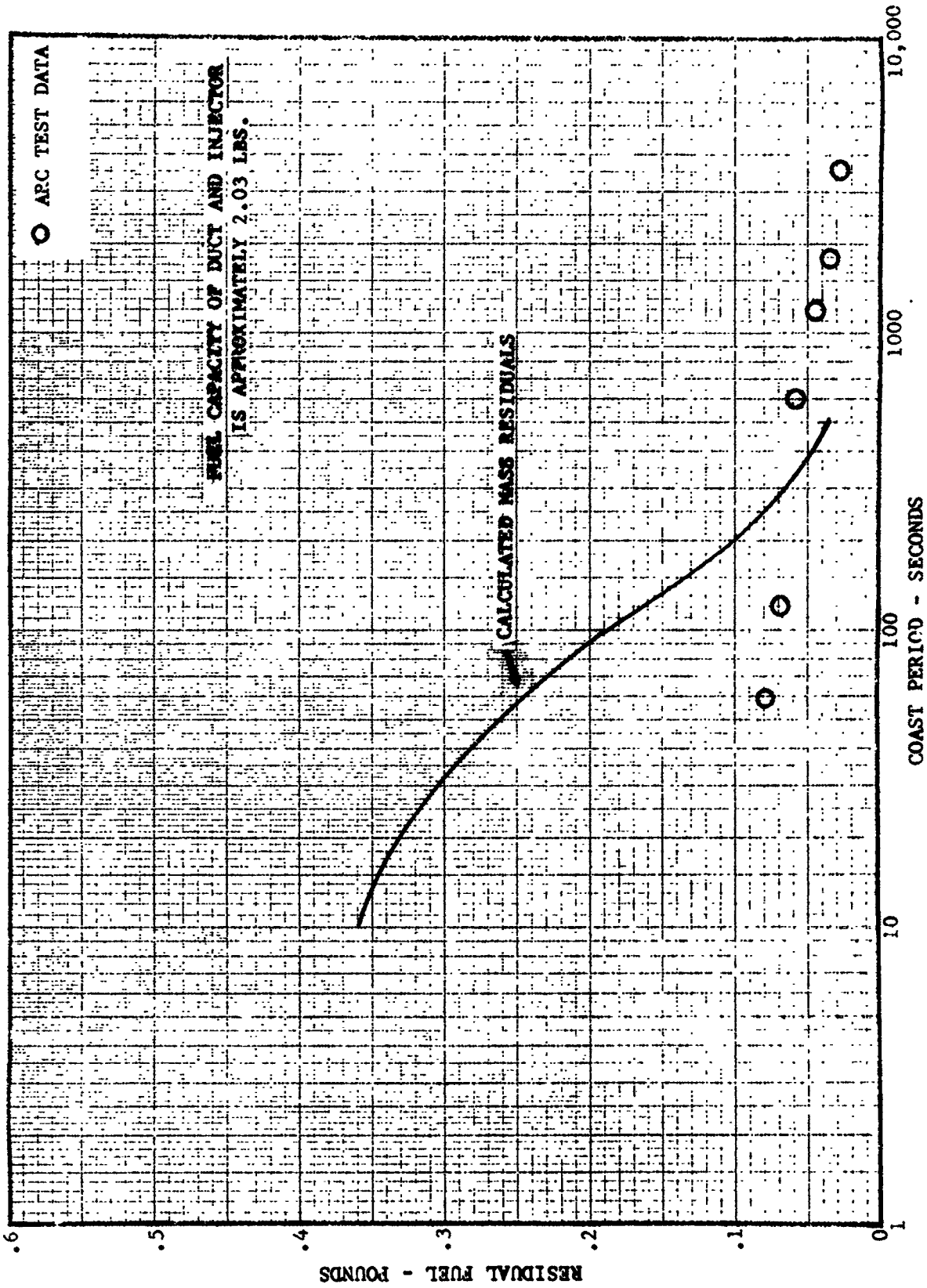


FIGURE 7-4 MASS RESIDUAL ASCENT ENGINE FUEL SIDE

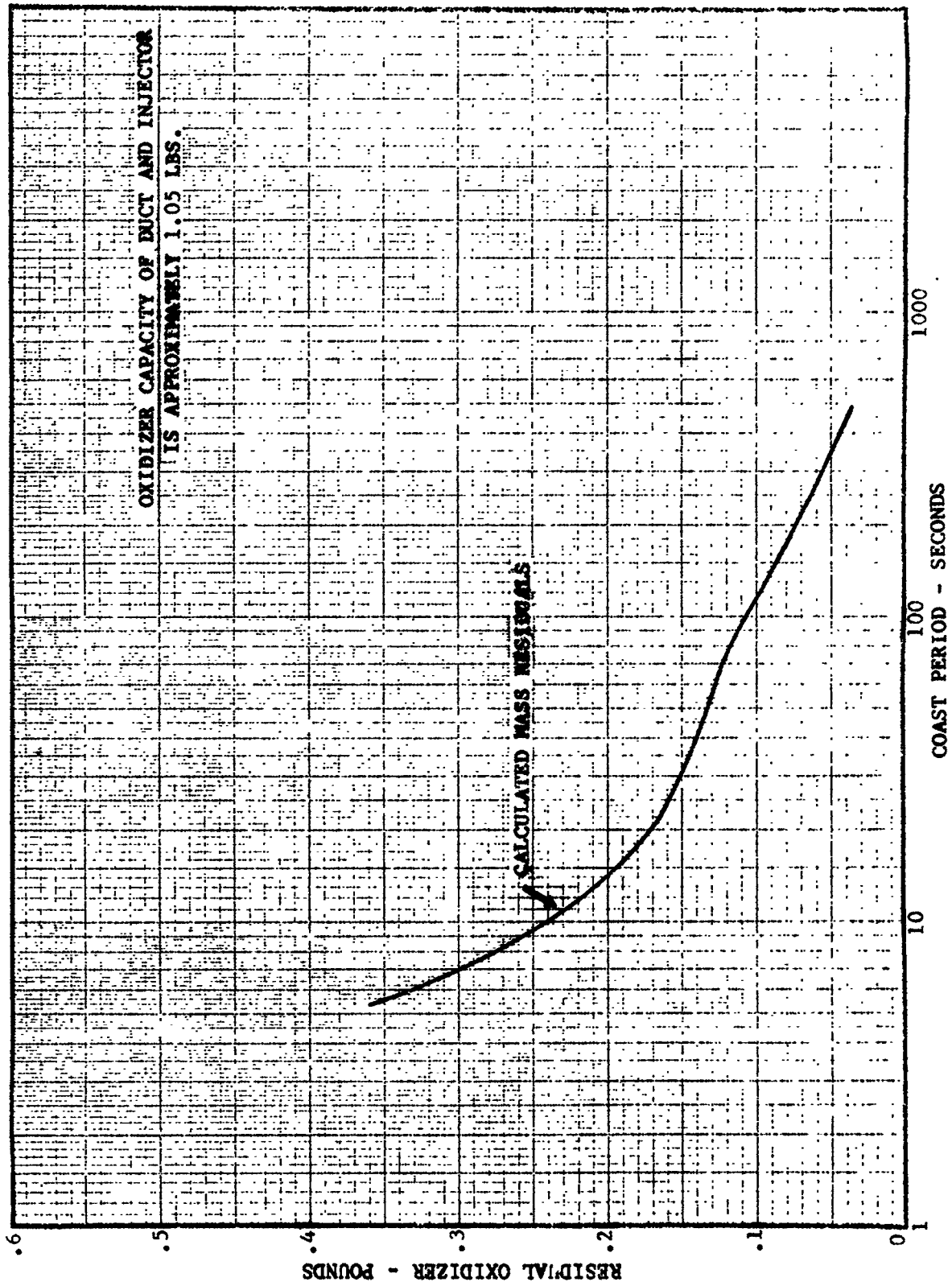


FIGURE 7-5 MASS RESIDUAL ASCENT ENGINE OXIDIZER SIDE

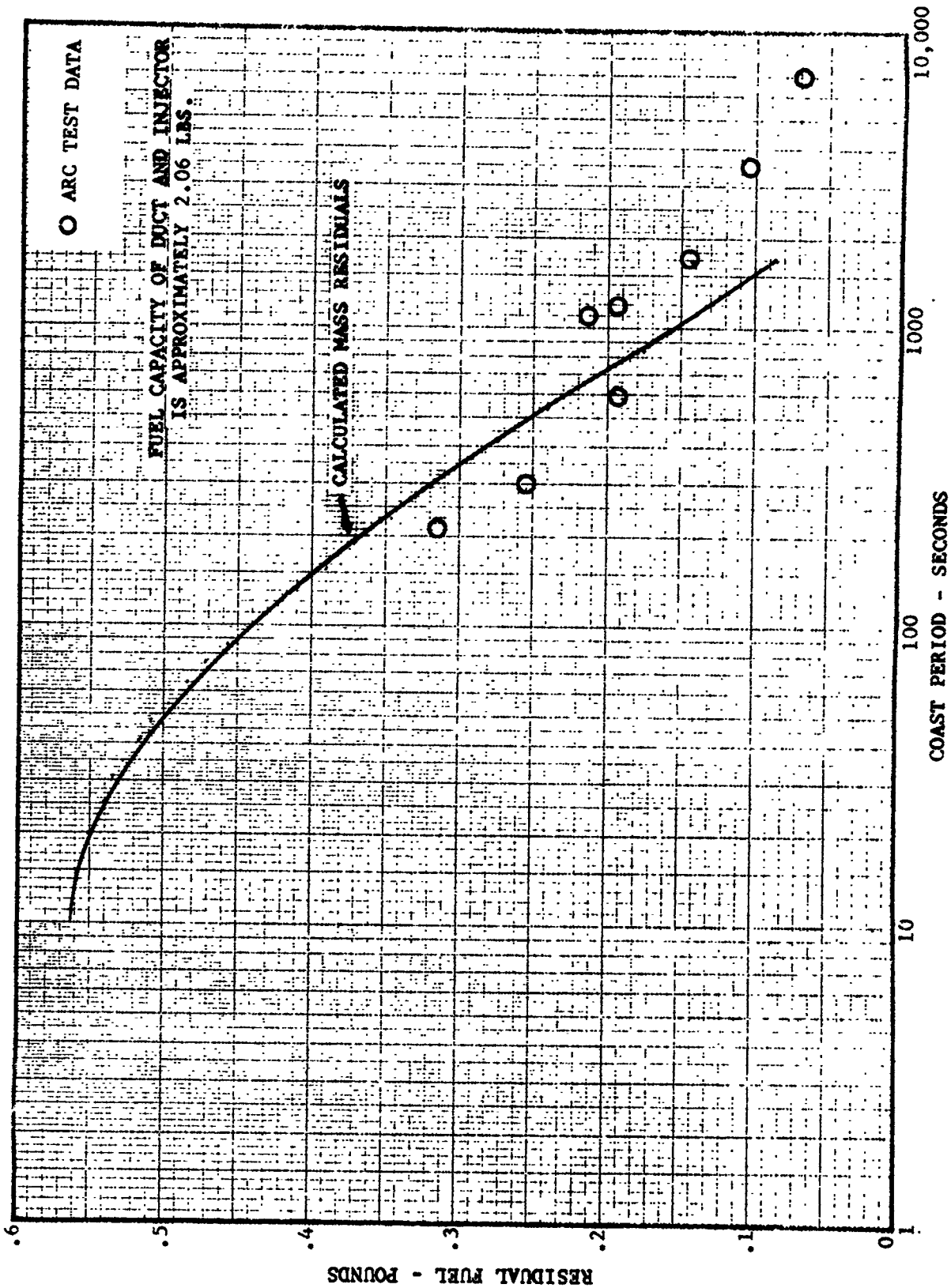


FIGURE 7-6 MASS RESIDUAL FOR DESCENT ENGINE FUEL SIDE

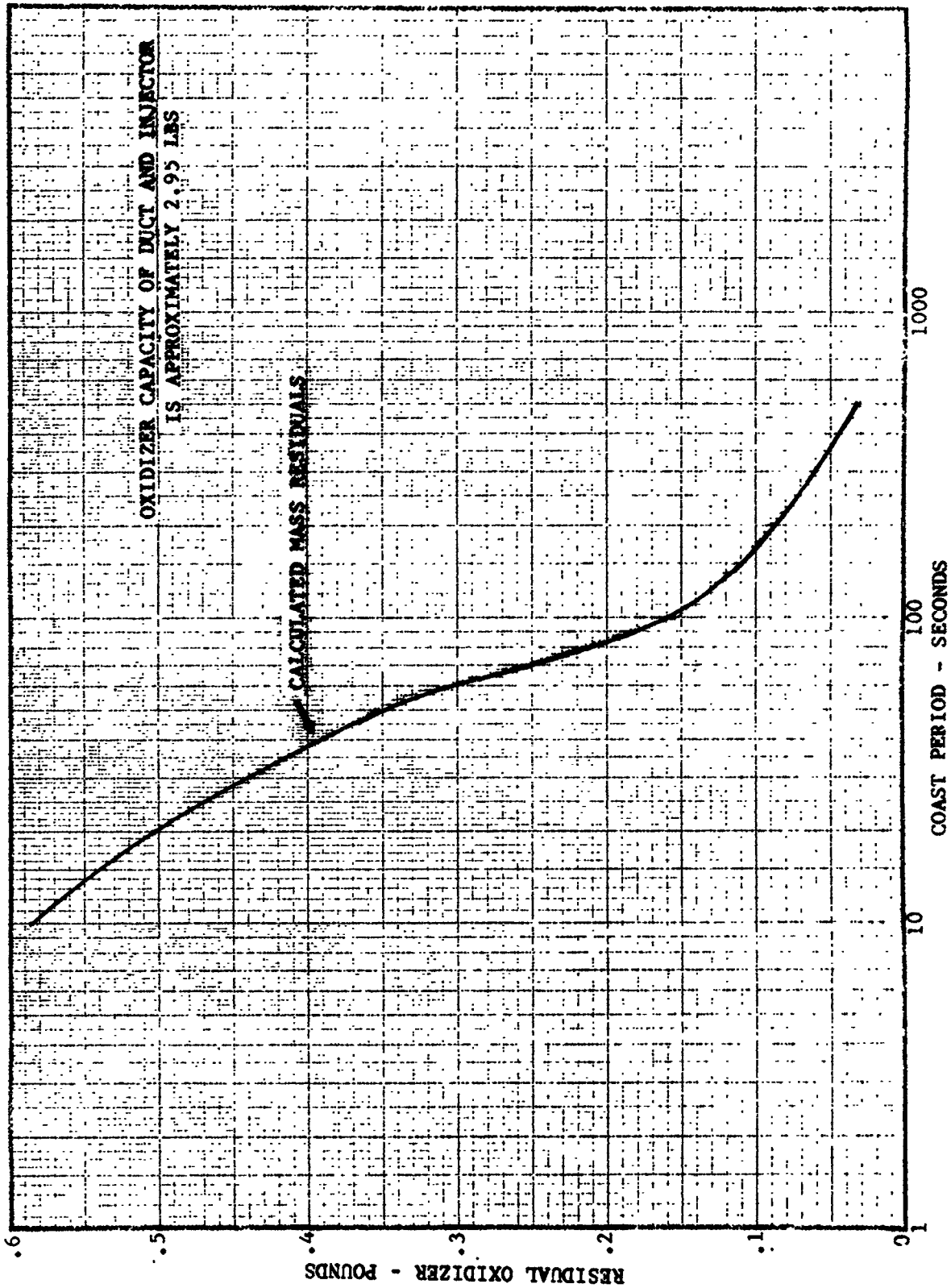


FIGURE 7-7 MASS RESIDUAL FOR DESCENT ENGINE OXIDIZER SIDE

7.1.4 Determination of Mass Residuals (Continued)

The change in priming times resulting from the presence of propellant residuals could be determined from a dynamic analysis of the priming process. No data are available on such an analysis. A reasonable estimate of the change in priming times can be made by assuming that the fractional change in priming time is directly proportional to the ratio of empty volume to total volume. This ratio is shown in the table along with the percent change in priming times. Note that these are maximum changes for coast times greater than 10 seconds since there will be smaller amounts of residual propellants at any later time.

Measured priming times taken from the Ascent checkout firing show fuel priming time to be .264 seconds and oxidizer priming to be .224 seconds. Using these values as nominal, one would expect the priming times on restart after a ten second coast to be .218 seconds for fuel and .175 seconds for oxidizer. Thus the oxidizer lead would increase from .040 seconds to .043 which is certainly not significant. An Ascent engine fuel lead could be obtained after a 10 second coast only if the oxidizer side were completely empty, while the fuel side retained the calculated amount of residuals. This would produce a nominal oxidizer priming time (.224 seconds) while the fuel priming time would be reduced to .218 seconds by the presence of residual fuel. Note that this is a worst case assumption for coast periods of more than 10 seconds, since the fuel residuals will decrease, and their effect will decrease, as coast times increase. In addition, test data and calculations do not support the assumption that all of the oxidizer residuals have been eliminated by the end of a 10 second coast.

An alternate approach is to assume that equal times are required to fill equal fuel and oxidizer side volumes. Simultaneous fuel and oxidizer injection will then occur when the empty volumes in the fuel and oxidizer sides are equal. This criteria provides an approximation to the maximum fuel residual volumes required to eliminate the oxidizer lead. Specifically, the oxidizer lead can be eliminated when the empty volume in the fuel side is equal to (or less than) the total oxidizer side volume. Therefore, the volume of fuel residuals required to eliminate the oxidizer lead is:

$$\text{Vol (fuel residuals)} = \text{Vol (fuel side)} - \text{Vol (oxid. side)}$$

For the ascent engine the required fuel residual volume is:

$$\text{Vol (fuel residuals)} = 62.7 - 20.1 = 42.6 \text{ in}^3$$

For the descent engine the required fuel residual volume is:

$$\text{Vol (fuel residuals)} = 80.1 - 56.6 = 23.5 \text{ in}^3$$

7.1.4 Determination of Mass Residuals (Continued)

The above calculations show that the ascent engine fuel side must contain 1.5 lbs of fuel and the descent engine fuel side must contain .8 lbs of fuel, when the oxidizer side is empty, in order to eliminate the oxidizer lead. The calculated and experimental test data show that these weights of fuel are not present at coast times of more than 10 seconds.

At shorter coast times (less than 10 seconds), the residual volumes will increase and tend to reduce the oxidizer lead. However, the concept of an "oxidizer lead" or a "fuel lead" is not valid at very short coast times since combustion is occurring for several seconds after shutdown. As a result, the incoming flow of propellants is injected at pressure and temperature conditions which produce smooth combustion. Restarts after short coast periods represent a continuation of the previous combustion process rather than a reignition of the combustion process. Test data confirm that "restarts" after coast periods of less than 10 seconds produce smooth "reignitions".

On the basis of these calculations, it can be concluded that the change in the lead lag relationship due to the volumes being partially filled is not important for the ascent engine. The changes that are observed are more likely caused by flow restrictions such as plugging of the screens. Due to instrumentation difficulties, a similar calculation for the descent engine cannot be made. However, the change in the lead/lag relationship is even smaller than for the ascent engine and there is no indication from the test data or combustion chamber photographs that the oxidizer lead was lost.

7.2 ARC COLD FLOW TEST ANALYSIS

This section presents and discusses selected test data from the cold flow tests run at the Atlantic Research Corporation (ARC) High Altitude Test Facility. The objective of the ARC test series was to investigate the propellant and injector phenomena occurring after engine shutdown in a vacuum. The test data were analyzed to determine the effects of significant test variables (coast time, initial temperatures, number of propellant flow pulses), and to provide a basis for comparing the cold-flow test results to the hot-firing test results. Temperature histories and propellant phase histories are presented to provide the basis for comparison. Appendix A of this report describes the ARC test facility and provides a description of the test series run with the Bell, Rocketdyne and TRW injectors.

7.2.1 Bell Ascent Injector, Phase I

Selected test data from the Phase I Bell ascent injector test series are presented in Figure 7-8. This figure shows the injector temperature history for Test #9, which was a 5-pulse fuel flow. No oxidizer simulant was used during this test. Quantitative data were limited because temperature data from only 4 thermocouples were reported. Fuel manifold pressure data were not reported because of doubtful accuracy of the 0-250 psia transducer in the pressure range of interest (0-5 psia).

Temperature data from test #9 show the injector cooling effect of repetitive fuel flow pulses. Thermocouple #12 was located at the bottom of the injector in the outer fuel manifold, and thermocouple #14 was located in the fuel duct, between the injector and the ball valves. The coast period following the first fuel flow produced the lowest reported temperature during this test, 2°F. The injector was cooled significantly (40°F) during the first two coast periods, but was cooled only 10°F during the third and fourth coast periods. The minimum injector temperature was essentially unchanged during the fifth period. Shortly after the first propellant pulse, the injector temperature fell below the freezing temperature of the fuel, and remained there during the rest of the test. However, no reduction in fuel flow was noted during the second through fifth fuel pulses. Motion pictures of the test showed that cones of frozen fuel were formed on the injector and baffle after the first fuel flow. These deposits are blown away by each succeeding fuel pulse, but reform immediately from the fuel "snow" flowing out of the injector orifices. It is apparent that during this test the injector orifices were not significantly blocked by the frozen fuel deposits, probably because the "snowy" consistency of the deposits was unable to support any significant pressure difference.

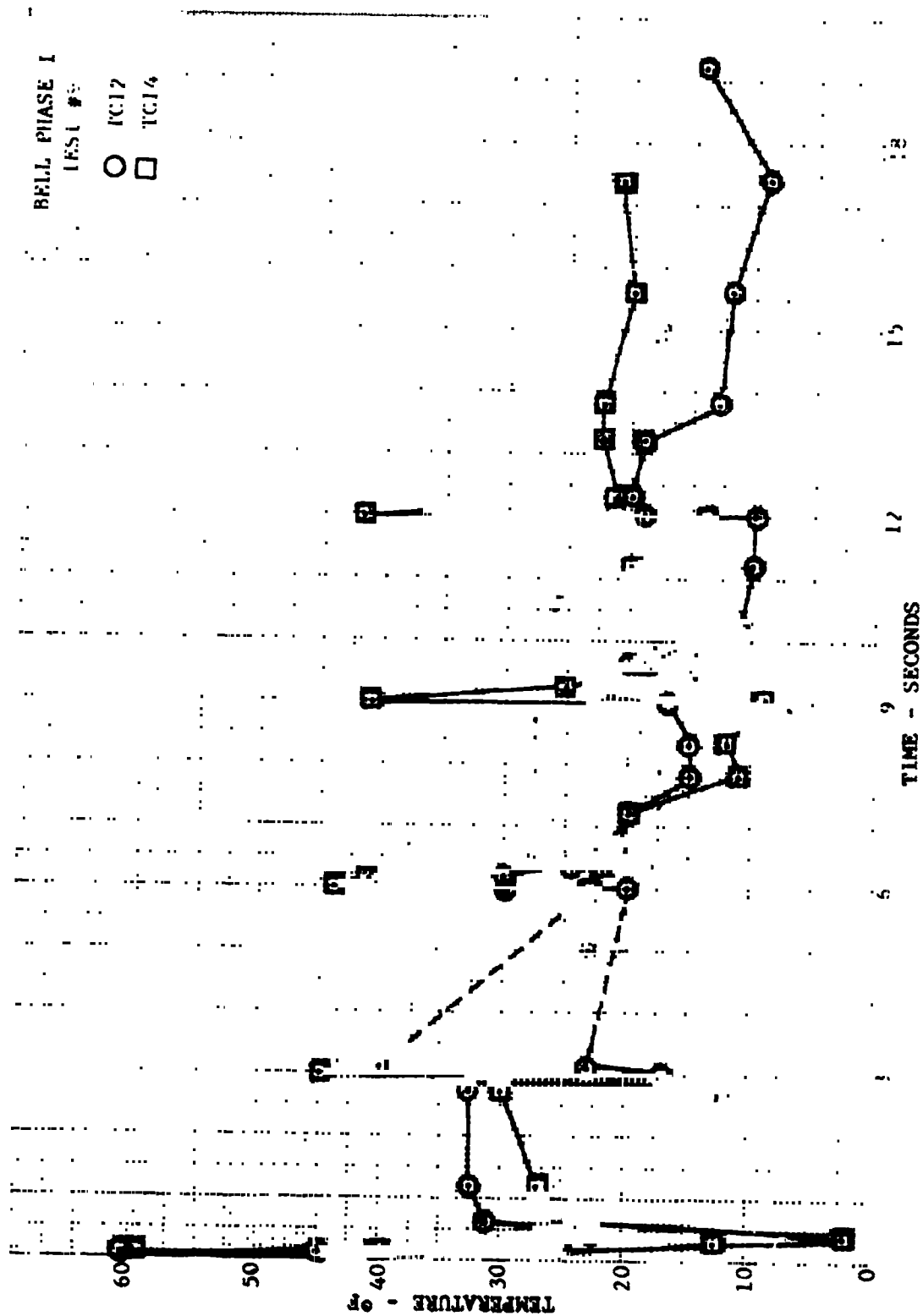


FIGURE 7-8 TEMPERATURE HISTORY FOR BELL INJECTOR, REPEATED PULSES

7.2.2 Bell Ascent Injector, Phase II

Selected test data from the Phase II Bell ascent injector test series are presented in Figures 7-9 through 7-14. These data are representative of the test results obtained during the Phase II program. Figures 7-9 through 7-12 show injector temperature histories. Fuel manifold temperatures are plotted versus fuel manifold pressures on Figures 7-13 and 7-14 so that propellant phase histories could be established.

The injector temperature histories, Figure 7-9 through 7-12 present thermocouple data for the first and second fuel flow pulses of test #46 (40°F) and test #60 (70°F). A total of 14 thermocouples were installed for the Phase II tests but data were reported for only four of them. Thermocouple data were presented for TC-1 (left side of outer fuel manifold), TC-8 (right side of outer fuel manifold), TC-12 (bottom of outer fuel manifold), and TC-14 (fuel duct). Thermocouples TC-8 and TC-14 were inserted into the propellant flow passages, and therefore indicate temperatures of the A-50 liquid. Temperature data from TC-14 were used to prepare the propellant phase histories presented on Figures 7-13 and 7-14.

These thermal histories show that the propellant in the fuel duct was cooled more rapidly, reached a lower temperature, and warmed more rapidly than did the propellant in the injector. These phenomena can be attributed to the varying heat sink and heat transfer properties of the components. The fuel duct has less mass than the injector, and is therefore cooled more rapidly, and to a lower temperature than the injector. However, when the injector is cooled to a low temperature, it remains at the low temperature for a longer period of time because it is thermally isolated from the valve assembly and propellant supply system by the fuel duct. Heat transferred from the valve body must first warm the propellant duct before the injector can be warmed.

The increase in fuel duct temperature to approximately 34°F, at 100-300 seconds after the first fuel pulse, is attributed to the collection of frozen hydrazine in the region of thermocouple TC-14. This interpretation is based on the fuel phase history, which is discussed in subsequent paragraphs. The increase in injector temperature beginning at about 2000 seconds (Test 46, second pulse) is attributed to the decreasing volume of frozen fuel residuals, which reduced the total cooling capacity of the sublimation process. The injector temperature increased when the rate of sublimation cooling decreased below the rate of conductive and radiative heating from the test facility.

The propellant temperature versus pressure data are plotted on the phase diagram for a 50-50 mixture (by weight) of hydrazine (N_2H_4) and UDMH (CN_2H_6). The 50-50 diagram shows the possible combinations of vapor, liquid and solid phases which can exist in various temperature and pressure regions. These regions are separated by phase boundaries which indicate the pressure and temperature limits for the existence

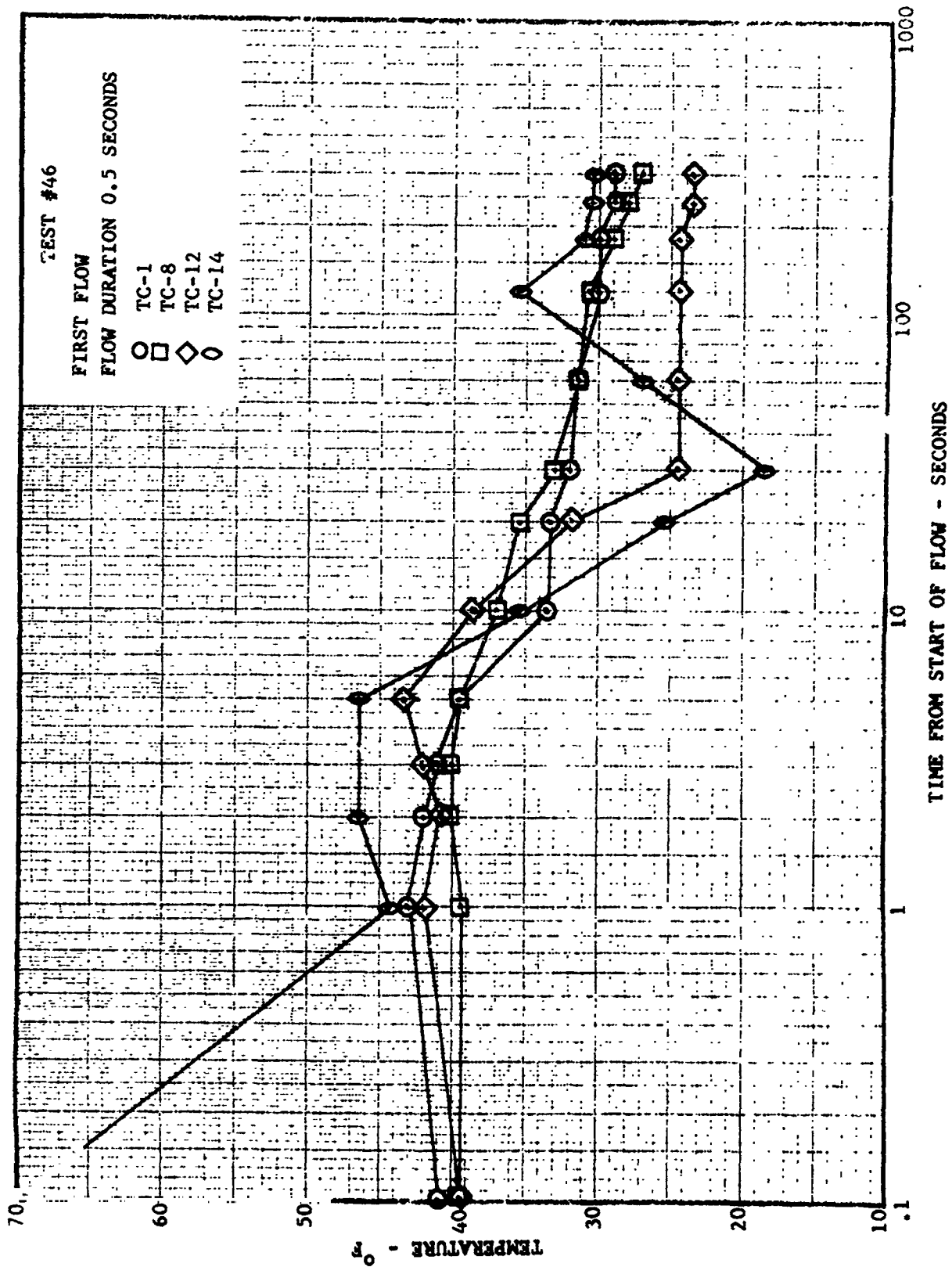


FIGURE 7-9 TEMPERATURE HISTORY FOR BELL INJECTOR

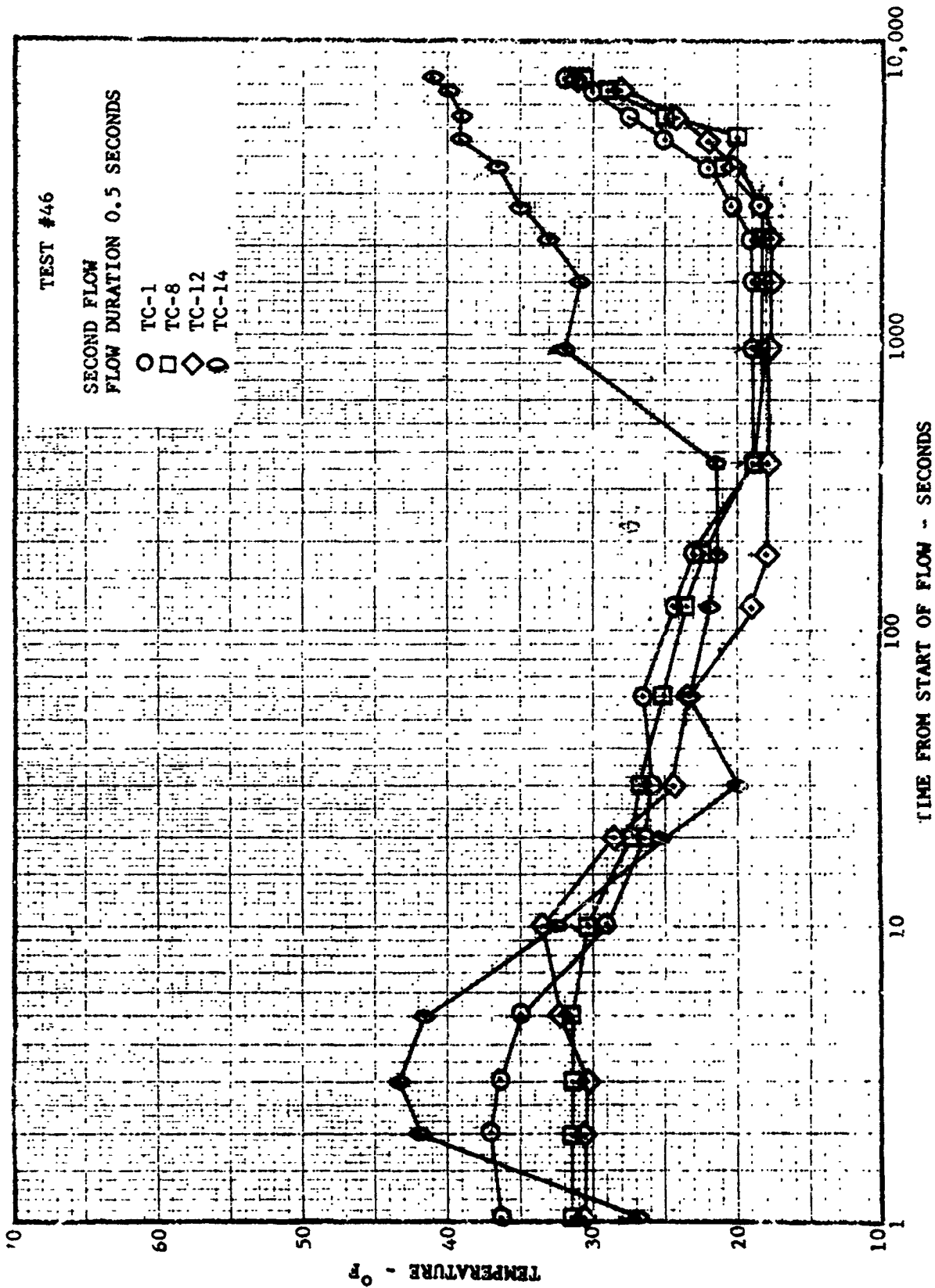


FIGURE 7-10 TEMPERATURE HISTORY FOR BELL INJECTOR

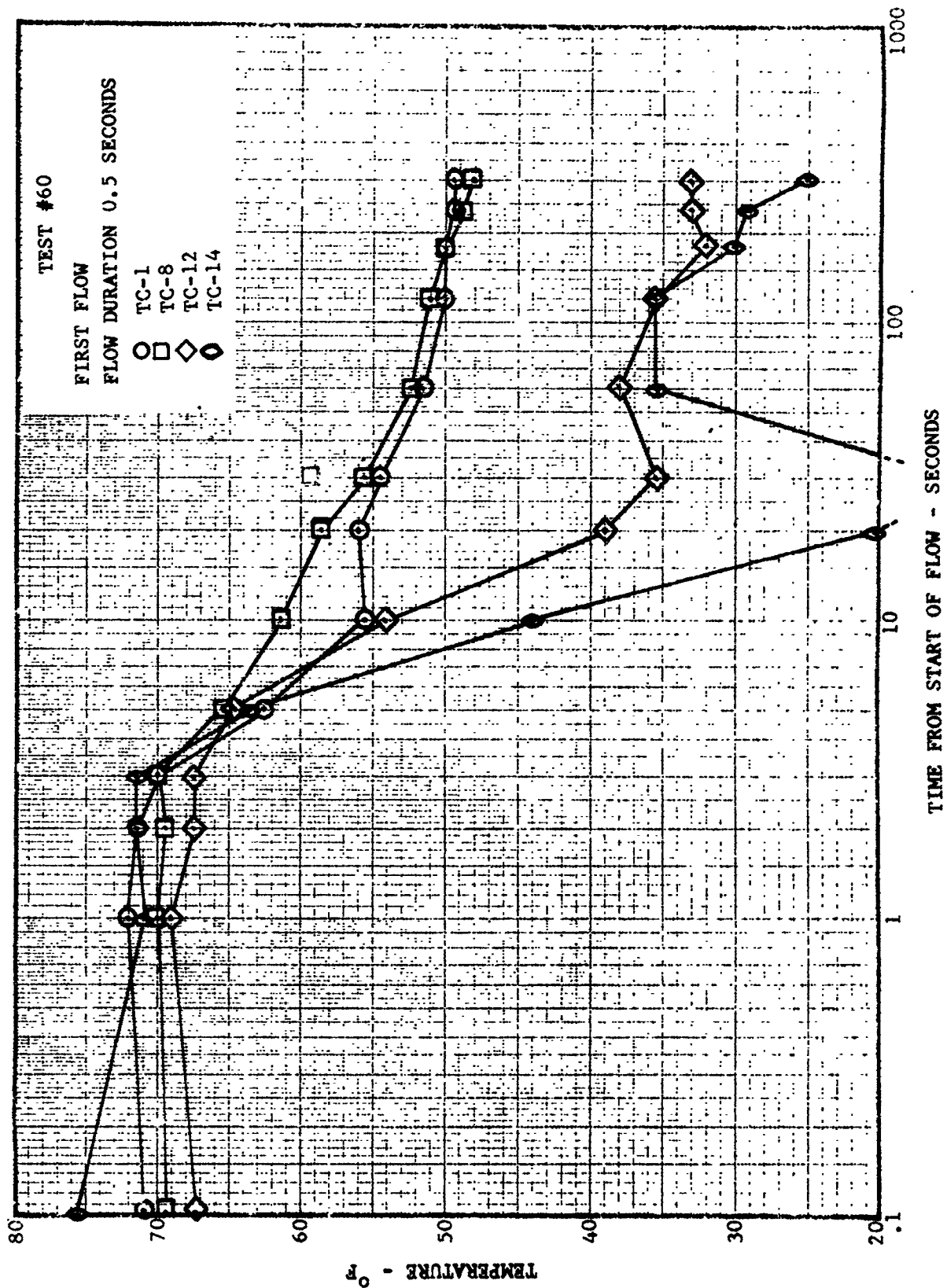


FIGURE 7-11 TEMPERATURE HISTORY FOR BELL INJECTOR

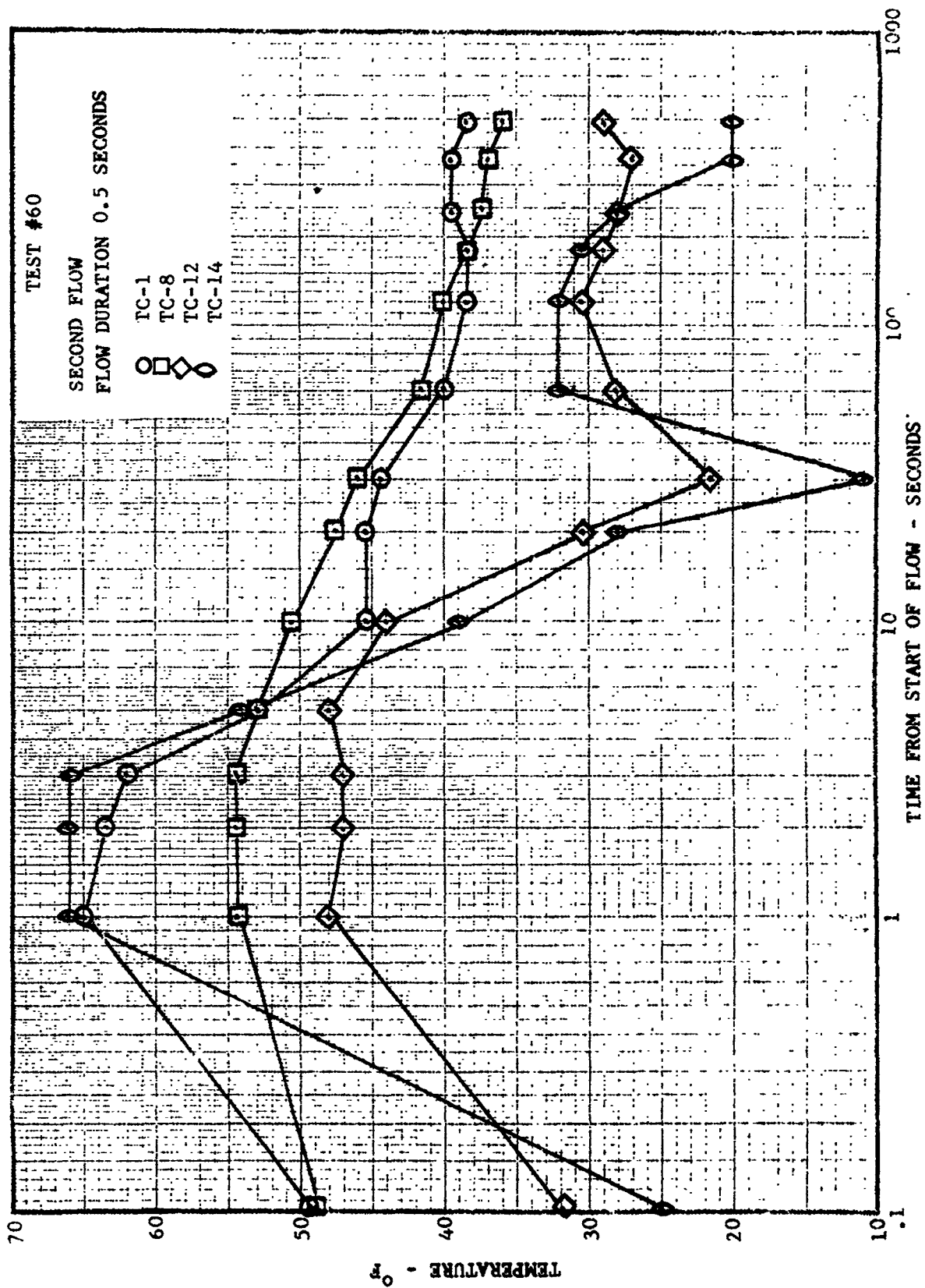


FIGURE 7-12 TEMPERATURE HISTORY FOR BELL INJECTOR

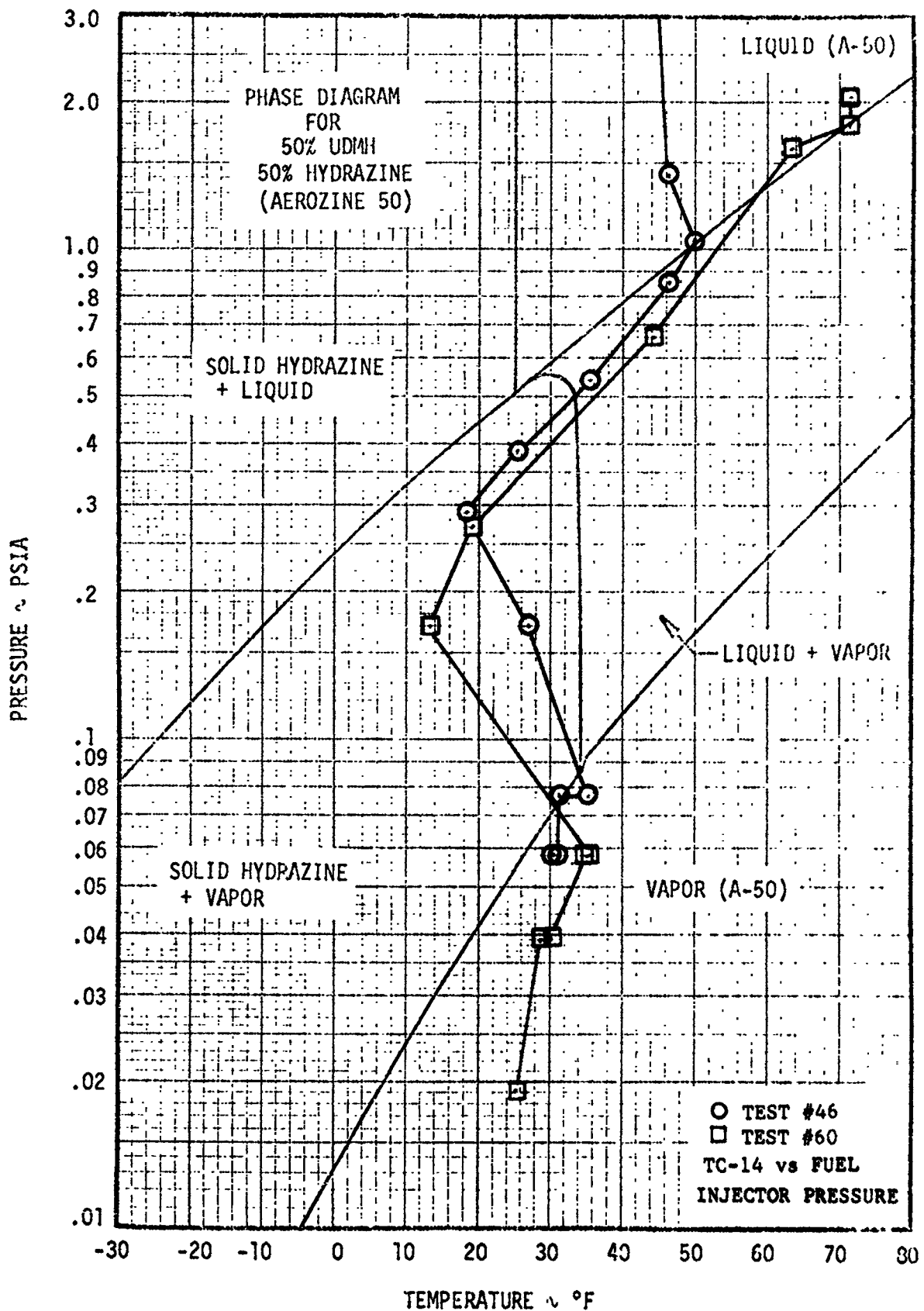


FIGURE 7-13 FUEL PHASE HISTORY, FIRST PULSE, BELL INJECTOR

D2-118246-1

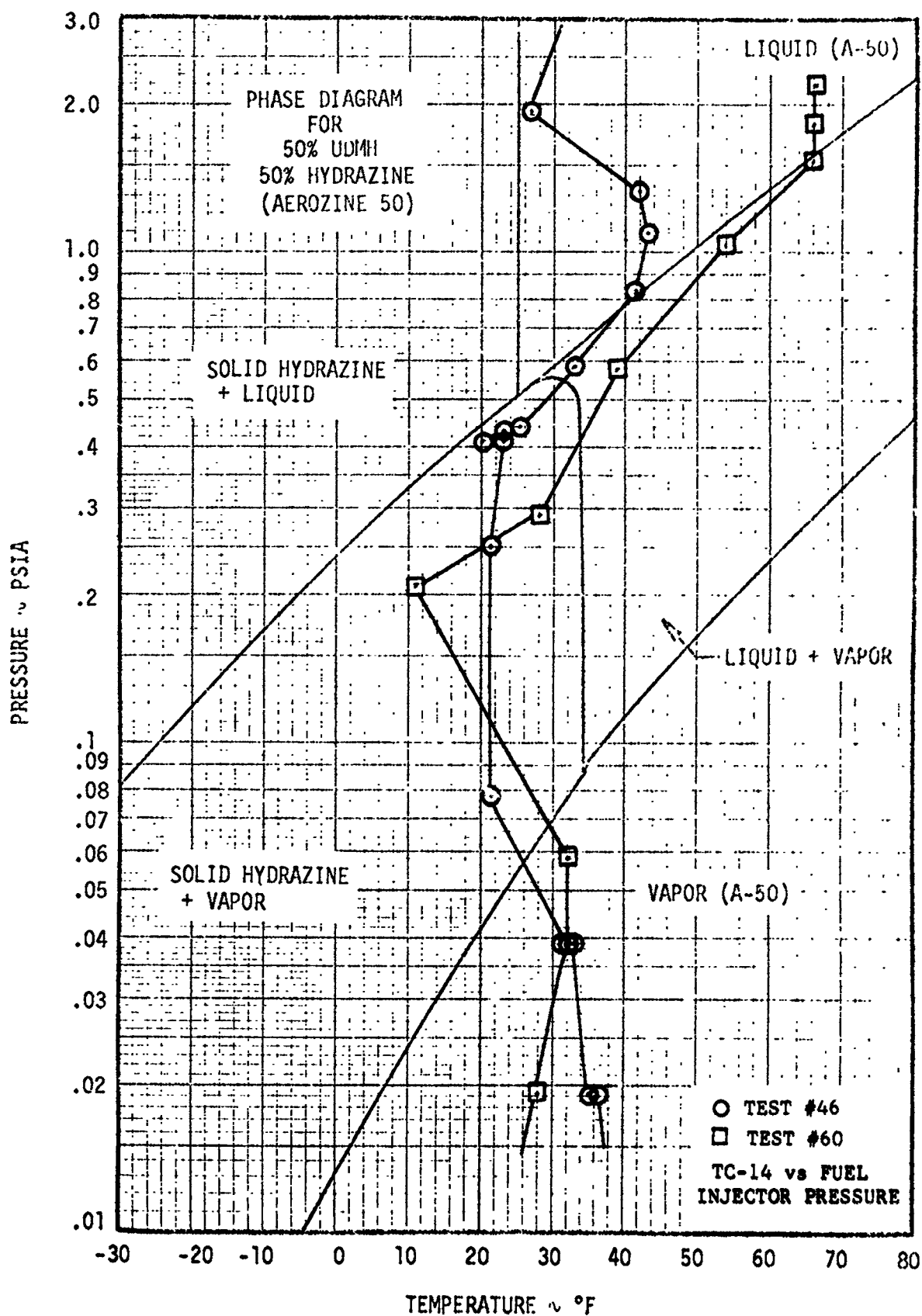


FIGURE 7-14 FUEL PHASE HISTORY, SECOND PULSE, BELL INJECTOR

7.2.2 Bell Ascent Injector, Phase II (Continued)

of single phases (liquid, solid, or vapor) or combinations of phases.

The phase diagram provides a useful frame of reference for evaluating propellant pressure-temperature or phase history, data. A brief discussion of test data from dual fuel pulse tests #46 and #60 (Figures 7-13 and 7-14) will illustrate the pressure-temperature data evaluation procedure. These figures show the temperature data from TC-14, located in the fuel duct, plotted against the pressure data from the 0-5 psia transducer located on the injector fuel manifold. The data for the first pulse of test #46 show an initial rapid pressure decrease without a corresponding temperature decrease. The propellant phase history crossed the phase boundary separating the liquid region from the liquid plus vapor region, at 1.0 psia and 50°F. In the liquid plus vapor region, continued pressure decreases resulted in temperature decreases because the liquid was cooled by evaporation. The evaporation, or boiling, process removed the heat of vaporization from the remaining liquid, thereby cooling it. The vapor formed during this process was principally UDMH, because UDMH has a significantly higher vapor pressure than hydrazine.

At a pressure and temperature of 0.5 psia and 34°F, the phase history for test #46 crossed the boundary separating the liquid plus vapor region from the solid hydrazine plus vapor region. The phase history would not have crossed this boundary if the evaporation process had been in thermodynamic equilibrium. An equilibrium process would have proceeded along the phase boundary, with vaporization of UDMH producing frozen hydrazine. The actual phase history indicates that the process was not in thermodynamic equilibrium and that liquid UDMH was present in the "solid hydrazine plus vapor" region. Evaporation of the UDMH cooled the residuals below the freezing temperature of the mixture, causing hydrazine to freeze out of the mixture. The relative concentration of frozen hydrazine increased, producing a liquid mixture which had an increasing concentration of UDMH. This occurred because the heat removed by the evaporation of one pound of UDMH (246 BTU) was sufficient to freeze approximately 1.5 pounds of hydrazine. The total amount of UDMH was continually decreased by evaporation, causing the rate of cooling to decrease. Heat transfer from the test facility then warmed the residuals to the freezing temperature of hydrazine.

At a pressure of 0.084 psia and a temperature of 34°F, the phase history crossed the boundary separating the "solid hydrazine plus vapor" region from the vapor region. This does not justify a conclusion that the residual propellants had completely evaporated or sublimed, because measurements of mass residuals show that significant amounts of propellant remained in the manifolds at this time (200 seconds). This disagreement between analysis methods is the result of the non-equilibrium propellant vaporization process.

7.2.2 Bell Ascent Injector, Phase II (Continued)

Comparison of the phase histories for tests #46 and #60 shows that an increase in initial propellant temperature from 42°F to 60°F caused an increase in the rate of fuel cooling. During test #60, the residual fuel was cooled approximately 30°F during the first 30 seconds of the test, but the residual fuel was cooled only 14°F during the first 30 seconds of test #46. The cooling rate was increased by the higher boiling rates resulting from the increase in vapor pressure between 42°F and 60°F.

The phase history for test #60 indicates that there were two "minimum" temperature periods during this test. This phenomena occurred during most of the Phase II Bell injector tests, but was more pronounced at warmer (70°F) initial propellant temperatures. The first "minimum" temperature occurred 30 seconds after the start of the fuel flow pulse. The temperature increase after this time occurred because the rate of evaporative cooling had decreased, allowing the duct temperature to increase to the freezing temperature of hydrazine (34°F). The decreased cooling rate indicated that the liquid UDMH was essentially depleted, and the temperature level indicated that the remaining fuel consisted of frozen hydrazine. Comparing the fuel residual data (Figure 3-1) to the evaporation required to cause complete freezing (see Section 7.1.2) confirms that sufficient fuel had been evaporated after 30 seconds to cause complete freezing of the residual hydrazine. The second "minimum" temperature occurred after the manifold pressure had decayed below the hydrazine triple point pressure, causing an increase in the rate of sublimation. The increased rate of sublimation caused decreasing duct temperatures, until the residual hydrazine was essentially depleted. After hydrazine depletion, heat transfer caused a temperature increase.

The phase histories for tests #46 and #60 show that the fuel started to boil in 3 to 5 seconds after the start of the 1/2 second fuel pulse, and started to freeze approximately 15 seconds after the start of the fuel pulse. These times were essentially the same for both 40°F and 70°F propellant temperatures and for both first and second coast periods.

7.2.3 TRW Descent Injector

Selected test data from the TRW descent injector test series are presented on Figures 7-15 through 7-20. Figure 7-15 is a temperature history of the injector for test #18, run at an initial propellant and injector temperature of 40°F. Figure 7-16 is the fuel phase history for the first coast period of tests #12 and #18, and Figure 7-17 is the fuel phase history for the second coast period of test #12. Figure 7-18 is the oxidizer phase history for tests #25 and #26. Figures 7-19 and 7-20 present a comparison between duct surface and immersion thermocouples.

The injector temperature history presents thermocouple data from the

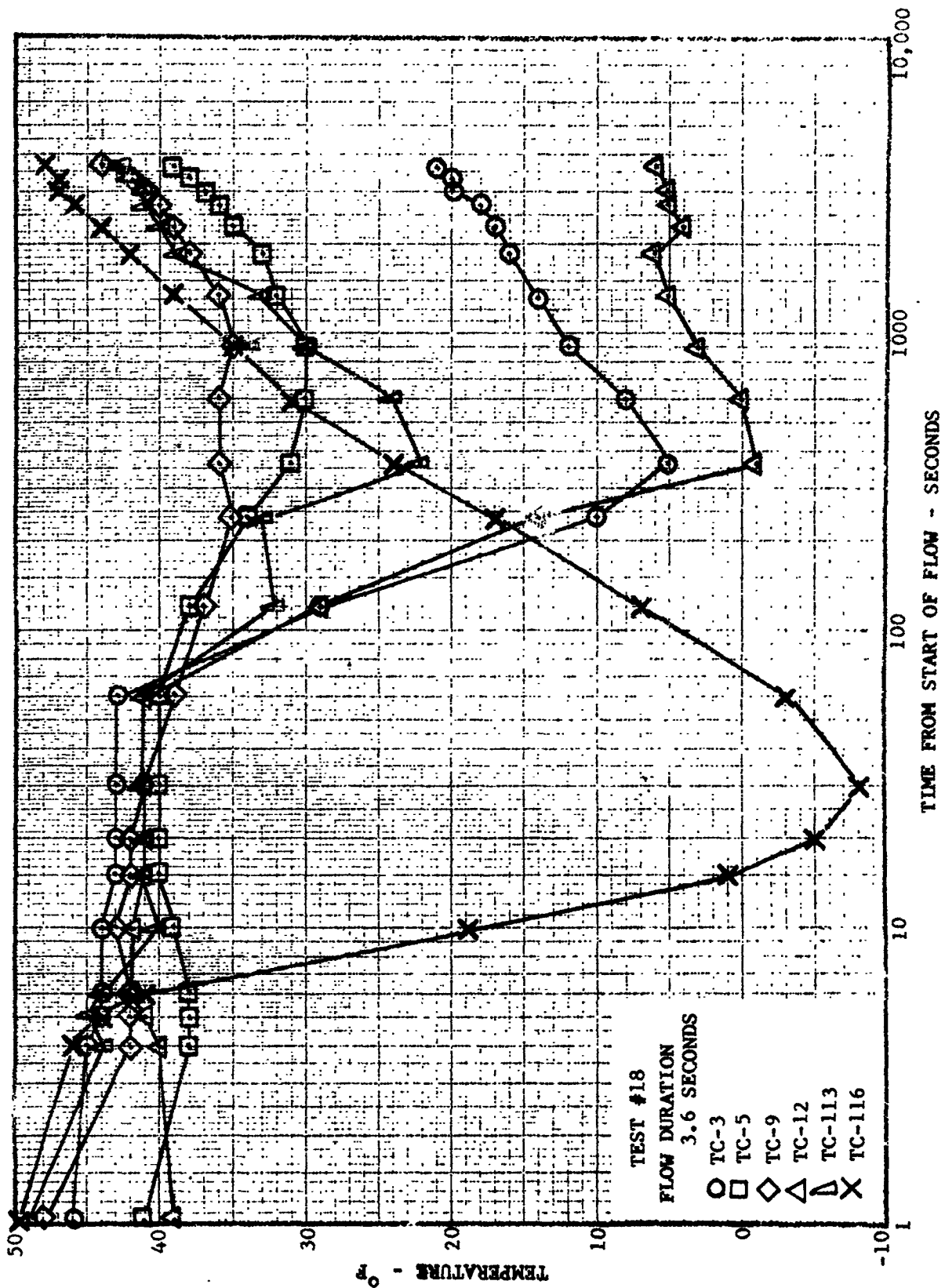


FIGURE 7-15 TEMPERATURE HISTORY FOR DESCENT INJECTOR

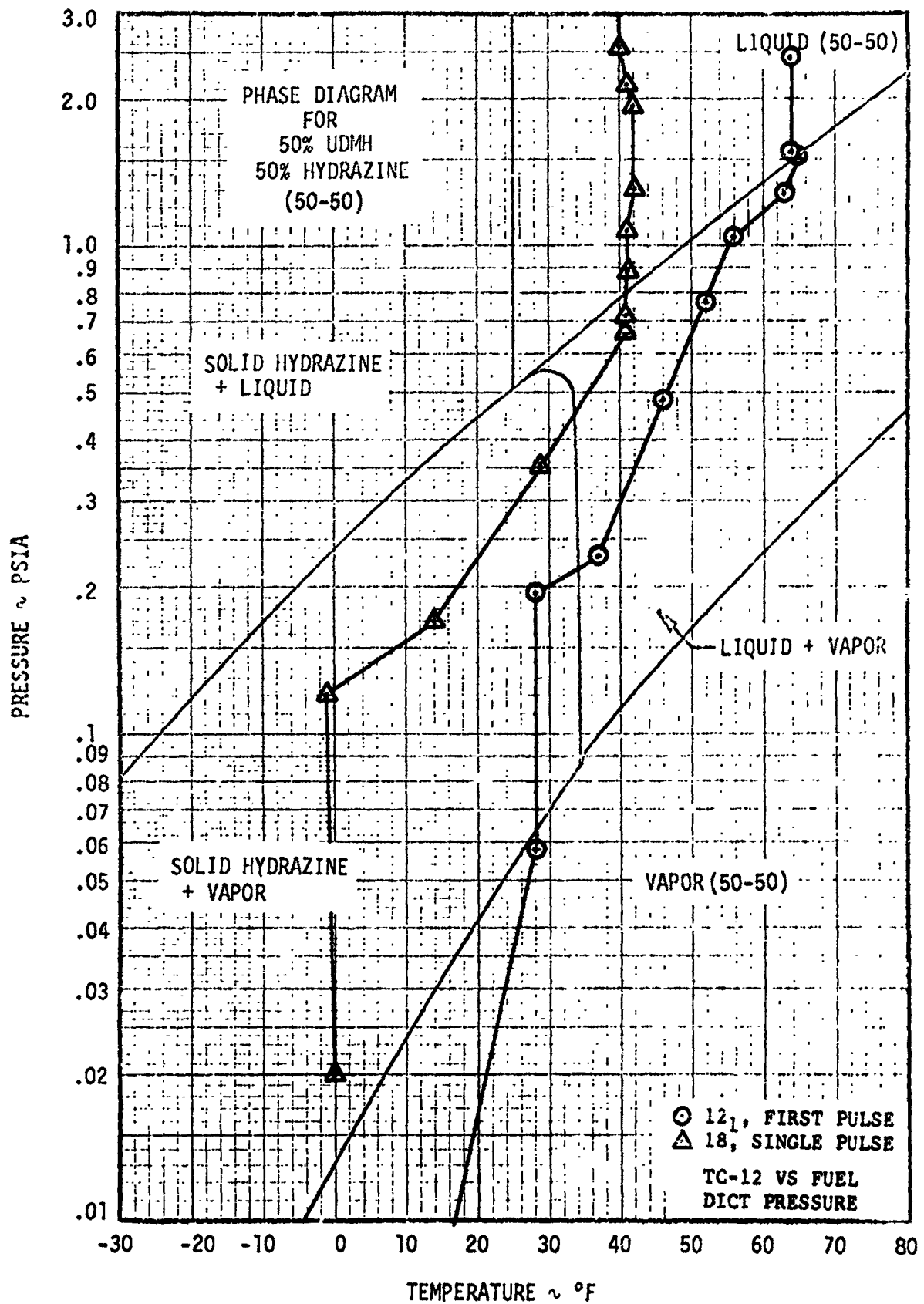


FIGURE 7-16 FUEL PHASE HISTORY FOR DESCENT INJECTOR

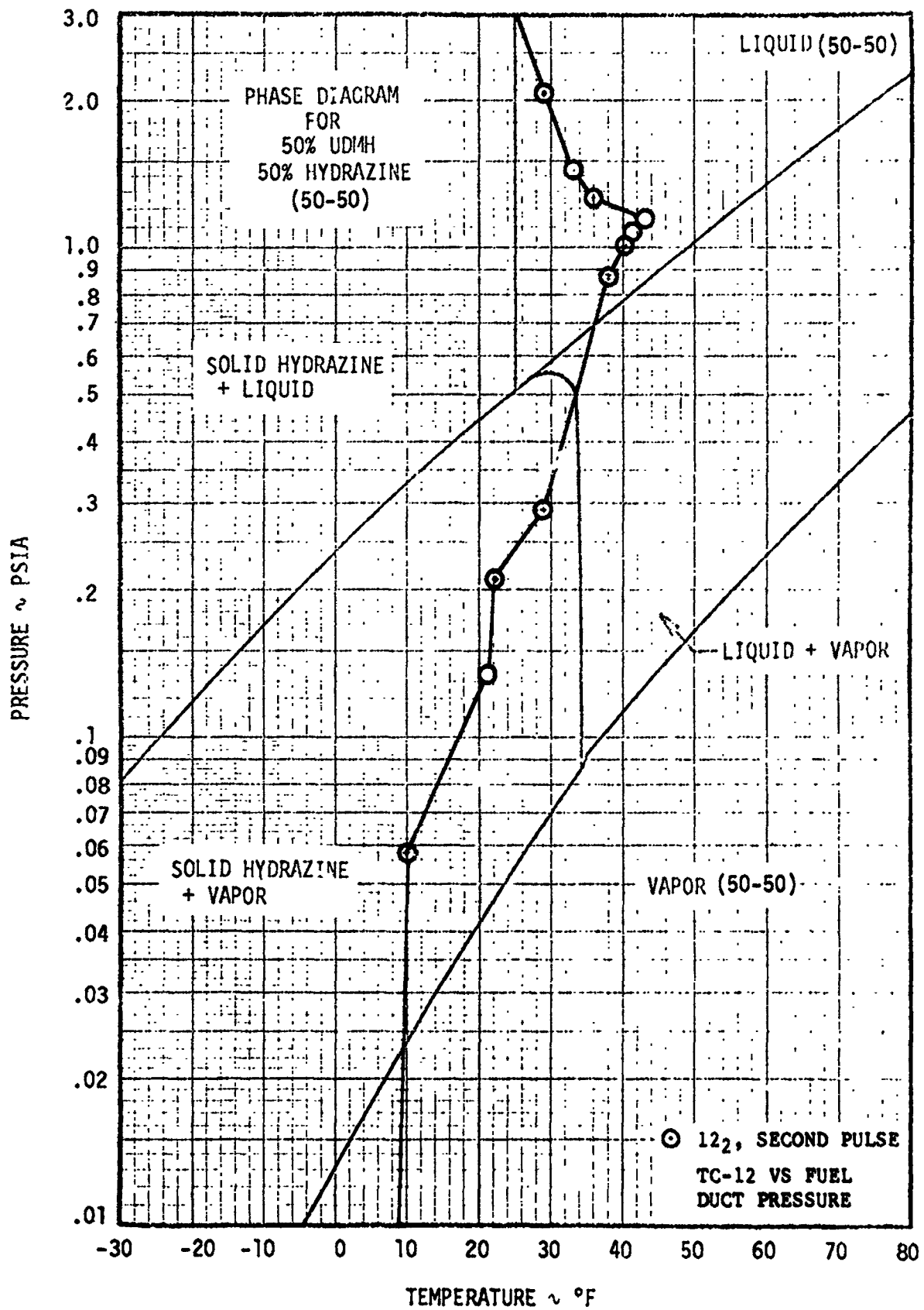


FIGURE 7-17 FUEL PHASE HISTORY FOR DESCENT INJECTOR

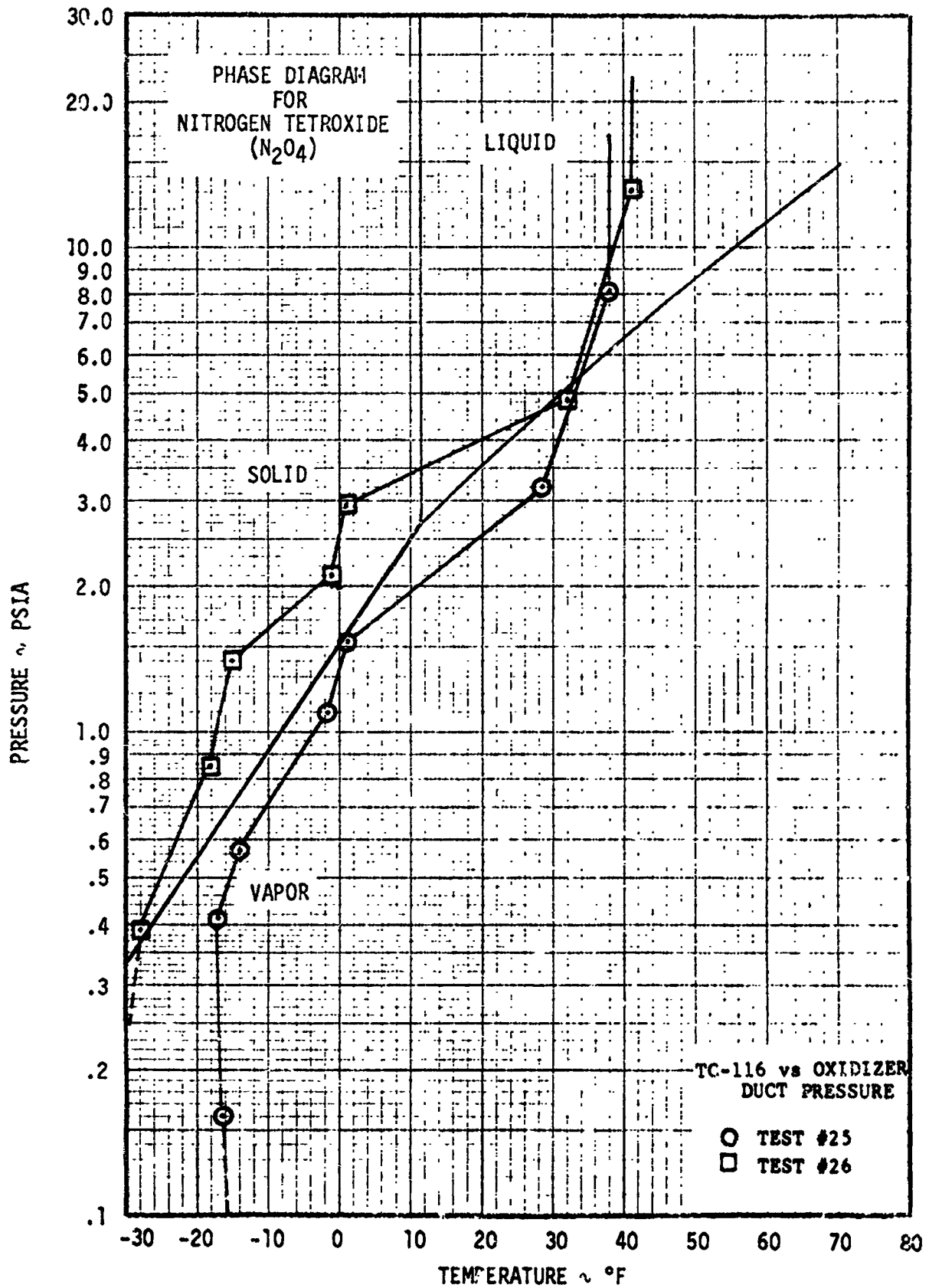


FIGURE 7-18 OXIDIZER PHASE HISTORY FOR DESCENT INJECTOR

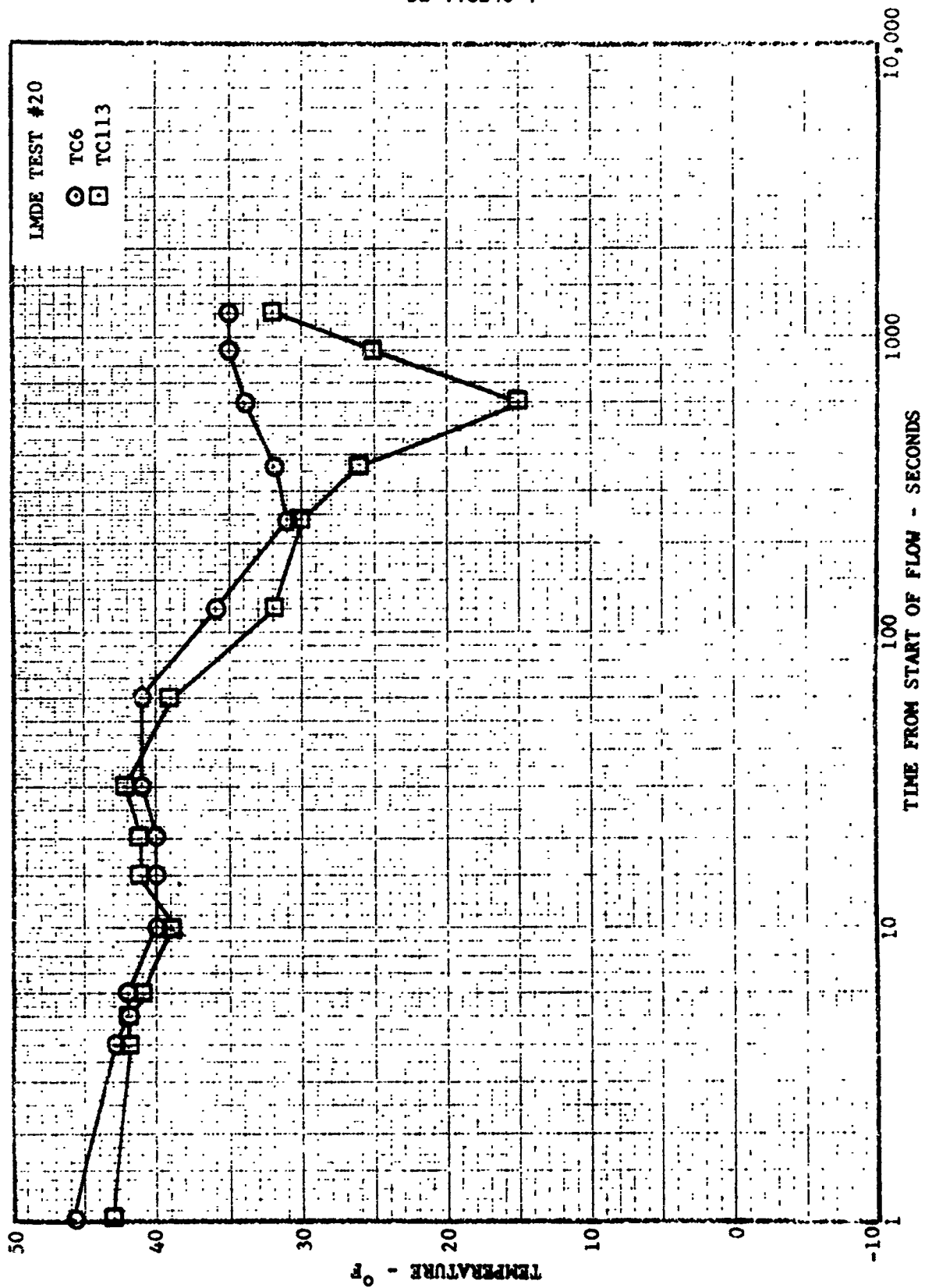


FIGURE 7-19 TEMPERATURE HISTORY FOR DESCENT INJECTOR

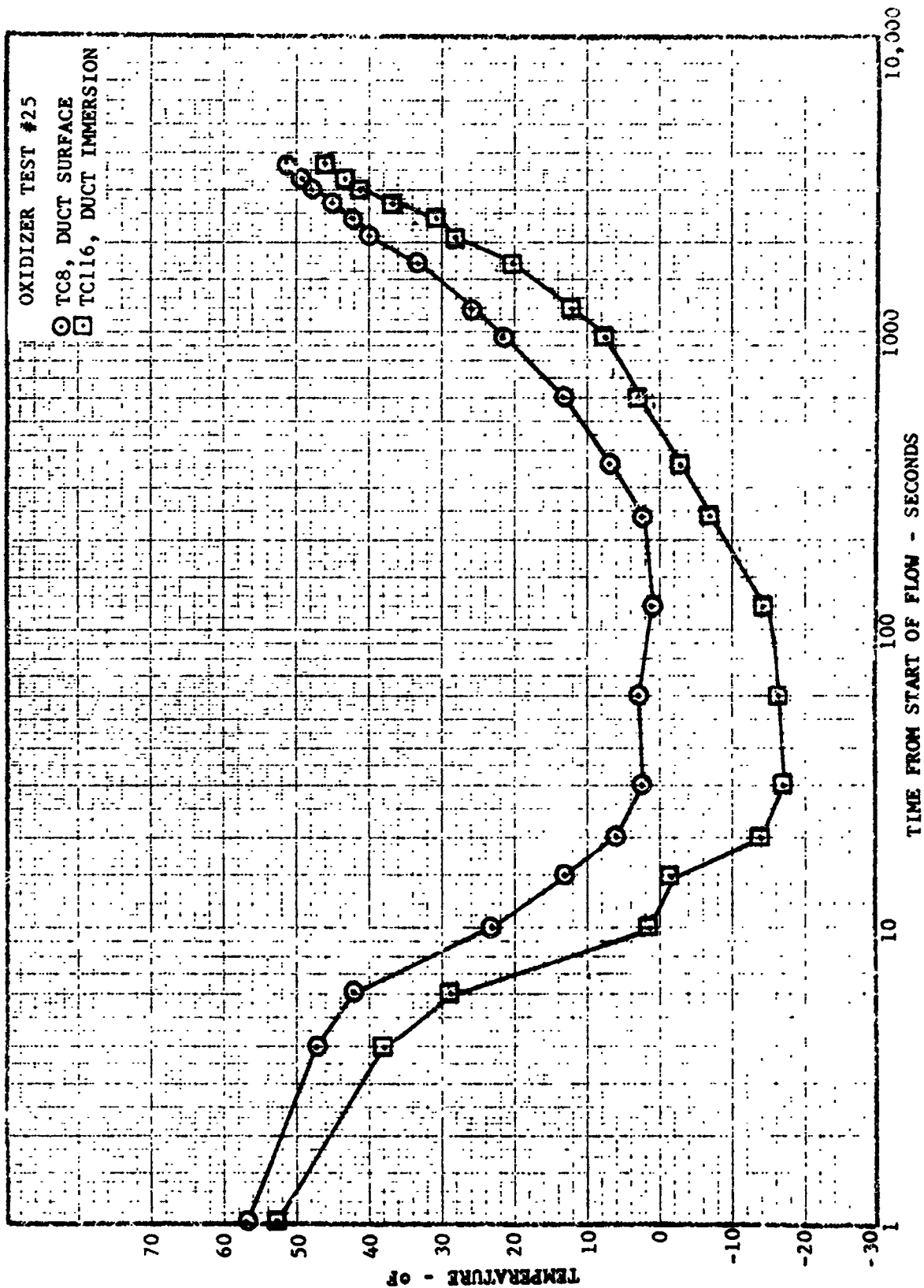


FIGURE 7-20 TEMPERATURE HISTORY FOR DESCENT INJECTOR OXIDIZER DUCT

7.2.3 TRW Descent Injector (Continued)

oxidizer duct immersion probe (TC-116), the fuel duct immersion probe (TC-113), the fuel manifold top (TC-5), side (TC-3) and bottom (TC-12), and the injector mounting flange (TC-9). The oxidizer duct thermocouple shows that the simulant (Freon TF) reached a minimum temperature (-6°F) and then increased in temperature before any significant fuel side cooling occurred. This effect was caused by a combination of high simulant vapor pressure and low fuel injector ΔP . The high simulant vapor pressure caused rapid evaporation and cooling on the oxidizer side. The low fuel injector ΔP caused low fuel vapor flow rates, which suppressed the fuel side evaporative cooling.

The fuel side cooling was significantly greater in the injector manifold than in the fuel duct, indicating that a major part of the fuel residuals were trapped in the injector manifold.

The low injector temperatures at one hour after the propellant flow indicates that frozen fuel residuals were still present. This conclusion is confirmed by the data from propellant residual measurements.

The fuel phase histories, Figures 7-16 and 7-17, are plots of the injector fuel manifold temperature (TC-12) versus the injector fuel manifold pressure. The external fuel manifold thermocouple, located at the bottom of the manifold, was chosen for the phase histories because residuals are located in this area for the longest period of time, producing the lowest measured fuel side temperatures. The main problem in using data from TC-12 is that it was located on the exterior of the 29.5 lb injector assembly. The large injector mass delays the response of TC-12, but the delay does not appear to significantly affect the test data. Comparison of TC-12 to TC-113 (the immersion probe in the fuel duct) shows that both probes have essentially the same response to the propellant temperature decrease which occurred at 60 seconds (see Figure 7-15).

The fuel phase histories for the initial coast period show that the time to the start of boiling varied significantly with the initial propellant/injector temperature. At an initial temperature of 40°F , boiling was indicated at 25 seconds, but at an initial temperature of 70°F boiling was indicated at only 5 seconds. Despite the variation in the time required to reach boiling conditions, the time required to reach freezing conditions was essentially the same, about 90 seconds, for both tests.

The fuel phase history for the second coast period of test #12 shows that the injector was warmed by the propellant flow, and that the occurrence of boiling was rapidly followed by the occurrence of fuel freezing. None of the fuel phase histories pass through the hydrazine triple point at 0.058 psia and 34°F .

7.2.3 TRW Descent Injector (Continued)

The oxidizer phase history, Figure 7-18 is a plot of the oxidizer duct immersion thermocouple (TC-116) versus the oxidizer duct pressure. The phase history indicates that boiling occurred within 5 to 6 seconds after the start of the 3.5 second oxidizer flow, and that freezing occurred approximately 8 seconds after the start of the flow. These conclusions are tentative because of indicated pressure instrumentation problems during these two tests. Comparing the pressure data from test #26 to the data from test #25 indicated that the data from test #26 are high by a factor of 1.5. This conclusion is substantiated by the fact that evaporative cooling of a single-component liquid cannot result in significant liquid super-cooling. Specifically, the phase history is not represented by the regime above and to the left of the liquid-vapor or solid-vapor phase boundaries.

The descent engine used for the Seattle hot-firing tests was instrumented with surface thermocouples on the injector and propellant ducts, but was not equipped with immersion thermocouples. The thermal response of the duct surface thermocouples was evaluated by using the cold-flow test data to compare the response of duct surface and duct immersion thermocouples.

Figure 7-19 compares the response of an immersion thermocouple (TC-113) located near the top of the fuel duct to the response of a surface thermocouple (TC-6) located at the midpoint of the duct. Both thermocouples showed the same response, within 2°F, during the first 60 seconds of the test, and were within 4°F during the first 240 seconds of the test. Beginning at 240 seconds, the immersion thermocouple indicated a significant temperature decrease that was not detected by the surface thermocouple. The maximum indicated temperature difference was 19°F at 600 seconds.

Figure 7-20 compares the response of an immersion thermocouple (TC-116) located near the bottom of the oxidizer duct to the response of a surface thermocouple (TC-8) located directly opposite from the immersion thermocouple. The temperature data at the beginning and end of the test indicate that the surface thermocouple is biased approximately 4-5°F higher than the immersion thermocouple. Temperature data from the initial cooling phase show a maximum temperature difference of 15-16°F after correcting for the indicated data bias.

7.2.4 Rocketdyne Ascent Injector

Selected test data from the Rocketdyne injector test series are presented on Figures 7-21, 7-22, 7-23, and 7-24. Figures 7-21 and 7-22 are injector temperature histories for tests #1 and #15, run at initial temperatures of 40°F and 70°F, respectively. The injector thermal histories present temperature data from TC-4 (lower fuel duct surface), TC-6 (lower fuel

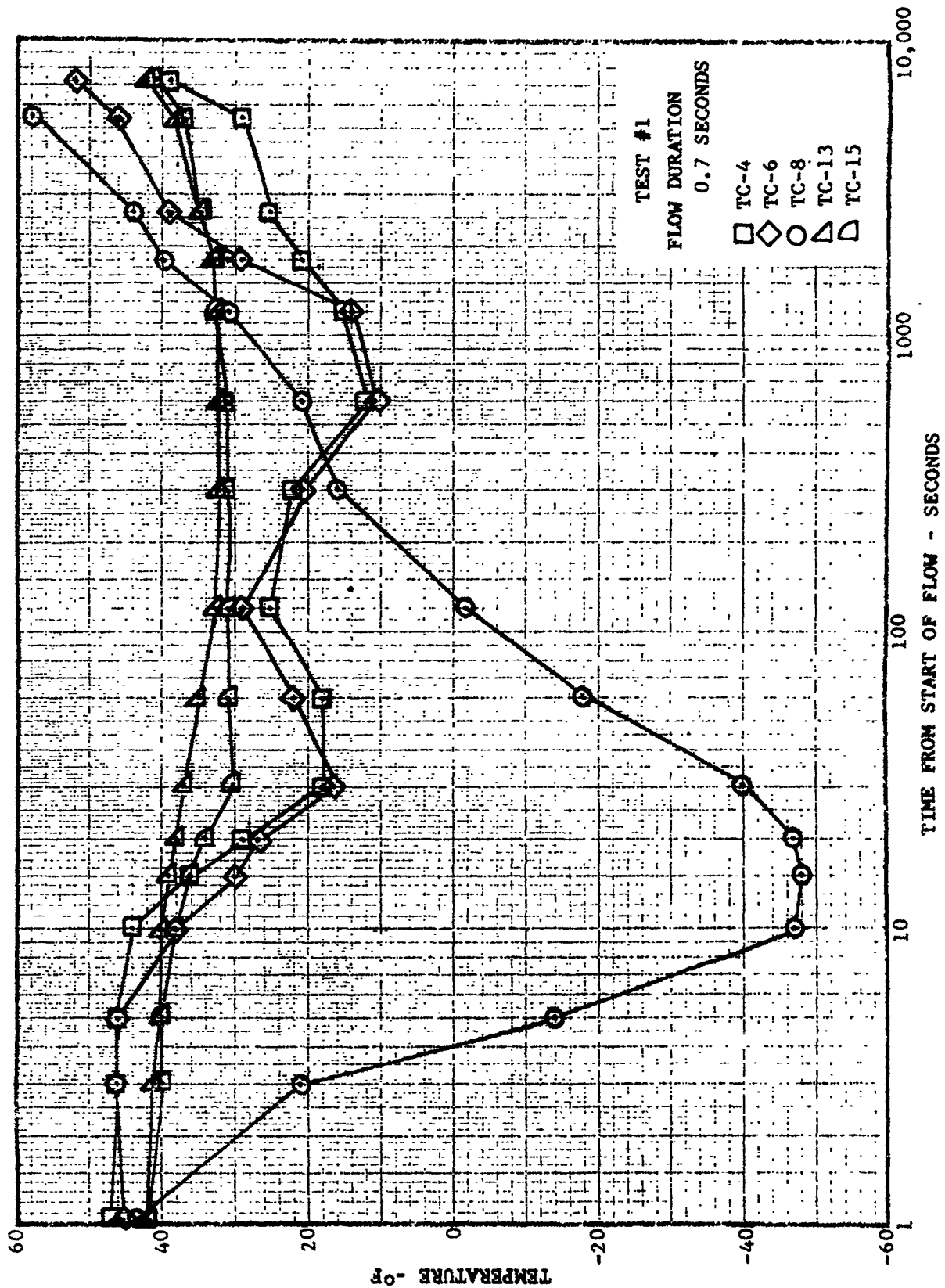


FIGURE 7-21 TEMPERATURE HISTORY FOR ROCKETDYNE INJECTOR

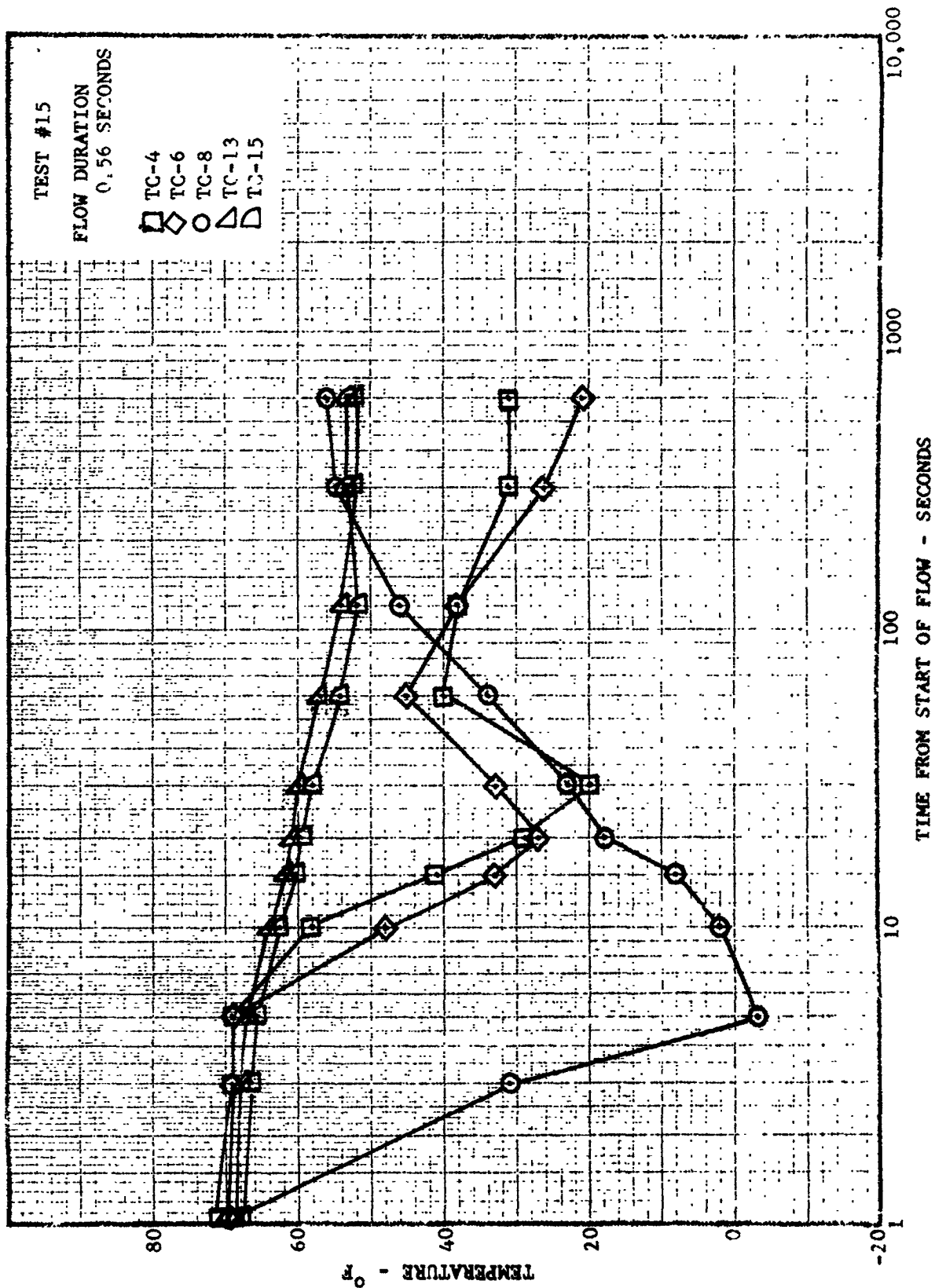


FIGURE 7-22 TEMPERATURE HISTORY FOR ROCKETDYNE INJECTOR

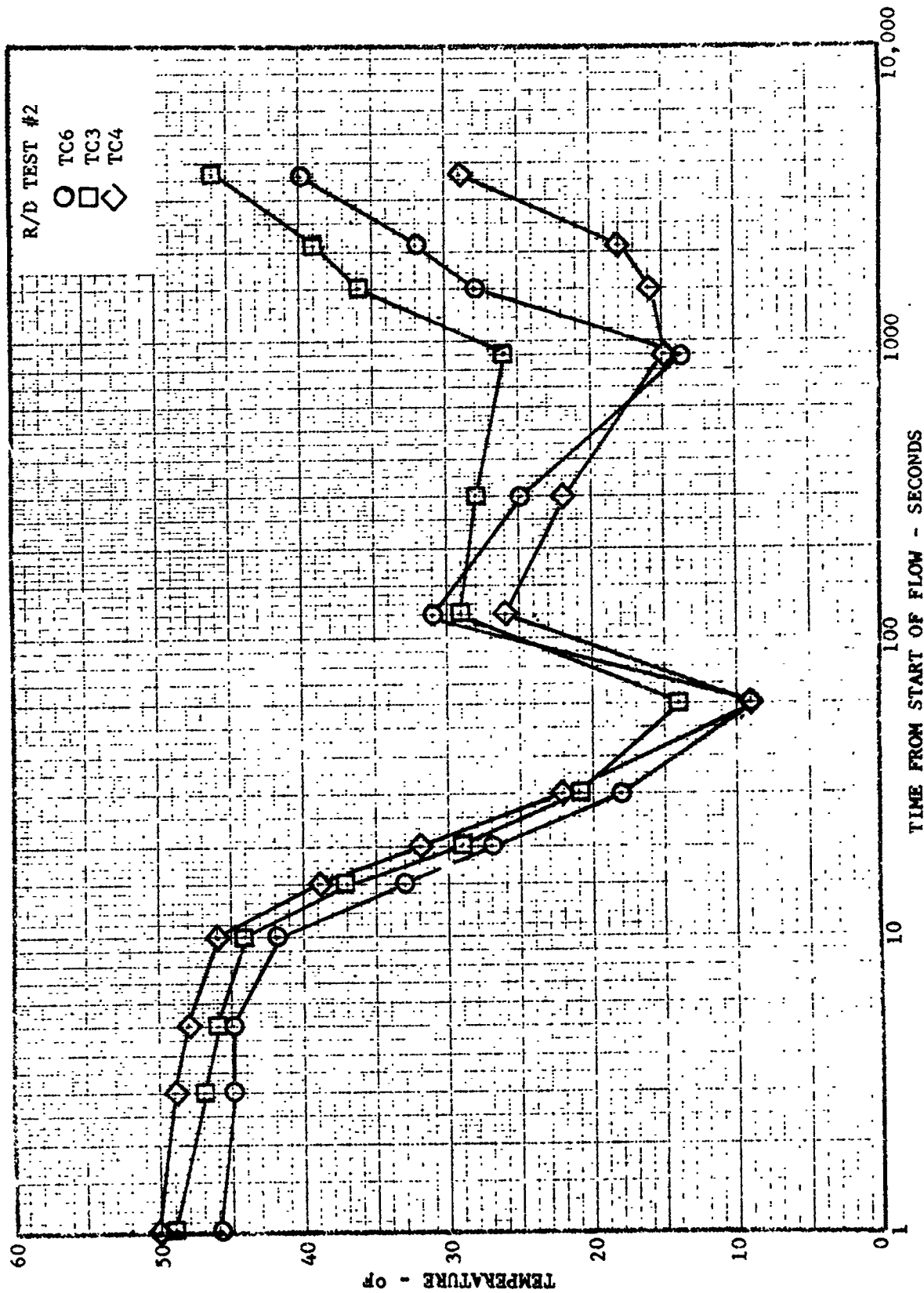


FIGURE 7-23 TEMPERATURE HISTORY FOR ROCKETDYNE INJECTOR

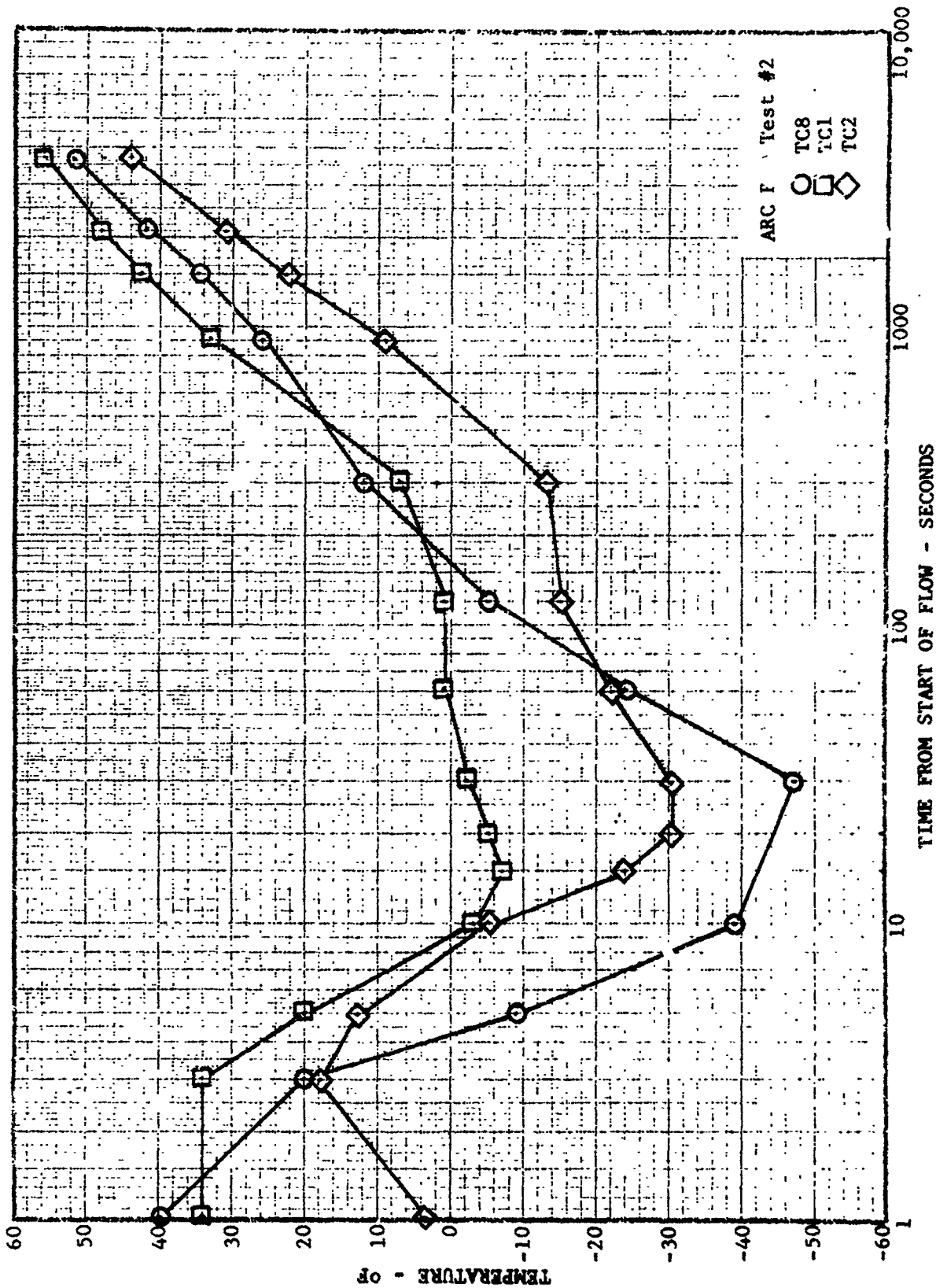


FIGURE 7-24 TEMPERATURE HISTORY FOR ROCKETDYNE INJECTOR

7.2.4 Rocketdyne Ascent Injector (Continued)

duct immersion thermocouple), TC-8 (midpoint oxidizer duct surface), TC-13 (injector back surface, near top), and TC-15 (injector back surface, near bottom). Phase histories for the Rocketdyne injector cannot be drawn because an error in injector instrumentation resulted in the loss of usable fuel manifold pressure data.

Both temperature histories indicated a decrease in fuel duct temperature approximately 5 seconds after the start of the 0.5 second duration propellant pulse. Based on the analysis of Bell injector phase histories, this temperature decrease was caused by fuel boiling in the ducts. The time required for the fuel to begin boiling was the same for both 40°F and 70°F initial temperatures. The fuel temperature decreased to the freezing value (34°F) at 12-15 seconds after the start of the propellant pulse.

The fuel duct temperature data showed that "minimum" fuel temperatures were reached at two distinct time periods. The first "minimum" occurred at 20 to 30 seconds, and the second "minimum" occurred at approximately 600 seconds. The fuel temperature increased approximately 10 to 20 degrees following the first minimum temperature period, and then decreased to the second "minimum" temperature region. Based on the previous analysis of Bell and TRW injector fuel phase histories, the first minimum temperature period is attributed to the rapid evaporation of UDMH, which cooled the residual fuel to a temperature below the freezing point of hydrazine (34°F). When the UDMH content of the residual had been significantly reduced, the duct temperatures increased. The second temperature decrease was caused by the sublimation of hydrazine after the fuel duct pressure decreased below the hydrazine triple point pressure of 0.058 psia.

The oxidizer duct temperature history was similar to the descent injector history. Specifically, the oxidizer duct temperature decreased to a minimum level before significant injector or fuel temperature reductions occurred. The oxidizer duct temperature reached a minimum within 5 to 10 seconds after the start of the propellant pulse, and then continuously increased to ambient. The minimum temperature was reached sooner when the initial temperature was 70°F than when the initial temperature was 40°F. This is attributed to the higher vapor pressure of the oxidizer simulant at 70°F, which increases the rate of boiling and thereby increases the rate of cooling.

The ascent engine used for Seattle hot-firing tests was instrumented with surface thermocouples on the injector and propellant ducts, but was not equipped with immersion thermocouples. The thermal response of the duct surface thermocouples was evaluated by using the cold-flow test data to compare the response of duct surface and duct immersion thermocouples.

7.2.4 Rocketdyne Ascent Injector (Continued)

Figure 7-23 compares the response of an immersion thermocouple (TC-6) located approximately 2 inches above the fuel duct elbow to the responses of a surface thermocouple (TC-3) located approximately 6 inches above the elbow and a surface thermocouple (TC-4) located on the bottom of the elbow near the valve assembly. All thermocouples showed the same response, within $\pm 1^\circ\text{F}$, until the minimum temperature was reached at 60 seconds. After this time, the response of the thermocouples was a function of the liquid level in the fuel duct. For example, TC-3 did not follow the decrease in fuel temperature at 300 seconds, indicating that the liquid level was below this thermocouple and that it was being cooled by heat transfer in the duct walls and by cold vapor flowing past it. TC-3 began to increase in temperature first, followed by the immersion thermocouple, TC-6. The surface thermocouple TC-4 remained at a low temperature ($15\text{--}18^\circ\text{F}$) for an additional 1000 seconds, indicating that the residual fuel was located near this thermocouple.

Figure 7-24 compares the response of an immersion thermocouple (TC-8) located approximately 3 inches above the oxidizer duct elbow to the responses of a surface thermocouple (TC-1) located approximately 6 inches above the elbow and a surface thermocouple (TC-2) located on the bottom of the elbow near the valve assembly. The thermocouple data show that neither of the surface thermocouples accurately followed the initial rapid decrease in simulant (Freon MF) temperature. The surface thermocouple at the bottom of the oxidizer duct (TC-2) followed the response of the immersion thermocouple with an initial time lag of 5 to 8 seconds, but did not indicate the low minimum temperature (-47°F) shown by the immersion thermocouple. The surface thermocouple at the midpoint of the duct began to show a temperature increase at 15 seconds, indicating that the simulant liquid level was below this thermocouple at that time.

Analysis of the oxidizer duct thermocouple response was complicated by the fact that the simulant (Freon MF) has a freezing point of -168°F and therefore did not freeze during these tests. The oxidizer has a freezing point of 12°F , which would tend to slow the rate of temperature decrease near this temperature when the oxidizer begins to solidify. However, it can be concluded that the surface thermocouples will indicate liquid temperatures with a time delay of 5 to 8 seconds during the initial temperature decrease. In addition, the surface thermocouples may indicate a temperature approximately 15 to 18°F higher than the true minimum oxidizer temperature.

7.3 ASCENT ENGINE TEST ANALYSIS

7.3.1 General

This section presents an analysis of the results from Phase I and Phase II Ascent engine restart tests conducted at the Boeing/Seattle test facility. The initial starts and restarts were analyzed to determine the effect of propellant residuals on the engine restarts. Coast phase data on propellant pressures and temperatures were plotted on phase diagrams. This method of data presentation provides a basis for determining the thermodynamic state of propellant residuals which were present at the ascent engine restarts. A summary of the test conditions and test results is presented in Tables 4-1 and 4-3.

The Seattle Phase I test series consisted of 5 tests. The checkout firing (A-0), consisted of only one start while the remaining four tests (A-1, A-2, A-3, and A-4) consisted of an initial firing followed by one restart at coast periods of 1500, 300, 90, and 30 seconds. Following the 30 second coast period (test A-4), all accelerometers saturated, indicating greater than 1000 g's on the facility transducers and greater than 35 g's on the flight transducers. Maximum accelerometer readings for the Phase I restarts, and the Phase II first restarts, are presented in Figure 7-25. These data show that the Phase I restarts, run with 60-65°F propellants, had lower maximum accelerometer readings than the Phase II restarts, run with 45-50°F propellants.

While no special attempt was made to saturate the propellants with helium for the Phase I tests, an analysis of the propellant for inert gas content was made for each test. For the oxidizer side, tests A-3 and A-4 had 0.142 and 0.163 scc/gram of dissolved helium respectively, which is greater than 1/2 of the saturation amount of 0.22 scc/gram at 190 psia. Similarly, the fuel side for all tests contained approximately 1/2 of the saturation amount.

The Seattle Phase II test series consisted of 10 tests. The two checkout runs, A-0-II₁ and A-0-II₂, consisted of one start for each test. The first checkout run was considered to be unsuccessful because an unplanned 200 millisecond restart occurred and the facility altitude was low during the coast period. The second checkout firing was successful. Tests A-5 through A-7 consisted of an initial start followed by two restarts. Tests A-8 through A-12 consisted of an initial start followed by one restart. Coast periods 200, 90, 60, 30, 15, 10, 2.5 and 1 second were tested during A-5 through A-12 respectively. Tests A-6, A-7, A-8 and A-9 (at coast periods of 90, 60, 30, and 15 seconds respectively) each had rough restarts as indicated by high pressure spikes and high accelerometer readings (see Figure 7-25). On test A-7, the second restart attempt was not successful. Test data indicate that the oxidizer side was plugged with frozen oxidizer.

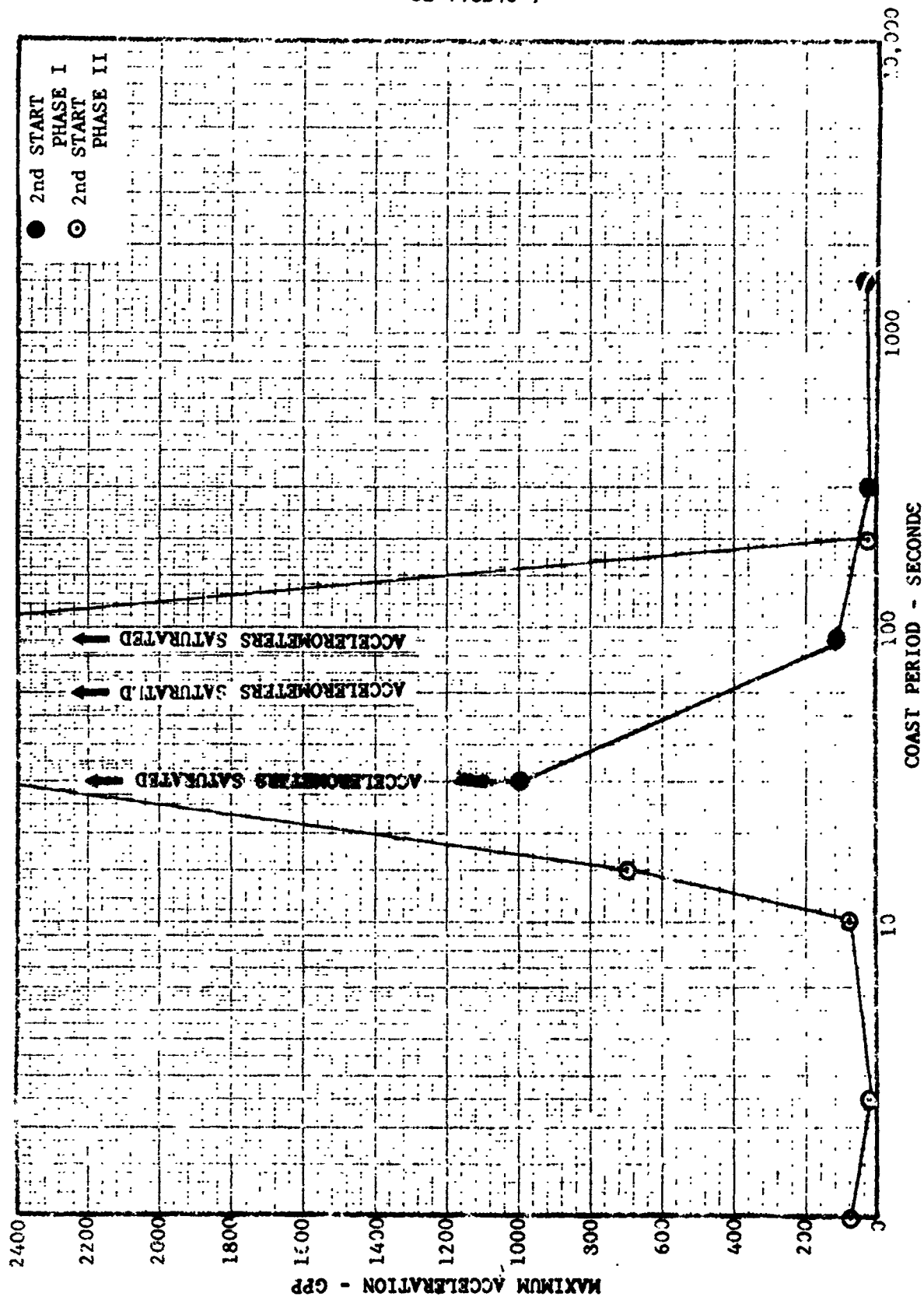


FIGURE 7-25 MAXIMUM ACCELEROMETER READING AT IGNITION VS
ASCENT ENGINE COAST PERIOD

7.3.2 Coast Phase Analysis

The fuel and oxidizer duct temperatures and pressures were plotted on phase diagrams to analyze the thermodynamic processes occurring during the coast phase. The data were plotted for time intervals of 5, 10, 15, 20, 25, 30, 40, 50, 60, 70, 80, 90, 100, 150, 200, 250, 300, 400, 500, 600, 700, 800, 900, and 1000 seconds following engine shutdown. The test coast time and data availability determined the time duration for which data were plotted.

The fuel phase histories for the initial coast period of Phase I tests A-0, A-3, and A-4 are in Figure 7-26. The fuel phase histories for the coast period following the restarts on tests A-2, A-3, and A-4 are in Figure 7-27. Comparison of Figures 7-26 and 7-27 shows that there was no significant difference between the first and second coast periods. The restart temperature data indicate that the fuel ducts were warmed to the temperature of the fuel supply before the onset of boiling.

The oxidizer phase histories for the initial coast period of Phase I tests A-3 and A-4, and for the coast period following the restarts of tests A-2, A-3, and A-4 are in Figure 7-28. These data show that the oxidizer ducts remained at a low temperature during and after the restart firings. In contrast to the fuel side, the oxidizer side was not warmed to the temperature of the propellant supply.

The oxidizer manifold phase histories indicate that the oxidizer is far out of thermodynamic equilibrium because the manifold pressure is much lower than the equilibrium oxidizer vapor pressure. This would indicate that the boiling process is very violent and sufficiently far from equilibrium to prevent any thermodynamic analysis of the process. It is not clear from the phase history data when boiling starts or when freezing starts. However, temperature data indicate that boiling does start prior to 5 seconds into the coast period and the freezing temperature of N_2O_4 is reached in about 15 seconds.

The fuel phase histories for typical Phase II tests (A-0-II, A-5, A-6, A-7) are shown in Figures 7-29, 7-30, and 7-31. Data on the initial coast period (Figure 7-29) show that the phase histories are quite consistent even though there was a 10°F variation in initial fuel temperature. The conditions existing in the fuel duct at coast times greater than 15 seconds appear to be independent of initial fuel temperature over the range of propellant temperatures tested. Initial hardware temperature does not appear to have a significant effect on the phase history following the start of boiling. This can be seen by comparing the process paths shown in Figures 7-29, 7-30, and 7-31, which show the phase histories for the initial, second, and third coast periods. Although the initial fuel duct temperature is about 10°F lower after the first restart, the phase history is not significantly affected.

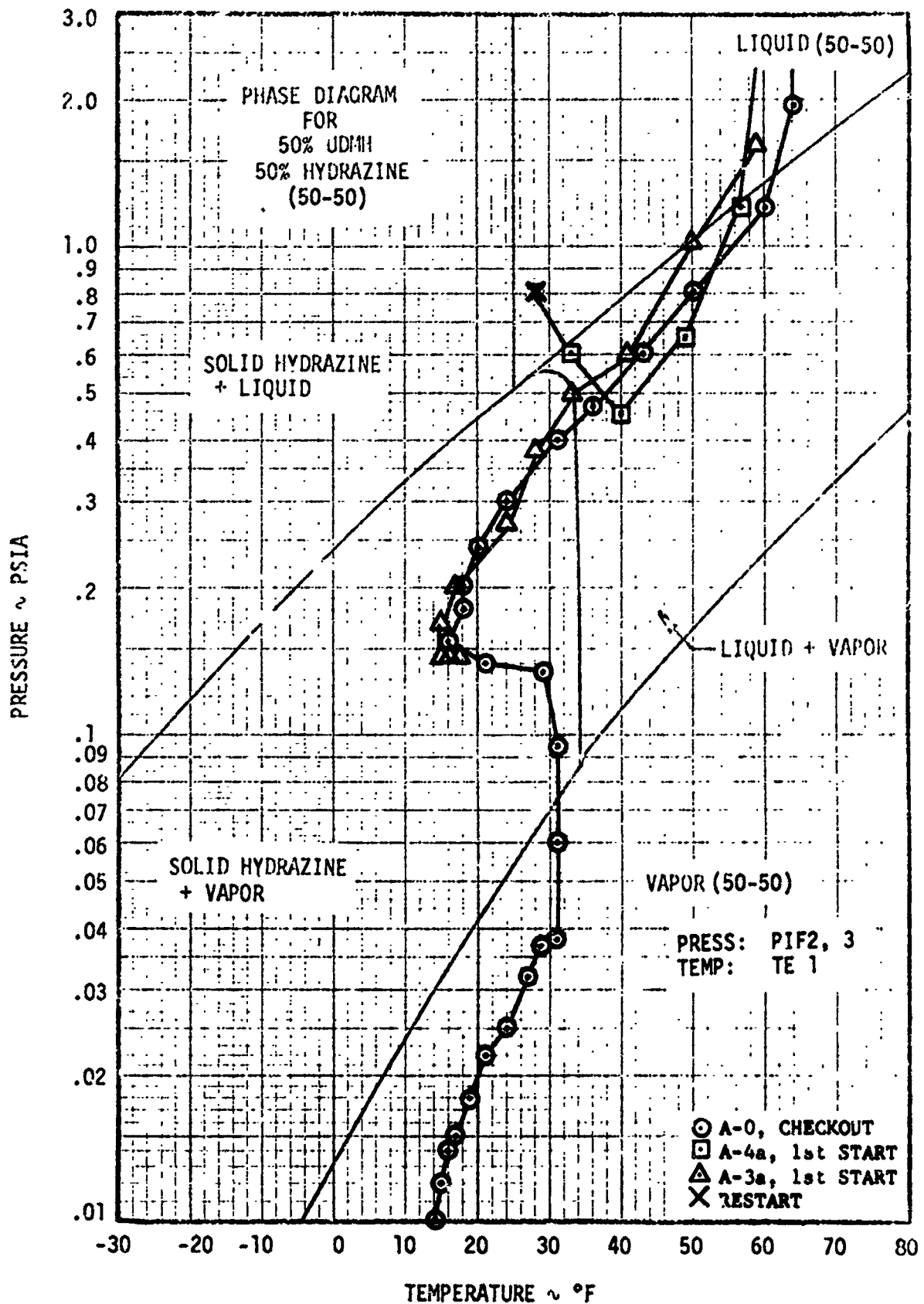


FIGURE 7-26 FUEL PHASE HISTORY FOR ASCENT ENGINE.

3

D2-118246-1

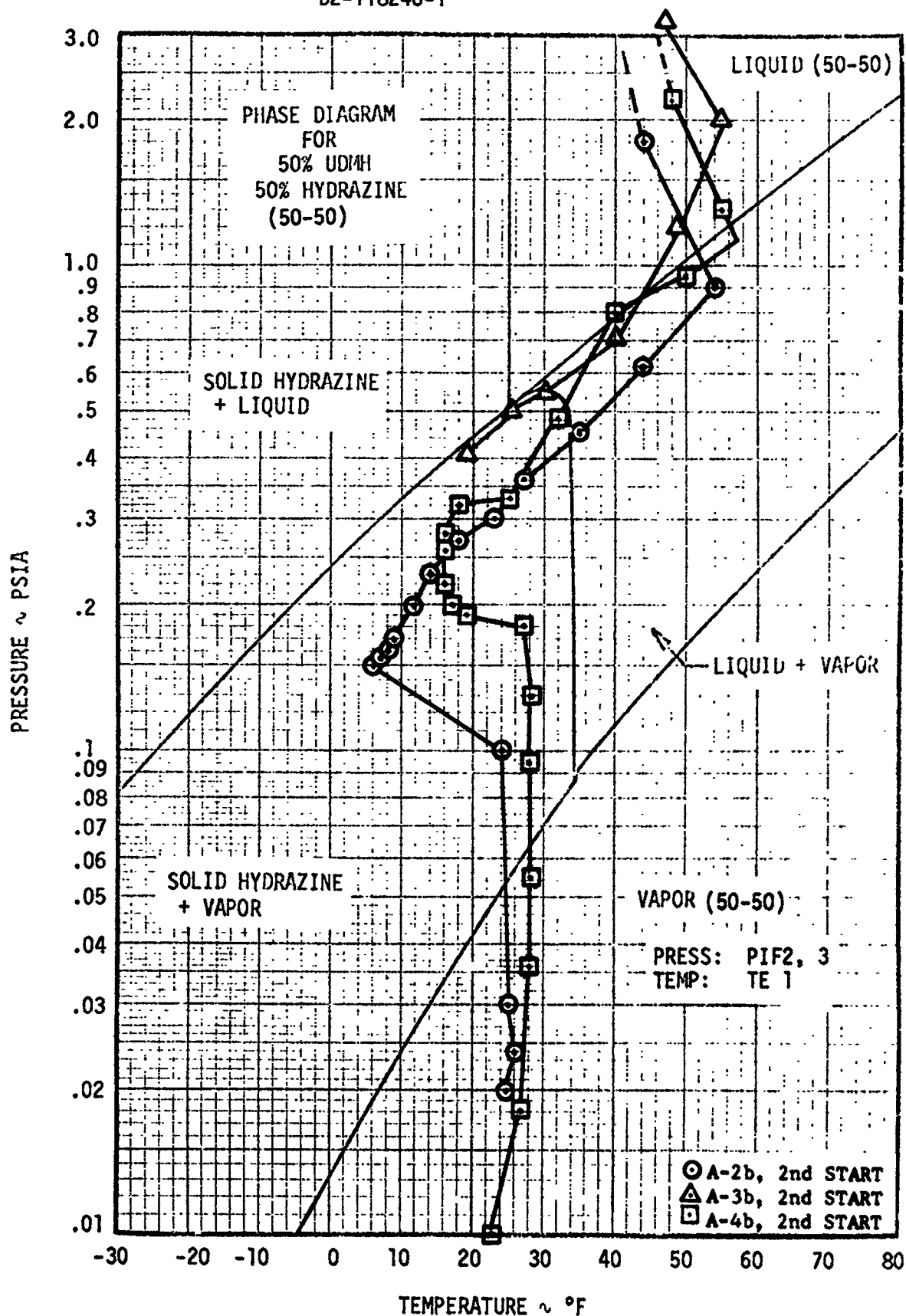


FIGURE 7-27 FUEL PHASE HISTORY FOR ASCENT ENGINE

D2-118246-1

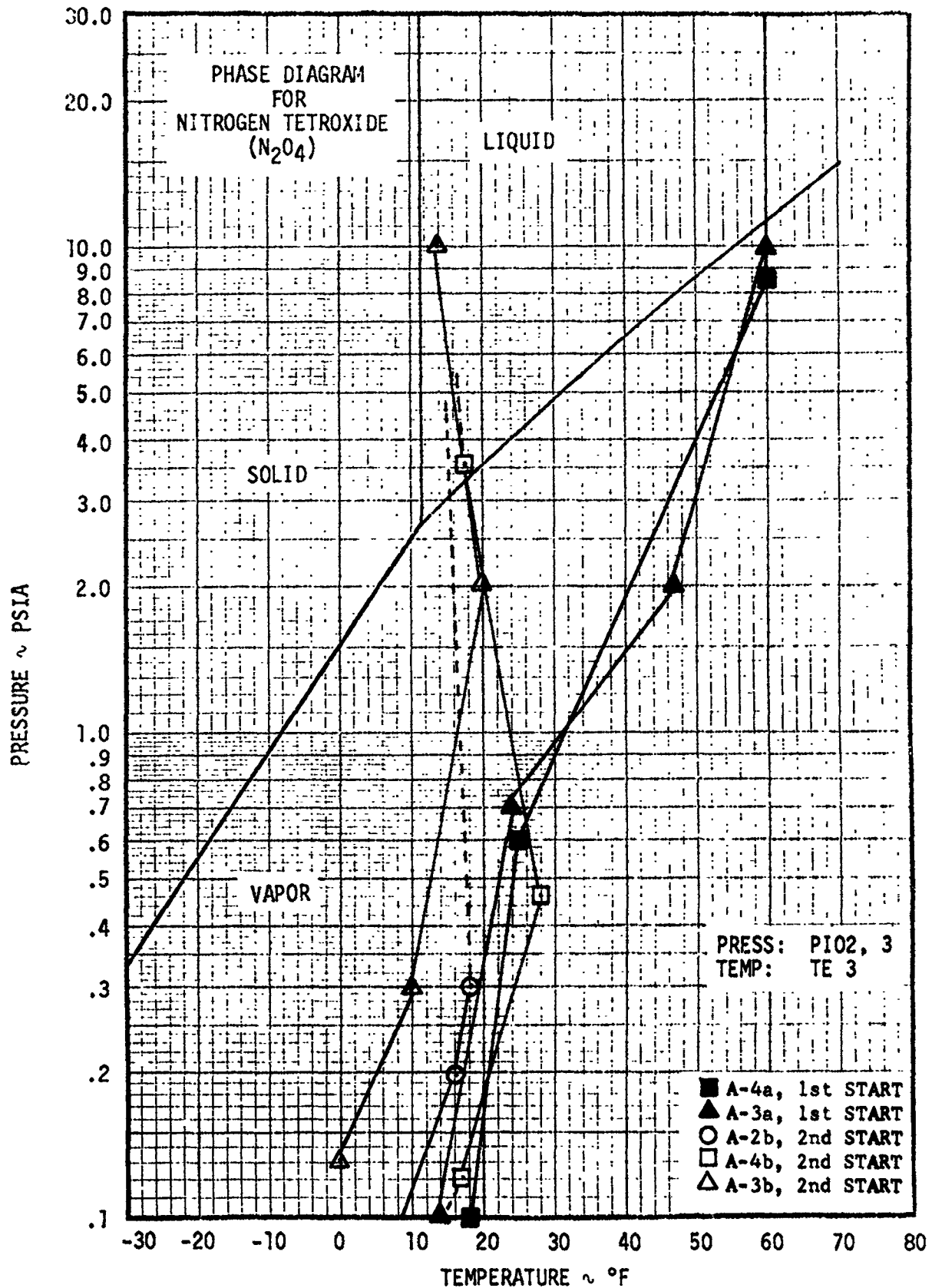


FIGURE 7-28 OXIDIZER PHASE HISTORY FOR ASCENT ENGINE

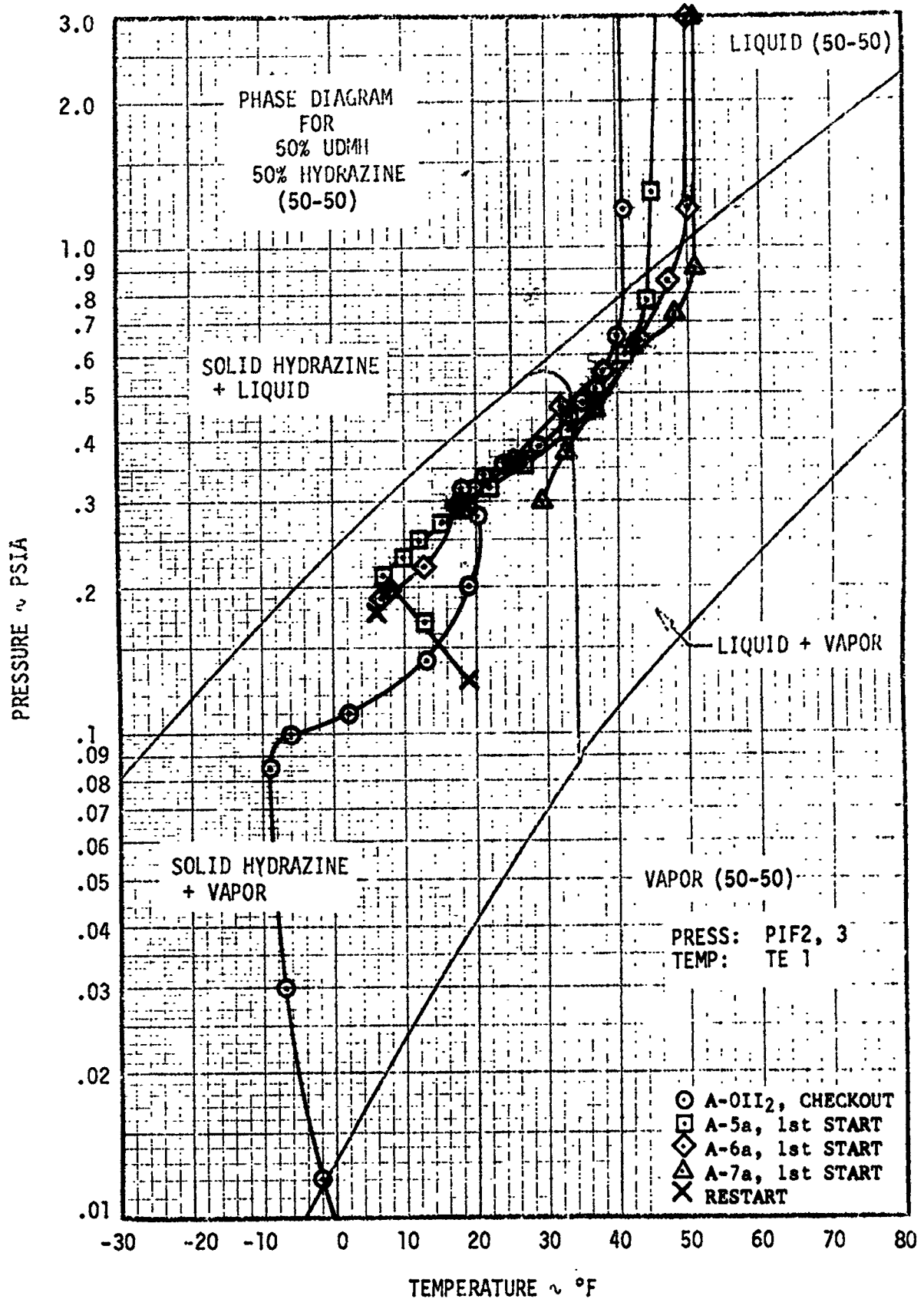


FIGURE 7-29 FUEL PHASE HISTORY FOR ASCENT ENGINE

D2-118246-1

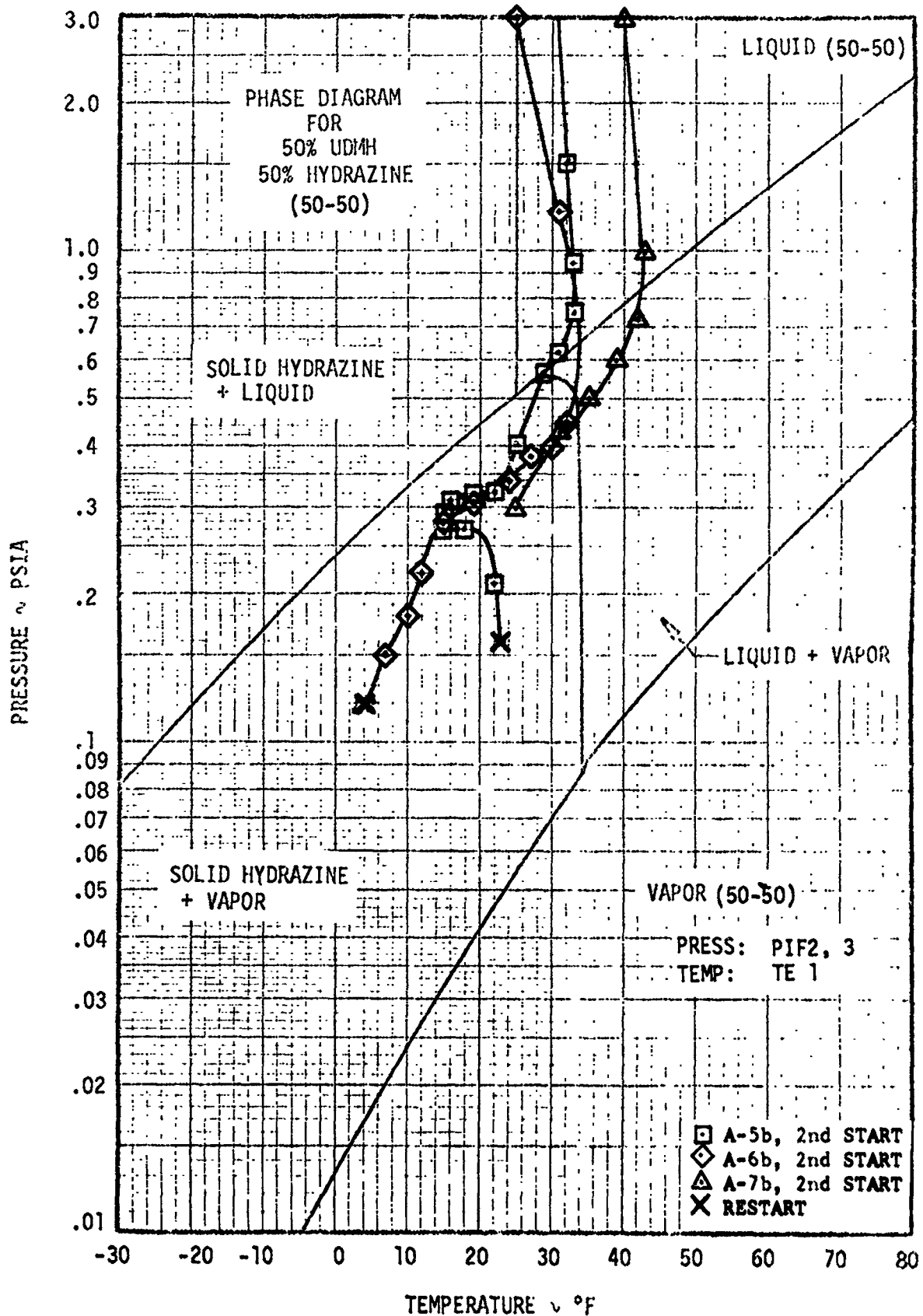


FIGURE 7-30 FUEL PHASE HISTORY FOR ASCENT ENGINE

D2-118246-1

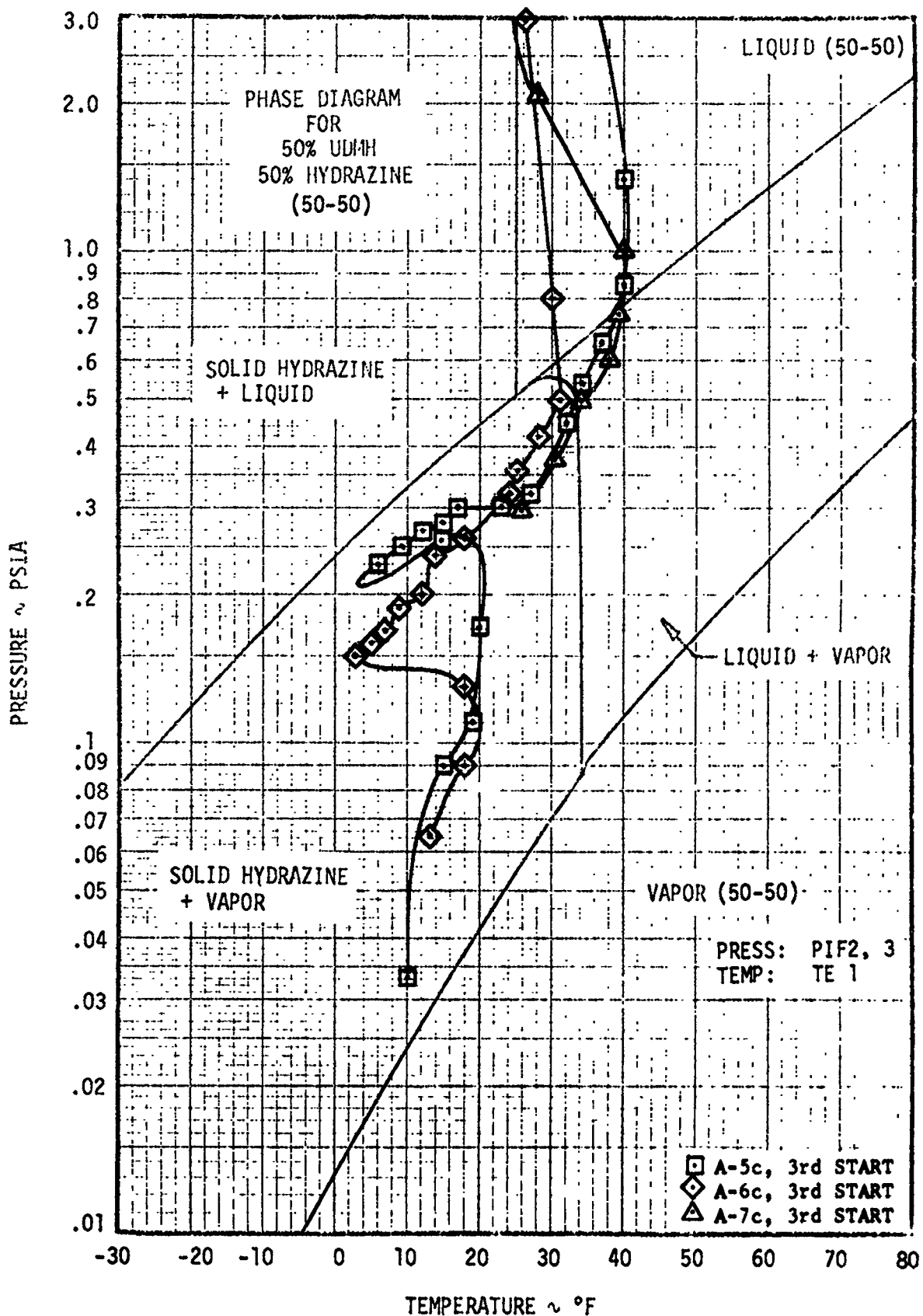


FIGURE 7-31 FUEL PHASE HISTORY FOR ASCENT ENGINE

7.3.2 Coast Phase Analysis (Continued)

The oxidizer phase histories for typical Phase II tests (A-0-II₂, A-5, A-6, and A-7) are shown in Figures 7-32, 7-33, and 7-34. The initial oxidizer temperature (see Figure 7-32) does not appear to have a repeatable effect on the phase histories. Comparison of phase histories obtained following the initial start and the first and second restarts (Figures 7-33 and 7-34) shows that the duct temperature does not increase to the bulk oxidizer temperature during or after the restart firings. This decrease in duct temperature cannot be attributed to thermocouple response time because the ARC cold flow tests (see Figure 7-24) indicated a maximum time delay of 5 to 10 seconds between thermocouples cemented to the duct surface (similar to the hot firing thermocouples) and thermocouples inserted into the oxidizer flow passage. Evaluation of the ARC data shows that the oxidizer duct is colder after each propellant flow.

Comparison of the phase histories for the Phase I and Phase II tests shows that the initial fuel and oxidizer temperatures have only a small effect on the time required to reach the fuel and oxidizer boiling and freezing points. The table below provides typical values from the initial coast periods of the Phase I and Phase II tests.

INITIAL PROP. TEMP. (°F)	FUEL		OXIDIZER	
	TIME TO BOIL (SEC)	TIME TO FREEZE (SEC)	TIME TO BOIL (SEC)	TIME TO FREEZE (SEC)
60	8	25	4	20
50	7	27	4	15
40	7	27	4	15

It is apparent that initial propellant temperature has a negligible effect on time to boil and time to freeze for propellants in the 40°F to 60°F temperature range.

Typical coast phase propellant phenomena are discussed in the following paragraphs.

Following shutdown there was a short period of time before the fuel manifold pressure dropped to the fuel vapor pressure. This time varied from test to test, but averaged about 7 seconds for the ascent engine. A time of this magnitude is far too long to be explained on the basis of an incompressible liquid in the dribble volume. It, however, can be explained by the effect of helium dissolved in the fuel coming out of solution as the manifold pressure decays. These helium bubbles can displace significant volumes of liquid in the injector (see Section 7.1.3), and maintain relatively high injector pressures for several seconds. An alternate possibility is that local hot spots exist in the injector, causing local boiling of the residuals and producing sufficient vapor to maintain injector pressure during this period. However, the injector

D2-118246-1

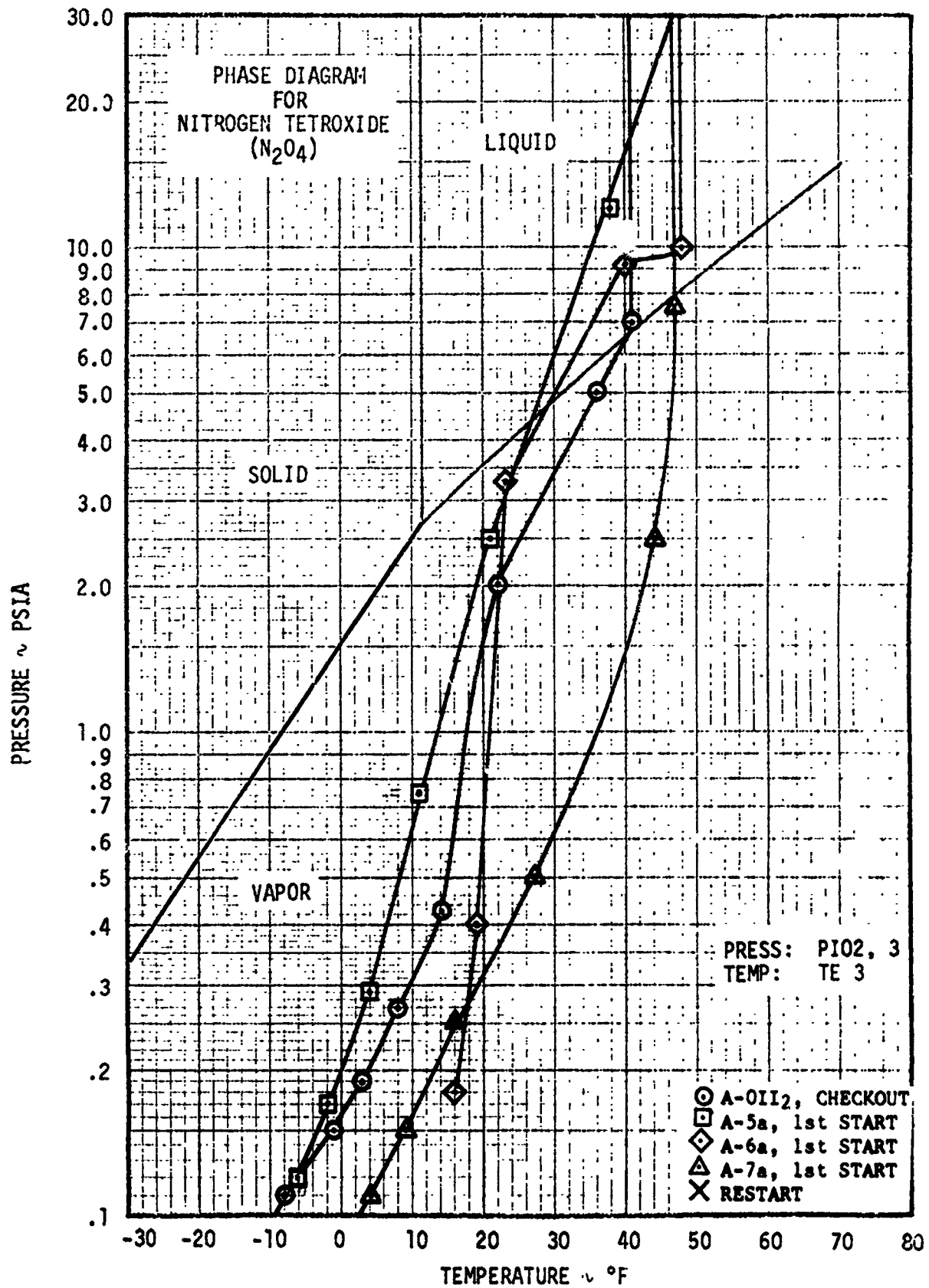


FIGURE 7-32 OXIDIZER PHASE HISTORY FOR ASCENT ENGINE

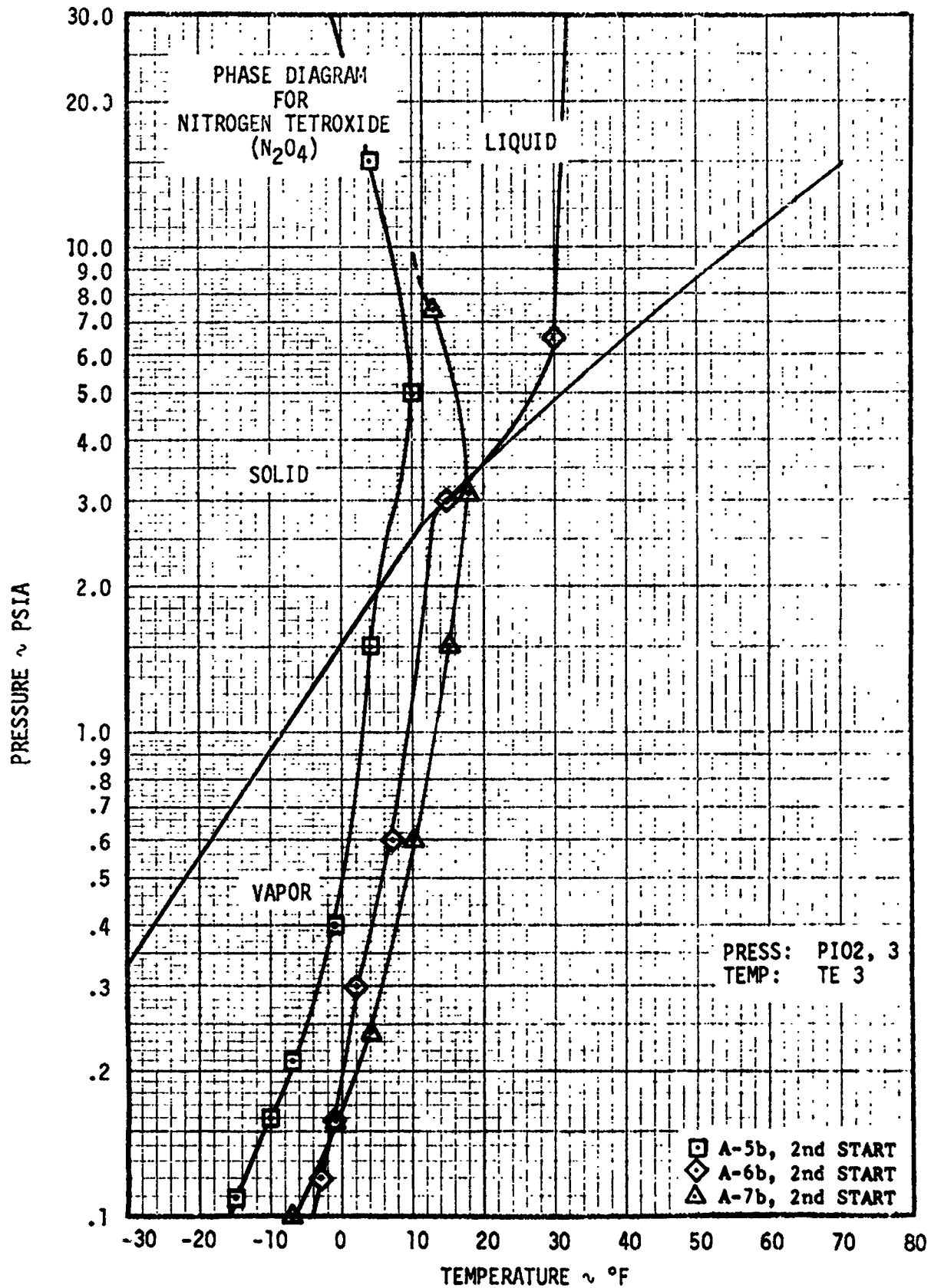


FIGURE 7-33 OXIDIZER PHASE HISTORY FOR ASCENT ENGINE

D2-118246-1

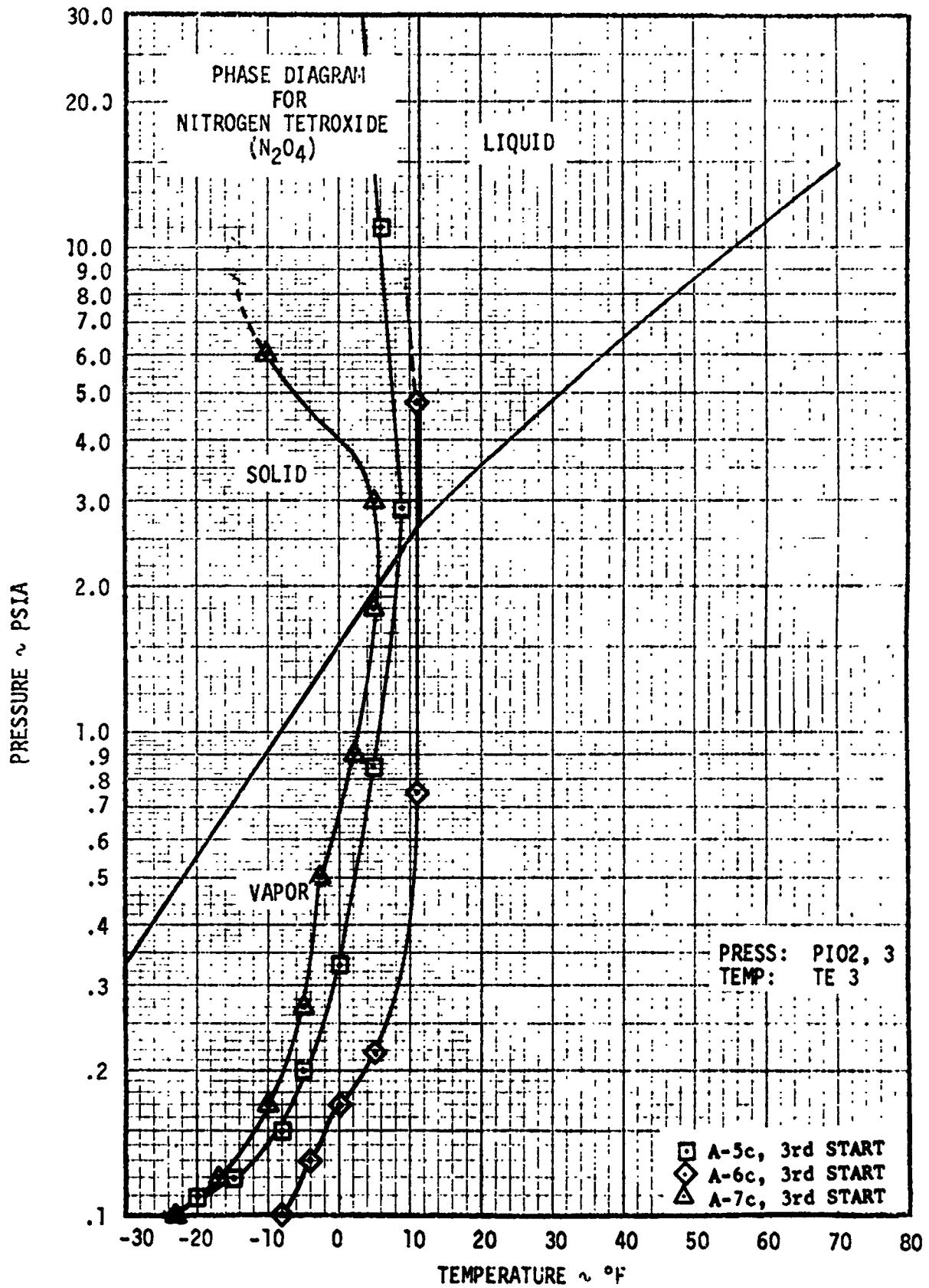


FIGURE 7-34 OXIDIZER PHASE HISTORY FOR ASCENT ENGINE

7.3.2 Coast Phase Analysis (Continued)

thermocouple data do not support the hypothesis that there were injector hot spots. The high speed movies show that fuel and oxidizer snow were deposited on the injector baffles after shutdown, indicating that the injector was not hot. In addition, the injector thermocouples do not indicate any significant temperature increase during the engine firing and the pressure produced by the weight of residuals in the injector is not large enough to cause the relatively high manifold pressures observed after shutdown. It is therefore concluded that the initial fuel manifold pressure decay is significantly affected by the effervescence of dissolved helium.

When the fuel manifold pressure decreases to the fuel vapor pressure the fuel will start to boil. The rapidity and violence of the boiling process is controlled primarily by the degree of superheat in the liquid. The data indicate that the liquid was superheated by 5 to 10°F during the early stages of the boiling process. The fuel was superheated because the fuel manifold pressure was significantly lower than the equilibrium fuel vapor pressure. The instrumentation had sufficient accuracy and adequate response characteristics to support the conclusion that the fuel was superheated. The accuracy of the pressure measurement is quoted to be ± 0.15 psia, which could account for the observed superheat only if the reading was consistently low. However, this is unlikely in that there is generally good agreement between this measurement and that obtained by the lower range measurement which has a quoted accuracy of ± 0.015 psia. The thermocouple used to obtain the temperature reading is a duct skin temperature transducer, which will be at a somewhat higher temperature than the liquid. However, the ARC cold flow tests show that the duct surface is within 30°F of the indicated liquid temperature.

As the boiling continued, the temperature dropped to the point where hydrazine started to freeze out of solution. Pure hydrazine freezes at about 34°F but a 50-50 liquid mixture with UDMH freezes at about 25°F. However, if the temperature of a 50-50 liquid mixture is lowered below 25°F, some of the hydrazine will freeze. This will change the liquid composition and decrease the freezing temperature of the remaining hydrazine-UDMH mixture. Thus, hydrazine can remain in the liquid state in the proper liquid composition down to -71°F. Since the temperature in the Seattle test dropped far below 25°F, one must conclude that the hydrazine is solidifying fast enough to increase the percentage of UDMH in the liquid. This increase in the percentage of UDMH in the liquid can also be shown by noting that the heat of vaporization of UDMH is about 1.5 times the heat of fusion of hydrazine. As a result, 1.5 pounds of hydrazine must freeze out of solution to balance the energy taken away by the evaporation of 1 pound of UDMH. The freezing temperature of the remaining hydrazine would therefore decrease. It is then possible to obtain very low temperatures before all of the hydrazine freezes out.

7.3.2 Coast Phase Analysis (Continued)

The temperature increase which occurred 75 seconds after engine shutdown is attributed to the essentially complete depletion of liquid residuals. As the manifold pressure continued to decrease, the sublimation rate of the frozen residuals was increased. This increased sublimation rate caused the duct temperature to decrease to -9°F at approximately 500 seconds after engine shutdown. The gradual temperature increase occurred because heat transfer from the engine and environment exceeded the heat removed by sublimation of the solid residuals. A thermal balance was reached at 12°F after approximately 1000 seconds of coast. This balance is not shown on the phase diagram because the manifold pressure is below the lower limit of the phase diagram.

The existence of significant amounts of frozen hydrazine residuals was confirmed by temperature data obtained from TE-8, which was located on the fuel duct near the ball valves. Since frozen hydrazine is heavier than the 50-50 liquid, it would settle to the low point of the fuel duct, at TE-8. This thermocouple indicated a minimum temperature of 25°F , the freezing temperature of the 50-50 mixture. The temperature then asymptotically increased to 34°F , the freezing temperature of pure hydrazine, but did not exceed this temperature for 3000 seconds, when the test was terminated.

Following shutdown, the pressure in the oxidizer manifold dropped quite rapidly and reached the vapor pressure of the N_2O_4 in about 5 seconds on most tests. The pressure continued to drop rapidly resulting in 5° to 15°F superheat in the liquid. This amount of superheat was sufficient to create very violent boiling and cooling of the remaining liquid. At about 15 seconds, the triple point temperature (12°F) of the N_2O_4 was reached. At this time the oxidizer manifold pressure was almost an order of magnitude below the triple point pressure. The boiling of the remainder of the liquid must have been very violent and one would expect all of the oxidizer to be frozen shortly after 15 seconds. The pressure and temperature continued to decrease, indicating that the solidified N_2O_4 was subliming for more than 500 seconds. There was no indication that any oxidizer ever freezes in the injector. During initial coast periods, the thermocouple on the duct-injector interface did not show temperatures below the freezing point of N_2O_4 . The thermocouple at the low point in the duct was always at the lowest temperature, indicating that the frozen N_2O_4 had settled to this point.

7.3.3 Start and Restart Firing Characteristics Analysis

The test data, summarized in Section 4, Table 4-3, show that several ascent engine restarts had significantly higher accelerometer readings than the initial starts. The characteristics of the initial starts were investigated to provide a baseline for evaluation of the restarts. The restart characteristics were then investigated to determine the effect of coast phase propellant phenomena on the restart characteristics.

7.3.3 Start and Restart Firing Characteristics Analysis (Continued)

Figure 7-35 shows the time from fire signal to ignition for all of the Phase II restarts. Ignition is defined as the first significant rise in chamber pressure, and includes the short-duration chamber pressure spikes which precoded the normal ignition transient by 20 to 30 milliseconds. The time to ignition is closely related to the fuel manifold priming times shown in Figure 7-36. Both the time to ignition and the fuel manifold priming times are significantly below normal for coast times less than 10 seconds, showing the effect of fuel residual volumes.

The relatively small oxidizer leads which occurred at coast times of less than 10 seconds did not produce rough restarts. The chamber pressure at 10 seconds is approximately 0.2 to 0.4 psia, which apparently provides a favorable condition for reignition even though the oxidizer lead is significantly lower than normal.

The Phase II oxidizer manifold priming times, for coast periods between 15 and 90 seconds, are increased by partial to essentially complete blockage of the oxidizer duct. This was clearly indicated during Test A-7 (see Figures 7-39 and 7-40), and is attributed to blockage of the oxidizer injector filter by frozen oxidizer residuals. When the flow was stopped, a large pressure pulse was produced. This pressure pulse was reflected upstream where it was detected by the interface pressure transducer. Figure 7-37 shows the maximum oxidizer interface pressure as a function of coast time for the ascent engine. The definite trend to increased interface pressures in the range from 10 to 60 seconds for first restarts was undoubtedly caused by partial plugging of the oxidizer filter. The three data points for second restarts are higher than the initial restart values because the oxidizer side temperature continues to decrease after each subsequent restart. It would appear that following the 90 second coast, the first restart did not have plugging but that the second restart did experience oxidizer side plugging. This is consistent with the fact that for repeated restarts the oxidizer continues to decrease in temperature which results in the retention of more oxidizer for each subsequent restart. Following the 15 second coast, the peak oxidizer interface pressure was higher than normal, but the oxidizer manifold priming time was normal. However, the oxidizer manifold pressure trace indicates that the oxidizer flow was not fully established at ignition, supporting the conclusion that partial oxidizer side blockage was experienced during this test.

The oxidizer phase history data (Figures 7-32, 7-33 and 7-34) show that oxidizer freezing can begin within 10 to 15 seconds after the initial start. The time to freezing decreases after the second and third starts, probably due to the lower duct temperatures during and immediately after the restart firings. The low duct temperatures can also result in increased amounts of frozen oxidizer residuals, causing partial blockage of the oxidizer filter, during third restarts for coast times in excess of 200 seconds (see Figure 7-37).

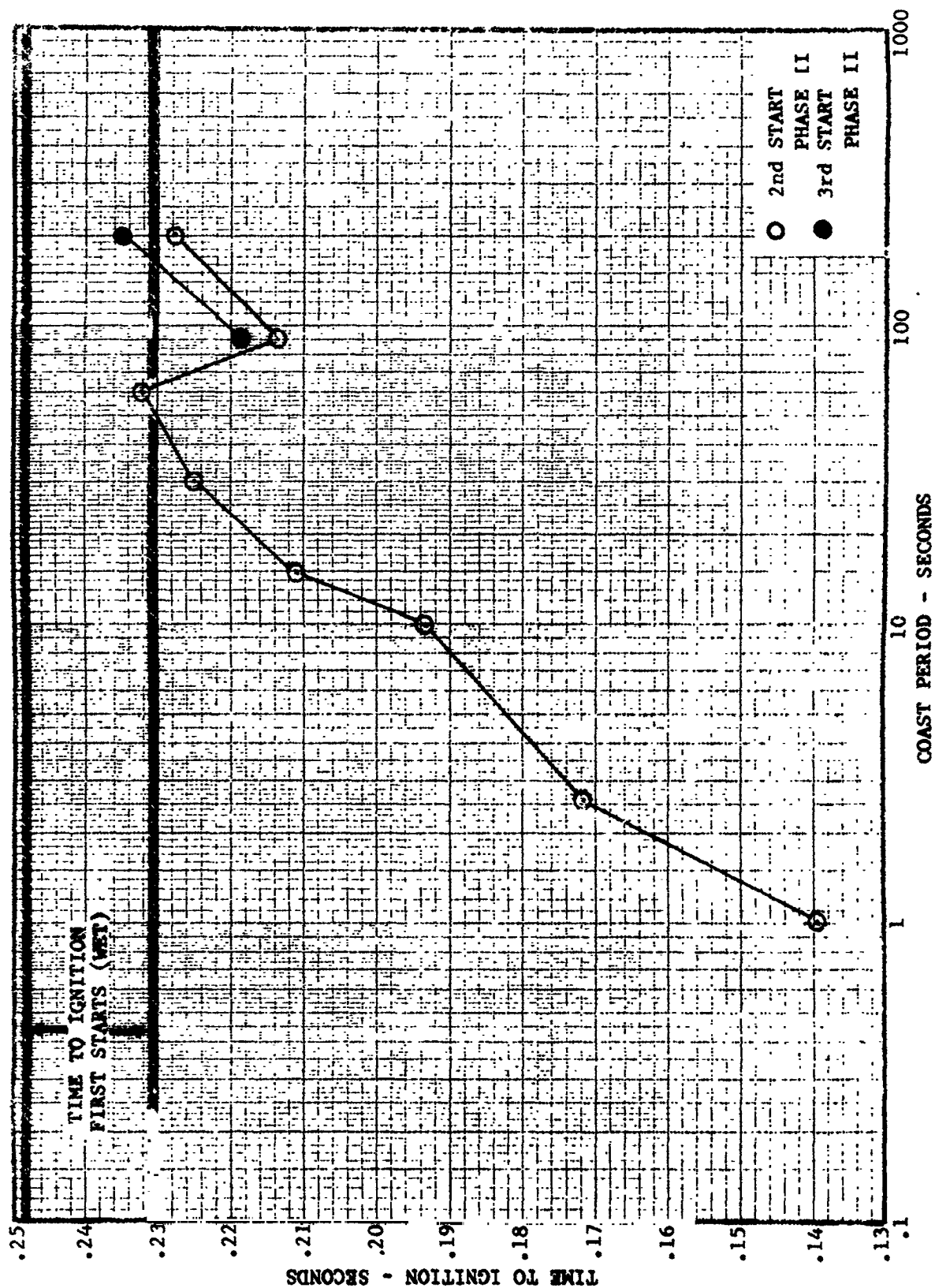


FIGURE 7-35 TIME TO IGNITION VS ASCENT ENGINE COAST PERIOD

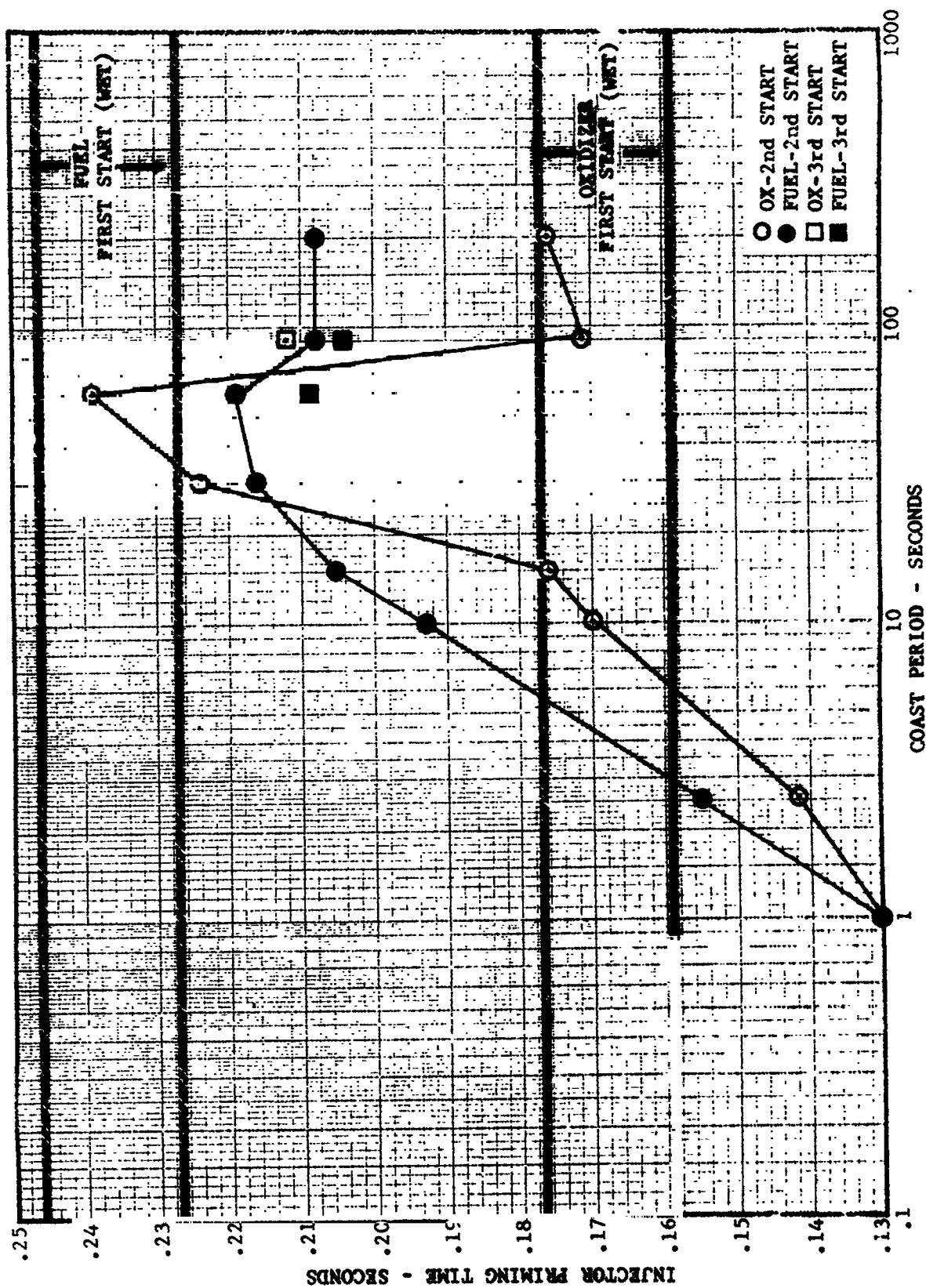


FIGURE 7-36 FUEL AND OXIDIZER INJECTOR PRIMING TIMES VS ASCENT ENGINE COAST PERIOD

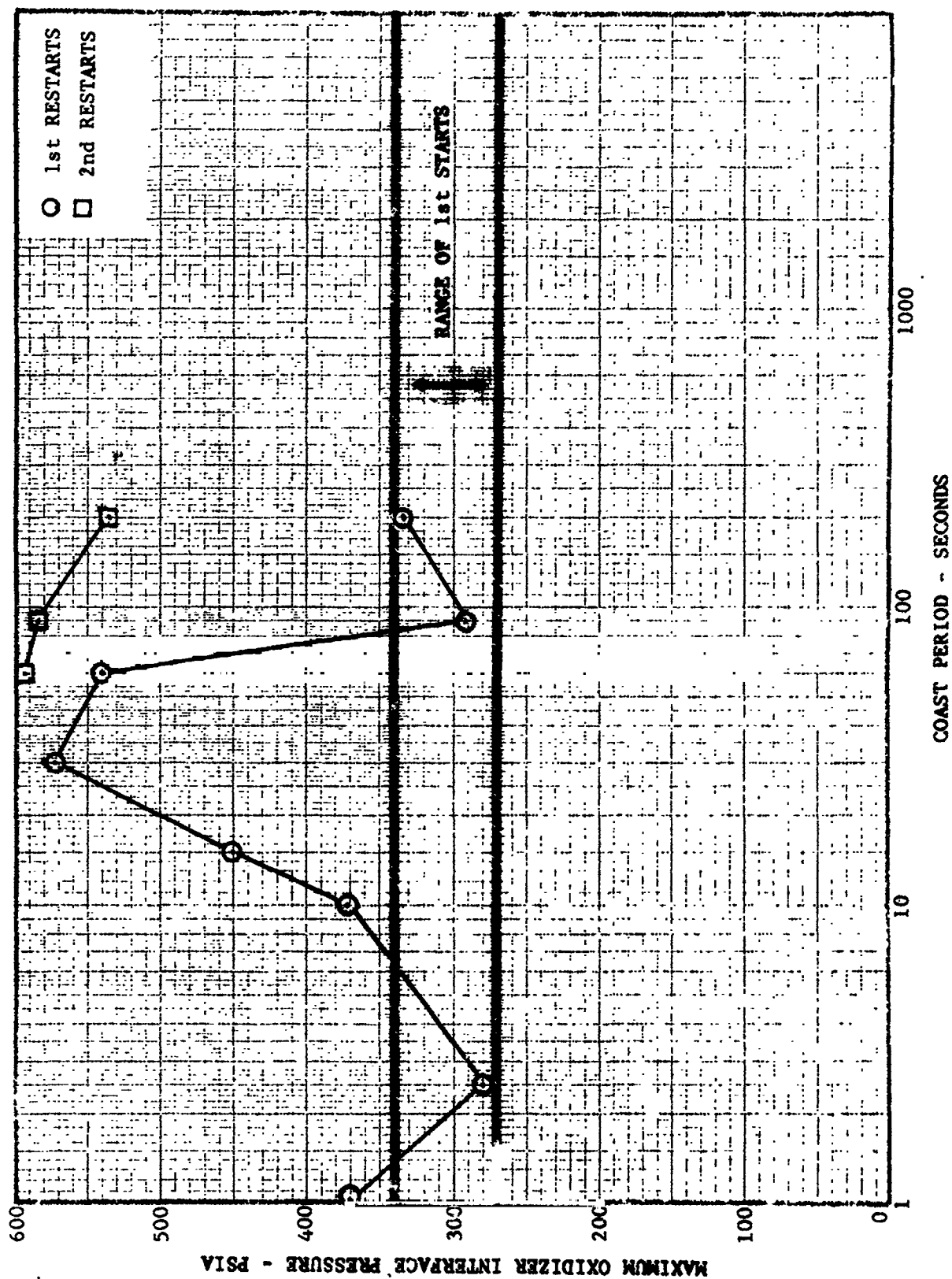


FIGURE 7-37 MAXIMUM OXIDIZER INTERFACE PRESSURE VS
ASCENT ENGINE COAST PERIOD

7.3.3 Start and Restart Firing Characteristics Analysis (Continued)

Calculated mass residual data (Figure 7-5) show that the oxidizer side still has approximately 25% of the total oxidizer side capacity after 10 seconds of coast. After 100 seconds of coast, approximately 10% of the total capacity is still present. Because of the horizontal orientation of the engine during the Seattle tests, these residuals are located in the bottom of the oxidizer duct at the engine valves. There is no evidence that oxidizer freezes in the injector internal flow passages. Thermocouples on the injector and at the injector/oxidizer duct interface always remain above the oxidizer freezing temperature. It is therefore concluded that the oxidizer filter is blocked when the frozen residuals, located near the ball valves, are forced against the filter during the priming process.

In every case where the oxidizer lead was lost, or the oxidizer flow was not fully established, high accelerometer readings were recorded. There was also a characteristic chamber pressure trace which had a sharp spike in chamber pressure at the time the fuel manifold pressure started to rise. In general, the chamber pressure returned to a low pressure and a normal chamber pressure rise occurred as soon as the oxidizer flow was fully established.

The only rough Phase II restart which did not indicate partial oxidizer side blockage was the first restart of Test A-6. Oxidizer priming time and peak interface pressure were within the normal range. The fuel manifold priming time was lower than the time for a 60 second coast, but was identical to the time for a 200 second coast, which produced a smooth restart. The time to ignition for A-6b was shorter than the times observed for 60 and 200 second coast periods, but the time interval between fuel manifold priming and ignition (5 ms) was within the normal range for initial wet starts (3 to 11 ms). The peak chamber pressure (441 psia) occurred during an apparently normal start transient. No cause for this overshoot, or the similar overshoot which occurred during Phase I test A-4b, has been established.

The peak fuel interface pressure as a function of coast time is presented in Figure 7-38. With the exception of the second restart after a 200 second coast, there is not enough variation away from the normal range to cause concern. The high fuel interface pressure at the 200 second point occurs at a time which does indicate that it is probably due to partial plugging of the fuel filter. This is the only time in any of the tests that this type of behavior was observed. Unfortunately most of the high response data from this test were lost so that additional information is not available. The relatively high fuel interface pressure at 3 seconds is a result of chamber pressure overshoot and not filter plugging.

The preceding data indicate that the restarts during test A-7 were significantly different from the initial starts. A detailed analysis of the data from the A-7 firings is presented in the following paragraphs.

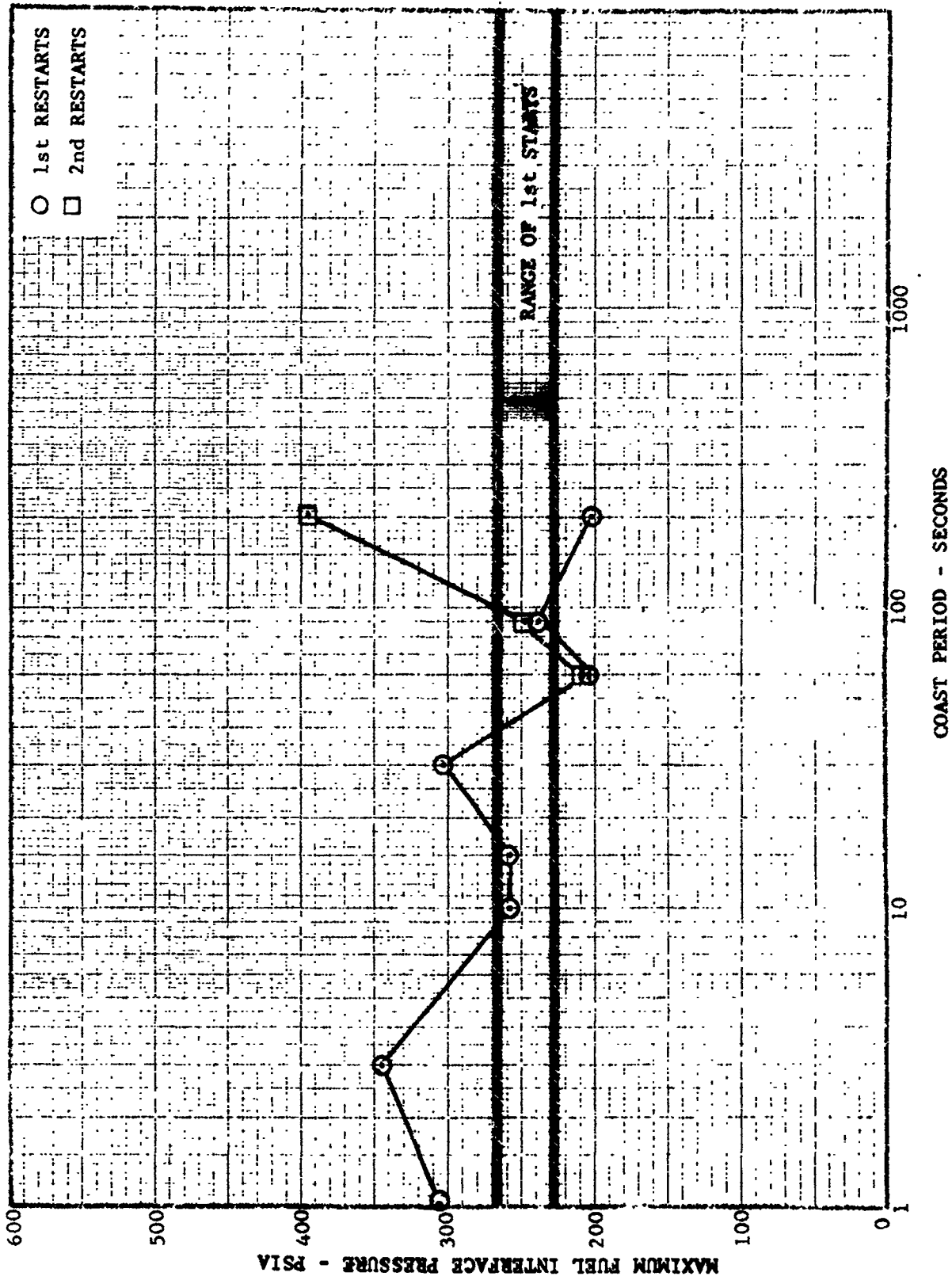


FIGURE 7-38 MAXIMUM FUEL INTERFACE PRESSURE VS ASCENT ENGINE COAST PERIOD

7.3.3 Start and Restart Firing Characteristics Analysis (Continued)

The oscillogram records of the fuel and oxidizer interface pressures for firings A-7a and A-7b are presented in Figure 7-39. The fuel manifold, oxidizer manifold and chamber pressure traces for these two firings are presented in Figure 7-40. The initial firing (A-7a) was a "dry" start. A "dry" start is one where there is no fuel or oxidizer between the ball valves and there is no fuel in the valve actuator lines. In contrast, a "wet" initial start is one where propellants are purposely bled into these volumes. The first restart firing (A-7b) occurred after a 60 second coast period, and was a hard restart. The oscillogram records for the second restart firing (A-7c) were essentially similar to the records for A-7b, except that the engine did not start, due to essentially complete blockage of the oxidizer flow by frozen residuals.

Initial Firing (A-7a)

Figure 7-39 shows that the oxidizer interface pressure remained constant for 65 ms. (milliseconds) after the fire signal. This occurred because the engine valves required 30 to 55 ms. to leave the closed position. The propellant valves were completely open by 125 ms. and the isolation valves were completely open by 185 ms. During the time when the valves were opening, the oxidizer interface pressure decreased to about 55 psig, indicating that the duct was being filled, and then reached a plateau of about 137 psig at 155 ms. This rapid pressure increase to 137 psig indicates that the duct had been filled, and the injector manifold was beginning to fill. A second rapid pressure increase occurred at 205 ms. This pressure increase indicates that the injector was full and a steady flow through the injector orifices was being established.

The fuel interface pressure remained constant for only about 25 ms. before decreasing. The subsequent pressure oscillation occurred because the engine ball valve actuators were being filled. During the time period when the engine valves were opening, the fuel interface pressure decreased, indicating that the fuel duct was being filled. The interface pressure then remained relatively constant at 77 psig until approximately 5 ms. prior to ignition.

Figure 7-40 shows that the oxidizer manifold pressure remained at essentially zero psia until 185 ms. after the fire signal. The two "steps", at 110 psia and 230 psia indicate injector manifold filling and the establishment of oxidizer flow through the injector orifices. The increase in manifold pressure at ignition shows the effect of increasing chamber pressure.

The fuel manifold pressure remained at essentially zero psia until ignition. The fuel manifold pressure and the chamber pressure then increased simultaneously.

D2-118246-1

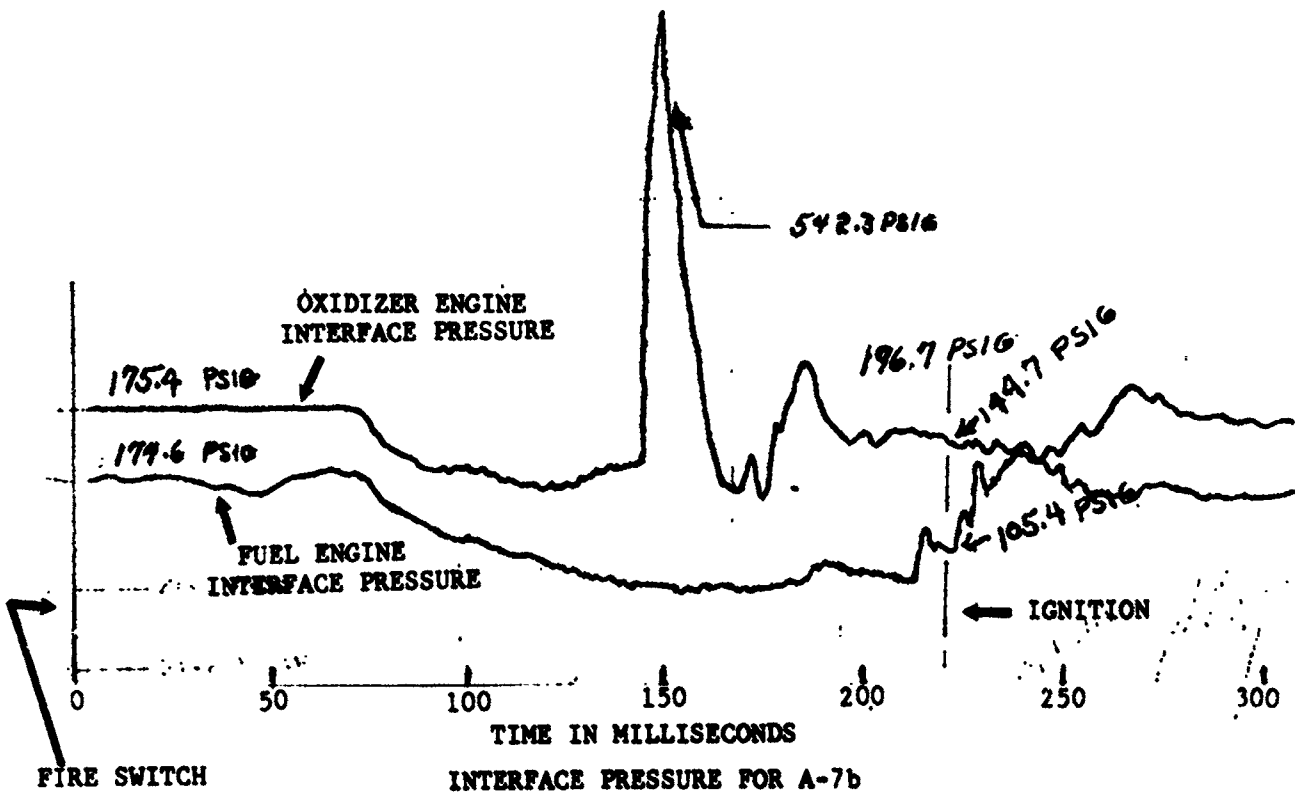
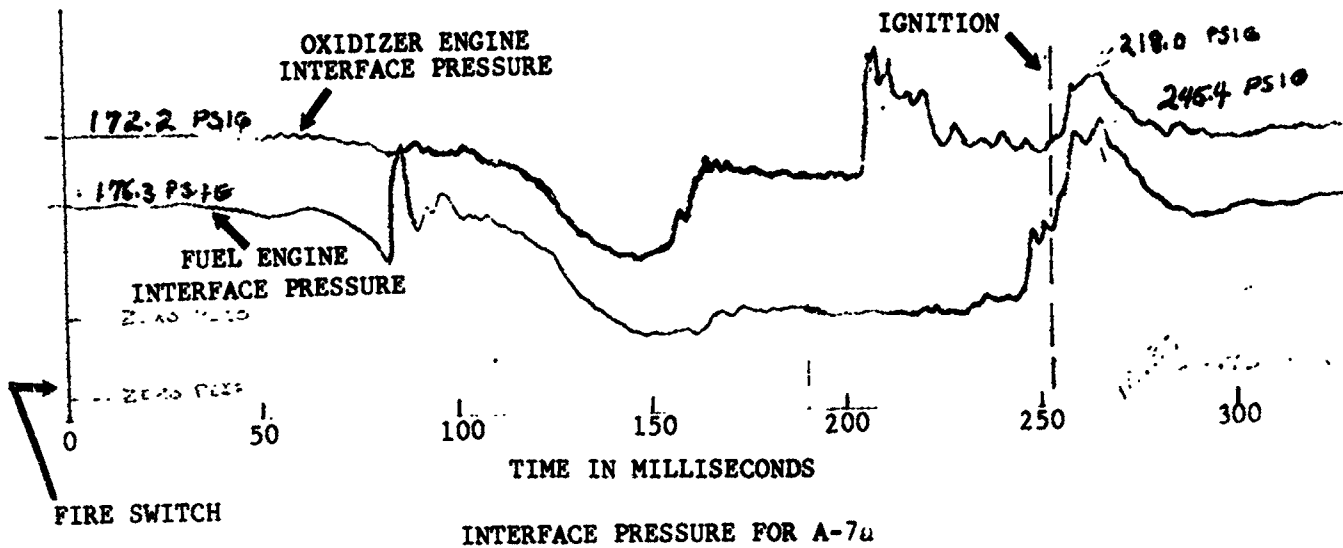
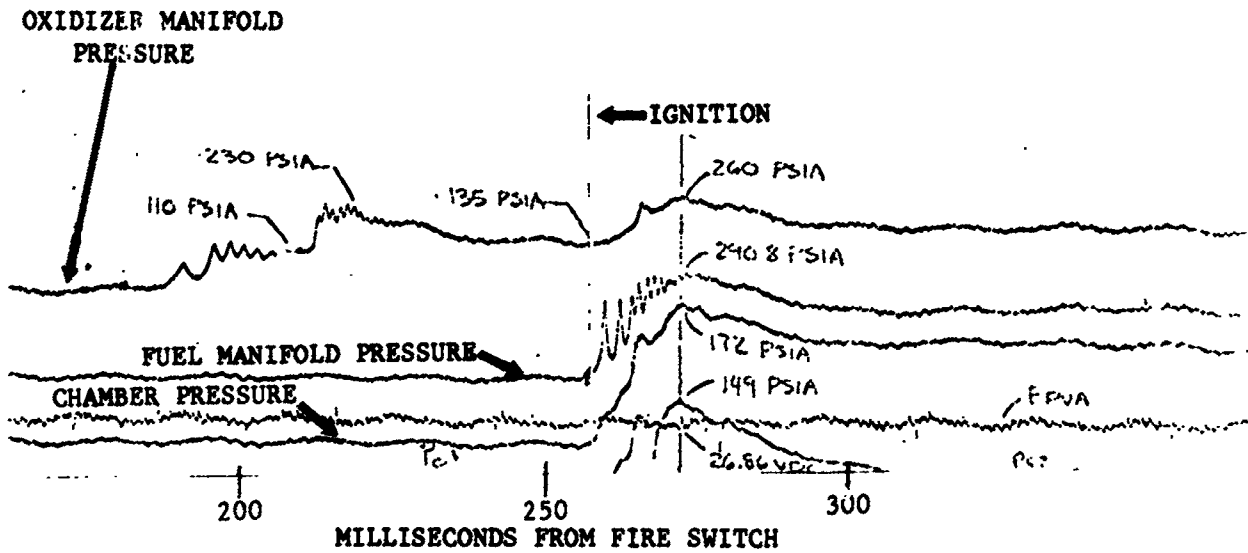
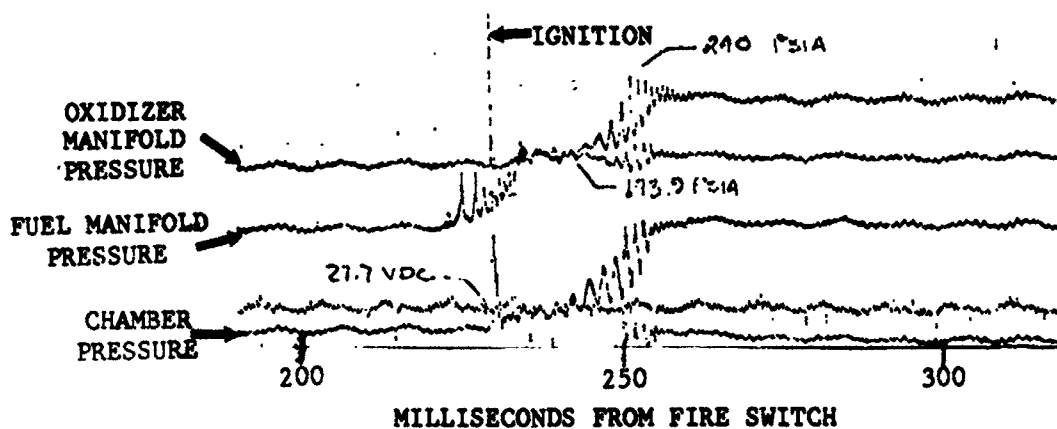


FIGURE 7-39 INTERFACE PRESSURE RECORDS FOR ASCENT ENGINE FIRINGS A-7a AND A-7b



P_c AND MANIFOLD PRESSURES FOR A-7a



P_c AND MANIFOLD PRESSURES FOR A-7b

FIGURE 7-40 CHAMBER PRESSURE AND MANIFOLD PRESSURE RECORDS FOR ASCENT ENGINE FIRINGS A-7a AND A-7b

7.3.3 Start and Restart Firing Characteristics Analysis (Continued)

The accelerometers responded during the manifold filling process, indicating a maximum of 13 g's peak-to-peak (gpp) when the oxidizer manifold pressure increased rapidly from 110 psia to 230 psia. At ignition, the flight accelerometer indicated a maximum of 31.5 gpp and the test facility accelerometers indicated a maximum of 70.7 gpp.

First Restart (A-7b)

The engine valves left the closed position between 50 and 65 ms. after the start signal, and reached full open position between 145 and 170 ms. The oxidizer interface pressure history for A-7b is essentially similar to the A-7a history until 140 ms. after the start signal. The large (542.3 psig) pressure spike at about 140 ms. is believed to have been caused by frozen oxidizer residuals being forced against the oxidizer injector filter (located at the duct/injector interface), causing a significant flow blockage. The oxidizer interface pressure was erratic until about 20 ms. prior to ignition, indicating that steady oxidizer flow was not established until this time.

The fuel interface pressure history for A-7b was essentially similar to the A-7a history until ignition. After ignition, the pressures were different because of the abnormal ignition characteristic of A-7b.

The oxidizer manifold pressure for A-7b remained at nearly 0 psia until 7 ms. after ignition. The manifold pressure then increased to steady state conditions at the same time the chamber pressure increased.

The fuel manifold pressure remained at essentially 0 psia until 13 ms. prior to ignition, indicating a definite fuel lead for this start. The fuel manifold priming time for A-7b was reduced from 257 ms. during A-7a to 219 ms., illustrating the combined effects of residual fuel and "wet" start conditions. However, the oxidizer priming time was increased from 185 ms. during A-7a to 239 ms. on A-7b, despite the presence of oxidizer residuals and "wet" start conditions, illustrating the blockage of the oxidizer side by frozen oxidizer residuals.

The chamber pressure had a 2 ms., 473 psia, spike at "ignition", and then decreased to about 20 psia before increasing to steady-state conditions. The complete spike is not visible on the oscillogram reproduction (Figure 7-40), but is visible on the original oscillogram records.

The accelerometers indicated 49 gpp when the oxidizer duct pressure spike, shown on the interface pressure record, occurred at 150 ms. The accelerometers were driven off-scale when the chamber pressure spike occurred at ignition.

High speed films of these two firings indicate that oxidizer flow from the injector occurred before fuel flow was established. The oxidizer appeared as a fine spray which gradually obscured the injector. During

7.3.3 Start and Restart Firing Characteristics Analysis (Continued)

the A-7a firing, this spray appeared 60 ms. prior to ignition, but during A-7b, the spray appeared only 40 ms. prior to ignition. In addition, the A-7b spray appeared to be less diffused and flowed from the bottom injector holes first, indicating that the oxidizer flow rate was reduced.

Second Restart (A-7c)

No significant combustion occurred during this attempted restart because of essentially complete blockage of the oxidizer side. This was indicated by the absence of a detectable increase in chamber pressure or injector oxidizer manifold pressure during A-7c. The valve actuation times and interface pressure histories were similar to those obtained during A-7b, except that the oxidizer interface pressure reached a higher peak pressure (see Figure 7-37), and continued to oscillate throughout the attempted firing. The accelerometers responded to the oxidizer interface pressure peak (37.1 gpp) and to fuel manifold priming (21 gpp) but did not produce an indication of ignition. High speed films show that fuel flow was definitely established first, and no oxidizer flow was visible prior to the time when the injector was obscured by spray. The only indication that any combustion occurred was the rise in exhaust gas temperature to 540°F. Normal exhaust gas temperature readings were approximately 1300°F.

7.4 DESCENT ENGINE TEST ANALYSIS

7.4.1 General

This section presents an analysis of the results from Phase I and Phase II Descent engine restart tests conducted at the Boeing/Seattle test facility. The initial starts and restarts were analyzed to determine the effect of propellant residuals on the engine restarts. Coast phase data on propellant pressures and temperatures were plotted on phase diagrams. This method of data presentation provided a basis for determining the thermodynamic state of propellant residuals which were present at the descent engine restarts. A summary of the test conditions and test results is presented in Tables 5-1 and 5-3.

The Seattle Phase I test series consisted of 5 tests. The checkout firing (D-0), consisted of one start while the remaining four tests (D-1, D-2, D-3, and D-4) consisted of an initial firing followed by one restart at coast periods of 1800, 300, 120, and 45 seconds. Following the 300 second coast period (test D-2), the restart showed a chamber pressure spike of 75 psia and a maximum accelerometer reading of 640 "g's" peak to peak in the X axis of the GSE accelerometer. This firing was the roughest restart encountered for the descent engine during Phase I and Phase II testing.

The Seattle Phase II test series consisted of 9 tests. The checkout firing (D-0II), consisted of one start while the remaining 8 tests, (D-5 through D-12), consisted of an initial start followed by two restarts. Coast periods of 120, 90, 50, 15, 5, 2, 375, and 170 seconds were tested during D-5 through D-12 respectively. None of these tests showed hard restart characteristics. The initial starts of tests D-9 and D-11 had the maximum peak chamber pressures of 55 and 53 psia. All of the restarts had lower maximum chamber pressure peaks. In general, the restarts were less severe than the initial starts and there was no significant difference between the first and second restarts.

7.4.2 Coast Phase Analysis

The fuel and oxidizer duct temperatures and pressures were plotted on phase diagrams to analyze the thermodynamic processes occurring during the coast phase. The data were plotted for time intervals of 5, 10, 15, 20, 25, 30, 40, 50, 60, 70, 80, 90, 100, 150, 200, 250, 300, 400, 500, 600, 700, 800, 900, and 1000 seconds following engine shutdown. The test coast time and data availability determined the time duration for which data were plotted. In the A-50 plot for test D-3a, the first point is at 7 seconds following shutdown, due to a lack of data for the 5 second point.

The fuel phase histories for Phase I tests D-2a, D-3a, and D-3b are in Figure 7-41. A comparison between D-3a and D-3b shows that there is no significant difference between the initial start and the restart as far

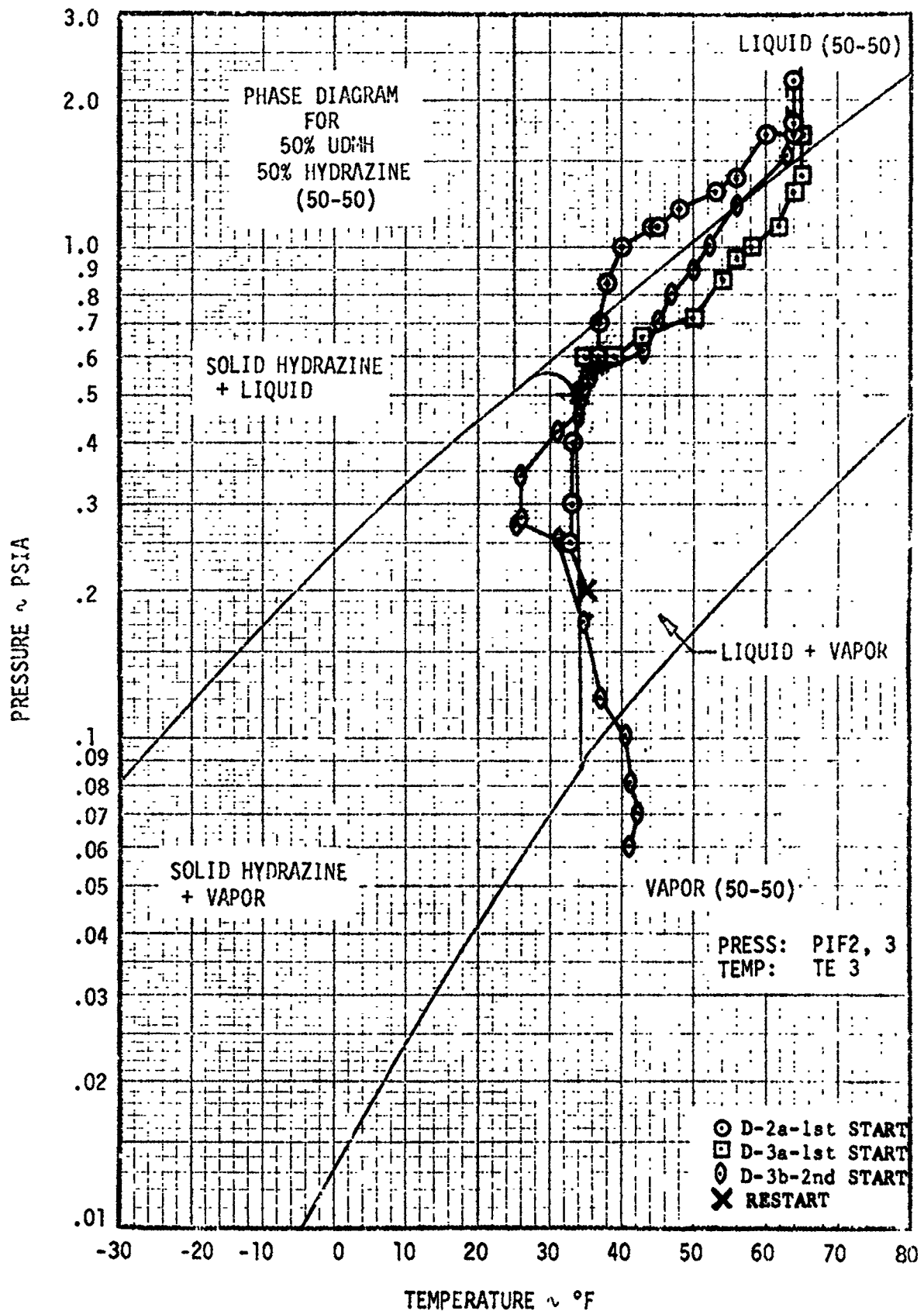


FIGURE 7-41 FUEL PHASE HISTORY FOR DESCENT ENGINE

7.4.2 Coast Phase Analysis (Continued)

as the fuel phase history is concerned. In general, the fuel phase histories show rather close agreement with equilibrium conditions for both the Phase I and Phase II tests.

The oxidizer phase histories for Phase I tests D-2a, D-3a, and D-3b are in Figure 7-42. Note that on D-3b the oxidizer side was not warmed up to the initial 65°F propellant temperature during the coast period and subsequent restart. Comparison of these data with the ascent engine data show that the oxidizer in the descent injector is much closer to equilibrium than the oxidizer in the ascent injector. The data points for coast times of 40, 50, 60, and 70 seconds are very close to the oxidizer triple point, which indicate that oxidizer is being frozen at nearly equilibrium conditions during this time period. This phenomena is typical of most Phase I and Phase II coast periods having a duration of more than 40 seconds.

The fuel phase histories for Phase II tests D0-II and D-11 are shown in Figures 7-43 and 7-44. Comparison of the phase histories for D0-II and D-11a (Figure 7-43) and D-11a, b, c (Figure 7-44) show that there are no major differences between the fuel phase histories for initial starts and restarts or for relatively small (11°F) changes in initial propellant temperature.

The oxidizer phase histories for Phase II tests D0-II and D-11 are shown in Figures 7-45 and 7-46. Comparison of the phase histories for D-11a, b, c indicates that the oxidizer temperature did not increase to the initial temperature of 46°F during the coast phases following restart firings D-11b and D-11c. The cause for this phenomena has not been established, although thermocouple response time may be a factor. Cold flow tests at ARC show that thermocouples cemented to the duct surface had a time lag of only 5 to 10 seconds relative to thermocouples inserted into the propellant ducts. This time lag occurred during the 3.5 second propellant flows, and during the subsequent coast periods. However, the time and temperature lags observed during cold flow tests do not have a sufficient magnitude to fully explain the 20 to 50°F temperature differences which were observed during the first 25 seconds of successive hot-firing coast periods.

Comparison of the phase histories for Phase I and Phase II tests show that the initial fuel and oxidizer temperatures have a significant effect on the time required to reach the fuel and oxidizer boiling and freezing points. The table below provides typical data from the initial coast periods of Phase I and Phase II tests.

D2-118246-1

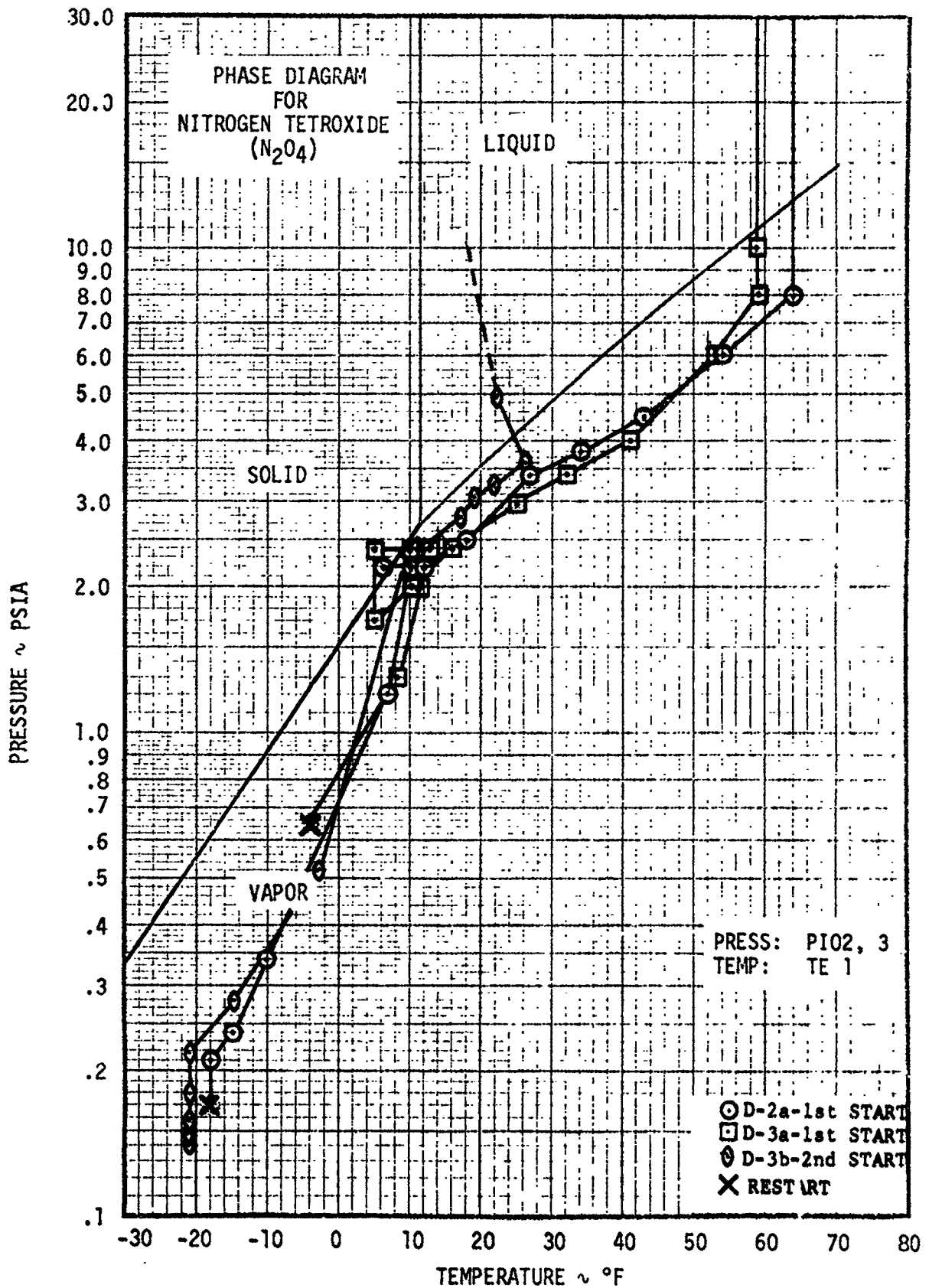


FIGURE 7-42 OXIDIZER PHASE HISTORY FOR DESCENT ENGINE

D2-118246-1

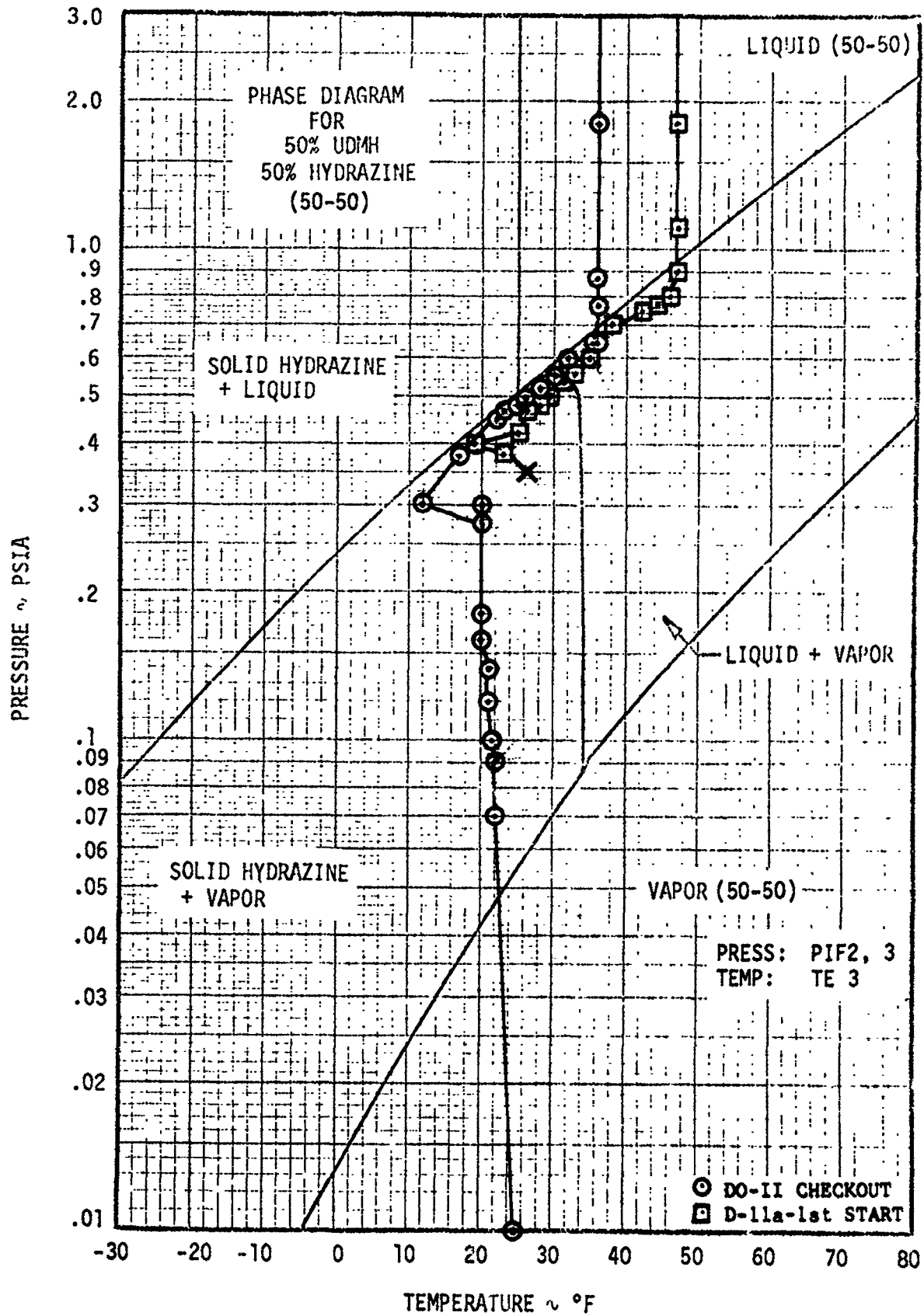


FIGURE 7-43 FUEL PHASE HISTORY FOR DESCENT ENGINE

D2-118246-1

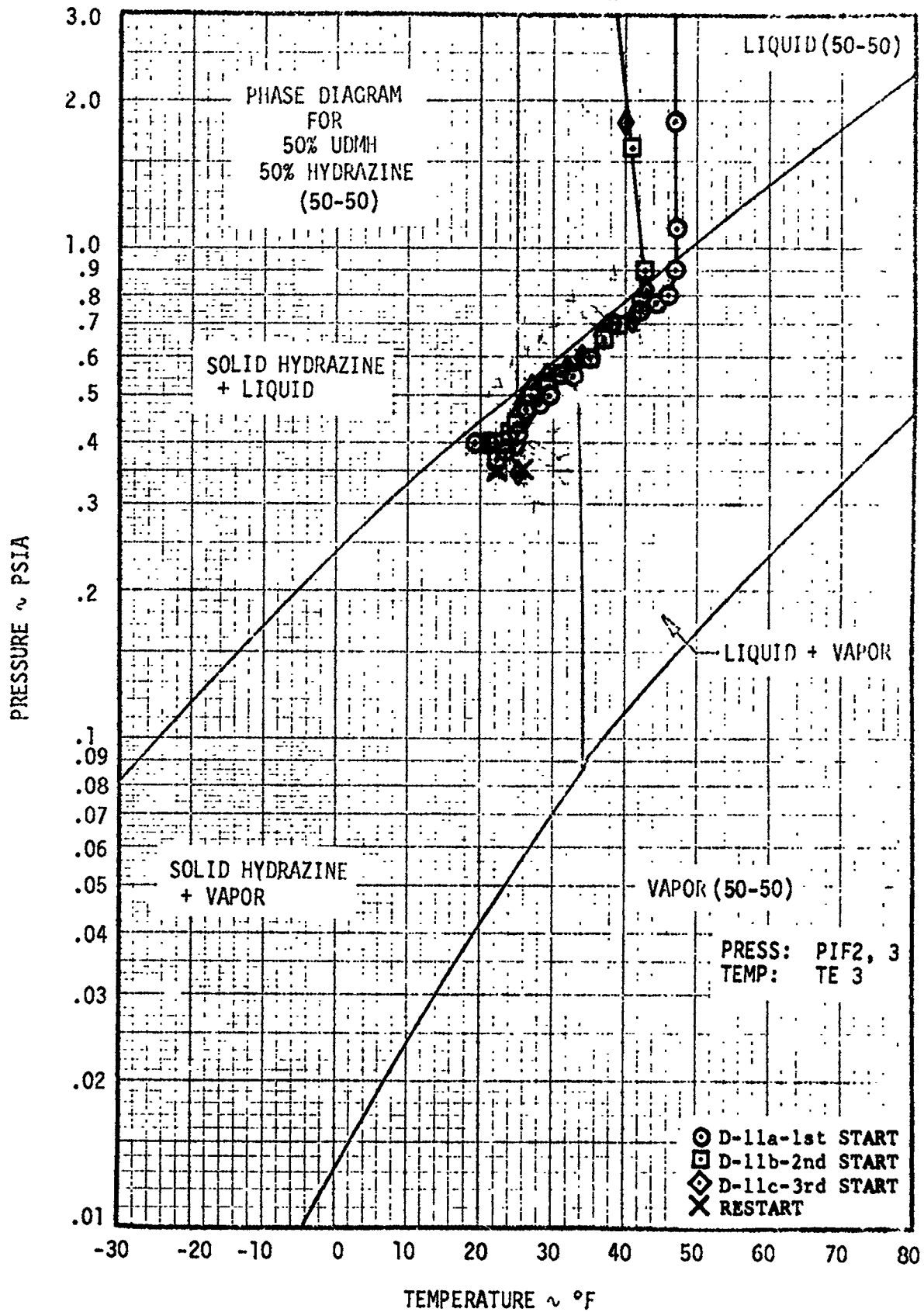


FIGURE 7-44 FUEL PHASE HISTORY FOR DESCENT ENGINE

D2-118246-1

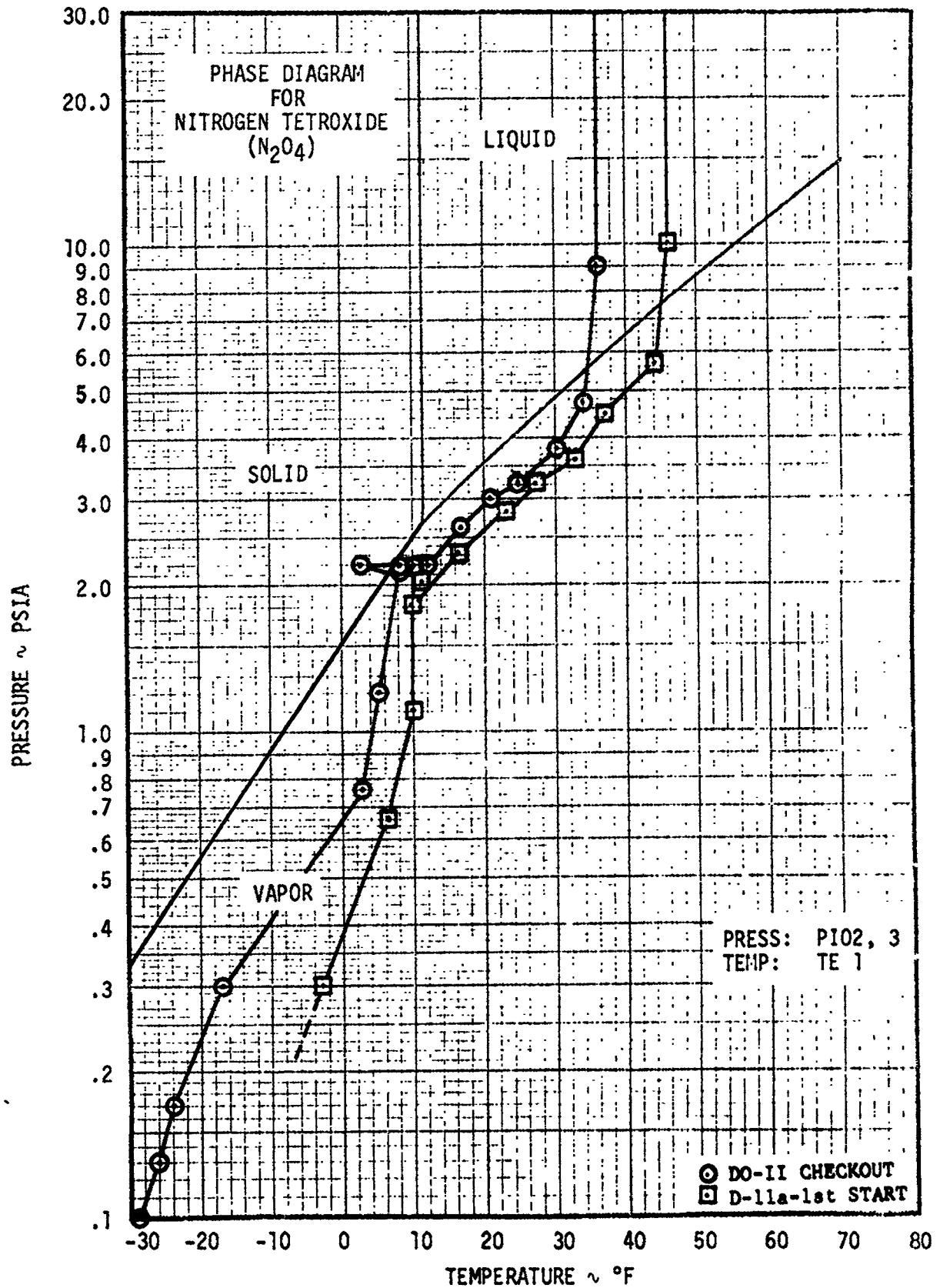


FIGURE 7-45 OXIDIZER PHASE HISTORY FOR DESCENT ENGINE

D2-118246-1

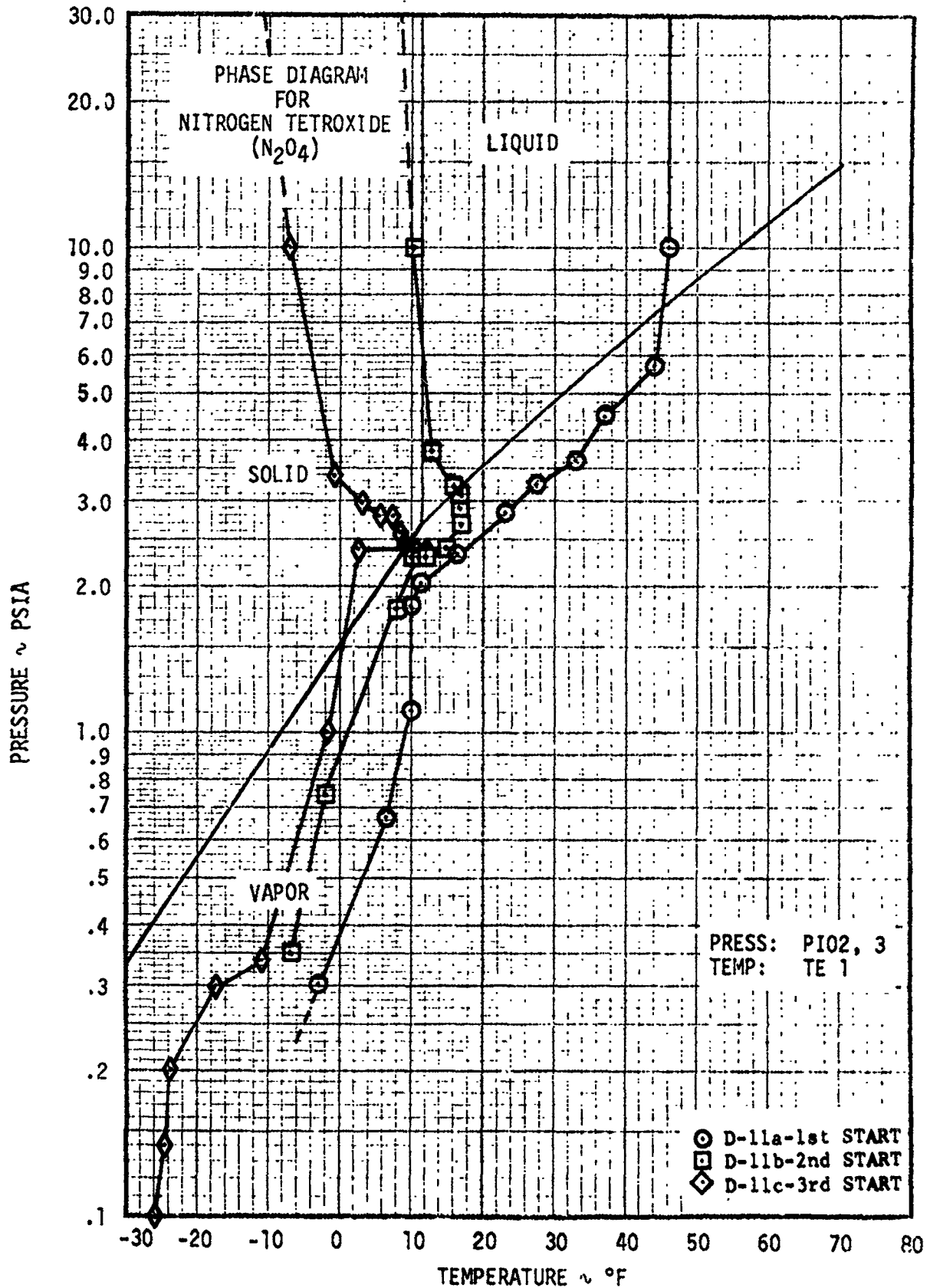


FIGURE 7-46 OXIDIZER PHASE HISTORY FOR DESCENT ENGINE

7.4.2 Coast Phase Analysis (Continued)

INITIAL PROP. TEMP. (°F)	FUEL		OXIDIZER	
	TIME TO BOIL (SEC)	TIME TO FREEZE (SEC)	TIME TO BOIL (SEC)	TIME TO FREEZE (SEC)
64	10	80	5	50
46	15	60	7	50
36	20	40	8	40

The "time to boil" is increased by a decrease in propellant temperature and vapor pressure. Because of the vapor pressure decrease, more time is required for the fuel and oxidizer manifold pressures to decay to the propellant vapor pressure. The "time to freeze" is decreased as propellant temperatures are decreased because less cooling is required to reach the freezing temperature.

Typical coast phase propellant phenomena are discussed in the following paragraphs.

Following shutdown there was a short period of time before the fuel manifold pressure dropped to the fuel vapor pressure. This time varied from test to test but averaged about 15 seconds for the Phase II tests. This time is far too long to be explained on the basis of an incompressible liquid in the dribble volume. However, the helium dissolved in the fuel will come out of solution as the manifold pressure decays. The helium bubbles can displace significant volumes of liquid in the injector, and maintain relatively high injector pressures for several seconds. The photographic coverage of the test tends to support this mechanism in that the fluid ejected immediately after shutdown appeared to be foamy. An alternate possibility is that local hot spots exist in the injector, causing local boiling of the residuals and producing sufficient vapor to maintain injector pressure during this period. However, the injector movies and the injector thermocouple data do not support the hypothesis that there were injector hot spots. The high speed movies show that frozen fuel and oxidizer were extruded from the injector after shutdown, indicating that the injector was not hot. In addition, the injector thermocouples do not indicate any significant temperature increase during the engine firing. The pressure produced by the weight of residuals in the injector is not large enough to cause the relatively high manifold pressures observed after shutdown. It is therefore concluded that the initial fuel manifold pressure decay is significantly affected by the effervescence of dissolved helium.

When the fuel manifold pressure decreased to the fuel vapor pressure, the fuel started to boil. As the fuel continued to boil, the fuel temperature dropped to the point where hydrazine started to freeze out of the

7.4.2 Coast Phase Analysis (Continued)

solution. Pure hydrazine freezes at about 34°F, but a 50-50 liquid mixture with UDMH freezes at about 25°F. However, if the temperature of a 50-50 liquid mixture is lowered below 25°F, some of the hydrazine will freeze. This will increase the percentage of UDMH in the liquid and decrease the freezing temperature of the remaining hydrazine/UDMH mixture. Thus, hydrazine can remain in the liquid state in the proper liquid composition down to -71°F. Since the fuel-side temperature dropped far below 25°F, one must conclude that the hydrazine was solidifying fast enough to increase the percentage of UDMH in the liquid. The freezing temperature of the remaining hydrazine will therefore decrease. It is then possible to obtain very low temperatures before all of the hydrazine freezes.

The fuel side temperature increase from 12°F to 20°F indicated that the fuel vaporization rate had decreased. The subsequent pressure decay at constant temperature results from a thermal balance between evaporative cooling and heat transfer from the engine and the test facility.

It is believed that the residuals were essentially all solidified at the time of the temperature increase (200-250 seconds) because by that time, sufficient fuel had been vaporized to freeze the remaining residuals (see Section 7.2).

The engine orientation allowed drainage of all of the oxidizer in the injector, and about half of the oxidizer in the duct. As a result, the oxidizer residuals were trapped primarily in the duct near the ball valve assembly.

The oxidizer manifold pressure reached the vapor pressure of the N_2O_4 in slightly less than 10 seconds. Boiling then occurred with around 5-10°F superheat in the liquid until the freezing temperature of the N_2O_4 was reached at about 35 seconds. In general, the oxidizer side maintained temperature and pressure values in the vicinity of the triple point for some time. In some tests, the pressure remained constant near the triple point pressure while the temperature decreased below the triple point temperature. This would indicate subcooling of the liquid. After 80 seconds, the pressure decreased sufficiently below the triple point pressure to indicate that all of the liquid had frozen. The continued temperature decrease was produced by sublimation of the frozen N_2O_4 . After 500 seconds, the duct temperature began to increase to ambient, and at about 1200 seconds the pressure had become sufficiently low that the readings were no longer reliable. The remaining N_2O_4 was probably expended at some time between 1200 and 1800 seconds, but it is not possible to determine exactly when the residuals were expended.

7.4.3 Start and Restart Firing Characteristics Analysis

A review of the test data, summarized in Section 5, Table 5-3, shows that only one restart (Phase I test D-2b) was significantly harder than the initial starts. In addition, this summary shows that the initial starts had significant run-to-run variations. The characteristics of the initial starts were investigated to determine correlating parameters and to provide a baseline for evaluation of the restarts.

The following paragraphs describe typical descent engine start and shutdown characteristics observed during the Seattle test series. The Phase II descent engine checkout firing, D-OII, was a typical dry start. After the fire signal, the valves started to open in about 40 milliseconds. All of the valves were completely open by 150 milliseconds. The fuel pressure at the engine interface remained constant at 218 psig for 25 milliseconds then dropped to 190 psig at 50 milliseconds, increased to 250 psig at 80 milliseconds, and returned to the steady state value at 100 milliseconds. The fuel interface pressure remained constant during the remainder of the firing and shutdown with some very small oscillations observed immediately after shutdown. The oxidizer engine interface pressure remained constant at 227 psig for 40 milliseconds then oscillated from 262 to 173 psig at a frequency of about 35 cps before damping out in about 300 milliseconds. The pressure then remained essentially constant throughout the firing and shutdown. Minor disturbances were observed immediately following ignition, and a rapidly damped 35 cps oscillation was observed about 300 milliseconds following shutdown.

The oxidizer manifold pressure remained constant at zero psia for 55 milliseconds following the actuation of the fire switch. The pressure then rapidly increased to 13.4 psia in about 50 milliseconds, and steadily increased to 24 psia at ignition (1.524 seconds after fire signal). The pressure decreased to 23 psia at ignition and continued to drop to 18.2 psia at 120 milliseconds after ignition. The pressure increased steadily to 62 psia at 1.3 seconds after ignition and remained at this level until after shutdown. Three hundred milliseconds after shutdown, the oxidizer manifold pressure decreased, reaching 8 psia at 5.5 seconds.

The fuel manifold pressure increased slowly from zero psia at the fire signal to 3 psia at ignition. It was not possible to determine when the fuel manifold was primed because there was no sudden increase in pressure in the time period immediately preceding ignition. At ignition, the fuel manifold pressure had a rapid increase to 8.5 psia. The pressure then increased steadily to 19.2 psia during steady-state engine operation.

The chamber pressure indicated essentially zero psia until ignition occurred 1.524 seconds after the start signal. At ignition, the chamber pressure increased rapidly from 0.8 psia to a peak of 33.1 psia, and then decreased in 10 milliseconds to 8.9 psia. The pressure continued to

7.4.3 Start and Restart Firing Characteristics Analysis (Continued)

decrease, reaching a low of 2 psia before beginning a smooth increase to a steady-state pressure of 14.5 psia.

The flight accelerometers show 40, 70, and 65 g's peak to peak readings along the X, Y, and Z axis respectively at the time of ignition. The facility accelerometers show 386, 80, and 246 g's at this time. No other accelerometer deflections were noted during or after the firing.

About 30 milliseconds following the shutdown signal the valves start to close. Three of the valves are closed within 300 milliseconds and the fourth closed at 450 milliseconds.

The high speed (1000 frames per second) Photosonics camera showed that the oxidizer spray appeared first 350 milliseconds after the fire signal. Ten milliseconds later, irregular fuel and oxidizer "snow" particles were observed. As the intensity of the oxidizer spray and fuel snow increased, a red glow appeared. The injector pintle was obscured about 300 milliseconds after the first oxidizer spray (650 ms. after fire signal). Approximately 1000 milliseconds after fire signal the film was completely black, indicating that the light source was obscured by material in the chamber. Significant combustion (ignition) was indicated by a brilliant red flash at approximately 1.520 seconds after the fire signal. Brown deposits, similar to those observed after shutdown, were observed on the thrust chamber window at engine start, and remained on the window for several milliseconds. The ignition transient had a duration of approximately 6 ms., after which the light intensity decreased significantly. Within 60 ms., combustion decreased to the extent that the pintle was clearly visible, and frothy oxidizer globules were seen coming from the pintle. The pintle was obscured 100 ms. after ignition by the increasing intensity of the combustion process. At 330 ms. after ignition, the combustion process had a noticeable change from the previous red color to an increasingly brilliant white color. The intensity of the combustion process had noticeable oscillations in intensity (confirmed by chamber pressure data) which lasted until steady-state conditions were reached.

Steady-state operation appeared to be very smooth. The first visual indication of shutdown (300 ms. after shutdown signal) was the appearance of oxidizer spraying towards the window. The combustion intensity decreased and changed to a red color as the oxidizer spray continued. The pintle was first observed 1.25 seconds after shutdown signal, with large globules of foamy oxidizer being blown off the end of the pintle, and foamy spray coming from the oxidizer orifices. Pulsations in combustion intensity were observed from 1.72 to 2.22 seconds after shutdown signal and were confirmed by chamber pressure data. The first indication of frozen oxidizer was observed 2.5 seconds after shutdown, when oxidizer "snow" was blown out of the bottom of the pintle. Significant amounts of solid fuel and oxidizer deposits were observed to "grow"

7.4.3 Start and Restart Firing Characteristics Analysis (Continued)

out of the fuel and oxidizer orifices during the period from 3.5 to 7.0 seconds after shutdown. The deposits were blown away but reformed immediately. Approximately 10 seconds after shutdown, viscous brown deposits were formed on the thrust chamber windows. These deposits boiled slowly, but never appeared to freeze, indicating that they were neither fuel nor oxidizer residuals.

Test data from the initial starts were analyzed to determine if the run-to-run variations between initial starts could be correlated. The magnitude of the initial chamber pressure pulse was plotted against the following parameters to determine if they correlated the run-to-run variations:

1. time from fire signal to ignition
2. initial propellant temperatures
3. fuel and oxidizer ullage pressures
4. fuel and oxidizer injector pressures at ignition
5. fuel and oxidizer dissolved gas content ($\text{He} + \text{N}_2$)

This evaluation showed that the initial propellant temperature and the oxidizer dissolved gas content provided limited correlations with the magnitude of the peak chamber pressure overshoot. The data presented in Figures 7-47 and 7-48 show that dry starts tended to become rougher as the dissolved gas content of the oxidizer increased, while wet starts tended to become rougher as the propellant temperature decreased. The wet starts (D-7a through D-12a) were not correlated by the measured gas content of the propellants in the run tanks. The wet starts were accomplished by admitting fuel and oxidizer into the volume between the isolation and bipropellant ball valves, and admitting fuel into the valve actuation system. This was accomplished at a pressure of 80 psi, with the result that the trapped propellant was probably saturated at a pressure of 80 psi instead of 240 psi. The reduced gas content of the trapped propellant apparently negates the correlation of start overshoot with bulk propellant gas content.

Test data from the restarts were analyzed to determine if the restart characteristics could be correlated by any of the following parameters:

1. coast time
2. temperature of fuel and oxidizer residuals
3. time from fire signal to ignition

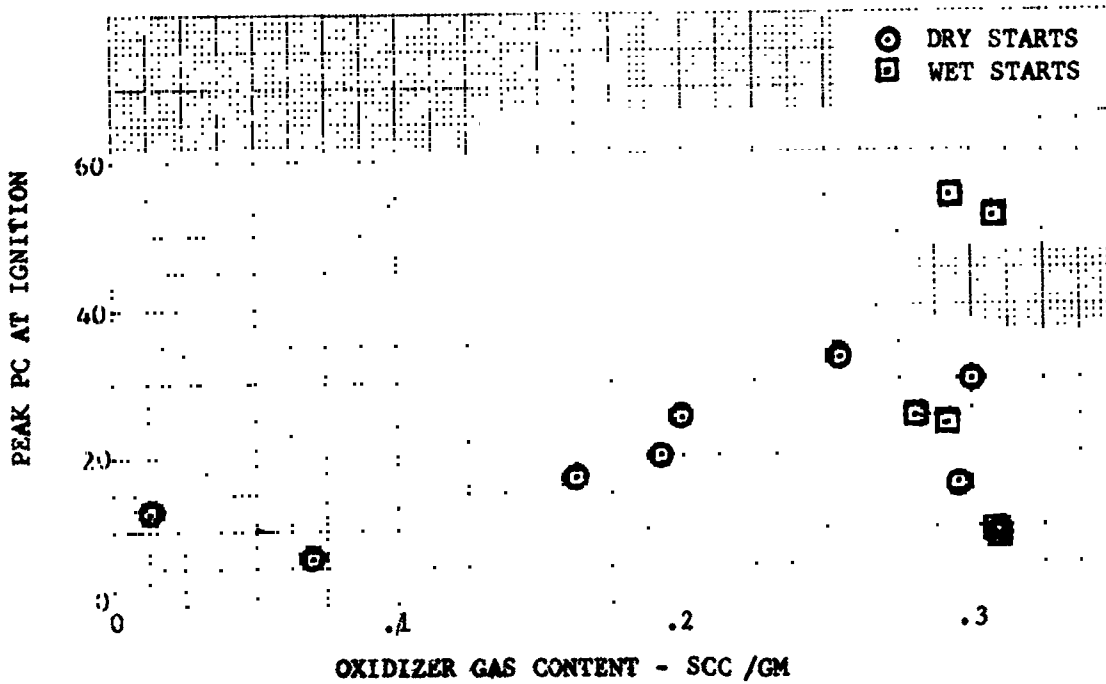


FIGURE 7-47 PEAK CHAMBER PRESSURE VS DESCENT ENGINE OXIDIZER GAS CONTENT

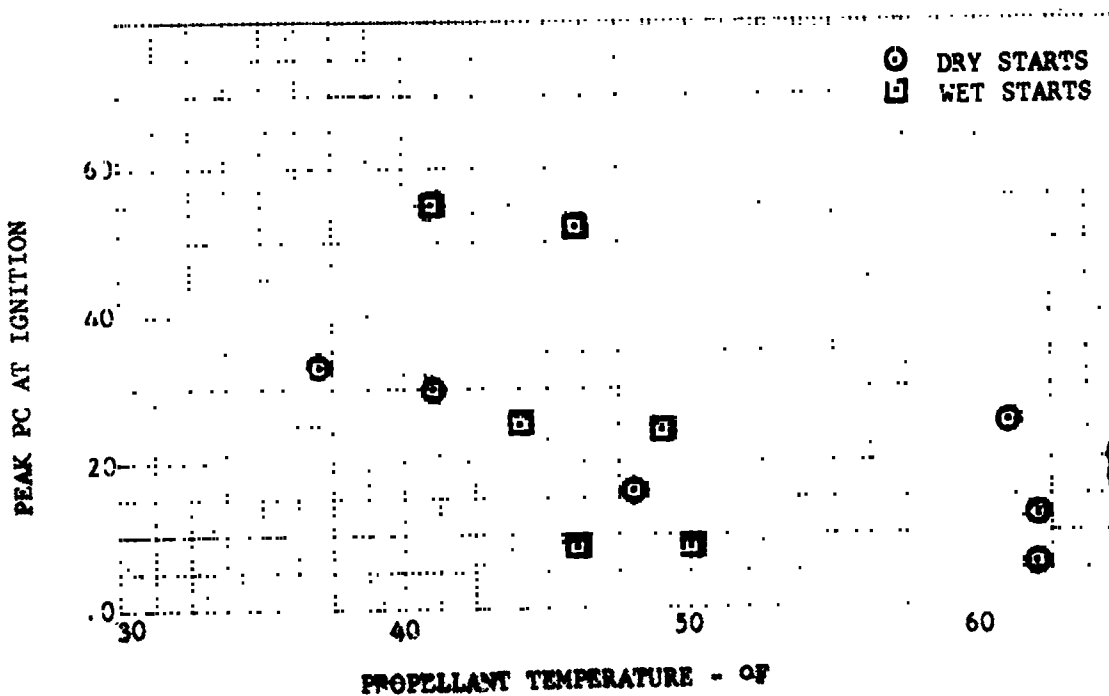


FIGURE 7-48 PEAK CHAMBER PRESSURE VS DESCENT ENGINE PROPELLANT TEMPERATURE

7.4.3 Start and Restart Firing Characteristics Analysis (Continued)

4. fuel and oxidizer injector pressures at ignition
5. fuel and oxidizer dissolved gas content
6. volume of fuel and oxidizer residuals

The peak value of the chamber pressure overshoot was used to characterize the restart ignition characteristics. This parameter was used because of the relatively long duration (10 milliseconds) of the pressure pulse.

Figures 7-49 and 7-50 present the most significant results of the attempted correlations. Figure 7-49 is a plot of the chamber pressure peak versus coast period, and Figure 7-50 is a plot of ignition delay versus coast period. Figure 7-49 shows that the Phase I restarts, conducted with propellant temperatures of 61-66°F, were significantly harder than the Phase II restarts, conducted with propellant temperatures of 41-50°F. However, only the Phase I test at a coast time of 316 seconds is significantly harder than the range of initial wet starts.

There is no evidence that the difference between fuel and oxidizer residual volumes has a significant effect on the ignition characteristics. At short coast times (less than 10 seconds), the residuals will tend to produce simultaneous fuel and oxidizer injection. However, these restarts had no measurable P_c overshoot or accelerometer readings, apparently because they occurred when the chamber pressure was still high enough (.3 psia) to produce very smooth reignition. The maximum difference between fuel and oxidizer residual volumes (see Section 7.2) occurs at coast times of 100 to 200 seconds. The restarts during this range of coast periods are not significantly different from the other restarts.

Figure 7-50 shows the effect of coast time on ignition delay. At short coast times, the ignition delay is significantly reduced by the presence of residual propellants. As the coast period increases, the ignition delay tends to increase toward the delay range for initial starts. The ignition delay, although related to the volume of residual propellants, does not appear to be related to the magnitude of the P_c overshoot.

Analysis of the descent engine restart tests did not result in any cause-and-effect relationship between the magnitude of the restart chamber pressure transient and the parameters listed above. Additional testing may result in a cause-and-effect relationship.

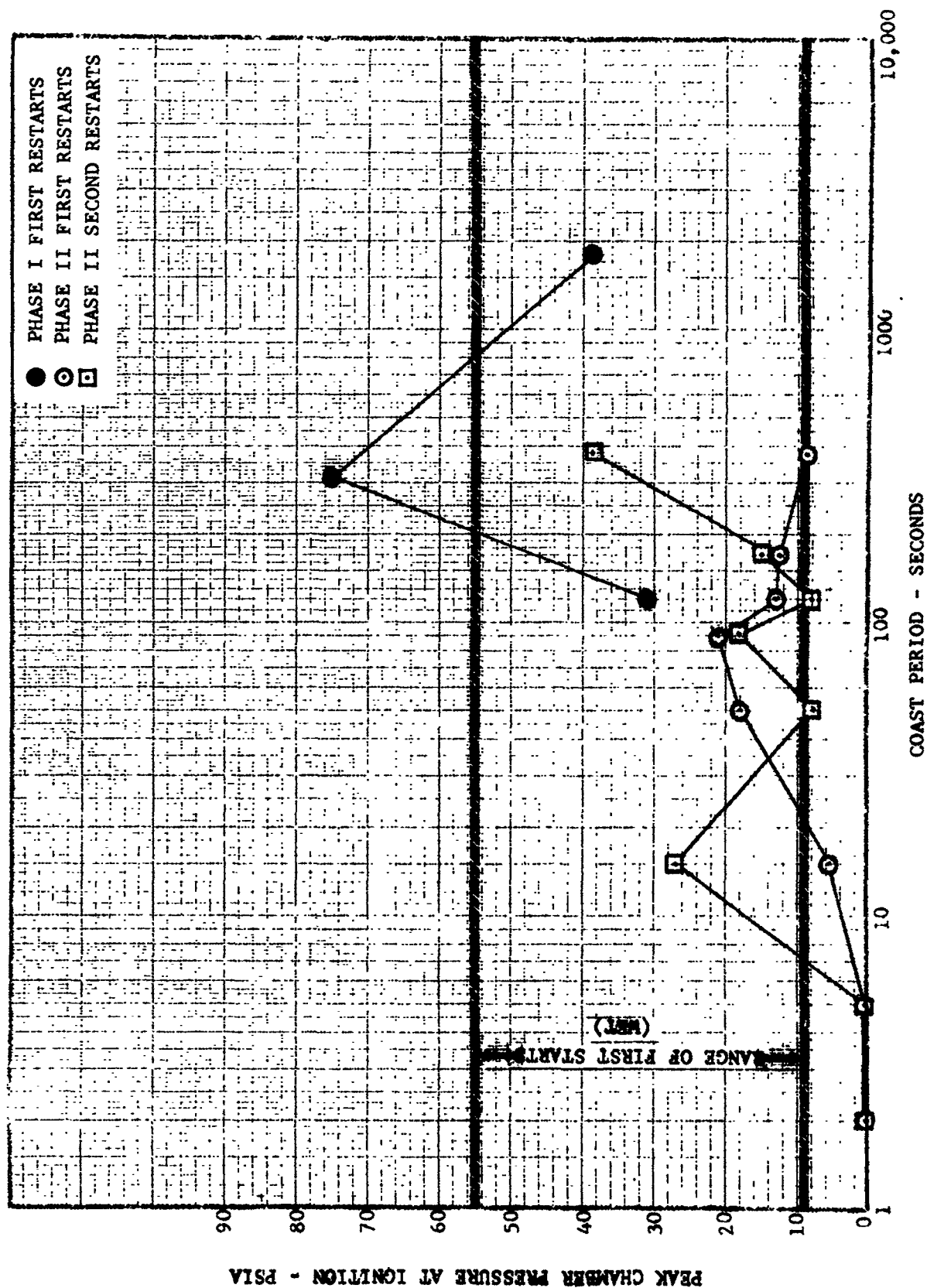


FIGURE 7-49 PEAK CHAMBER PRESSURE VS DESCENT ENGINE COAST PERIOD

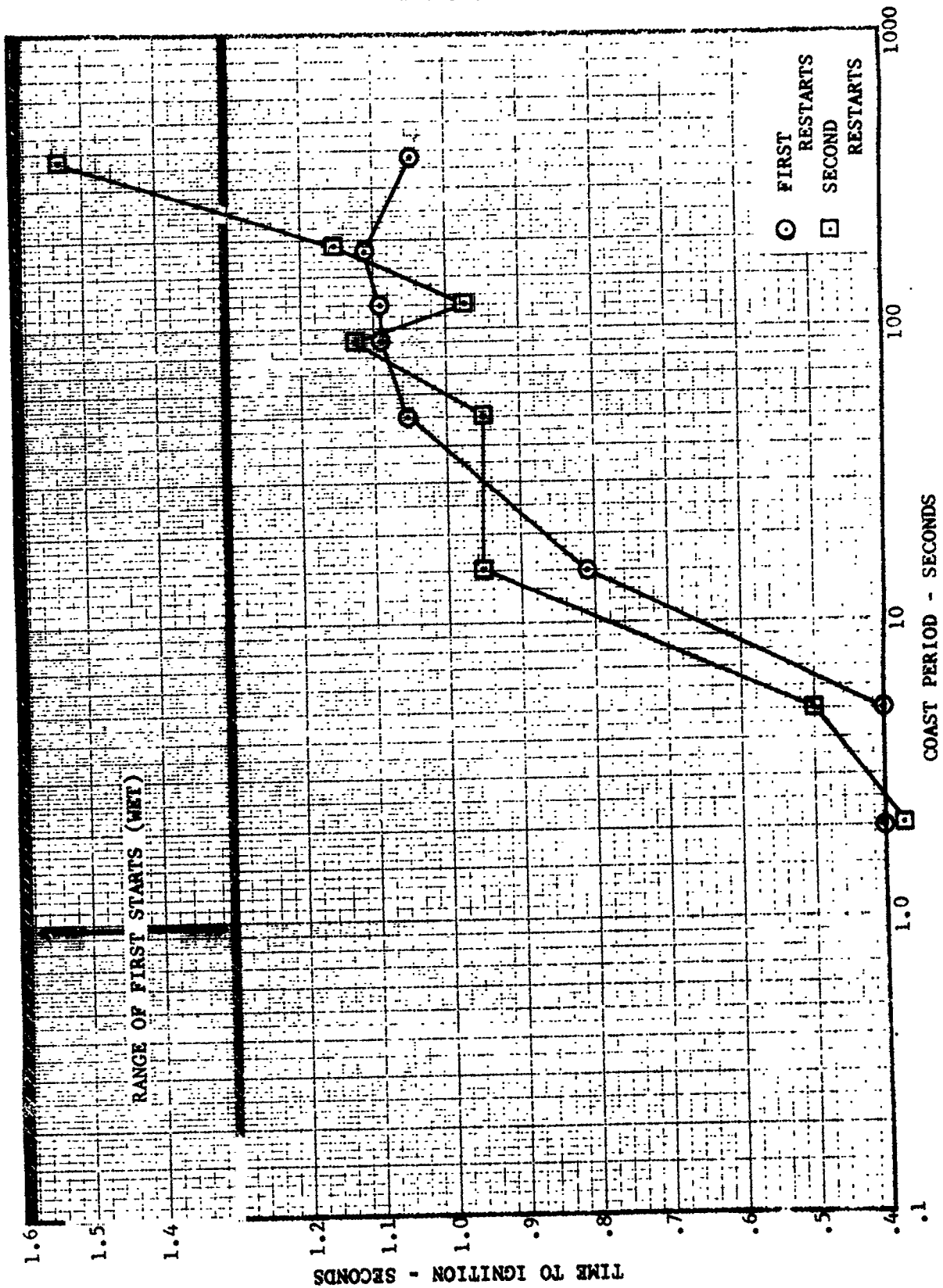


FIGURE 7-50 TIME TO IGNITION VS DESCENT ENGINE COAST PERIOD

7.5 SPS COLD FLOW TEST ANALYSIS

7.5.1 General

This section presents and analyzes SPS injector test data from cold flow tests conducted at AEDC. These tests were conducted to investigate the phenomena occurring when residual propellants in the injector and inlet ducts are exposed to a low pressure environment. The test data were analyzed to determine the effects of coast time and initial propellant temperatures, and to provide a basis for comparing the cold flow test results with the hot firing test results. Propellant temperature histories and phase histories are presented to provide this basis for comparison. Appendix D of this report describes the AEDC test facility and test article, and provides a description of the test series.

7.5.2 Phase I Tests - Oxidizer

Eleven tests were conducted during this phase of cold flow testing with initial propellant temperatures ranging from 15 to 65°F. Phase histories for tests I-3, I-6 and I-11 are presented in Figure 7-51. The pressure and temperature measurements were taken in the propellant inlet duct very near the bipropellant ball valve flange. These histories show that the oxidizer was out of thermal equilibrium for all three tests. Data from tests I-6 and I-3 showed an abrupt drop in pressure at 4-5 seconds that was accompanied by a small decrease in temperature. The time of this sudden decrease in pressure correlates very closely with visual observations which indicated that all liquid was gone, and only frozen material remained in the duct.

From these phase diagrams it is also evident that an increase in the initial oxidizer temperature caused an increase in the rate of cooling. This was caused by more violent boiling at the warmer temperatures, which increased the rate of heat removal from the remaining oxidizer.

Injector manifold and inlet duct temperature histories, Figure 7-52, show that the inlet duct initially cooled at about the same rate as the injector manifold, but finally reached a much lower temperature. This was expected because the test article was oriented so that the injector face was the high point and the inlet duct was the low point. Therefore, the inlet duct was the last volume to retain liquid. The inlet duct exterior skin thermocouple, located near the duct immersion probe, indicates that the duct skin did not get as cold as the frozen oxidizer inside of the duct.

7.5.3 Phase II Tests - Fuel

Ten tests were conducted during this phase of testing with initial propellant temperatures ranging from 34°F to 79°F. Selected test data from the Phase II tests are presented in Figures 7-53 and 7-54. These data are typical of the test results obtained during this phase of testing.

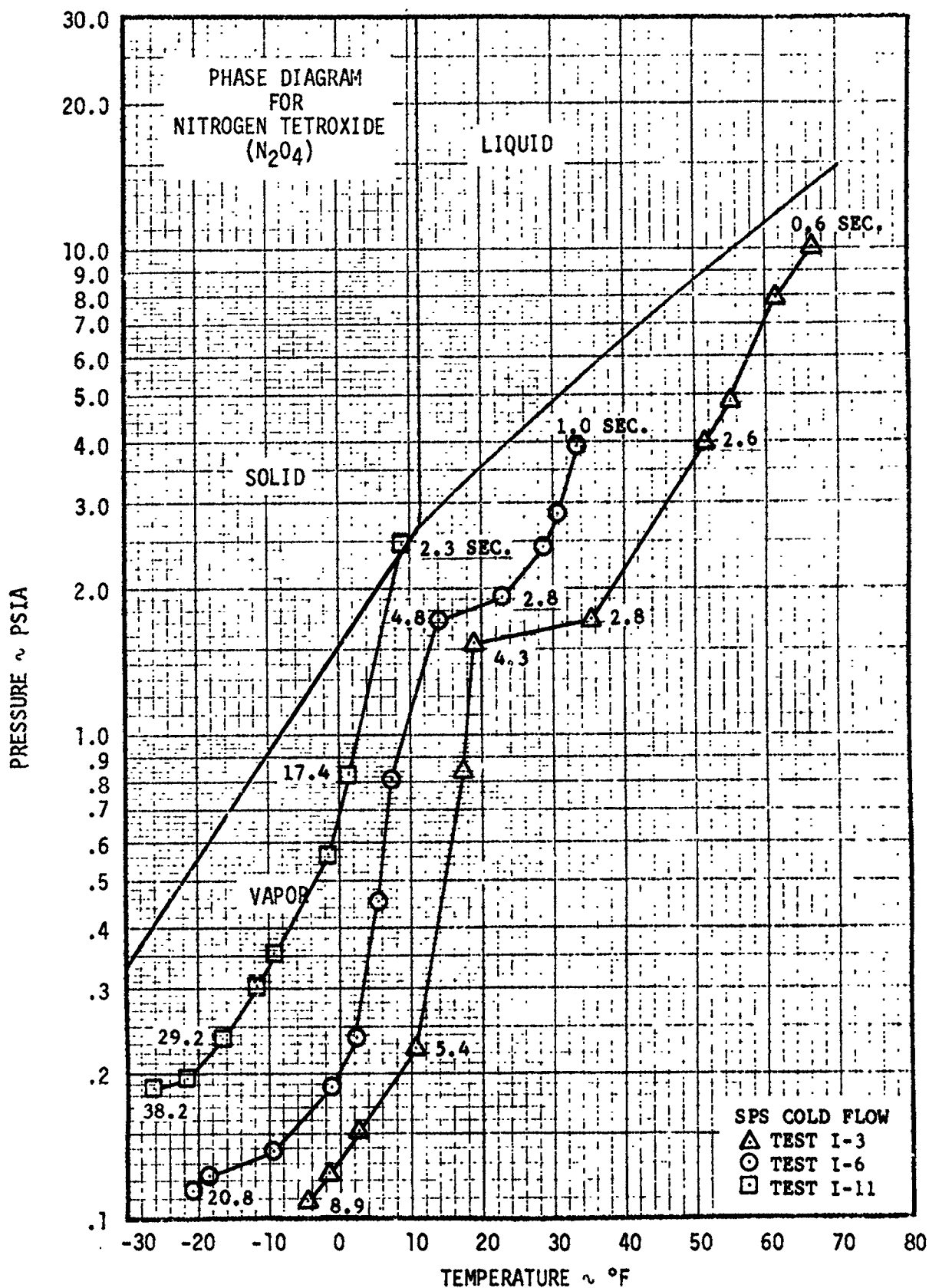


FIGURE 7-51 OXIDIZER PHASE HISTORIES SPS INJECTOR INLET DUCT

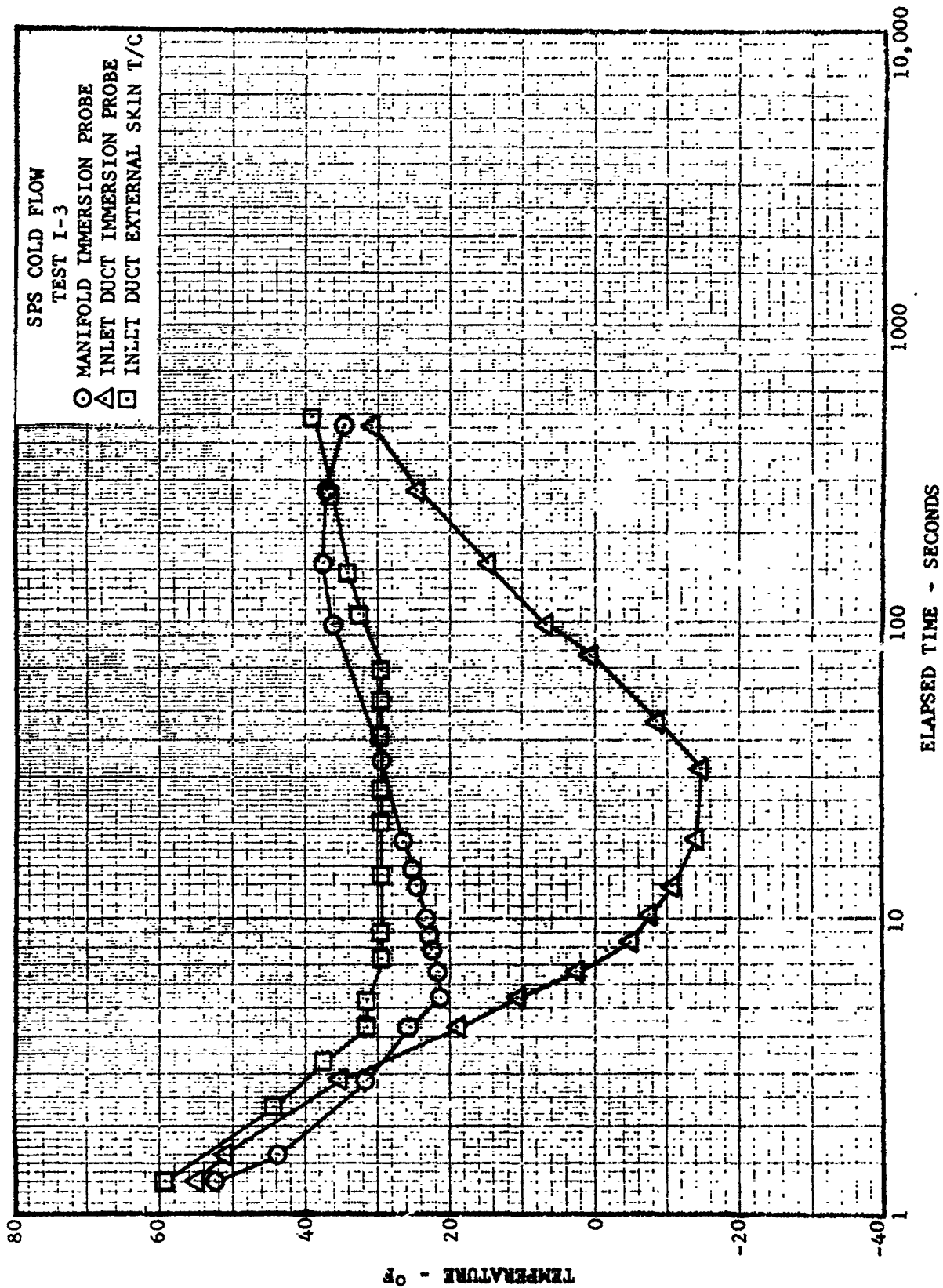


FIGURE 7-52 TEMPERATURE HISTORIES SPS INJECTOR MANIFOLD AND INLET DUCT

7.5.3 Phase II Tests - Fuel

The phase diagram shown in Figure 7-53 shows fuel duct temperature plotted against fuel duct pressure. Data is presented for three tests conducted with initial propellant temperatures of 73°F, 56°F, and 34°F. These phase histories show that the time to the start of freezing was a strong function of the initial propellant temperature. In addition, the data indicate that the fuel boiling process was far from being in thermodynamic equilibrium. In general, the phase histories were similar to the Bell ascent injector data, which are described in detail in Section 7.2.

Figure 7-54 shows a comparison of injector manifold and inlet duct immersion probes. These thermal histories show that the inlet duct temperature initially cooled at about the same rate as the injector manifold, but the duct eventually reached a colder temperature. This response pattern was typical of all SPS cold flow tests. Figure 7-54 also presents data for a surface thermocouple located on the duct exterior near the duct immersion probe. These data show that the duct surface thermocouple response was similar to the immersion probe response for the first 100 seconds of the test. The observed initial temperature bias was probably caused by instrumentation inaccuracy. After 100 seconds, the surface thermocouple did not respond accurately to the decrease in internal duct temperature. A maximum temperature difference of 15°F was indicated.

Comparison of the fuel and oxidizer temperature histories (Figures 7-54 and 7-52) shows that the oxidizer side was cooled more rapidly and reached a lower temperature than the fuel side. This result is typical of the ascent engine and descent engine tests also. This phenomena occurs because the oxidizer has a much higher vapor pressure than the fuel, which causes more violent boiling, an increased cooling rate, and earlier depletion of the residuals.

7.5.4 Phase III Tests - Fuel and Simulated Oxidizer (Freon MF)

Six tests were conducted during this phase with initial propellant temperatures ranging from 23 to 80°F for the simulant and 36 to 85°F for the fuel. This testing was accomplished by simultaneously filling the injector with fuel and simulated oxidizer (Freon MF). The test data showed that at similar initial conditions the fuel (only) tests and the fuel plus simulated oxidizer tests reached the same minimum temperature.

Although the same minimum temperature was reached, for a given initial propellant temperature, the fuel plus simulated oxidizer tests showed decreased times to reach the minimum temperature and to deplete the residual propellant.

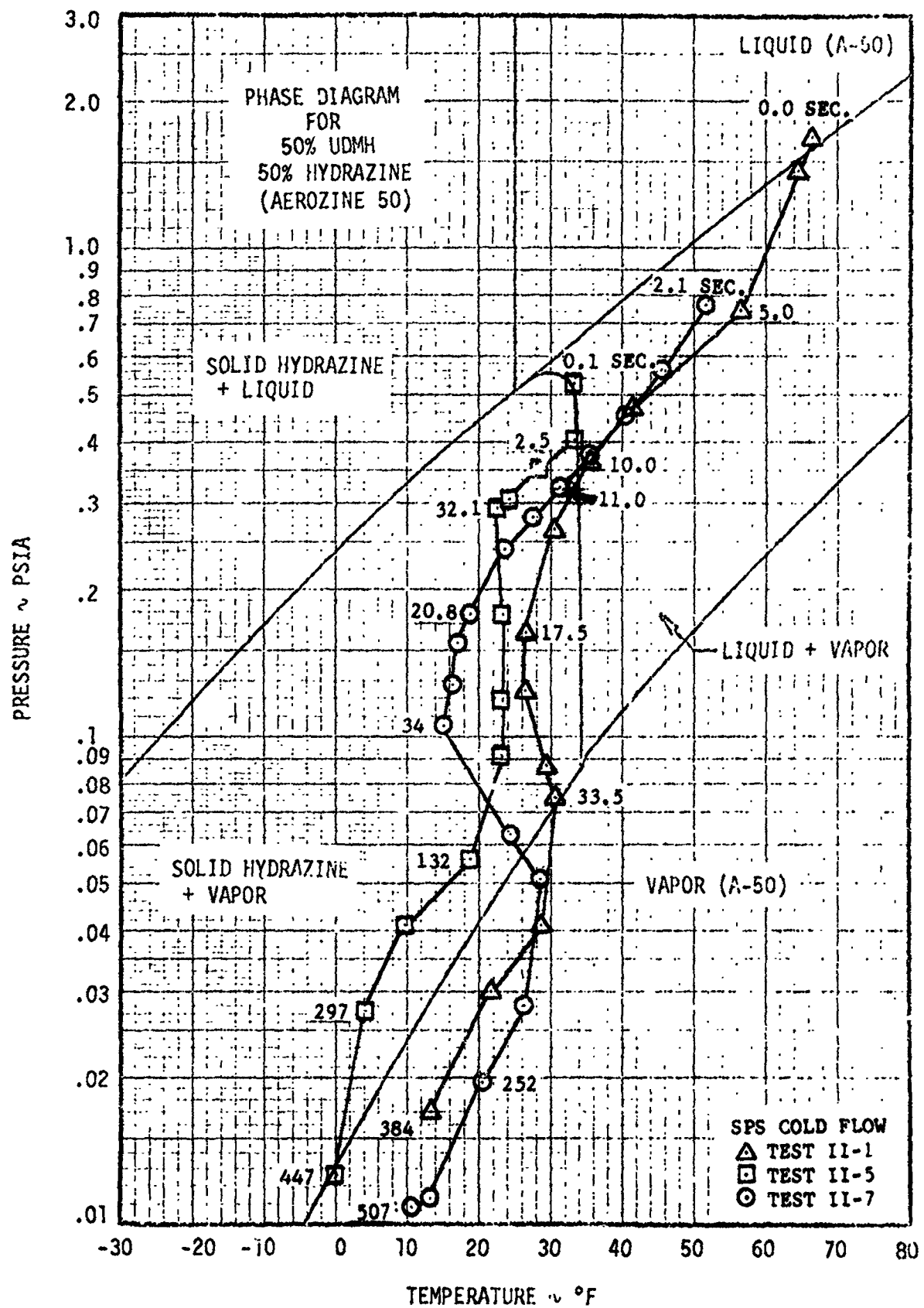


FIGURE 7-53 FUEL PHASE HISTORIES SPS INJECTOR INLET DUCT

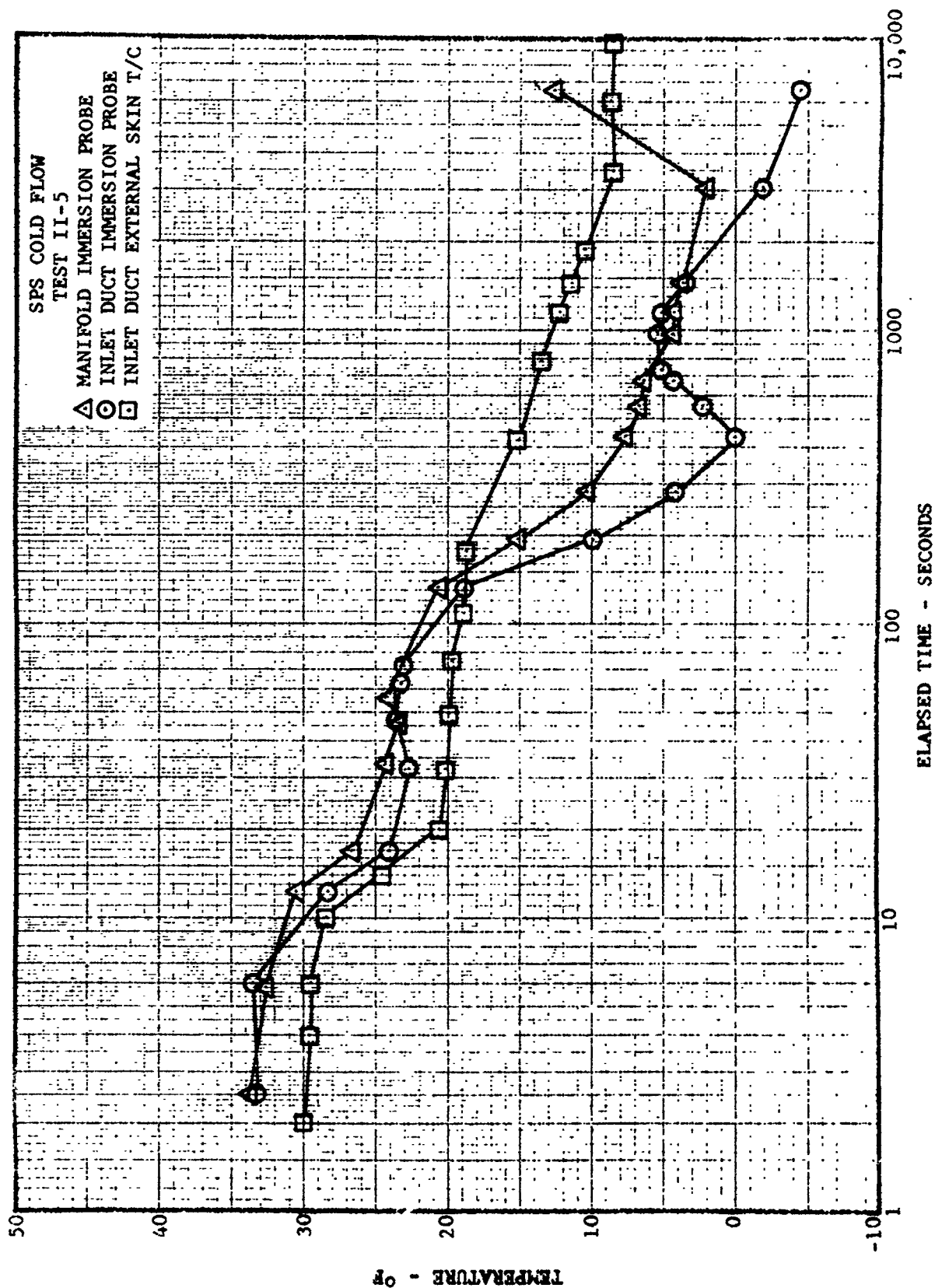


FIGURE 7-54 TEMPERATURE HISTORIES SPS INJECTOR MANIFOLD AND INLET DUCT

7.5.4 Phase III Tests - Fuel and Simulated Oxidizer (Freon MF) (Continued)

Figure 7-55 presents fuel duct immersion probe temperature histories from tests II-7 (Fuel only) and III-2 (Fuel plus simulant) to illustrate this phenomena.

As shown, the duct temperatures were similar during the first 2300 seconds of the test. The data from test III-2 show that the minimum duct temperature (-8°F) was reached at 2300 seconds, and that the duct temperature subsequently increased. In contrast, the data from test II-7 show a continuing temperature decrease until 5800 seconds after the start of the test.

The temperature increase after 2300 seconds, or 5800 seconds, occurred because the fuel residuals were essentially depleted. The longer time-to-depletion indicates that the fuel (only) test had a larger amount of residual fuel than did the fuel plus simulant test. The similarity of the temperature histories up to 2300 seconds, which would produce similar sublimation rates, supports this conclusion. Tests II-9 and III-4, also run at similar initial temperatures, produced the same type of results.

In general, the fuel (only) tests appeared to have more residual fuel than the fuel plus simulant tests for all tested temperatures. This result was not expected, because the increased cooling produced by the use of test fluids in both the fuel and oxidizer sides would be expected to increase the amount of frozen fuel residuals. It is possible that the fuel plus simulant tests did not have full fuel manifolds, because the additional time required to condition both the fuel and simulant to the required initial temperature (by evaporation of the test fluids) may have resulted in partial depletion of the fuel prior to the test.

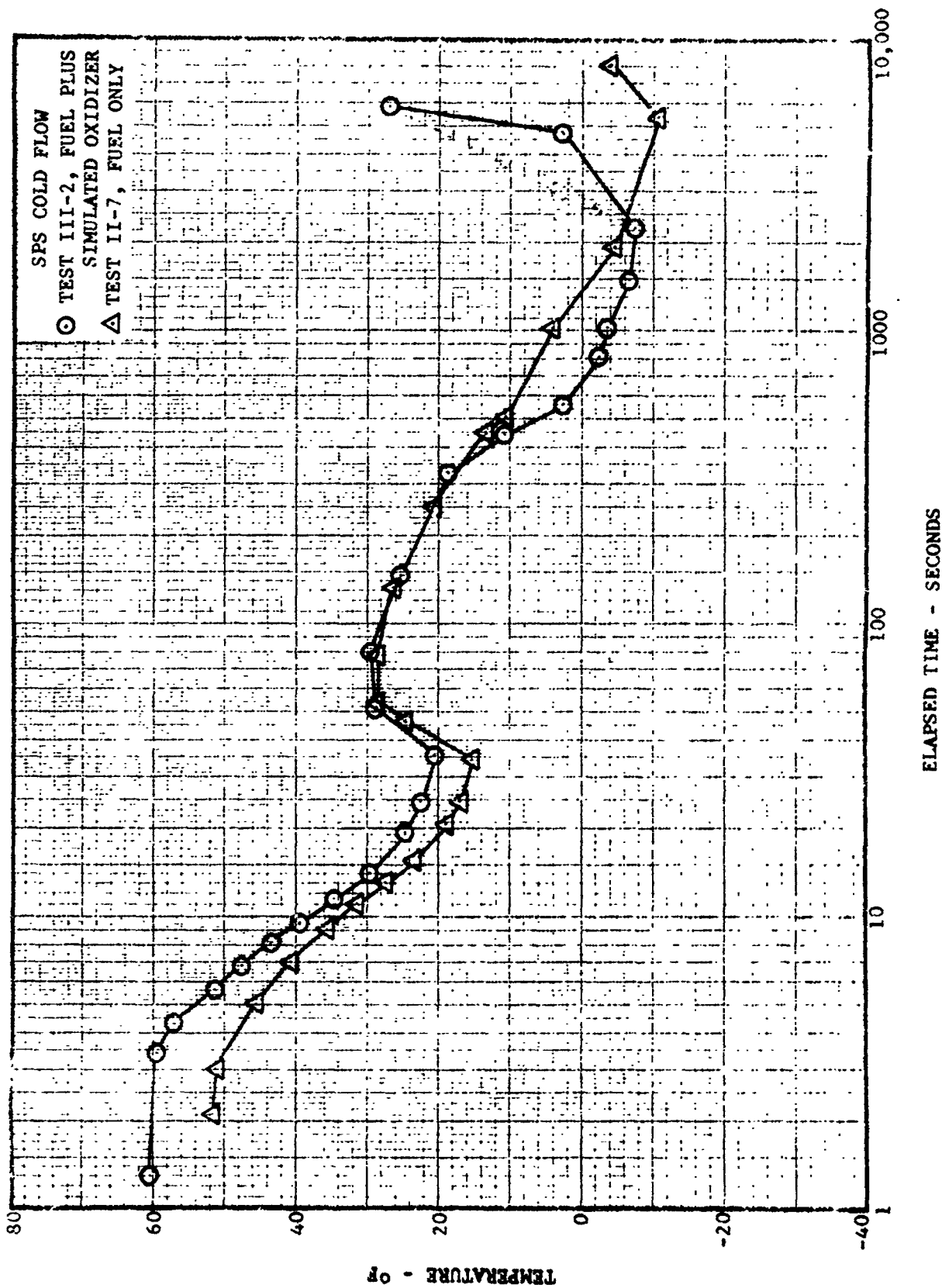


FIGURE 7-55 TEMPERATURE HISTORIES SPS INJECTOR INLET DUCT
COMPARISON FUEL ONLY AND FUEL PLUS SIMULATED OXIDIZER

7.6 SPS ENGINE TEST ANALYSIS

7.6.1 General

This section presents an analysis of the SPS engine restart tests conducted at AEDC. The coast phase data for propellant pressures and temperatures are presented on phase diagrams to provide a basis for determining the thermodynamic state of propellant residuals. The initial starts and subsequent restarts were analyzed to determine the effect of propellant residuals on engine restarts. A summary of test conditions and test results is presented in Tables 6-1 and 6-2.

During the AE series of tests, unusually high acceleration and chamber pressure spikes were occurring in a random manner. The magnitude of these spikes was sufficient to shake loose accelerometer installations and cables and to over-range the high response pressure transducers for almost every start. This series was terminated when it became apparent that the photographic window in the combustion chamber had been damaged.

After evaluation of the photographic coverage and test data, it was concluded that the high accelerations and pressure spikes were the result of thermal and shock sensitive residues accumulating in the combustion chamber. Elimination of these residues was accomplished by increasing the duration of the last firing in a restart sequence from 0.37 seconds to 0.50 seconds to allow the heat from combustion to vaporize or decompose the accumulated residues.

7.6.2 Coast Phase Analysis

The effect of evaporative cooling is clearly shown by the temperature measurements in the injector manifolds with the possibility of propellant freezing first occurring in the oxidizer manifold. During a typical shutdown transient, Figure 7-56, the oxidizer manifold pressure decreases to the triple-point pressure for N_2O_4 in about 7 seconds. Figure 7-57 depicts injector temperatures during the coast period after a 0.37 second pulse. The grouping of points around $10^\circ F$ for the oxidizer injector temperature (TOJ) correspond to the phase change at the triple-point of the oxidizer. Below this temperature all boiling is complete and the residual oxidizer is a solid. The fuel injector temperature (TFJ) indicates two minimum points during the coast period. This is typical of fuel side temperature profiles and the cause for this phenomena is discussed thoroughly in Section 7.3.2. The first minimum corresponds to the vaporization of the more volatile UDMH component. The second minimum is caused by the sublimation of hydrazine.

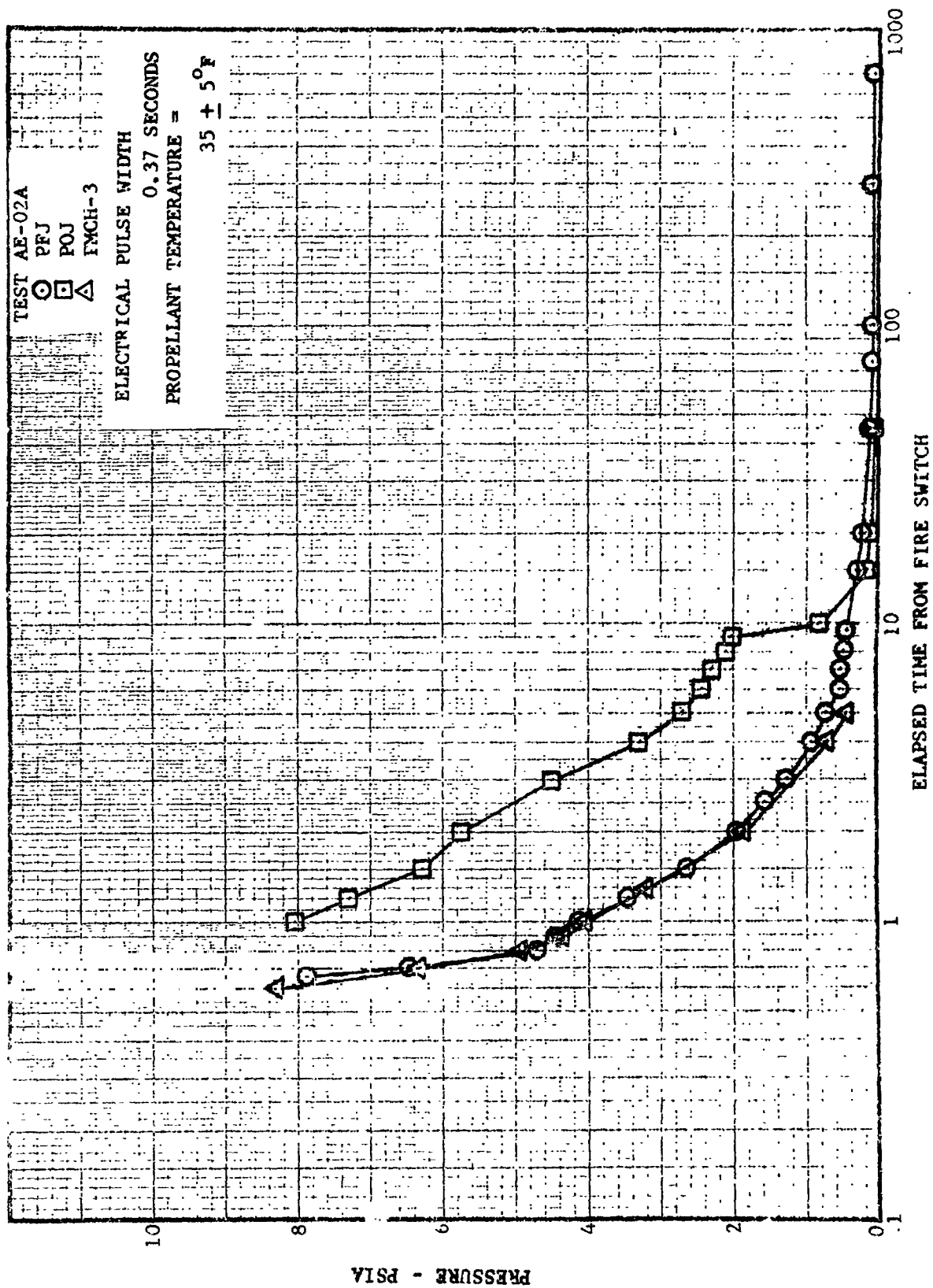


FIGURE 7-56 HISTORIES SPS INJECTOR AND COMBUSTION CHAMBER PRESSURE

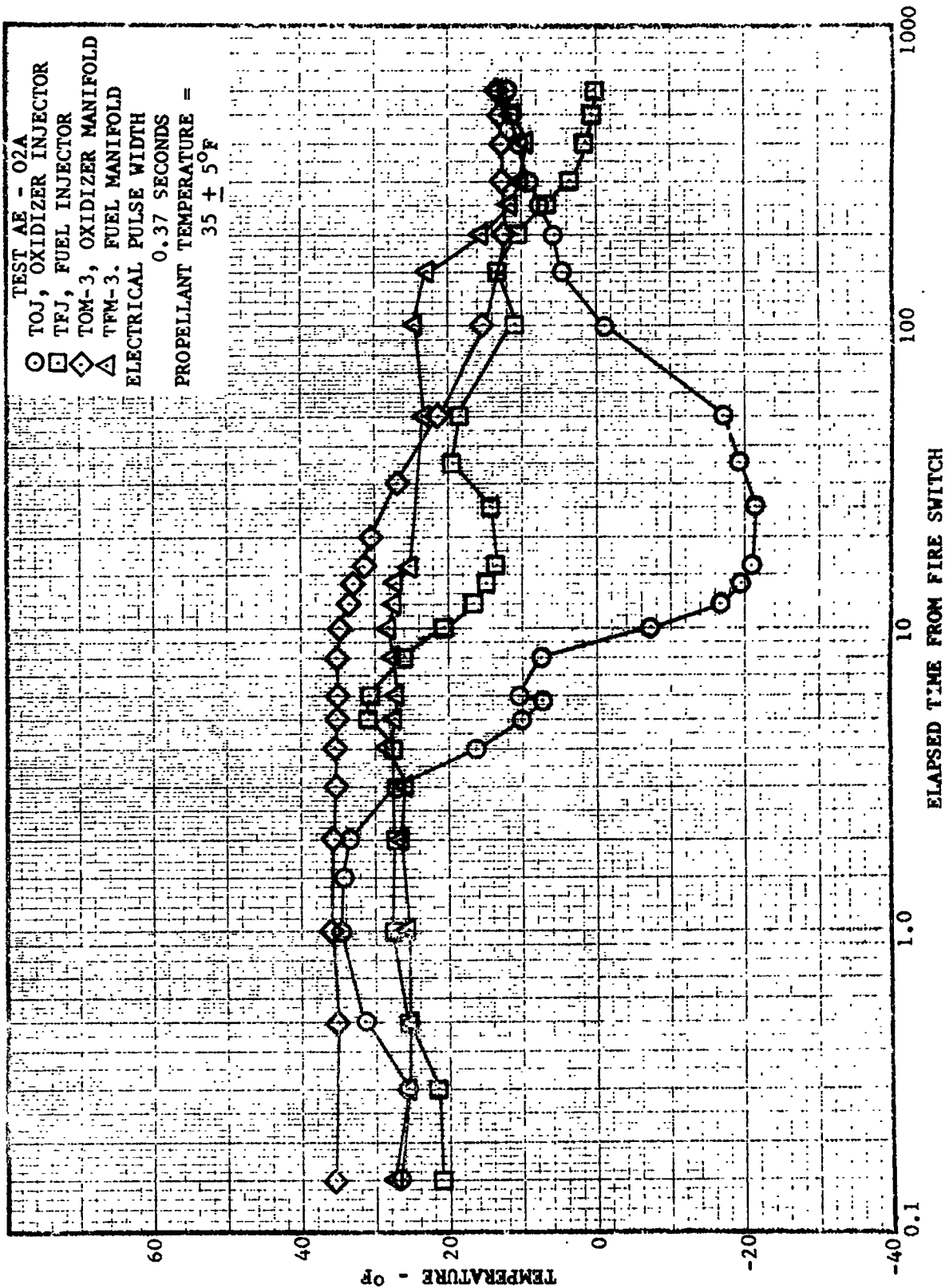


FIGURE 7-57 TEMPERATURE HISTORIES SPS INJECTOR AND INLET DUCT

7.6.2 Coast Phase Analysis (Continued)

Figure 7-58 shows a temperature-time history following a 0.50 second duration firing. The additional heat from the longer firing appears to shift the temperature-time history of residual propellants toward shorter venting, freezing, and sublimation times. The increase in firing duration from 0.37 to 0.50 seconds appears to have had only a minor effect on the rate or magnitude of cooling the hardware exposed to oxidizer. However, the increased heat input may have changed the vaporization rate of the fuel sufficiently to cause the fuel manifold temperature to reach its first minimum value approximately 5 seconds sooner and the second minimum approximately 200 seconds sooner than the shorter firing. The effect of increased firing duration is not clear because the 0.50 second firing occurred after the injector assembly had been significantly cooled during the previous two coast periods.

The oxidizer manifold cooled much more rapidly than the fuel manifold, as can be expected from a comparison of the propellant properties. As seen in Figure 7-58, when the oxidizer reaches its minimum temperature, there was a difference of approximately 40°F between the two manifolds. The cooling rate of the fuel manifold was probably influenced by this large temperature difference.

Unfortunately there are very little data from which phase diagrams can be constructed. However, Figure 7-59 shows the phase diagrams for the fuel side tests AE-02A, AE-04A, and AE-04B and several observations can be made from these. First, it appears that the fuel stays very close to equilibrium up to approximately 13 seconds. At this time, the UDMH is essentially all evaporated and the hydrazine is solidified. The sublimation of the hydrazine is apparently a very slow process, continuing over 600 seconds. The data show that there is very little difference between the process for the three tests even though one is a restart and the other two are initial starts.

The phase diagram for the oxidizer side is shown in Figure 7-60. The data show that the oxidizer stays very close to equilibrium. Boiling starts at about 2 seconds, the residual oxidizer is solidified in approximately 5 seconds and then sublimates slowly for times exceeding 600 seconds. There does not appear to be a significant difference between the restart and the initial start but the available information is not sufficient to determine if this is generally true.

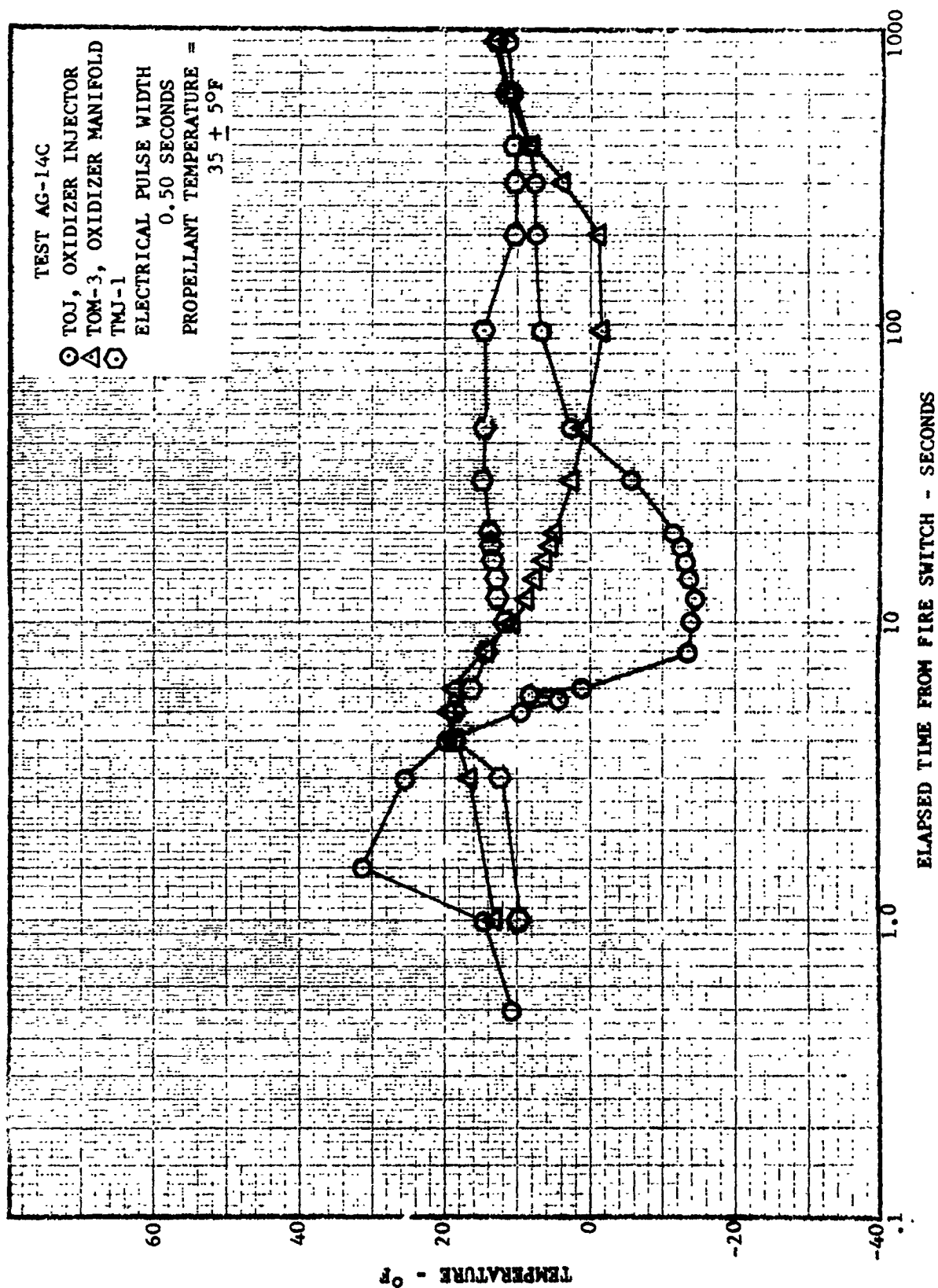


FIGURE 7-58 TEMPERATURE HISTORIES SPS INJECTOR AND MANIFOLD

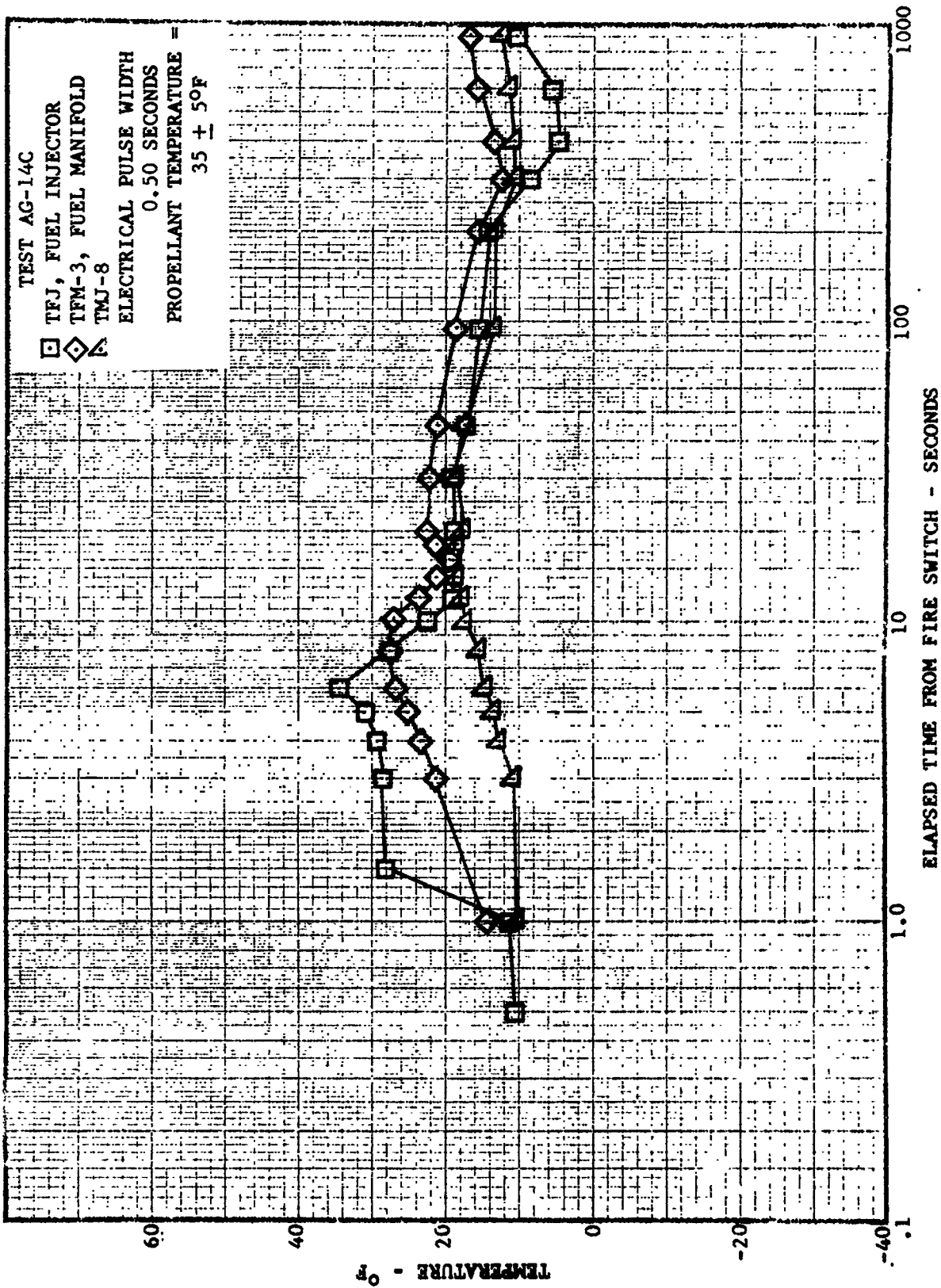


FIGURE 7-58 TEMPERATURE HISTORIES SPS INJECTOR AND MANIFOLD (CONCLUDED)

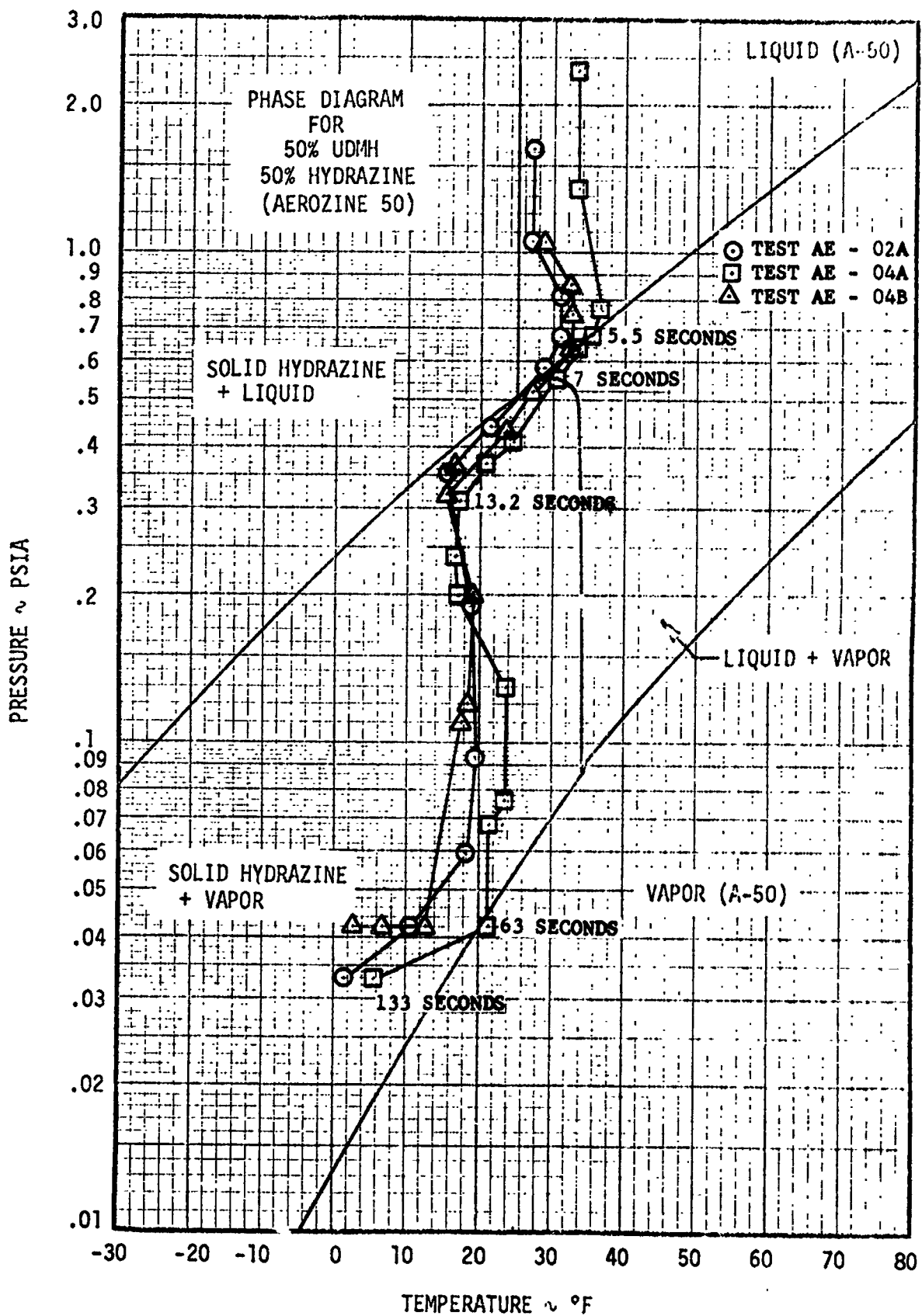


FIGURE 7-59 PHASE HISTORIES SPS INJECTOR

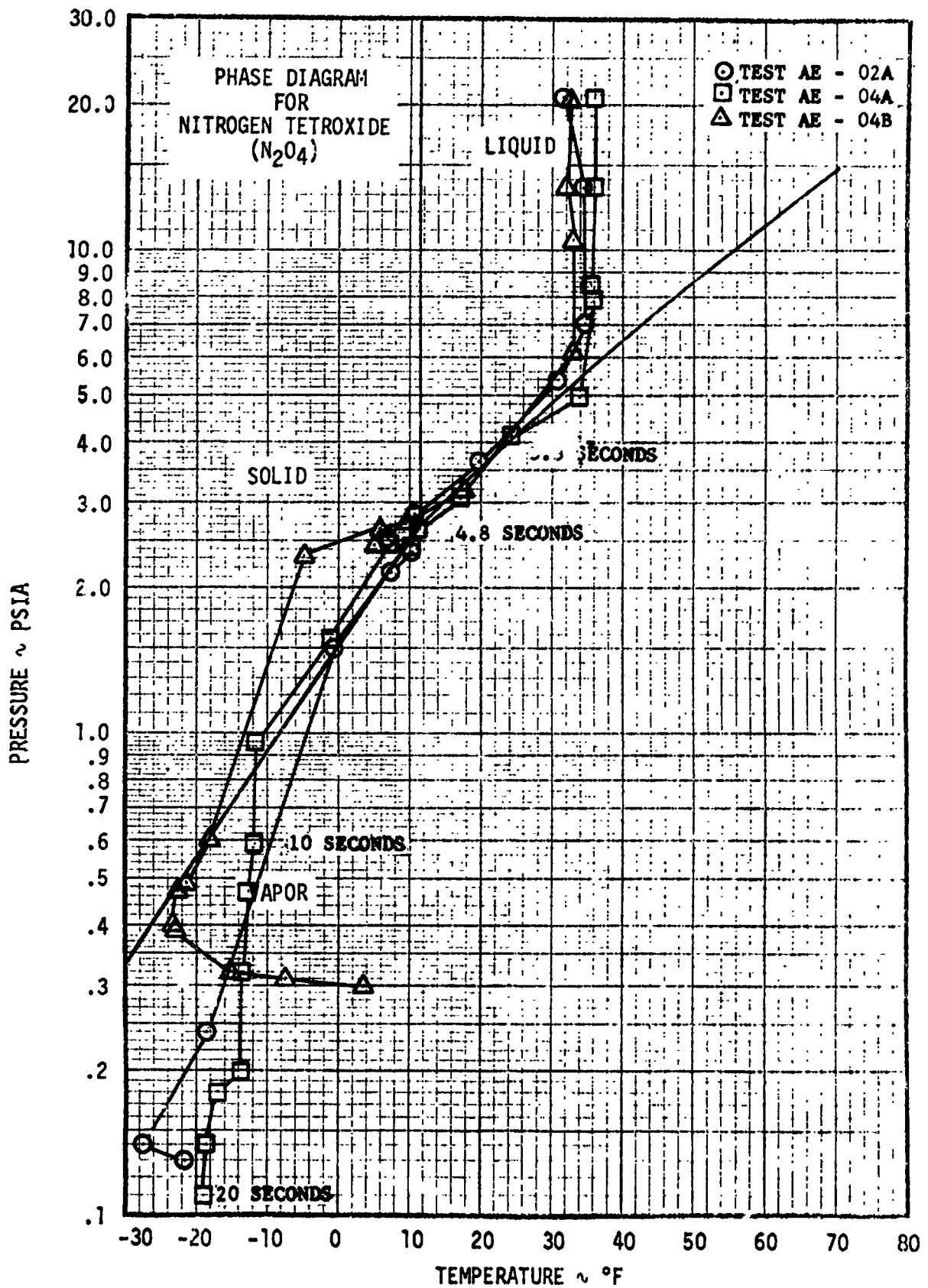


FIGURE 7-60 PHASE HISTORIES SPS INJECTOR

7.6.3 Start and Restart Firing Characteristics Analysis

The peak accelerations experienced with $35 \pm 5^\circ\text{F}$ propellants and an electrical pulse width of 0.37 seconds are plotted against coast duration in Figure 7-61. This figure shows the most severe test occurs at a coast period of 20 seconds. The peak level at 60 seconds is approximately one-third less than at 20 seconds, while the levels at 600 and 1800 seconds are comparable to levels reached on first starts. The least severe test occurred at a coast period of 7 seconds. Chamber pressure spikes versus coast duration are shown in Figure 7-62. These data show very little correlation to the accelerometer data, except that the maximum restart chamber pressure spikes occur between 20 and 180 seconds. At 600 and 1800 seconds, the restart chamber pressure spikes are comparable to first starts. From test data acquired during the AE series of tests, it appears that hard starts (accelerations greater in magnitude than on the initial start of a test sequence) were also associated with repeated short duration pulses, regardless of coast duration.

Accelerometer data for the AE test series show an increase in magnitude for restarts made after an initial 0.37 second firing. This was verified during the AG test series with a sequence of four restarts following a 0.37 second initial firing. All but one restart experienced acceleration levels higher than the initial start, and the last two restarts indicated acceleration levels more than two times the initial start. The data from restarts following a 0.50 second initial firing indicate that the restart will experience less severe accelerations than were experienced following a 0.37 second initial firing.

Acceleration data for restarts using $65 \pm 5^\circ\text{F}$ propellants are shown in Figure 7-63. Although these data are extremely limited, it is evident that the peak accelerations are of a lesser magnitude than with cold propellants ($35 \pm 5^\circ\text{F}$). Both the volume and phase of the residuals can affect the severity of engine restarts. Because of a lack of injector manifold pressure data (either oxidizer or fuel), it is not possible to evaluate manifold priming times to establish a propellant lead/lag relationship. This also limits the establishment of propellant phase histories during the shutdown transients and coast periods.

Several fuel manifold priming times from the AG test series are plotted in Figure 7-64. These data, as expected, show a decrease in priming time as coast time decreases. However, the magnitude of change is not large between 7 second and 1800 second coast periods. The point at 20 seconds appears to be associated with valve timing since both the initial start and first restart are comparable, but are higher than the other data.

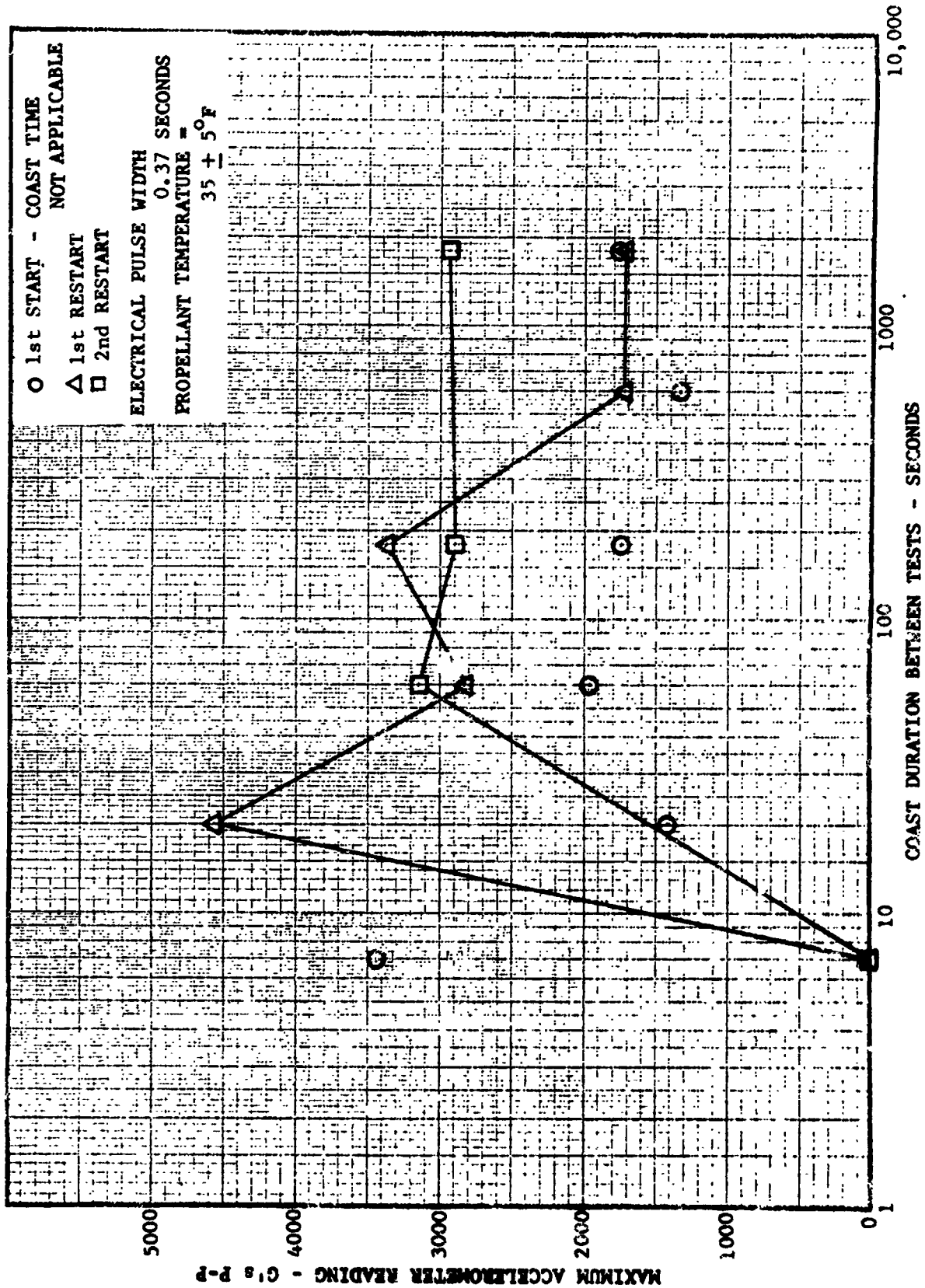


FIGURE 7-61 MAXIMUM ACCELERATION VS COAST TIME SPS ENGINE

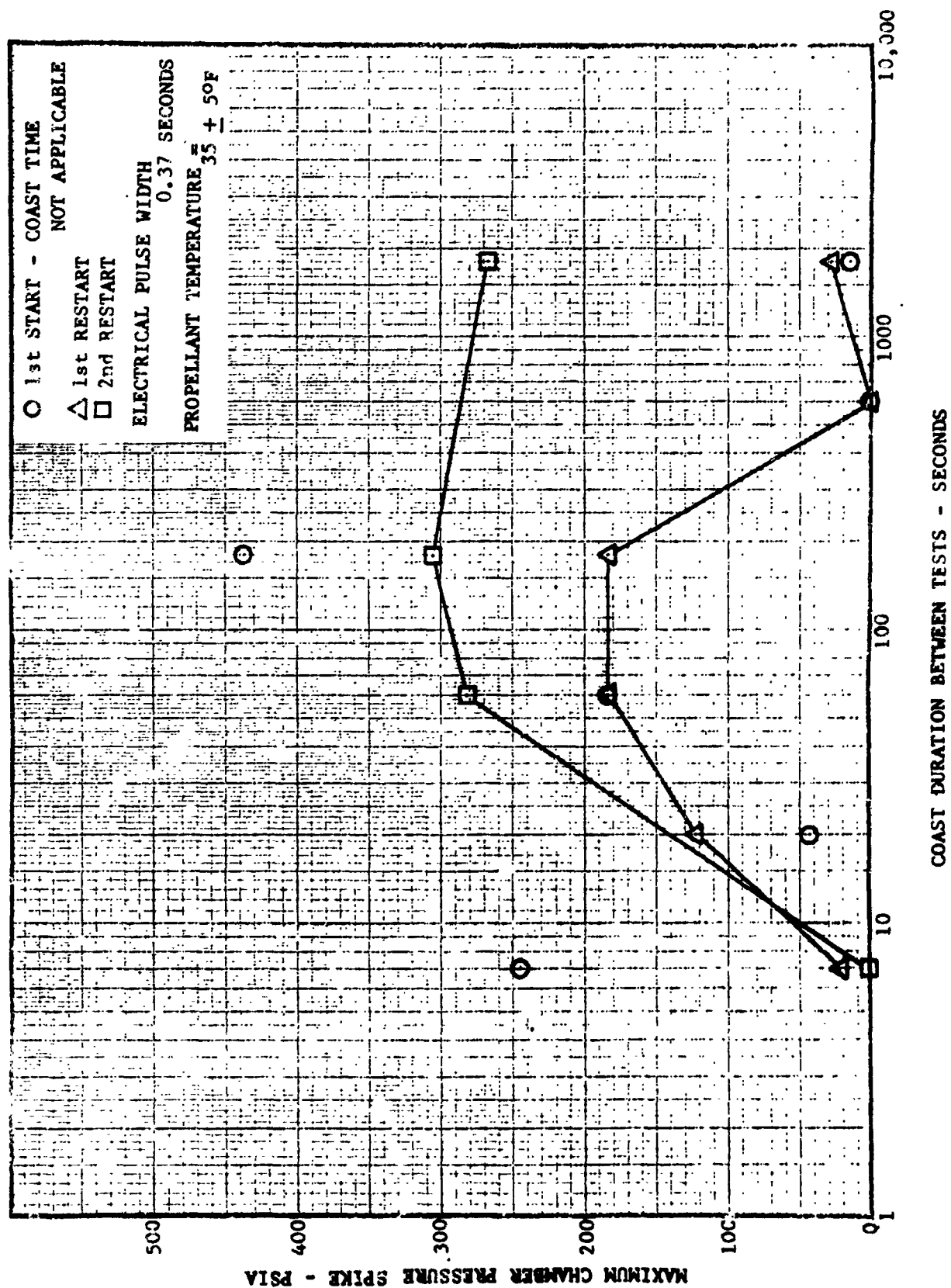


FIGURE 7-62 MAXIMUM CHAMBER PRESSURE SPIKE VS COAST TIME SPS ENGINE

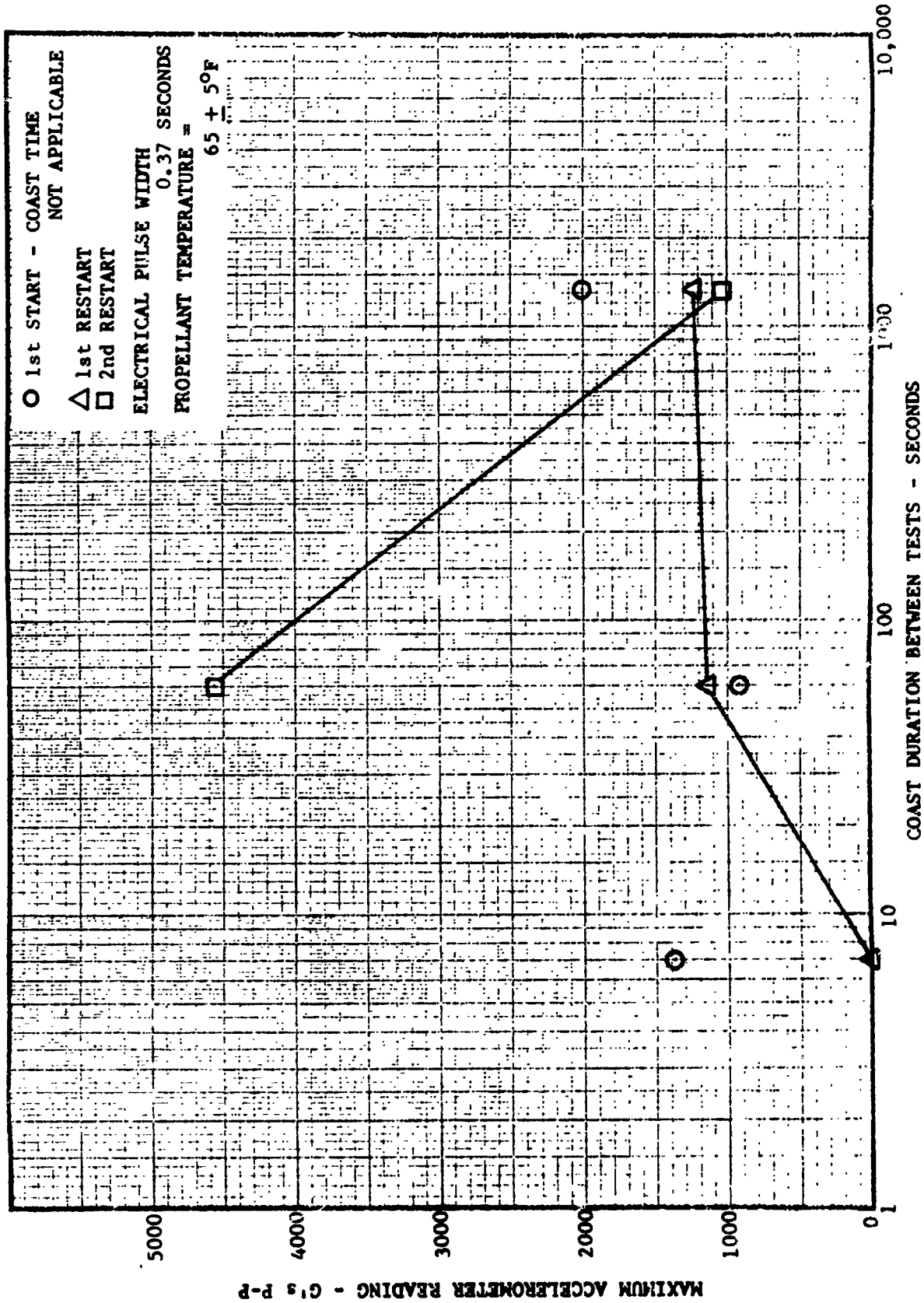


FIGURE 7-63 MAXIMUM ACCELERATION VS COAST TIME SPS ENGINE

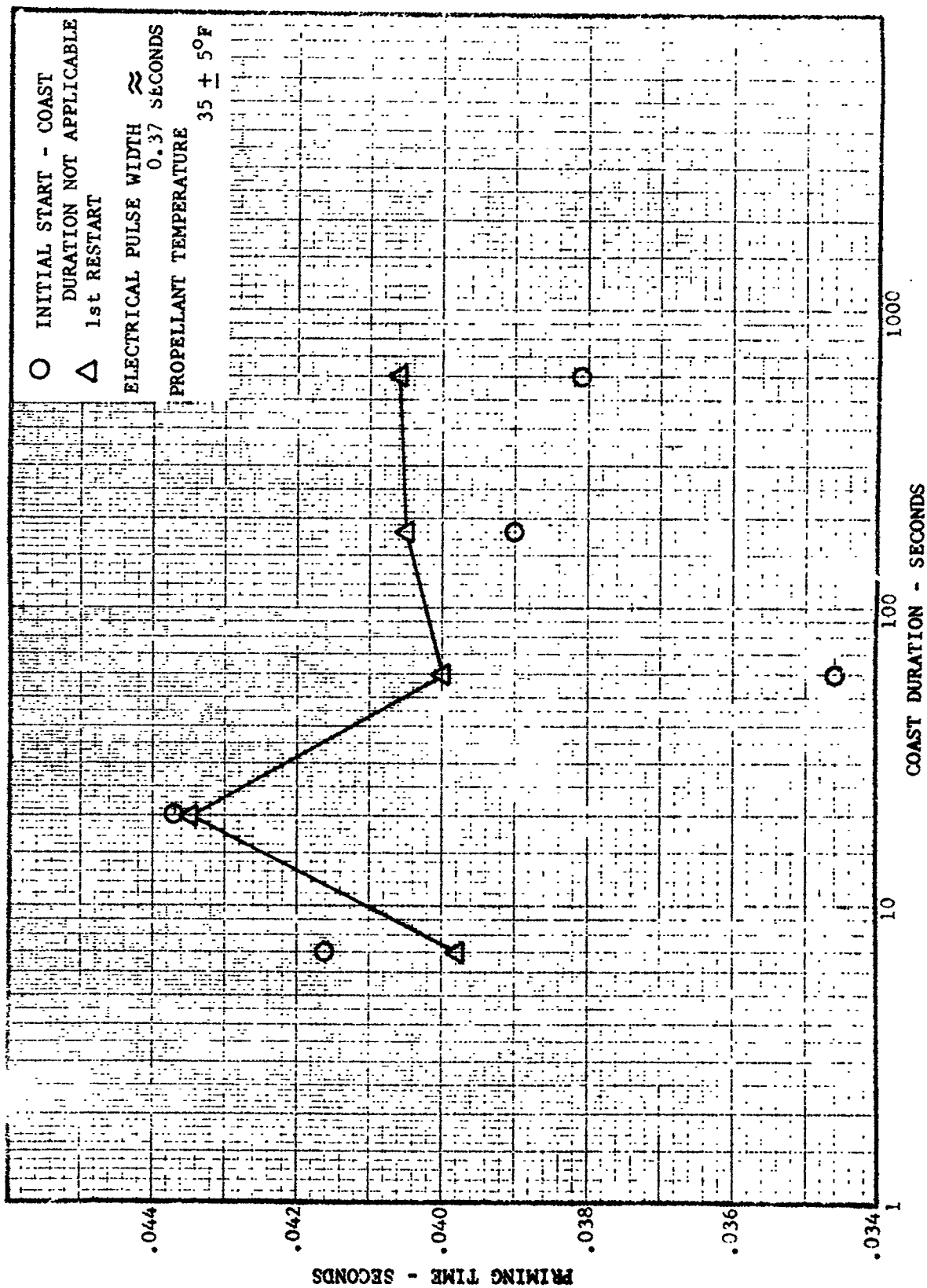


FIGURE 7-64 FUEL MANIFOLD PRIMING TIME VS COAST DURATION SPS ENGINE

7.6.4 Inbleed Tests Analysis

During tests AD-02, AD-03, and AD-04 oxidizer was bled into the injector and allowed to freeze prior to engine start. The oxidizer inbleed tests were accomplished by introducing a single propellant at a constant flow rate into the injector manifold just downstream of the injector ball valve. During propellant inbleeding, the engine exit pressure was maintained at a simulated pressure altitude of approximately 300,000 feet. The ignition transients were accomplished with a known volume of propellant which had vaporized sufficiently to reduce the pre-ignition hardware temperatures and freeze propellant.

Three oxidizer inbleed tests were conducted to simulate adverse starting conditions. The first inbleed was conducted with $35 \pm 5^\circ\text{F}$ propellants. An oxidizer volume equivalent to 32% of the total oxidizer manifold volume was inbled through a tap in the injector inlet duct at a slow rate to promote freezing in the injector passages. Five seconds after terminating the inbleed, the engine was started. Phase history data indicate that the oxidizer in the injector should be liquid or a liquid/solid mixture while the propellant in the chamber is in the solid phase. The second oxidizer inbleed was conducted with $35 \pm 5^\circ\text{F}$ propellants and an oxidizer volume equivalent to 75% of the total oxidizer manifold volume. The engine was started 220 seconds after terminating the inbleed. Phase history data indicate only solidified propellant should be present in either the injector or the chamber. During evaporative cooling of the oxidizer, considerable cooling of the fuel side resulted and, because of extremely low hardware temperatures, a delayed ignition occurred. Acceleration and pressure spikes were higher than those observed on the first test. The third oxidizer inbleed was conducted with $35 \pm 5^\circ\text{F}$ propellants and a propellant volume equivalent to 141% of the total oxidizer manifold volume. The engine was started after 60 seconds. Phase history data indicate only solid oxidizer is present in either the injector or chamber. Since the hardware temperature did not get as cold as in the second test, the ignition delay was less and the acceleration levels decreased slightly, although the pressure spikes increased. In general, the peak acceleration data for the oxidizer inbleed tests show values less than those reached by the first engine restart after coast periods of 60 and 180 seconds.

During tests AG-16, AG-17, and AG-18 fuel was bled into the injector prior to engine start. The hard start conditions resulting from a fuel inbleed were not as severe as anticipated and it did not appear to significantly affect the magnitude of the initial combustion pressure spike. The fuel inbleed tests were accomplished by introducing a single propellant at a constant flow rate, into the injector manifold just downstream of the injector ball valve. During the propellant inbleeding the engine exit pressure was maintained at a simulated pressure altitude of approximately 300,000 feet.

7.6.4 Inbleed Tests Analysis (Continued)

A total of three fuel inbleed tests were conducted. Since the engine was started approximately 30 seconds after terminating the inbleed for all the tests, the primary variable is the quantity of fuel inbled. Temperature and phase history data indicate that the fuel should be in the liquid/solid region. This is the same region (coast periods 20 - 180 seconds) in which the highest acceleration and chamber pressure spikes were reached during the restart tests. For the first fuel inbleed test, a volume equivalent to 0 - 25 percent of the total fuel manifold volume of $35 \pm 5^\circ\text{F}$ fuel was inbled through a tap in the injector just downstream of the injector ball valve. For the second test a volume equivalent to 25 percent of the total fuel manifold volume of $35 \pm 5^\circ\text{F}$ propellant was inbled and for the third test a volume equivalent to 50 percent of the total fuel manifold volume of $35 \pm 5^\circ\text{F}$ propellant was inbled.

In all fuel inbleed tests, peak acceleration levels are equal to or greater than those reached during restarts for the worst case coast periods (20 - 180 seconds). The most severe test occurred at 25 percent fuel inbled with no apparent trend towards increasing acceleration or chamber pressure spike levels as the quantity of inbled fuel was increased.

SECTION 8 - CORRELATION OF TEST RESULTS AND APPLICATION TO FLIGHT

8.0 GENERAL

This section presents the results of studies conducted to correlate test results between engines and between hot firing and cold flow tests using the same engines. Test results were also evaluated to determine if the effects of gravity forces could be isolated so that "zero-gravity" results can be predicted. The capability to correlate test results between engines can reduce the testing required for new engine designs. The capability to correlate test results between cold flow and hot firing tests can allow a reduction in the requirements for costly hot firing engine performance tests.

8.1 CORRELATION OF APS, DPS, AND SPS RESTARTS

Data analysis did not reveal any direct correlation of hard restarts between the APS, DPS, and SPS engines. The lack of correlation is the result of configuration differences between the engines. Configuration differences are indicated by Table 8-1, which presents volume, weight, and orifice area data for the three injectors. The differences in injector and duct configurations were significant even though all test engines were fired in an essentially horizontal position.

However, a correlation was obtained with respect to the thermodynamic process occurring during the coast phase following engine shutdown. The principle correlating factor is the ratio of injector assembly volume to injector orifice area. This correlation is discussed in Section 8.2.

The restart characteristics of the engines, as determined by ground testing, are briefly summarized in the following paragraphs.

DPS

The DPS engine did not have any repeatable hard restart problems, and did not show any evidence of potential problems for up to two restarts at coast periods of from 2 to 1800 seconds. Although the DPS engine has an oxidizer injector filter, there was no evidence that this filter was plugged. The injector configuration, which allowed significant amounts of oxidizer residuals to drain out, did not appear to cause fuel leads and consequent hard restarts.

APS

The APS engine experienced several hard restarts which can be conclusively attributed to frozen oxidizer residuals plugging the oxidizer injector screen. This occurred only when significant amounts of frozen oxidizer were present. At longer coast times (greater than 200 seconds) and shorter coast times (less than 15 seconds) there was insufficient frozen oxidizer to produce significant filter blockage. No engine structural damage was observed after the hard restarts.

SPS

The SPS engine had several hard restarts, but most of the hard restarts, and several of the hard "initial starts" appeared to be caused by the accumulation of explosive residues following repetitive short duration (0.37 second) firings. The short duration firings did not reach a steady state condition. Such firings are conducive to the formation and retention of explosive residues. The same phenomena has been responsible for RCS engine failures. The remaining hard restarts were not significantly harder than the range of first starts observed during the AEDC test program. No engine structural damage resulted from the hard restarts.

VOLUMES, IN ³	APS	DPS	SPS
DOWNSTREAM OF BALL VALVES TO PROP. DUCTS			Block I
FUEL	4	2.3	15
OXIDIZER	2	2.3	15
PROPELLANT DUCTS			
FUEL	49.8	15.9	53
OXIDIZER	9.5	42.1	41
INJECTOR			
FUEL	8.9	61.9	43
OXIDIZER	8.6	12.2	76
TOTAL FUEL	62.7	80.1	111
OXIDIZER	20.1	56.6	132
INJECTOR ORIFICE AREA, IN ²			
FUEL	.203	.084	.945
OXIDIZER	.275	.065	1.42
RATIO OF VOLUME TO ORIFICE AREA			
FUEL	308	954	118
OXIDIZER	73.1	870	93
ASSEMBLY WEIGHT, POUNDS			
BALL VALVE ASSEMBLY	27	17.0	123.8
PROPELLANT DUCTS			
FUEL	2.0	5.6	-
OXIDIZER	1.4	7.5	-
INJECTOR	10.5	29.5	46



Estimated; Includes propellant ducts

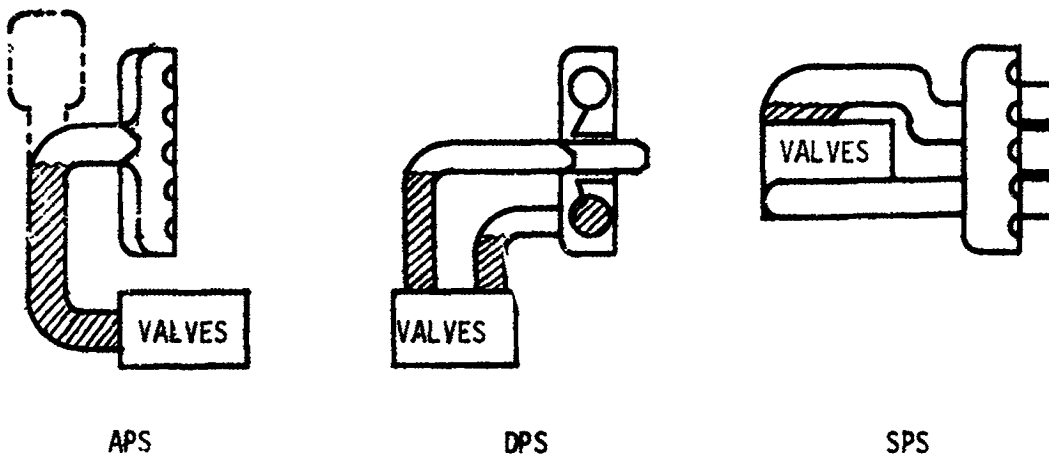
TABLE 8-1

COMPARISON OF APS, DPS, SPS ENGINE CONFIGURATIONS

8.1 CORRELATION OF APS, DPS, AND SPS RESTARTS (Continued)

The observed restart characteristics of the three engines can be partially explained by evaluating the effect of injector and duct configuration on the location and volume of the residual propellants. Further investigation of the injector flow phenomena which occur after engine shutdown will be required to complete the evaluation.

The relevant basic configuration differences between the injectors are shown on the sketches below. These sketches illustrate how the location and volume of the residuals are affected by the injector and duct configuration.



The APS hard restarts were caused by frozen oxidizer blocking the injector filter. The APS sketch shows that significant amounts of oxidizer can be trapped and frozen in the oxidizer duct. A significant volume of frozen fuel is present in the fuel duct. When the engine is restarted, the frozen oxidizer is forced directly into the oxidizer filter, but the frozen fuel is forced into the "tomato can," significantly reducing the probability that fuel will plug the fuel injector filter.

The DPS engine data showed no indications of hard restart problems, although restarts occurred with frozen fuel and oxidizer in the ducts. The slow starting characteristics at 10% thrust and the large injector orifices apparently prevent the frozen residuals from blocking flow passages and significantly altering the normal oxidizer lead.

The SPS engine does not have any filters which can be blocked by frozen residuals, but it is susceptible to fuel leads in the hub area of the injector. This is caused by the direct fuel flow path from the fuel duct to the injector orifices in the hub. In the outer rings of the

8.1 CORRELATION OF APS, DPS, AND SPS RESTARTS (Continued)

injector, the fuel must first flow through the injector baffles before reaching the fuel injector orifices, producing an oxidizer lead in the outer injector rings. As a result, the SPS engine is particularly vulnerable to blockage of the oxidizer flow paths because of the marginal oxidizer or oxidizer vapor lead in the hub area. Partial blockage of the oxidizer flow paths can delay the oxidizer flow and cause a fuel lead. It is interesting to note that the hardest restart during the AG series and the minimum oxidizer manifold temperature both occurred after 20 seconds of coast. The possible existence of a fuel lead at 20 seconds cannot be confirmed because of the loss of manifold pressure instrumentation during the AG test series.

8.2 CORRELATION OF COLD FLOW AND HOT FIRING TESTS

A comparison of hot firing temperature and pressure data with similar cold flow data shows that the same basic boiling and freezing phenomena occurred during both the hot firing and cold flow tests. Representative hot firing test data are presented in Sections 7.3, 7.4, and 7.6. Representative cold flow test data are presented in Sections 7.2 and 7.5.









Although the same basic phenomena were observed during cold flow and hot firing tests, the significant phenomena, such as the beginning of boiling or freezing, occurred at different coast times. Table 8-1 presents a summary of representative coast times at which the beginning of boiling and freezing were observed. The summary in Table 8-2 shows that the effect of initial propellant temperature on time to boil and time to freeze was consistent between cold flow and hot firing tests. Specifically, the initial ascent engine propellant temperature did not have a significant effect on the time to boil or freeze during either the cold flow or hot firing tests. In contrast, the initial descent engine propellant temperature had a significant effect on the time to boil or freeze during both the cold flow and hot firing tests.

The summary in Table 8-2 also shows that the time to boiling and freezing was significantly different between the cold flow and hot firing tests. This is attributed to the effect of chamber pressure on the propellant venting process during the engine shutdown phase. The "chamber pressure" measured during cold flow tests was actually the altitude chamber pressure, which was significantly lower than the chamber pressure that would result from propellant combustion in a thrust chamber. At the present time, the effect of chamber pressure on the flow rate through the injector orifices cannot be precisely calculated, although the general characteristics of the flow are known. During the propellant flow and immediately after termination of the flow the liquid flow rate out of the injector will be increased by any reduction in the "chamber pressure" existing at the injector face. When the flow through the injector orifices becomes two phase (liquid plus gas) or single phase (gas only), the chamber pressure level may affect the flow rate out of the injector.

None of the cold flow tests could be characterized with respect to the effect of "chamber pressure" on the shutdown transient, because data were not obtained during the cold flow "shutdown" phase. However, it is believed that the difference between the hot firing chamber pressure decay and the cold flow "chamber pressure" decay caused the major differences between otherwise similar hot firing and cold flow tests.

Evaluation of the data showed that the times to boiling and freezing for hot firing tests were correlated by the ratio of injector assembly volume to injector orifice area. The volume-to-area ratio for the fuel and oxidizer sides of the APS, DPS, and SPS injector assemblies was obtained from Table 8-1. Figures 8-1 and 8-2 show the correlation

D2-118246-1

TEST SERIES	INITIAL PROP. TEMP. (°F)	FUEL		OXIDIZER	
		TIME TO BOIL (SEC)	TIME TO FREEZE (SEC)	TIME TO BOIL (SEC)	TIME TO FREEZE (SEC)
DPS Hot Fire	64	10	80	5	50
	46	15	60	7	50
	30	20	40	8	40
DPS Cold Flow	70	5	90	5	9
	40	25	90	N/A	N/A
APS (Rocketdyne) Cold Flow	70	5	15	N/A	N/A
	46	5	12	N/A	N/A
APS Hot Fire	60	8	25	4	20
	50	7	27	4	15
	40	7	27	4	15
SPS Cold Flow	65	-	-	0 	4
	33	-	-	0 	5
	15	-	-	0 	2
	73	0 	10	-	-
	56	0 	11	-	-
	34	0 	2-1/2	-	-
SPS Hot Fire	65	7		3	
	35	8-1/2	9-1/2	5	15



Static test, start of boiling is start of test.

Exterior skin thermocouple did not indicate freezing temperature.

TABLE 8-2 COAST PHASE TEST RESULTS SUMMARY

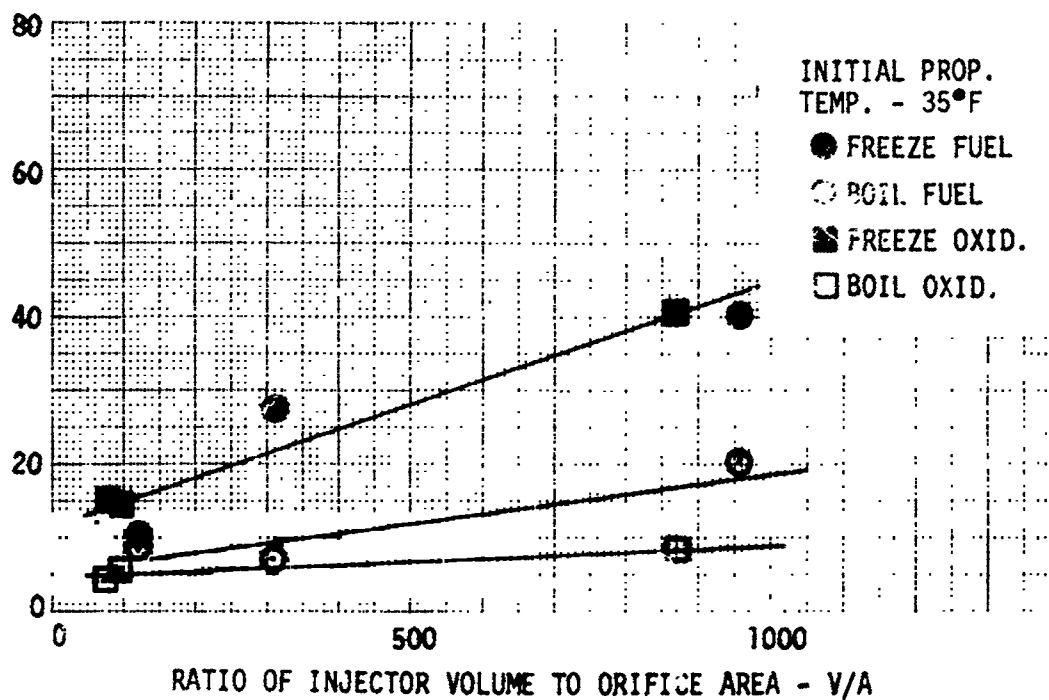


FIGURE 8-1 CORRELATION OF HOT FIRING COAST PHASE RESULTS (35°F)

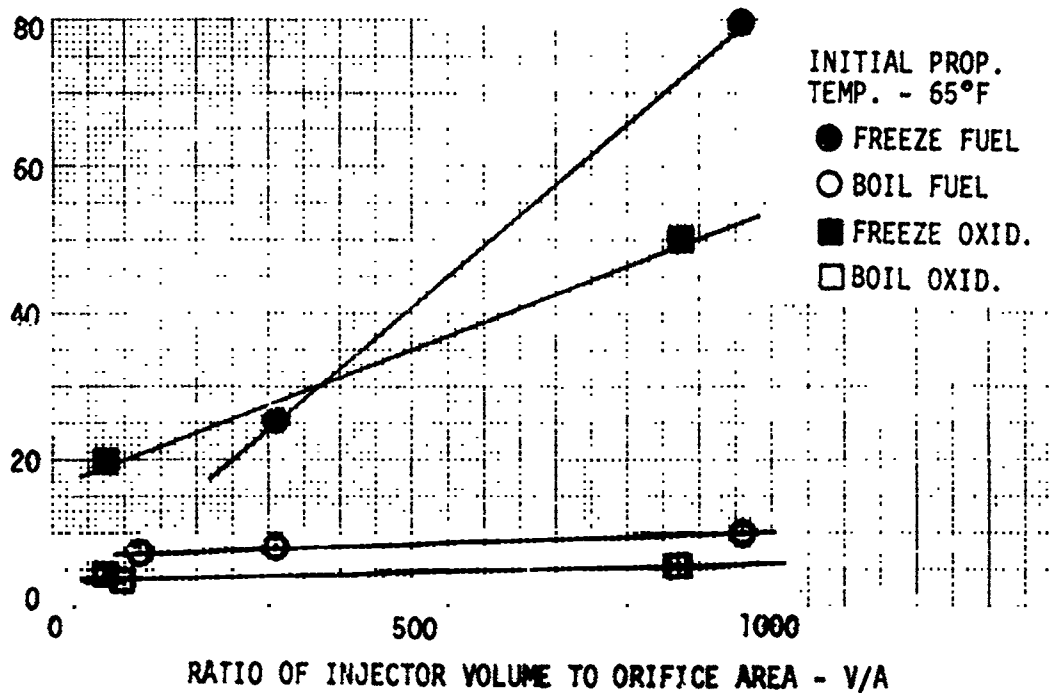


FIGURE 8-2 CORRELATION OF HOT FIRING COAST PHASE RESULTS (65°F)

8.2 CORRELATION OF COLD FLOW AND HOT FIRING TESTS (Continued)

between the times to boil or freeze and the injector volume-to-area ratios. These correlations are presented for the hot firing tests only. The cold flow data correlation is not presented because oxidizer data were not obtained during the Rocketdyne injector tests, facility problems were experienced during the DPS tests (see Appendix A) and the SPS injector orientation was significantly different from the orientation of the APS and DPS injectors.

The observed correlation confirms the effect of relative orifice area (as measured by the injector volume-to-orifice-area ratio) on the suppression of gas effervescence, boiling and evaporation. The phase histories in Section 7 show the effect of injector volume-to-area ratio on the boiling and vaporization processes. Typical DPS phase histories, such as Figures 7-43 and 7-45, show that the relatively small DPS fuel and oxidizer injector areas tended to reduce the rate of boiling and to produce phase histories which were close to equilibrium. Typical APS fuel histories, such as Figure 7-29 show that the fuel boiling process, was more rapid and farther from equilibrium than the DPS process, illustrating the effect of an increase in relative orifice area. The APS oxidizer phase histories, such as Figures 7-32, were much farther from equilibrium than the DPS oxidizer histories, showing the effect of a significant increase in relative orifice area. The SPS phase histories, such as Figures 7-59 and 7-60 show that the fuel and oxidizer processes were very rapid but close to equilibrium. The temperature data for these histories were obtained from immersion thermocouples in the injector flow passages, with the result that these temperature data are not directly comparable to the duct surface temperature data used in the APS and DPS phase histories. SPS phase histories, using duct thermocouple temperature data, indicated that the fuel and oxidizer in the ducts were far from thermodynamic equilibrium. The SPS data presented in Table 8-2 and Figures 8-1 and 8-2 were obtained from propellant duct surface thermocouples.

8.3 APPLICATION TO FLIGHT

In a "zero-gravity" flight environment, there will be no gravity-produced drainage of propellants from the injectors and ducts. Neither will there be any residual propellants "trapped" in the ducts and injectors by gravity forces. A reduction in the amount of drainage will increase the severity of hard restarts, but a reduction in the volume of "trapped" propellants will decrease the severity of hard restarts. The key problem is the determination of the importance of gravity effects relative to the boiling and gas effervescence effects on propellant expulsion.

Temperature and phase history data from the SPS firings tend to indicate that the effects of gravity are less significant than the effects of boiling and effervescence. This tentative conclusion is based on a comparison of the SPS temperature-time histories with the DPS and APS histories. This comparison shows that the SPS injector was significantly cooled by fuel residuals which were present for more than 60 seconds and by oxidizer residuals which were present for more than 30 seconds. Residuals were present for relatively long periods even though all of the residuals could have drained out within a few seconds. It appears that liquid and solid residuals are retained in the engine by gas bubbles formed during gas effervescence and boiling. On the basis of this comparison of test data, it is tentatively concluded that the boiling and effervescence of dissolved gases have a significant effect in determining the initial volume of residual propellants.

Additional data on the magnitude of these effects relative to the effect of gravity-related phenomena (drainage and "trapping") can be obtained by conducting hot firing tests with the engines in a vertical nozzle-down orientation. Changing from a horizontal attitude, as used for the Boeing/Seattle tests, to a vertical attitude, will have the following effects on the volume of trapped residuals (refer to the illustrations in Section 8.1):

	FUEL	OXIDIZER
APS	Significant decrease	Significant decrease
DPS	Significant increase	Significant decrease
SPS	Negligible	Negligible

Comparison of test data from nozzle-down firings to data from the horizontal firings will allow the relative importance of gravity effects and thermodynamic effects to be determined.

Proposed testing of the APS, DPS, and SPS engines in a vertical-down attitude at WSTF can be used to prove or disprove the ability of the boiling and gas effervescence phenomena to significantly affect the

8.3 APPLICATION TO FLIGHT (Continued)

the initial volume of residual propellants. Due to the significant effect of orientation on propellant drainage in the APS engine, data from WSTF restart testing of this engine can prove, or disprove, the controlling influence of boiling and effervescence phenomena on engine restarts. In particular, if the APS data indicate that significant residuals are present for times on the order of 20 to 30 seconds, or hard restarts occur as the result of oxidizer injector screen blockage, the controlling influence of boiling and effervescence will be confirmed.

SECTION 9 - CONCLUSIONS AND RECOMMENDATIONS

9.1 CONCLUSIONS

1. Run time, propellant temperature, propellant gas saturation, engine start transient characteristics, and engine orientation (as related to gravity effects) are the prime parameters that must be considered in determining the restart characteristics of hypergol engines. Indications are that:

The probability of a hard restart increases as the propellant temperature is lowered;

Short firings can lead to hard restarts due to propellant freezing and the formation of detonable compounds;

The susceptibility of an engine to hard restarts is lower for an engine with a relatively long normal start transient time.

Definite conclusions relating engine orientation (gravity effects) and propellant gas saturation to engine restart characteristics require test data not available during this program. Recommendations for further work to obtain these data are presented in Section 9.2.

2. Cold flow testing can be formulated to provide data that will allow the determination of propellant temperatures and coast times required to establish the proper range of variables that must be covered by a hot firing test program. Recommended requirements for these cold flow tests are presented in Appendix E (Volume II). An additional theoretical investigation of injector flow processes is also required before the capability to correlate cold flow and hot firing test results is established. Recommendations for such an investigation are presented in Section 9.2.

9.2 RECOMMENDATIONS

1. Additional restart tests should be conducted with the APS, DPS, and SPS engines in a vertical, nozzle-down orientation. These tests would provide data required to determine the relative importance of gravity effects (drainage) and thermodynamic effects (boiling and gas effervescence). Specific test objectives for each of the engines are listed below.

APS

Determine coast period which produces hard restarts. Remove injector filters, and repeat the test to verify that filter blockage by frozen propellants was the cause of hard restarts.

DPS

Conduct restart tests at different throttle settings to verify restart capability in the event that start procedures are modified, and to determine the effect of varying injector area/injector volume ratio on restart phenomena. These tests are necessary to provide basic experimental data for further development of correlation and prediction techniques.

SPS

Verify restart capability for the Block II engine.

2. A simple computer program should be developed and utilized for parametric analyses of significant test variables such as volume, orifice area, and initial temperatures. This will supplement the existing test analysis and support the other recommended actions.
3. A theoretical investigation of injector flow processes should be made. The specific area to be investigated is the time period at and immediately after shutdown when liquid, two-phase and gas flows are occurring, and should include better definition of the non-equilibrium processes. These analyses could provide a capability to correlate cold flow and hot-firing test results that would be particularly valuable on future programs.